Serial No. 07-0555A
Docket No. 50-336

ENCLOSURE 1

WESTINGHOUSE REPORT

WCAP-16896-NP, REV 1

MILLSTONE UNIT 2 RCS SURGE, SPRAY, SHUTDOWN COOLING, SAFETY INJECTION, CHARGING INLET, AND LETDOWN/DRAIN NOZZLES STRUCTURAL WELD OVERLAY QUALIFICATION

(Non-Proprietary)

(161 pages)

MILLSTONE POWER STATION UNIT 2
DOMINION NUCLEAR CONNECTICUT, INC.

Westinghouse Non-Proprietary Class 3

WCAP-16896-NP
Revision 1

April 2008

Millstone Unit 2 RCS
Surge, Spray, Shutdown Cooling, Safety Injection, Charging Inlet, and Letdown/Drain Nozzles Structural Weld Overlay Qualification

Westinghouse

WCAP-16896-NP
Revision 1

Millstone Unit 2 RCS Surge, Spray, Shutdown Cooling, Safety Injection, Charging Inlet, and Letdown/Drain Nozzles Structural Weld Overlay Qualification

Gordon Z. Hall*

April 2008

Reviewer: David F. Baisley*
Major Reactor Component Design & Analysis I

Approved: John Ghergurovich*
Manager
Major Reactor Component Design & Analysis I

* Electronically approved records are authenticated in the Electronic Document Management System.

Westinghouse Electric Company LLC
P.O. Box 355
Pittsburgh, PA 15230-0355

Record of Revisions

Rev	Date	Revision Description
0	3/2008	Original Issue
1	See EDMS	• At Dominion's request, the language in the document was revised to indicate that the impact of the added weld overlay mass on existing primary stress qualification is documented in [36]. • Reference [36] added. • Revised pages: Cover, Record of Revision, 6-1, 6-18, 7-1, 7-21, 8-1, 8-19, 9-1, 9-21, 10-1, 10-17, 11-1, 11-20, 12-1, 13-4.

TABLE OF CONTENTS

LIST OF TABLES

LIST OF FIGURES

LIST OF FIGURES (Cont.)

LIST OF FIGURES (Cont.)

LIST OF FIGURES (Cont.)

NOMENCLATURE

ΔK_I	stress intensity factor range, ksi√in (MPa√m)
A	constant in crack growth law for Alloy 82/182 welds
A	cross-section area, in^2
A_i	polynomial coefficients in through-wall stress distributions
C	scaling parameter for temperature effects in crack growth law
da	crack growth, inches
$\left(\frac{da}{dN}\right)_{air}$	crack growth rate in air, inch/cycle (m/cycle)
F_{env}	environmental factor for stainless steel welds
F_x, F_y, F_z	forces along x, y, and z-directions, kips
G_j	boundary correction factors in stress intensity factor
h	weld overlay wall thickness, inches
K_I	stress intensity factor, ksi√in (MPa√m)
K_{max}	maximum stress intensity factor range, ksi√in (MPa√m)
K_{min}	minimum stress intensity factor range, ksi√in (MPa√m)
m	exponent in crack growth law for Alloy 82/182 welds
M_x, M_y, M_z	moments about x, y and z-axis, in-kips
n	material property slope in crack growth law
P	primary stress component, ksi
Q	secondary stress component, ksi
Q	shape factor in stress intensity factor formulae
R	stress intensity factor ratio, K_{min} / K_{max}
R_i	inside radius, inches
R_o	outside radius, inches
S	scaling factor for load ratio
S_m	ASME Code allowable stress intensity, ksi
S_y	yield strength, ksi
S_u	ultimate tensile strength, ksi
T	metal temperature, °F (°C)
t	wall thickness, inches
Z	section modulus, in^3
σ	stress perpendicular to the plane of the crack
σ_m, σ_b	membrane and bending stresses, ksi
Φ	elliptical angle in crack shape definition

LIST OF ABBREVIATIONS

ANSI	American National Standards Institute
ASME	American Society of Mechanical Engineers
BWR	boiling water reactor
CGR	crack growth rate
CI	charging inlet
CS	carbon steel
DM	dissimilar metal
DNC	Dominion Nuclear Connecticut Inc.
DO	dissolved oxygen
DW	deadweight
EPU	extended power uprate
FCG	fatigue crack growth
FEA	finite element analysis
GMAW	gas-metal arc welding
GTAW	gas-tungsten arc welding
HAZ	heat-affected zone
HU	heatup
ID	inside diameter
IGSCC	intergranular stress corrosion cracking
ISI	in-service inspection
LOCA	loss-of-coolant accident
LWR	light water reactor
MOPCD	modified operating procedure cooldown
MOPHU	modified operating procedure heatup
NRC	Nuclear Regulatory Commission
OBE	operating basis earthquake
P	pressure
PDI	Performance Demonstration Initiative
PT	penetration testing
PWR	pressurized water reactor
PWSCC	primary water stress corrosion cracking
RCL	reactor coolant loop
RCS	reactor coolant system
RSS	root-sum-of-the-squares
RV	relief valve
SAW	submerged arc weld
SDC	shutdown cooling
SI	safety injection
SMAW	shielded-metal arc welding
SQRT	square root
SS	stainless steel
SSE	safe shutdown earthquake
SWOL	structural weld overlay
TGSCC	transgranular stress corrosion cracking
TH	thermal
UT	ultrasonic testing
WOL	weld overlay

1 INTRODUCTION

Weld overlay (WOL) is a repair and/or mitigation technique used to reinforce nozzle safe-end regions and pipes susceptible to primary water stress corrosion cracking (PWSCC). In this report, the term "repair" is used to describe the application of WOL as either a pre-emptive or repair activity. ASME Code Case N-740 [1] and the Dominion Nuclear Connecticut Inc. (DNC) Alternative Request [3] were used for the WOL design. ASME Code Case N-740 permits the use of weld deposit on austenitic stainless steel (SS) piping to increase the wall thickness of the affected region. This method demonstrates the acceptability of the repaired defects in accordance with ASME Code Section XI IWB-3640 [6]. Use of Code Case N-740 prior to NRC approval has required an Alternative Request [3] to the NRC for their approval.

The process identified Code Case N-740 may be used to design either a pre-emptive or repair overlay. The WOL involves both the application of a specified thickness and a length of weld material over the region of interest in a configuration that ensures that the structural integrity is maintained. The weld material, Alloy 52/52M, is applied by the gas-tungsten arc welding (GTAW) process. Alloy 52/52M is considered highly resistant to intergranular stress corrosion cracking (IGSCC), transgranular stress corrosion cracking (TGSCC), and PWSCC. The reinforcement material forms a structural barrier to stress corrosion cracking and produces a compressive residual stress condition at the inner portion of the pipe that mitigates future crack initiation and/or propagation.

The approach outlined in ASME Code Case N-740, ASME Code Section XI IWB-3640, and the DNC Alternative Request [3] is consistent with the requirements in NUREG-0313, Revision 2 [4] for boiling water reactor (BWR) coolant pressure boundary piping. The design must consider limitations on the welding process and control, as well as accommodate the need for ultrasonic testing (UT) examinations of the WOL and the original weld. Additionally, the impact of the resulting WOL repair on the existing design qualification of the piping system and nozzle safe-end must be addressed.

Due to the proximity of the safe-end-to-piping SS butt-weld to the nozzle-to-safe-end dissimilar-metal (DM) butt-weld, the WOL will cover the nozzle-to-safe-end weld, as well as cover and extend past the safe-end-to-piping weld. Therefore, this report describes the geometry of the WOL repairs for the SS butt-welds, as well as the dissimilar-metal butt-welds of the reactor coolant system (RCS) spray, surge, shutdown cooling outlet (SDC), safety injection (SI), charging inlet (CI), and letdown/drain nozzles. Furthermore, this report provides the technical basis for application of the overlay. A summary of the finite element analysis (FEA) performed to determine the residual stresses that result from the structural weld overlay (SWOL) is provided. The methodology used in the WOL design qualification and the results that demonstrate the acceptability of the design are also provided.

Several locations in this report contain proprietary information. Proprietary information is identified and bracketed. For each of the bracketed locations, the reason for the proprietary classification is provided, using a standardized system. The proprietary brackets are labeled with three different letters, "a", "c", and "e", which stand for:

a. The information reveals the distinguishing aspects of a process or component, structure, tool, method, etc. The prevention of its use by Westinghouse's competitors, without license from Westinghouse, gives Westinghouse a competitive economic advantage.

c. The information, if used by a competitor, would reduce the competitor's expenditure of resources or improve the competitor's advantage in the design, manufacture, shipment, installation, assurance of quality, or licensing of a similar product.

e. The information reveals aspects of past, present, or future Westinghouse- or customer-funded development plans and programs of potential commercial value to Westinghouse.

2 BACKGROUND

In September 2003, a small leak was discovered from an Alloy 132 (similar to Alloy 182) butt-weld on a pressurizer relief nozzle in Tsuruga Unit 2. Samples removed for the destructive examination contained the entire weld and a portion of the base metal on each side of the weld. Metallurgical failure analysis showed that the cracks initiated from the inside surface, were axially-oriented, and were intergranular or interdendritic in nature. The metallurgical analysis concluded that the nozzle failure was caused by PWSCC in the nozzle weld [5]. Similar indications were found in the D. C. Cook Unit 1 safety nozzle in the spring of 2005. In 2006, circumferential indications consistent with PWSCC were found at Wolf Creek prior to performing an overlay repair.

WOL repairs were first applied to address IGSCC in the weld heat-affected zones (HAZs) of BWR SS piping as an alternative to pipe replacement. Since 1982, WOL repairs have been used extensively in BWR SS piping and safe-end welds (over 1,000 in service) to repair flawed weldments. These WOL repairs have produced favorable compressive residual stresses on the inner portion of the pipe wall [4], thereby minimizing further crack growth. Many BWR WOLs were applied using SS. However, in recent years, Alloy 52/52M has been used.

DNC has decided to install a SWOL on one RCS surge nozzle, two RCS spray nozzles, one shutdown cooling outlet nozzle, four safety injection nozzles, two charging inlet nozzle, and five letdown/drain nozzles. Installation is scheduled to begin in the spring of 2008. This report documents the technical basis for these WOL mitigations. Figures 2-1 through 2-6 show the typical configurations for RCS spray, RCS surge, shutdown cooling, safety injection, charging inlet, and letdown/drain nozzles, respectively.

In accordance with ASME Code Case N-740, weld metal is applied circumferentially around the affected region and in its vicinity to restore ASME Code Section XI margins. An analysis of the repaired/mitigated weld is performed to ensure that any remaining flaws in the affected region will not further propagate to an unacceptable condition. According to ASME Code Case N-740, the WOL is designed to maintain all the structural requirements by conservatively assuming that a through-wall defect has penetrated 360° of the circumference of the original nozzle-to-safe-end dissimilar-metal butt-weld and the original safe-end-to-piping similar-metal butt-weld. The WOL provides a replacement pressure boundary and an effective barrier to prevent any further crack growth because of the excellent corrosion resistance inherent in the chemistry of the Alloy 52/52M weld deposits. Either ERNiCrFe-7 (Alloy 52, UNS06052) or ERNiCrFe-7A (Alloy 52M, UNS06054) will be used as the overlay filler material. Both Alloy 52 and Alloy 52M are listed in the ASME Code, Section II and Section IX, and are acceptable for use under the ASME Code. Alloy 52/52M nickel-based weld repair material is used rather than austenitic SS because SS welds cannot be effectively applied over Alloy 82/182 buttering and welds. The use of Alloy 52/52M nickel-based repair material is also consistent with the DNC Alternative Request [3].

All welding will be accomplished using the GTAW process. The requirements specified in the DNC Alternative Request [3] will be used for the repair examinations. The impact of the SWOL on the original Code of Construction qualifications for these nozzles is evaluated. The original Codes of Construction and design specifications are:

- ANSI Code for Pressure Piping B31.7, Class 1, 1969 [33]
- Design Specification 18767-31-5, Rev. 16 [30]

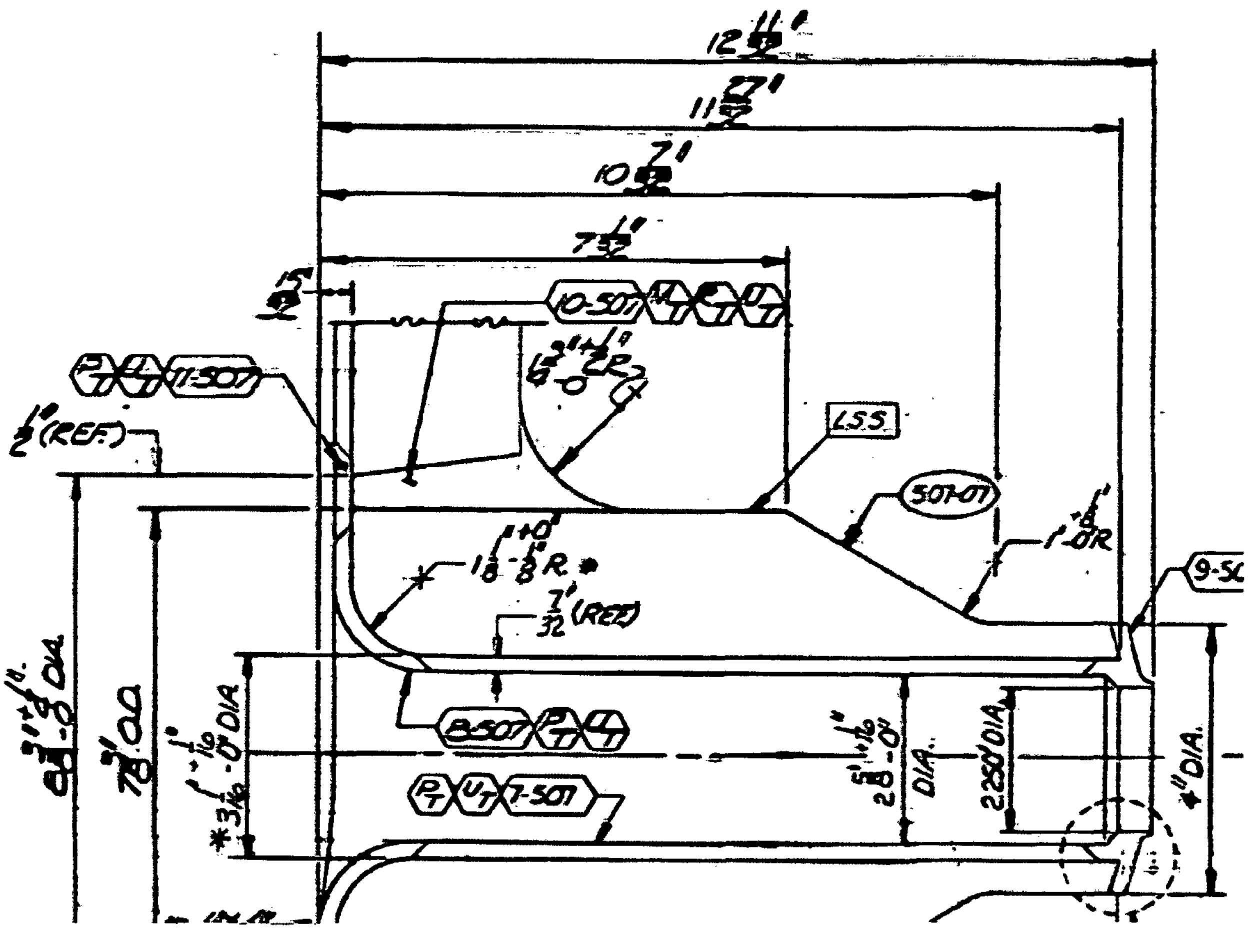

Figure 2-1: RCS Spray Nozzle Geometry for Millstone

Note: All measurements are in units of inches.

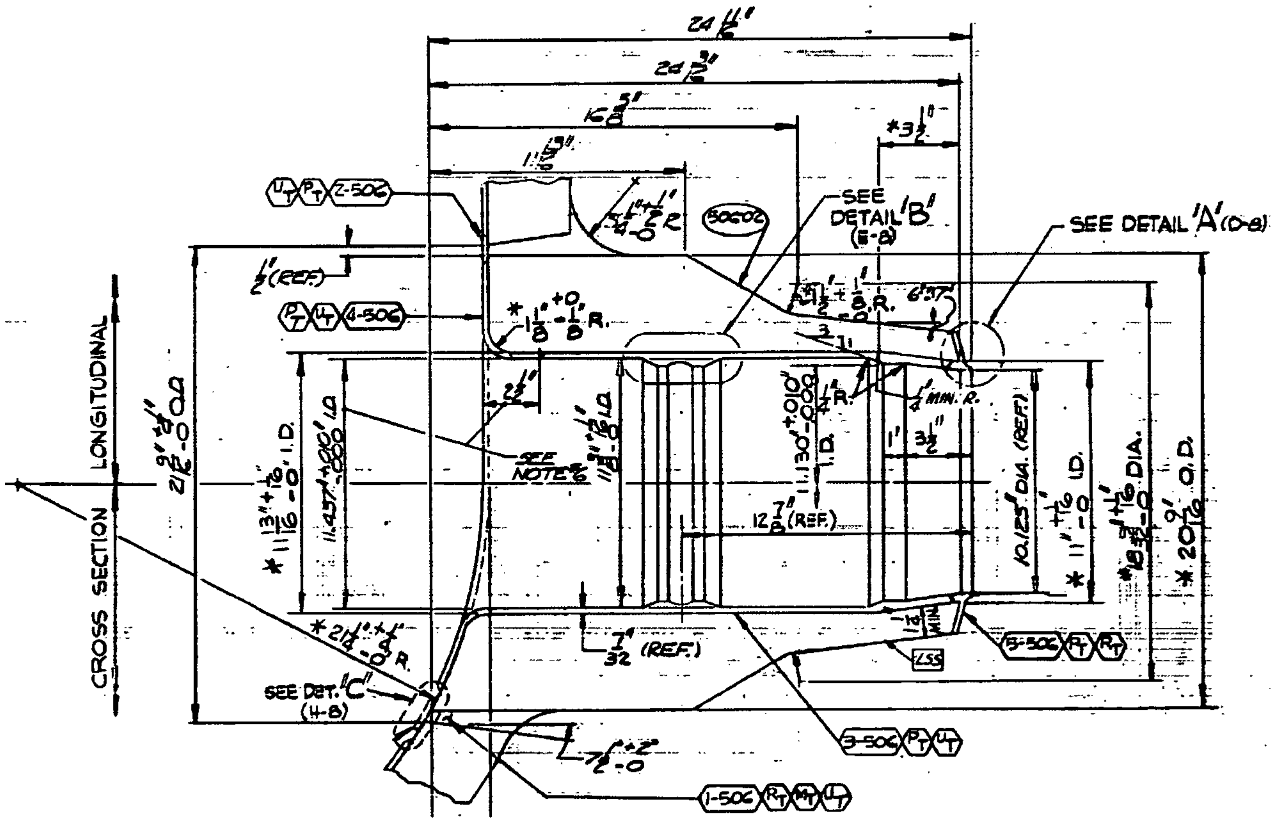

Figure 2-2: RCS Surge Nozzle Geometry for Millstone

Note: All measurements are in units of inches.

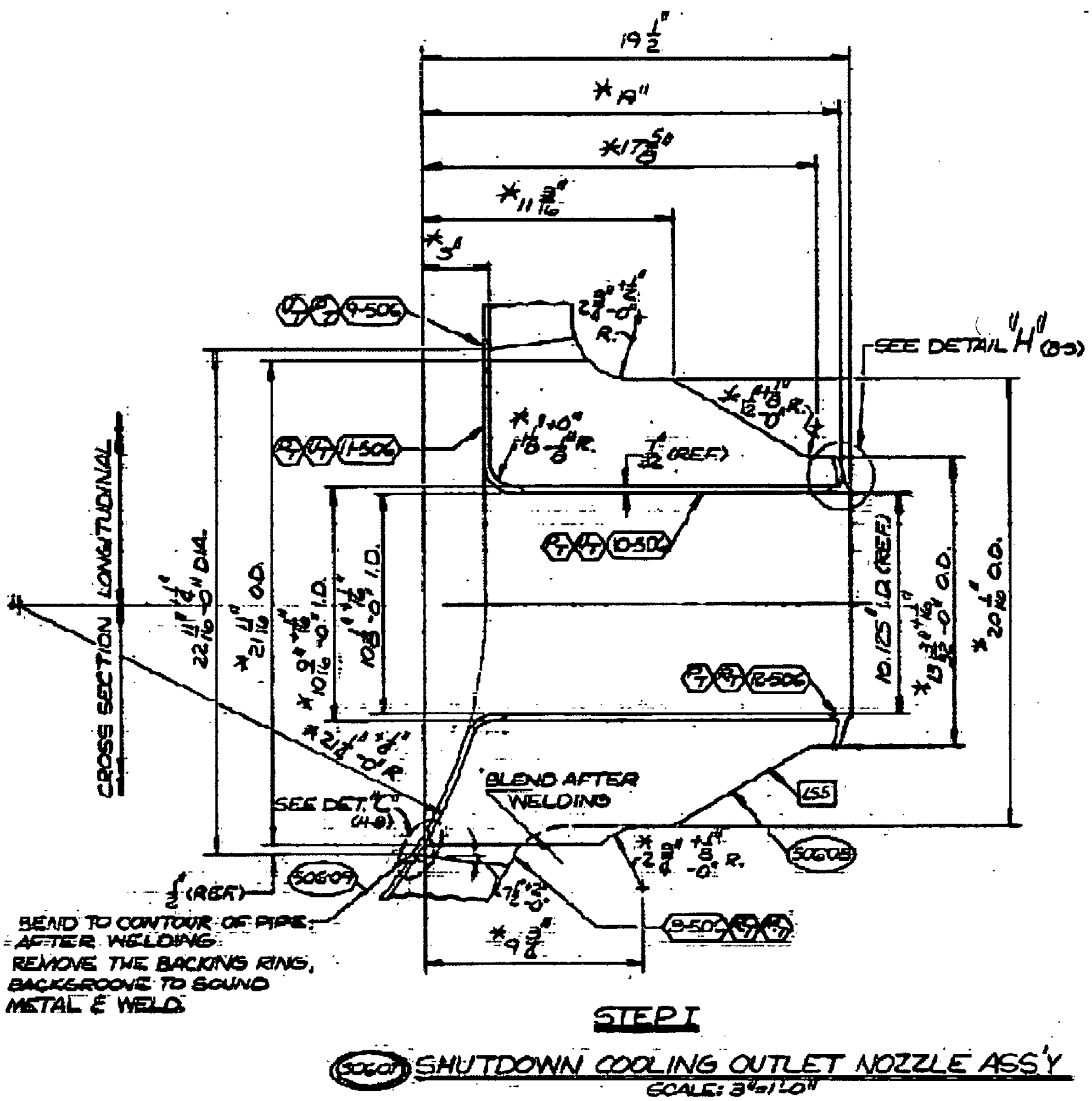

Figure 2-3: Shutdown Cooling Nozzle Geometry for Millstone

Note: All measurements are in units of inches.

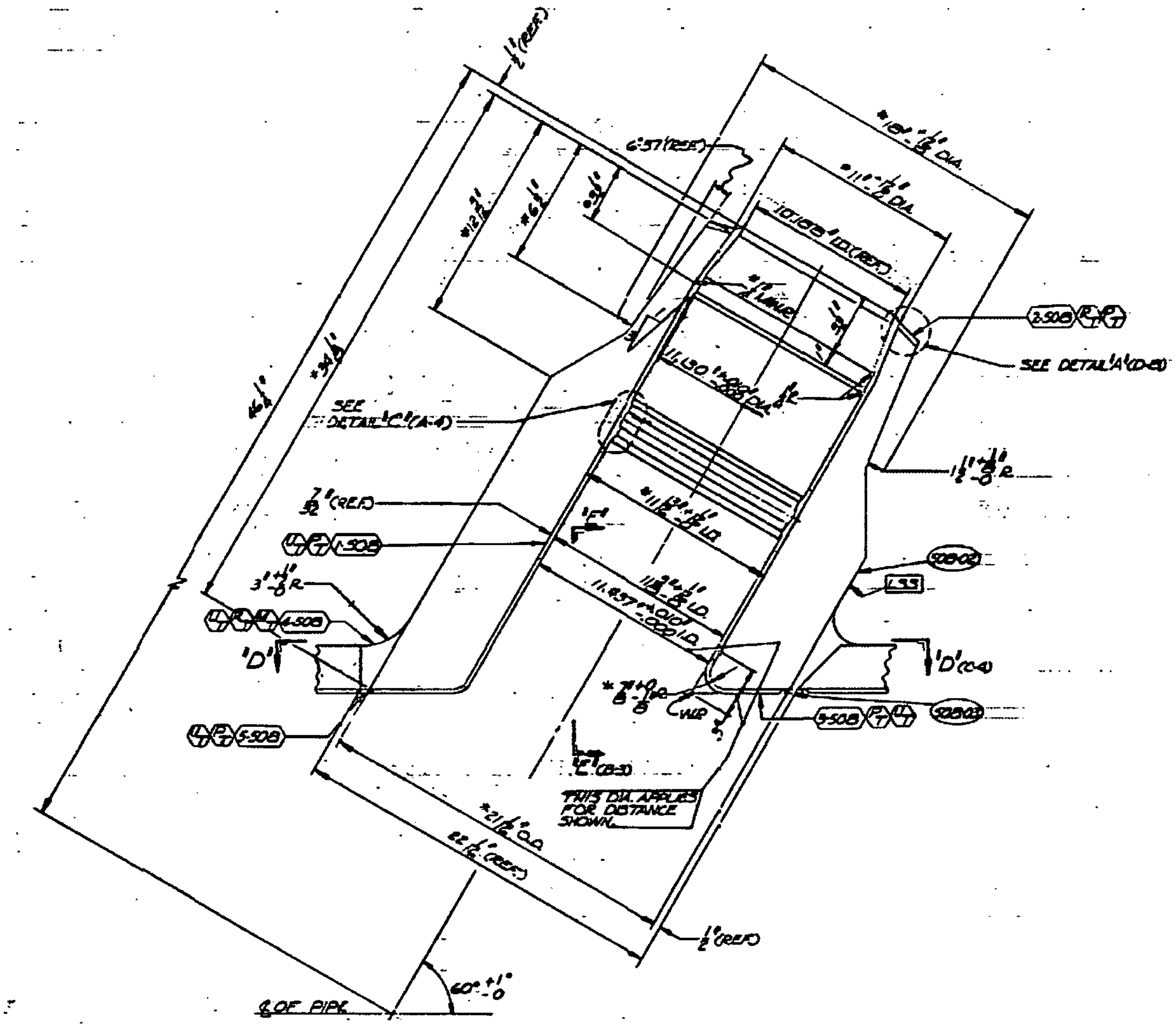

Figure 2-4: Safety Injection Nozzle Geometry for Millstone

Note: All measurements are in units of inches.

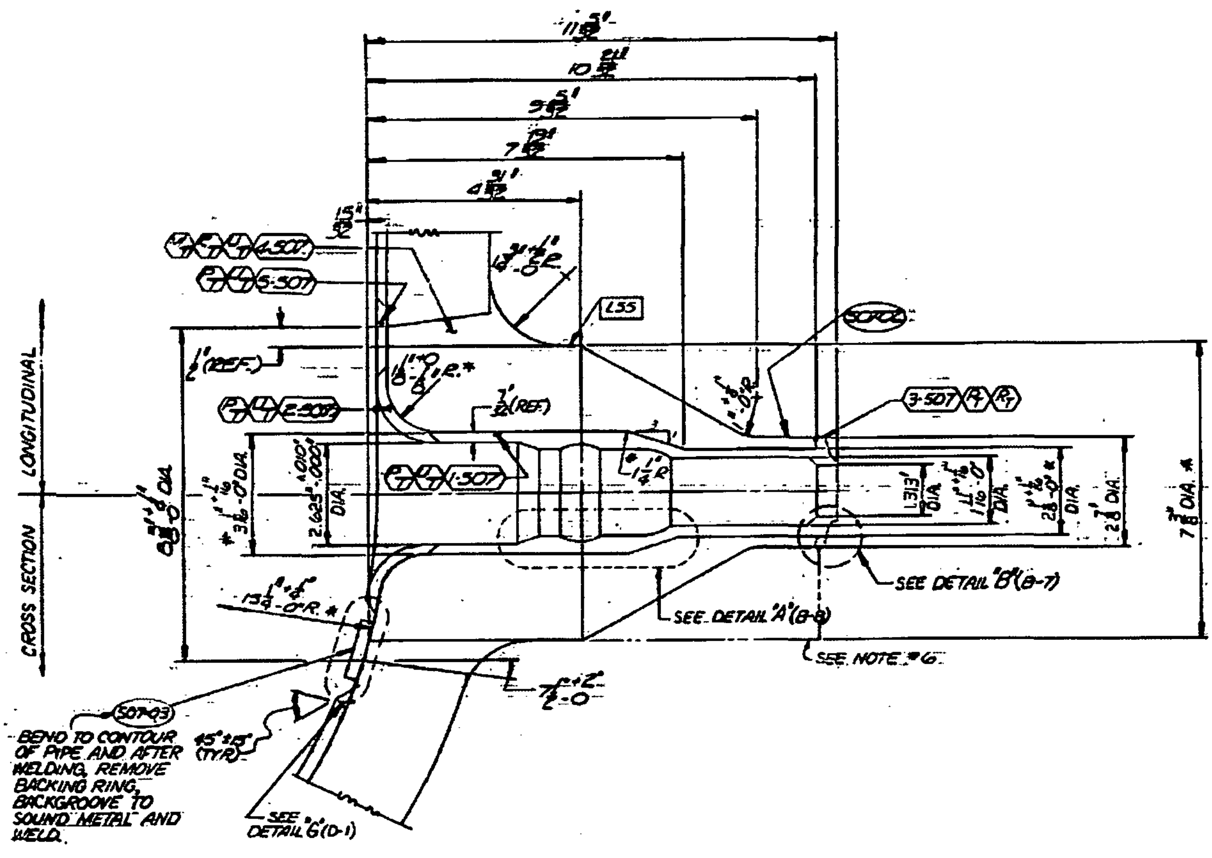

Figure 2-5: Charging Inlet Nozzle Geometry for Millstone

Note: All measurements are in units of inches.

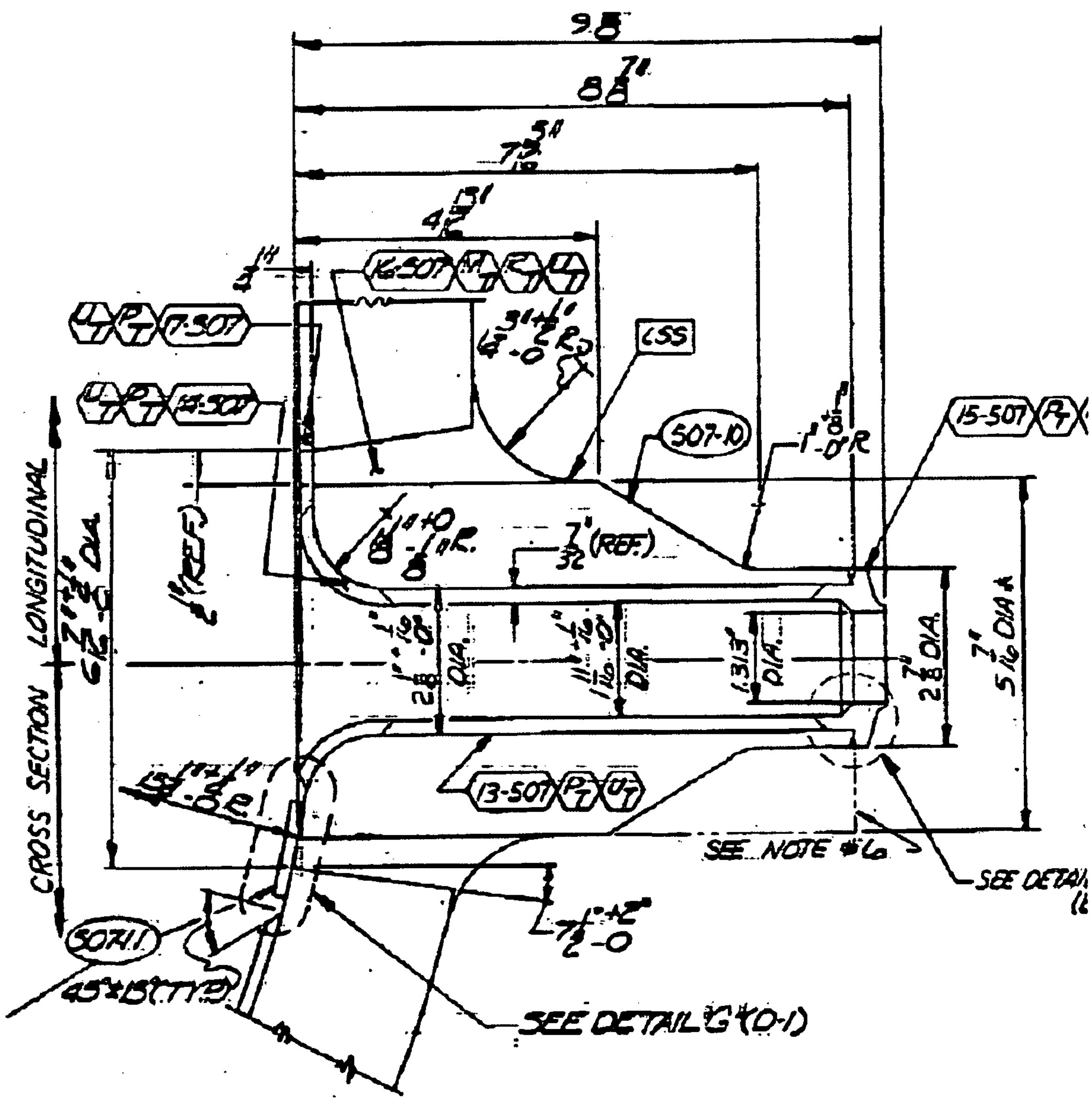

Figure 2-6: Typical Letdown/Drain Nozzle Geometry for Millstone

Note: All measurements are in units of inches.

3 WELD OVERLAY DESIGN METHODOLOGY

The design of the SWOL thickness/length is performed in accordance with ASME Code Cases N-740 and ASME Section XI IWB-3640 to demonstrate that the RCS nozzles weld overlays will provide a structural barrier that is reliable and durable. A flaw that is 100% through the original weld thickness for the entire circumference of the weld has been assumed in the weld overlay design.

The lifetime of the overlay is evaluated using the actual size of the flaw that is discovered by the UT examination. A series of flaw sizes was evaluated, and plots of design life versus flaw depth were created in advance. When the examinations are complete, these figures can be used to determine the remaining design life for each overlay. The figures are provided in the following sections.

The methodology discussed in this section is applied to the SWOL evaluation of the RCS nozzles. The weld overlay design sizing calculations are documented in [2].

3.1 CODE CASE N-740 WELD OVERLAY DESIGN

The weld overlays will extend around the full circumference of the dissimilar-metal butt-weld region and safe-end-to-piping similar-metal butt-weld region for the required length and thickness. In accordance with ASME Section XI IWB-3640 [6], the maximum allowable flaw depth for axial and circumferential flaws is 75% of the wall thickness for wrought base metals, cast SS, GTAW, and GMAW. The maximum allowable flaw size for SMAW and SAW is 60% of the wall thickness. This 60% limitation is included primarily for conservatism due to the low toughness value of the SS flux welds and is not directly applicable to the high toughness of the Alloy 82/182 weld, which is the weld of interest. This limitation has been removed from Section XI IWB-3640 in later Code editions. Therefore, the maximum allowable depth of 75% of the wall thickness is used in the weld overlay design. Using this maximum flaw depth as the upper limit, the actual allowable flaw size is then calculated in accordance with the flaw evaluation procedures of ASME Section XI Appendix C [6], and acceptance criteria based on plant-specific loadings at the nozzle. This is an iterative calculation and the overlay thickness is increased until the flaw evaluation criteria are satisfied for all applicable loadings.

For the Millstone Unit 2 RCS nozzle safe-end regions, the maximum allowable flaw depth, based on plant-specific nozzle loadings and geometry, is 75% of the wall thickness. Therefore, the required weld overlay repair thickness can be determined by the following equation:

$$\frac{t}{(t+h)} = 0.75$$

where,

t = wall thickness at the location of indication
h = thickness of weld overlay repair

According to ASME Code Case N-740, the axial length and end slope of the weld reinforcement are recommended to provide smooth load redistribution from the nozzle to the weld overlay and back to the pipe. The applicable stress limits of the ASME Section III Code of Construction are usually satisfied if the full length of the weld overlay was extended axially at least $0.75\sqrt{Rt}$ beyond each end of the postulated flaws, prior to deposition of the weld overlay. (R and t are the outer radius and nominal wall thickness of the pipe/nozzle, respectively.) The adequacy of this thickness, transition length, and weld envelope was verified by the subsequent ASME Code evaluation. Since crack growth can occur anywhere within the susceptible Alloy 82/182 weld material, the length of the weld overlay is assumed to be measured from the base metal/weld interface on the outside surface of the affected weld region. To avoid stress risers, the weld overlay material was blended into the pipe and nozzle side. The maximum end slope was specified as 30°, which provides a transition consistent with the recommendation of MRP-169 [28]. Additional evaluation of a 45° end slope SWOL design showed the end slope has insignificant affect on the structural integrity. The weld overlay repair is to be applied 360° around the component to provide a full structural barrier. The weld overlay repair designs for the RCS nozzles are shown schematically in Figures 3-1 through 3-6 [8].

3.2 WELD OVERLAY DESIGN FOR EXAMINATION

Examination requirements are a controlling factor in the weld overlay repair design. Based on the current industry examination techniques, the radius of curvature at any geometric transition must be at least 4 inches to ensure proper operation of the examination probes. The SS safe-end-to-pipe weld is located very close to the Alloy 82/182 weld; therefore, the SWOL was designed for both welds. This was done to provide for the inspectability of both welds. The length of the weld overlay must be sufficient to examine an area that is 0.5 inch beyond each weld toe and as deep as the outer 25% of wall thickness; otherwise, full examination coverage cannot be claimed in accordance with the examination procedure. PT examination of the nozzle and pipe surface shall occur prior to application of the weld overlay.

The length of the weld overlay was extended and blended into the low-alloy steel nozzle outer diameter taper to permit UT examination of the adjacent weld and minimize stress concentration on the nozzle outer diameter. Since the outside diameter of the nozzle is larger than that of the safe-end, the weld overlay thickness on the safe-end is increased to allow a smooth-transition surface for UT examination. The final weld overlay length and thickness, after considering the UT examination requirements, may exceed the length and thickness required for a full SWOL repair in accordance with ASME Code Case N-740.

The minimum weld overlay design thickness required to meet structural requirements is shown in the weld overlay design drawings (Figures 3-1 through 3-6) [8]. The cross-hatched areas represent weld deposits that are added to facilitate volumetric examination. Therefore, the weld overlay design values (thickness and length) provided in this report are considered minimum values. Additional weld passes or a larger weld overlay thickness within the specified tolerance on the drawings will not invalidate the design.

a,c,e

Figure 3-1: RCS Spray Nozzle Typical Weld Overlay Design

"a", "c", and "e" proprietary classifications identified in Section 1 (Introduction) of this document.

a,c,e

Figure 3-2: RCS Surge Nozzle Weld Overlay Design

"a", "c", and "e" proprietary classifications identified in Section 1 (Introduction) of this document.

a,c,e

Figure 3-3: Shutdown Cooling Nozzle Weld Overlay Design

"a", "c", and "e" proprietary classifications identified in Section 1 (Introduction) of this document.

a,c,e

Figure 3-4: Safety Injection Nozzle Typical Weld Overlay Design

"a", "c", and "e" proprietary classifications identified in Section 1 (Introduction) of this document.

a,c,e

Figure 3-5: Charging Inlet Nozzle Typical Weld Overlay Design

"a", "c", and "e" proprietary classifications identified in Section 1 (Introduction) of this document.

a,c,e

Figure 3-6: Letdown/Drain Nozzle Typical Weld Overlay Design

"a", "c", and "e" proprietary classifications identified in Section 1 (Introduction) of this document.

4 MATERIAL PROPERTIES AND FRACTURE ANALYSIS METHODS

4.1 MATERIALS

All nozzles documented herein are made of A105 Grade 2 material with the exception of the safety injection nozzle, which is made of A182-F1 material. The safe-ends for all nozzles are made SSs: SA-182 TP 316 for the spray, charging inlet, and letdown/drain nozzles; A351 Gr CF8M for the surge, shutdown cooling, and safety injection nozzles. The SS piping is made of A376 TP 316 for the spray, shutdown cooling, letdown/drain, and charging inlet nozzles; A351 Gr CF8M for the surge nozzle; A403 TP 316 for the safety injection nozzle. The safe-end-to-nozzle weld material is Alloy 82/182. The surge and shutdown cooling nozzles use 304 SS for the safe-end-to-piping weld material. The spray, safety injection, charging inlet, and letdown/drain nozzles use A376 TP 316 for safe-end-to-piping weld material. The materials for these components are specified in the DNC Alternative Request [3]. The physical properties used for these materials are based on available data provided in the ASME Code [9 and 10] and other publications and reports [11 through 15, 18, and 19]. All transient stress and structural evaluations used the original Code of Construction stress allowables to determine the impact of the weld overlay.

4.2 WELD OVERLAY MATERIAL PROPERTIES

The weld overlay material, Alloy 52/52M, is a nickel-based alloy that is highly resistant to stress corrosion cracking. The substantial chromium content also gives Alloy 52/52M outstanding resistance to oxidizing chemicals, which makes it an ideal weld material for weld overlay repairs. Alloy 52/52M has properties similar to SB-166 and SB-167 (N06690) ASME Code materials. The material properties used in the design calculations for the weld overlay were obtained from [9].

4.3 ALLOWABLE FLAW SIZE METHODOLOGY

The allowable flaw size is not directly calculated as part of the flaw evaluation process for SSs [6]. Instead, the failure mode and allowable flaw size are incorporated directly into the flaw evaluation technical basis; therefore, they are used in the tables of "Allowable End-of-Evaluation Period Flaw Depth to Thickness Ratio," in paragraph IWB-3640 of [6]. A more accurate determination of the allowable depth can be made using the methodology of ASME Section XI [6], Appendix C.

Rapid, nonductile failure is possible for ferritic materials at low temperatures, but is not applicable to SSs. In SS and nickel-based alloy materials, the higher ductility leads to two possible modes of failure, plastic collapse or unstable ductile tearing. The second mechanism can occur when the applied J integral exceeds the J_{IC} fracture toughness, and some stable tearing occurs prior to failure. If this mode of failure is dominant, the load-carrying capacity is less than that predicted by the plastic collapse mechanism.

The allowable flaw sizes of paragraph IWB-3640 of [6] for the high-toughness base materials were determined based on the assumption that plastic collapse would occur and would be the dominant mode of failure. All repair welding will be accomplished using the GTAW process. Therefore, the appropriate failure bending stress equation for P_b' from ASME Code Section XI [6], Appendix C, paragraph C-3320, was used for the evaluation.

4.4 CRACK GROWTH METHODOLOGY

The fatigue crack growth (FCG) analysis involves postulating a flaw at the region of concern. The objective of this analysis is to determine the service life required for the flaw to propagate through the original wall thickness to an allowable depth. The determination of this process was previously discussed. The flaw is subjected to cyclic loads due to the applicable design thermal transients. The design thermal transients considered in the analysis were distributed equally over the plant design life. Figures 6-10, 6-11, 7-10, 7-11, 8-10, 8-11, 9-10, 9-11, 10-10, 10-11, 11-10, and 11-11 provide examples of remaining service life based on design transient cycles spread over either 40 years of original design life, or 60 years of extended life. This representation was selected to enable the curves to be used to predict the remaining life, regardless of how the fatigue cycles are handled in license renewal. This is valid for the SS weld, which is not susceptible to PWSCC, and to those portions of the 82/182 weld where a compressive stress field has been established by the weld overlay process. This topic and the results will be discussed further in the applicable sections for each nozzle.

The input required for a fatigue crack growth analysis is essentially the same information necessary to calculate the range of stress intensity factor (ΔK_I), which depends on the crack size, crack shape, geometry of the structural component where a crack is postulated, and the applied cyclic stresses.

Once ΔK_I is calculated, the fatigue crack growth due to a particular stress cycle can be calculated based on the fatigue crack growth model published in [20 through 23]. The incremental growth is then added to the original crack size, and the analysis proceeds to the next cycle or transient. The procedure is repeated until all the transients predicted to occur in the remaining design life of operation have been analyzed.

Stress Intensity Factor

One of the key elements of the fatigue crack growth calculation is the determination of the driving force or crack tip stress intensity factor (K_I). In all cases, the crack tip stress intensity factor for the fatigue crack growth calculation utilized a representation of the actual stress profile rather than a linearization. The stress profile was represented by a cubic polynomial:

$$\sigma(x) = A_0 + A_1 \frac{x}{t} + A_2\left(\frac{x}{t}\right)^2 + A_3\left(\frac{x}{t}\right)^3$$

where,

- x = distance into the wall from inside surface
- t = wall thickness
- σ = stress perpendicular to the plane of the crack
- A_i = coefficients of the cubic polynomial fit

The stress intensity factor calculation for a semi-elliptical surface flaw in a cylinder was carried out using the expressions from [23 and 24]. The boundary correction factors for the loading conditions utilized for surface flaws are provided in these references. The boundary correction factors for various locations along the crack front (Φ) can be obtained using an interpolation method. Stress intensity factors for a semi-elliptical surface flaw in a cylinder can be expressed using the general form:

$$K_I(\Phi) = \left[\frac{\pi a}{Q}\right]^{0.5} \sum_{j=0}^{3} G_j\ \left(a/c,\ a/t,\ t/R_i,\ \Phi\right) A_j$$

where,

- a/c = ratio of crack depth (a) to half-crack length (c)
- a/t = ratio of crack depth (a) to thickness of a cylinder (t)
- t/R_i = ratio of thickness (t) to inside radius (R_i)
- Φ = elliptical angle along the crack front
- G_j = G_0, G_1, G_2, G_3 are boundary correction factors
- Q = shape factor $= \int_0^{\pi/2} \left(\cos^2\Phi + \frac{a^2}{c^2}\sin^2\Phi\right)^{1/2} d\Phi$

Fatigue Crack Growth Rate Reference Curves for Nickel-Based Alloys

Crack growth rate (CGR) reference curves for Alloy 52/52M, 82, and 182 materials have not been developed in the ASME Code Section XI; therefore, information available from the literature [20 through 23] was used. Based on the results reported in [20 through 23], a crack growth rate curve was developed for application in the air environment for INCONEL® Alloy 600 material, as shown below. The crack growth rate is a function of both stress ratio R (K_{min}/K_{max}) and the range of the applied stress intensity factor (ΔK_I).

$$\left(\frac{da}{dN}\right)_{air} = CS\left(\Delta K\right)^n (F_{weld})(F_{env})$$

$$C_{A600} = 4.835 \times 10^{-14} + (1.622 \times 10^{-16})T - (1.490 \times 10^{-18})T^2 + (4.355 \times 10^{-21})T^3$$

$$S = [1 - 0.82R]^{-2.2}$$

$$n = 4.1$$

where,

- T = operating temperature (°C)
- ΔK = stress intensity factor range, $MPa\sqrt{m}$
- R = stress ratio, K_{min}/K_{max}
- $\left(\frac{da}{dN}\right)_{air}$ = crack growth rate, m/cycle

F_{weld} = factor for weld

F_{env} = environmental factor

According to [20], the fatigue CGR of high-nickel alloys in the light water reactor/pressurized water reactor (LWR/PWR) environment can be correlated to that in the air environment using:

$$CGR_{env} = CGR_{air} + A(CGR_{air})^m$$

By performing a least-square curve fitting of the FCG data on Alloy 600 in high-purity water with ~300 ppb DO (dissolved oxygen), it was concluded in [23] that the best values of A and m for CGR of Alloy 600 in the LWR/PWR environment are:

$A = 4.4 \times 10^{-7}$
$m = 0.33$

This model was proposed by Chopra et al. in [23]. It was judged conservative for this application since it includes data for water environments with oxygen contents up to 10 ppb, as shown in Figure 4-1. The typical PWR water chemistry has an oxygen level that is too low to measure, since it is scavenged by the presence of a hydrogen overpressure.

The fatigue CGR in a water environment for an Alloy 182 weld is a factor of 10 higher than that for Alloy 600 material. This CGR is assumed to be also applicable to the Alloy 82 weld material in the dissimilar-metal weld region.

Fatigue Crack Growth Rate Reference Curves for Stainless Steel

The reference crack growth law shown in Figure 4-2 was used for the SS material, and appears in Section XI, Appendix C for air environments. Its basis is provided in [26]. For water environments, an environmental factor of two was used, based on the crack growth tests in PWR environments reported in [27].

$$\frac{da}{dN} = CS\left(\Delta K\right)^n F_{env}$$

where,

$\frac{da}{dN}$ = CGR, inches per cycle

C = material coefficient $C = 10^{\left[-10.009+8.12E-04T-1.13E-06T^2+1.02E-09T^3\right]}$

$S = 1.0$ for $R \le 0$

$S = 1 + 1.8R$ for $0 < R \le 0.79$;

$S = -43.35 + 57.97R$, for $0.79 < R < 1.0$

n = material property slope = 3.30

ΔK = stress intensity factor range, $ksi\sqrt{in}$

F_{env} = environmental factor (= 1.0 for air environment, and = 2.0 for PWR environment)

Fatigue Crack Growth Curves for Alloy 52/52M SWOL Material

Since the SWOL will be applied before any inspections can be completed, the possibility of discovering an almost through-wall flaw during the final Performance Demonstration Initiative (PDI) qualified UT inspection of the completed weld overlay needs to be addressed. Based on the residual stress distributions at the Alloy 82/182 weld that the residual stresses under normal operating condition do not remain compressive through 100% of the original wall thickness, PWSCC may become an active crack growth mechanism at the Alloy 82/182 weld if an existing flaw propagates under fatigue crack growth mechanism to the portion of the original wall where the residual stresses become tensile. Using the current PWSCC crack growth rate, the service life required for such a flaw to propagate under PWSCC to reach 100% through the original wall would be quite short. Even though this is an unlikely scenario, additional FCG analyses were performed at the Alloy 82/182 weld location for a postulated, 100% through the original wall flaw. If crack growth continues beyond the original Alloy 82/182 weld metal, it will grow into the Alloy 52/52M SWOL. No primary water stress corrosion crack growth needs to be considered for the postulated 100% through-wall flaw because the weld overlay material, Alloy 52/52M, is considered highly resistant to PWSCC. In accordance with the test data for Alloy 52 weld material, the fatigue crack growth rate in the water environment is similar to that for Alloy 600 in a water environment, and therefore, it is assumed to be applicable to the Alloy 52/52M weld overlay material. To model this effect, the scaling factor for temperature effects is:

$$C_{A690} = 5.423 \text{ X } 10^{-14} + (1.83 \text{ x } 10^{-16})T - (1.725 \text{ x } 10^{-18})T^2 + (5.49 \text{ x } 10^{-21})T^3$$

The scaling factor for load ratio effects, S(R) parameter, for Alloy 52/52M is the same as for the case of Alloy 82/182 material.

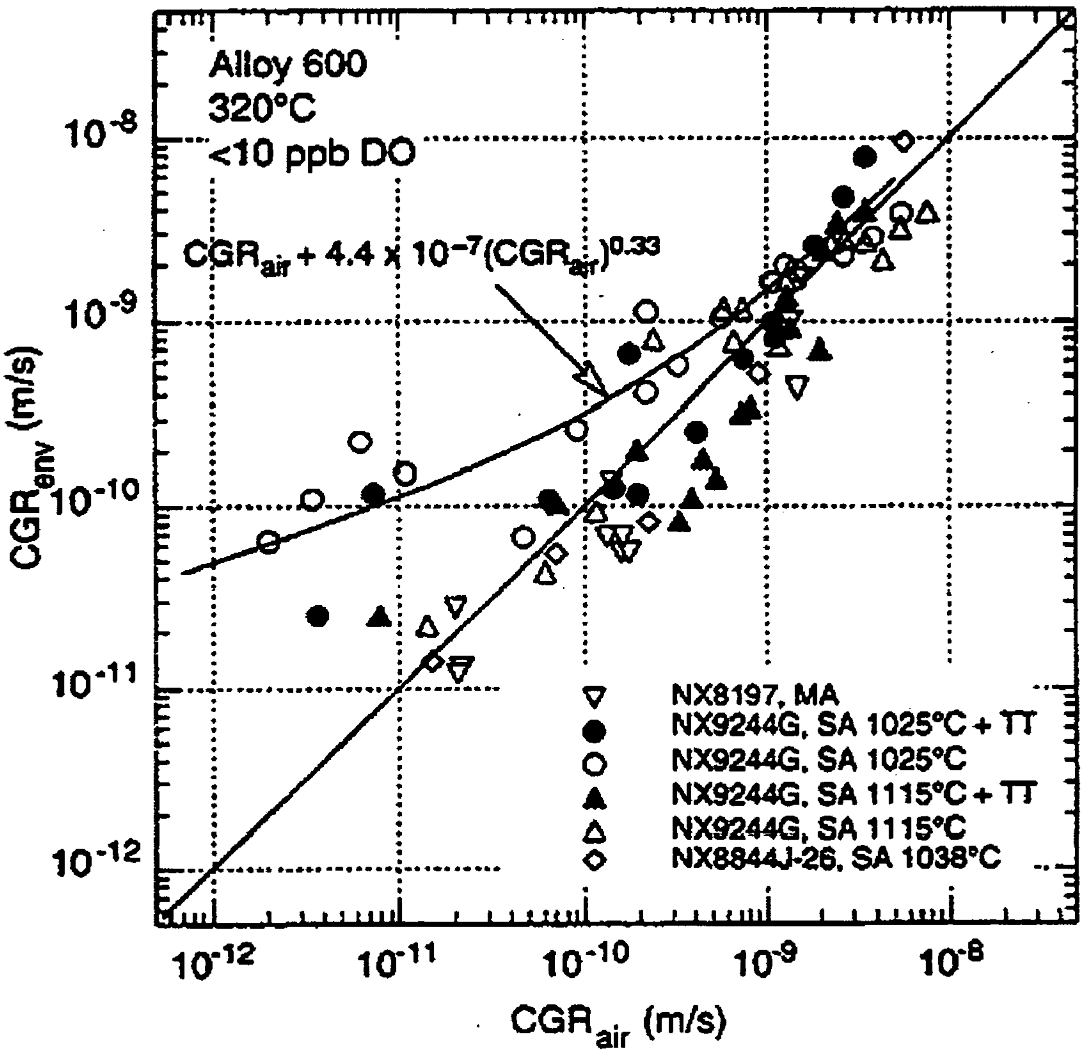

Figure 4-1: Fatigue Crack Growth Model Development for Alloy 600 and Associated Welds in PWR Water Environment

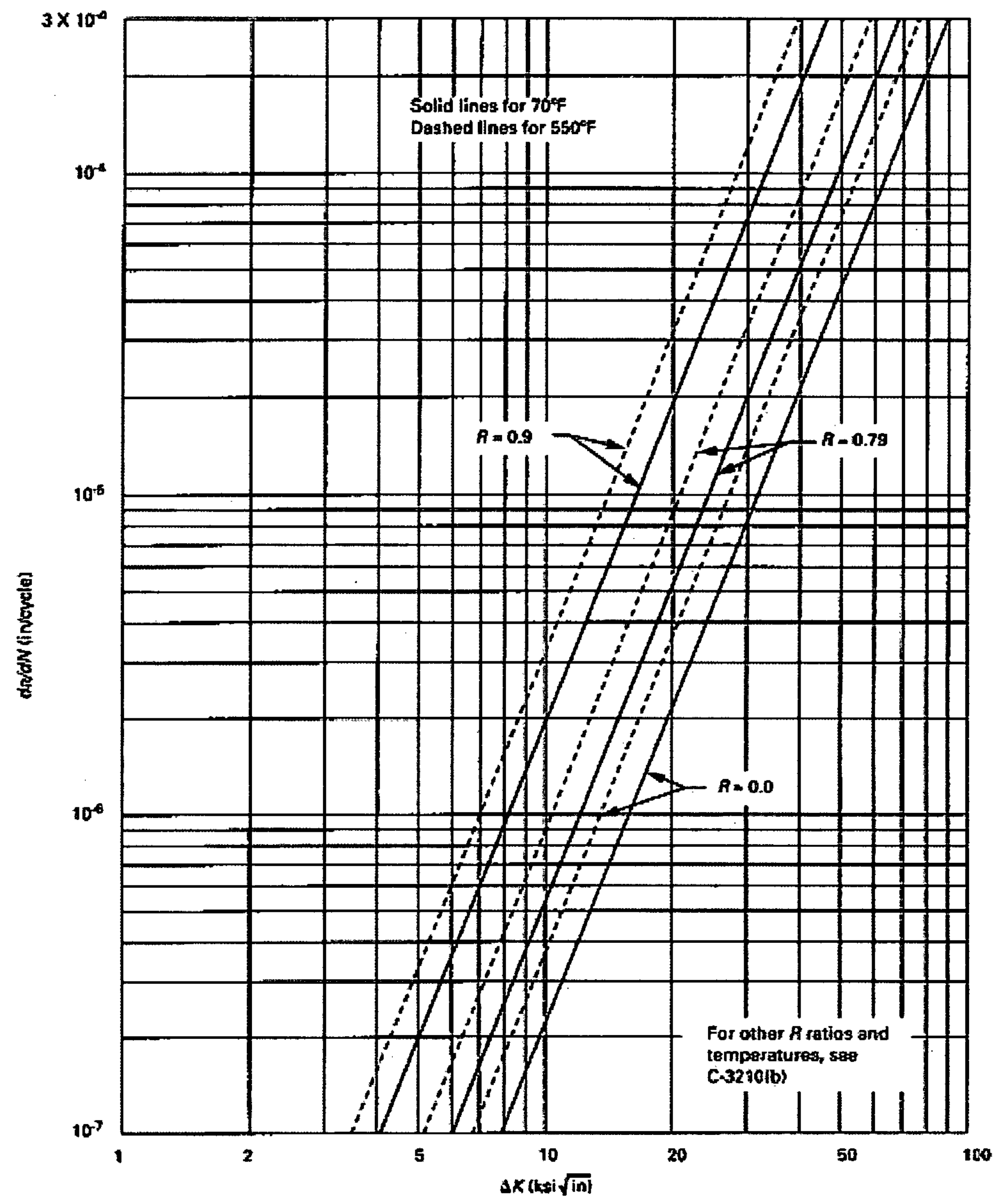

FIG. C-8410-1 REFERENCE FATIGUE CRACK GROWTH CURVES FOR AUSTENITIC STAINLESS STEELS IN AIR ENVIRONMENTS

Figure 4-2: Reference Crack Growth Rate Curves for SS in Air Environments

5 WELD OVERLAY FINITE ELEMENT ANALYSIS

5.1 OBJECTIVE OF THE ANALYSIS

The objective of this analysis is to determine the stresses produced by the RCS nozzle SWOLs, which will be used to demonstrate the acceptability of the mitigation/repair in accordance with Section XI requirements. Finite element analyses were performed to simulate the WOL process and obtain the resulting residual weld stresses. These finite element analyses were performed using the ANSYS®[1] FEA program [16]. Then, crack growth evaluations were performed using the finite element stress results to demonstrate that the SWOL is sized adequately and within allowable crack growth limits.

5.2 FINITE ELEMENT MODELS

The finite element models use PLANE42/PLANE25 for the structural elements and PLANE55 for the thermal elements, each with four nodes. The models are axisymmetric and use isotropic, temperature-dependent material properties, as summarized in Section 4. Higher-order elements are not used in this application because the plasticity treatment in the elements derives no significant benefit from the higher-order shape functions. The typical analysis sequence involves a heat transfer analysis that determines applicable heat flow and temperatures (steady-state or transient). The same model is used for the structural analysis, with the element type changed from PLANE55 to PLANE42 and the appropriate structural boundary conditions applied. The nodal temperatures were read into the structural model to capture the steady-state or transient thermal stresses. The results for each particular nozzle type are documented in Sections 6 through 11.

5.3 WELD OVERLAY SIMULATION

Analyses were performed to determine residual weld stresses in the RCS nozzle dissimilar-metal and SS butt-weld regions to support the ASME Section XI evaluations. [

]a,c,e

---

[1] ANSYS, ANSYS Workbench, CFX, AUTODYN, FLUENT and any and all ANSYS, Inc. product and service names are registered trademarks or trademarks of ANSYS, Inc. or its subsidiaries located in the United States or other countries.

"a", "c", and "e" proprietary classifications identified in Section 1 (Introduction) of this document.

The structural analysis was performed using a similar process. Each area was applied using the "birth option," and the temperatures were read into the model. A time-history elastic-plastic analysis was performed for the entire WOL application. Once the WOL simulation was completed, the normal operating loads (temperature and pressure) were applied to the model. Several cycles of ambient temperature and normal operating loads were applied until the stresses achieved "shakedown" (i.e., subsequent cycles did not produce significant stress changes).

All six nozzle types were conservatively analyzed assuming a 50% through-wall inside diameter (ID) weld repair of the Alloy 82/182 weld to simulate the initial stress state due to either weld repair or as-fabricated weld stresses. The ID repair was applied as four radial layers, each repair layer consisting of one weld area. [

]a,c,e The approaches used for the nozzles have been shown to produce a conservative simulation of residual weld stresses as compared to test data [17].

"a", "c", and "e" proprietary classifications identified in Section 1 (Introduction) of this document.

6 WELD OVERLAY DESIGN QUALIFICATION ANALYSIS: RCS SPRAY NOZZLE

6.1 INTRODUCTION

This section provides the WOL design qualification analysis to demonstrate the adequacy of the SWOL design for the RCS spray nozzle. The effectiveness of a WOL with Alloy 52/52M weld material is demonstrated using crack growth analysis, per IWB-3640 [6], to ensure that the WOL does not deteriorate during service. Using the residual weld stresses developed by the finite element model of the WOL process, future crack growth was evaluated at the RCS spray nozzle safe-end weld locations using the operational design transients affecting the WOL region. The advantage of the Alloy 52/52M material is its high resistance to PWSCC, which minimizes the possibility for future PWSCC crack growth. Since the purpose of the SWOL is to mitigate/repair a potentially cracked dissimilar-metal butt-weld, performing crack growth analyses using the ASME Code Section XI methodology is the accepted method to address the fatigue qualification of the WOL region for the RCS spray nozzle.

The effect of the SWOL on the existing fatigue qualification of the RCS spray nozzle outside the WOL region is addressed in accordance with ANSI B31.7 requirements considering the effect of the applicable thermal transient stresses, structural discontinuities, and bimetallic effects resulting from the SWOL.

6.2 LOADS

The loads used for the design of the spray nozzle weld overlay are listed in Table 6-1. These loads are considered in [2] and specified in [31]. The load combinations considered in the design are listed in Table 6-2. The transients considered in the spray nozzle fatigue and FCG evaluations are shown in Table 6-3. The pipe end loads used for fatigue and FCG evaluations are listed in Table 6-4. Theses loads are considered in [7] and specified in [31]. The nozzle loads and transients used for the design and FCG analysis are bounding for the actual nozzle loads and the plant-specific transients [7, 31, and 30].

Table 6-1: Enveloping RCS Spray Nozzle Loads Used for Weld Overlay Design [31]

Load Type	Axial Force F_a (kips)	Bending Moment M_b (in-kips)
DW	-0.129	2.492
OBE	0.752	17.518
SSE	1.504	35.037

Notes:
DW = Deadweight Loads
OBE = Operating Basis Earthquake Loads
SSE = Safe Shutdown Earthquake Loads

Table 6-2: Load Combinations

Condition	Load Combination	Service Level
Design	DP + DW + DS	Design
Normal/Upset	TR(1) + DW + NT(1)	Level A/B
Emergency	DP + DW + MS + NT(1)	Level C
Test	TP + DW	Test

Notes:
1. Not applicable to WOL design sizing
DW = Deadweight
DP = Design Pressure
TP = Test Pressure
TR = Level A/B Transient Loadings (Thermal and Pressure)
NT = Thermal Expansion
DS = Design Seismic
MS = Maximum Seismic

Table 6-3: Applicable Thermal Transients for RCS Spray Nozzles

Number	Transient	Cycles	Level
1	Plant Heatup, 100°F / hr	500	A
2	Plant Cooldown, 100°F / hr	500	A
3	Plant Loading, 5% / min	15,000	A
4	Plant Unloading 5% / min	15,000	A
5	Step Load Increase 10%	2,000	A
6	Step Load Decrease 10%	2,000	A
7	Reactor Trip	400	B
8	Loss of Turbine Generator Load/Loss of Reactor Coolant Flow	80(3)	B
9	Loss of Secondary Pressure	5	C
10	Hydrostatic Test	10	TEST
11	Leak Test	200	TEST
12(1)	Seismic (Positive)	200	B
13(1)	Seismic (Negative)	200	B
14	Zero Load	710(2)	-

Notes:
1. The design specification [30] states 200 cycles of OBE and 200 cycles of design basis earthquake. For this analysis, 400 cycles of design basis earthquake will be used.
2. The total cycles for this transient consist of 500 heatup and cooldown cycles, 10 hydrostatic test cycles, and 200 leak test cycles.
3. The total cycles for this transient consist of 40 Loss of Turbine Generator Load cycles and 40 Loss of Reactor Coolant Flow cycles.

Table 6-4: Enveloping RCS Spray Nozzle Loads for Fatigue and FCG Evaluations

Condition	Force (kips)			Moment (in-kips)		
	F_x	F_y	F_z	M_x	M_y	M_z
Deadweight	0.001	-0.064	-0.006	-0.036	0.024	-0.072
Thermal	-0.072	-0.016	0.286	8.136	-2.604	4.632
Design Seismic	0.200	0.320	0.121	17.247	16.562	3.072
Maximum Seismic	0.400	0.640	0.242	34.494	33.124	6.144

Notes:

Axial force = F_y
Shear force = $\sqrt{(F_x^2 + F_z^2)}$
Torsion moment = M_y
Bending moment = $\sqrt{(M_x^2 + M_z^2)}$

6.3 WELD OVERLAY DESIGN SIZING

The minimum WOL thickness was determined based on a through-wall flaw in the original pipe. The methodology used to determine the WOL design thickness and length is discussed in Section 3. Using that methodology, radii from the design geometry, shown in Table 6-5, are used to design the minimum SWOL parameters. As-designed inside and outside radii at the thickest portion of the Alloy 82/182 and SS welds are presented here. The thickest portion results from considering the smallest inner radius ($R_{i\text{-}min}$) and the largest outer radius ($R_{o\text{-}max}$). By using the maximum wall thickness of the design geometry, conservative SWOL design thickness and length are achieved. The WOL length was based conservatively on the recommended length, per Code Case N-740:

$$L_{WOL} = 0.75\sqrt{Rt}$$

where,

$R = R_{o\text{-}max}$ = outside radius
$t = R_{o\text{-}max} - R_{i\text{-}min}$ = wall thickness at the location of indication

The WOL length (L_{WOL}) will extend from the weld/base metal interface on either side of the Alloy 82/182 and SS welds, as shown in Figure 6-1. The WOL thickness (t_{WOL}) was determined using the following equation:

$$t_{WOL} = t/0.75 - t$$

The minimum WOL design dimensions are shown in Table 6-6.

In accordance with ASME Section XI IWB-3640, the criterion from Section XI, Appendix C is used to evaluate the maximum post-WOL stresses resulting from the actual applied loadings. To determine the applied post-WOL stresses, the minimum post-WOL thicknesses are considered, which produces a conservative method to determine stresses for comparison to the allowable stress criterion. The thinnest portion of the Alloy 82/182 and SS welds results from considering the largest inner radius ($R_{i\text{-}max}$) and the smallest outer radius post-WOL ($R_{o\text{-}min\text{-}WOL}$). These parameters and the resulting geometric section properties are presented in Table 6-7.

The applied bending stresses were calculated by:

$$\sigma_b = \frac{M_b}{Z}$$

M_b is per Table 6-1 and Z is per Table 6-7.

$$Z = \frac{\pi(R_{o-\min-wol}^{\;4} - R_{i-\max}^{\;4})}{4(R_{o-\min-wol})}$$

$R_{i\text{-max}}$ and $R_{o\text{-min-wol}}$ are per Table 6-7.

The applied membrane stresses were calculated by:

$$\sigma_m = \sigma_p + \frac{F_a}{A_x}$$

where,

$$\sigma_p = \frac{\pi R_{i-\max}^{\;2}}{\pi\left(R_{o-\min-wol}^{\;2} - R_{i-\max}^{\;2}\right)} P$$

F_a is per Table 6-1.

A_x is per Table 6-7.

$A_x = \pi \; (R_{o\text{-min-wol}}^2 - R_{i\text{-max}}^2)$

$R_{i\text{-max}}$ and $R_{o\text{-min-wol}}$ are per Table 6-7.

P = 2,235 psig [2]

The allowable stress intensity S_m (at 650°F) used in the sizing of the Alloy 52/52M (N06690) overlay is 23.3 ksi [9]. This allowable is based on the annealed condition of SB-166/SB-167. The normal operating pressure, 2,235 psig, was used for the calculation.

The resulting stresses, determined by using the previous equations, as well as the loads and load combinations from Tables 6-1 and 6-2, respectively, are listed and compared to the Code allowable in Table 6-8.

Table 6-5: RCS Spray Nozzle Geometry for WOL Design Calculations [2]

Alloy 82/182 Weld			Stainless Steel Weld		
Inside Radius $R_{i\text{-min}}$ (in)	**Outside Radius $R_{o\text{-max}}$ (in)**	**Wall Thickness t_{design} (in)**	**Inside Radius $R_{i\text{-min}}$ (in)**	**Outside Radius $R_{o\text{-max}}$ (in)**	**Wall Thickness t_{design} (in)**
1.313	2.000	0.688	1.312	1.750	0.438

Table 6-6: RCS Spray Nozzle Minimum Weld Overlay Repair Design Dimensions [2]

Alloy 82/182 Weld		Stainless Steel Weld	
t_{WOL} (in)	L_{WOL} (in)	t_{WOL} (in)	L_{WOL} (in)
0.33	0.88	0.15	0.66

Table 6-7: RCS Spray Nozzle Geometry for Stress Check in Post-Weld-Overlay Condition [2]

Alloy 82/182 Weld				Stainless Steel Weld			
Inside Radius $R_{i\text{-}max}$ (in)	Outside Radius $R_{o\text{-}min\text{-}WOL}$ (in)	Cross-Sectional Area A_x (in^2)	Section Modulus Z (in^3)	Inside Radius $R_{i\text{-}max}$ (in)	Outside Radius $R_{o\text{-}min\text{-}WOL}$ (in)	Cross-Sectional Area A_x (in^2)	Section Modulus Z (in^3)
1.313	2.105	8.509	6.218	1.346	1.900	5.649	4.030

Table 6-8: RCS Spray Nozzle Post-SWOL Stress Comparison [2]

	Normal/Upset		Emergency/Faulted	
Location	Applied Stress σ_b (ksi)	Allowable Stress P_b (ksi)	Applied Stress σ_b (ksi)	Allowable Stress P_b (ksi)
Alloy Weld	3.218	9.950	6.035	21.211
SS Weld	4.965	9.040	9.312	20.205

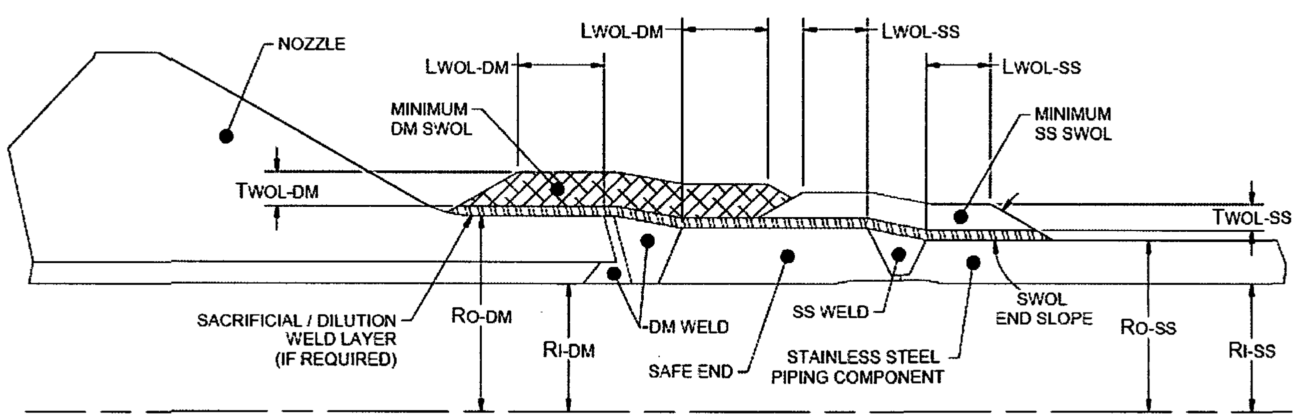

Figure 6-1: Weld Overlay Design Parameters for the RCS Spray Nozzle
(Not drawn to scale.)

6.4 WELD OVERLAY RESIDUAL WELD STRESS RESULTS

As described in Section 5.3, the finite element model was developed to capture the parts of the structure in the vicinity of the RCS spray nozzle safe-end with the SWOL. This includes a portion of the spray nozzle attached to the nozzle safe-end and a length of SS pipe attached to the safe-end. An ID weld repair was considered in the finite element model. The finite element model and boundary conditions are shown in Figures 6-2 and 6-3. The nozzle is fixed in the axial direction to simulate the rest of the nozzle. The end of the SS piping is coupled in the axial direction to simulate the remaining portion of the SS piping not included in the model. The model assumes that a 50% through-wall weld repair was performed from the inside surface of the spray nozzle to safe-end Alloy 82/182 butt-weld.

The final residual weld stresses, including normal operating pressure and temperature conditions, are shown in Figures 6-4 and 6-5 for selected stress cuts in the Alloy 82/182 and SS welds. The locations of the stress cuts are provided in Figure 6-2. The axial and hoop stress contours in the RCS spray nozzle after the weld overlay application are provided in Figures 6-6 and 6-7.

Figure 6-4 shows the axial and hoop residual stresses for the Alloy 82/182 weld, at normal operating conditions after the SWOL. The stresses are compressive up to about 80% of the original pipe wall thickness. This stress distribution is favorable due to the generally compressive stress field because it minimizes the potential for crack growth in the dissimilar-metal weld region. Similarly, Figure 6-5 shows the axial and hoop stresses for the stainless weld. They remain compressive for more than 80% of the original pipe wall at normal operating conditions. Therefore, the potential for FCG is minimized.

Acceptable post-WOL residual stresses (i.e., stresses that satisfy the requirements for mitigating PWSCC) are those that are sufficiently compressive over the entire length and circumference of the inside surface of the Alloy 82/182 weld (at operating temperature, but prior to applying operating pressure and loads). Acceptable post-WOL residual stresses also have a total stress, after application of operating pressure and loads, that remains less than 10 ksi tensile [28]. This target level has been selected as a conservatively safe value, below which PWSCC initiation, or growth of small initiated cracks, is unlikely. Additionally, the residual plus operating stresses must remain compressive through some portion of the weld thickness away from the inside surface. The residual stresses in the Alloy 82/182 weld of the RCS spray nozzle, resulting from the WOL, are well below this stress level through 80% of the original weld thickness.

Figures 6-8 and 6-9 show the axial and hoop stresses on the inside surface (in the vicinity of the alloy weld and buttering) remain compressive after SWOL. The maximum resultant bending moment for normal operating condition is 18.302 in-kips. The resulting maximum bending stresses in the Alloy 82/182 weld and SS weld are 2.109 ksi and 3.035 ksi, respectively [32]. The pipe bending stresses are low, and are considered to have negligible effect on the residual weld stress results.

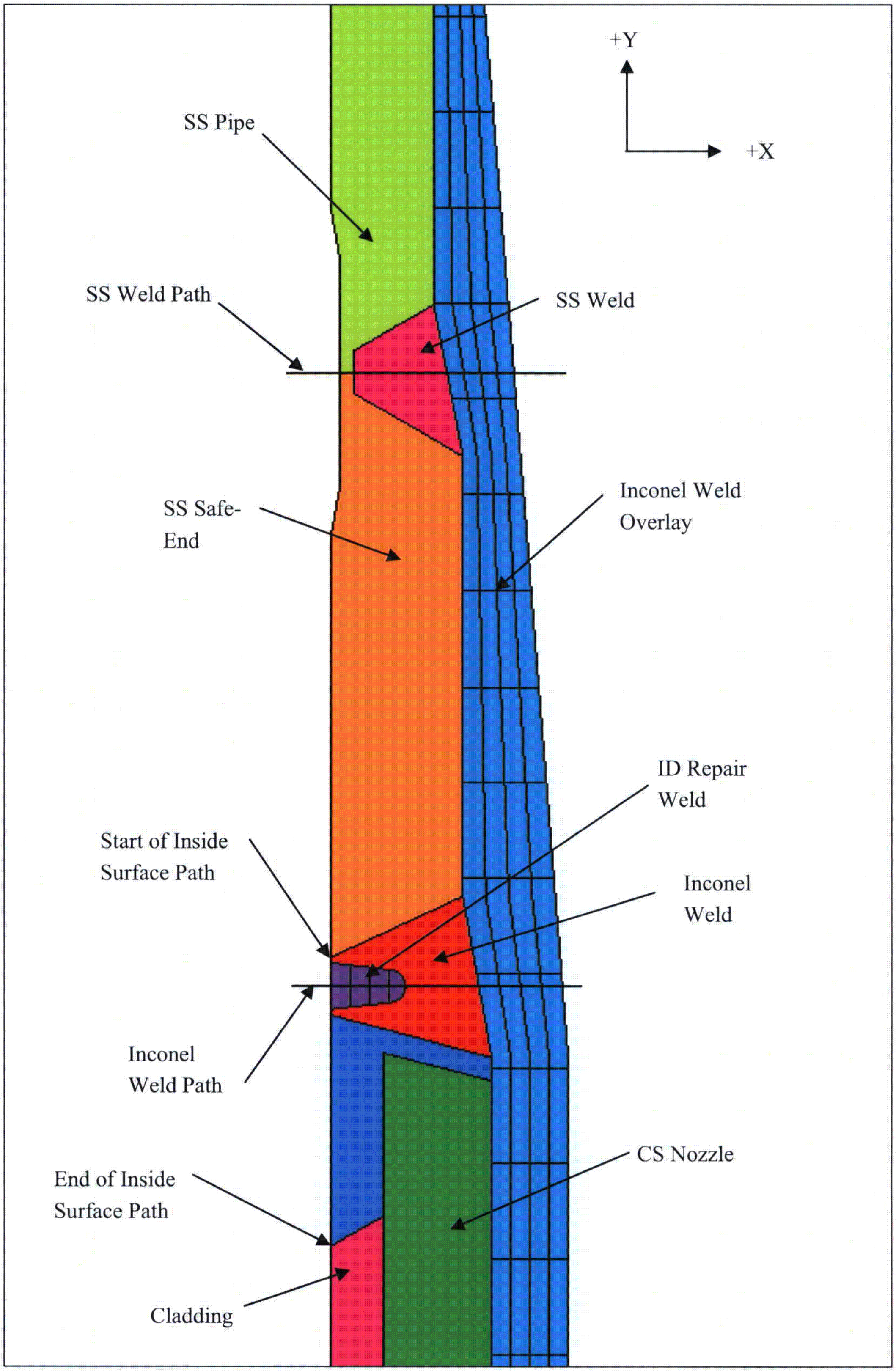

Figure 6-2: ANSYS Model of RCS Spray Nozzle

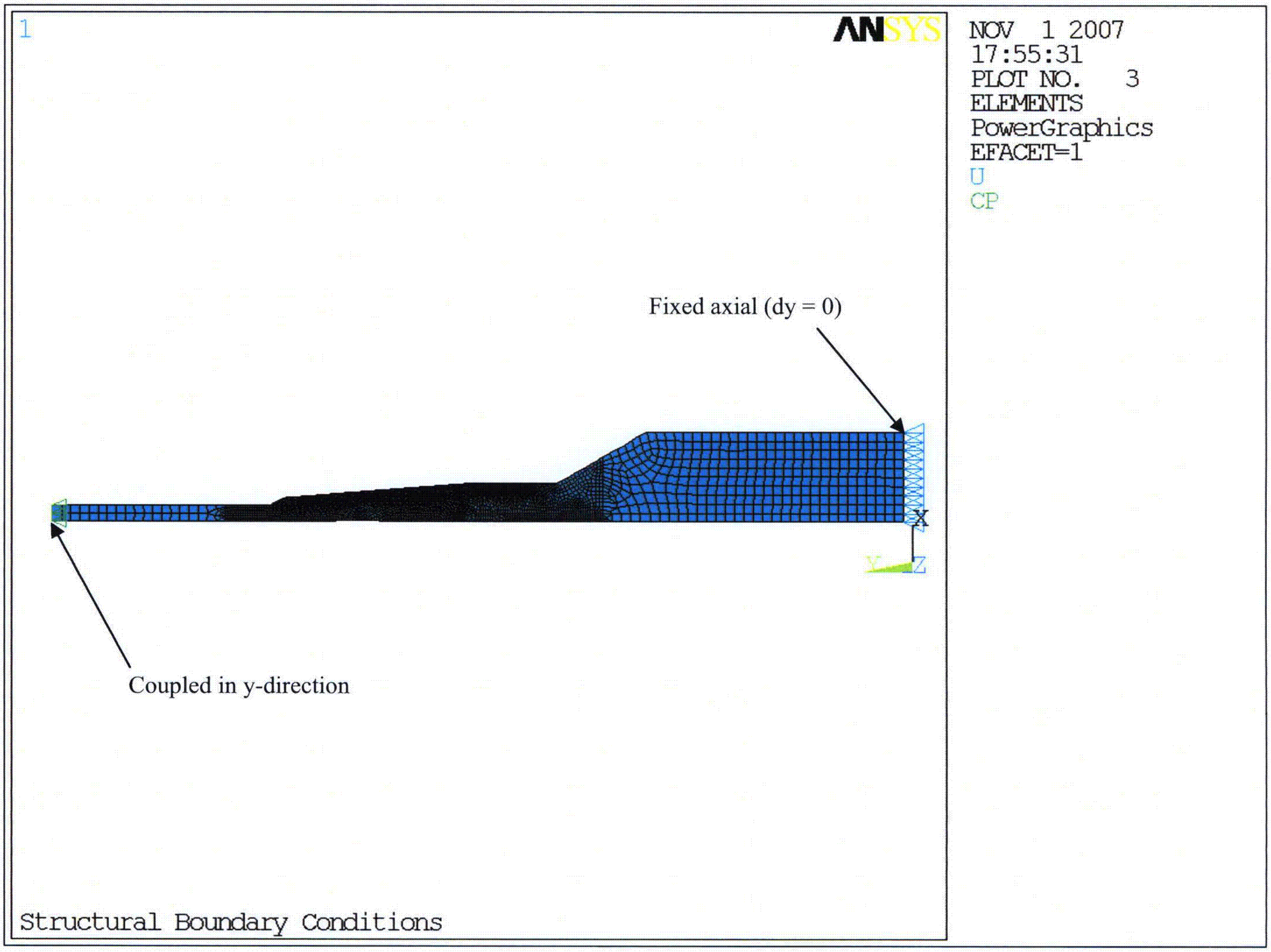

Figure 6-3: Finite Element Model and Structural Boundary Conditions

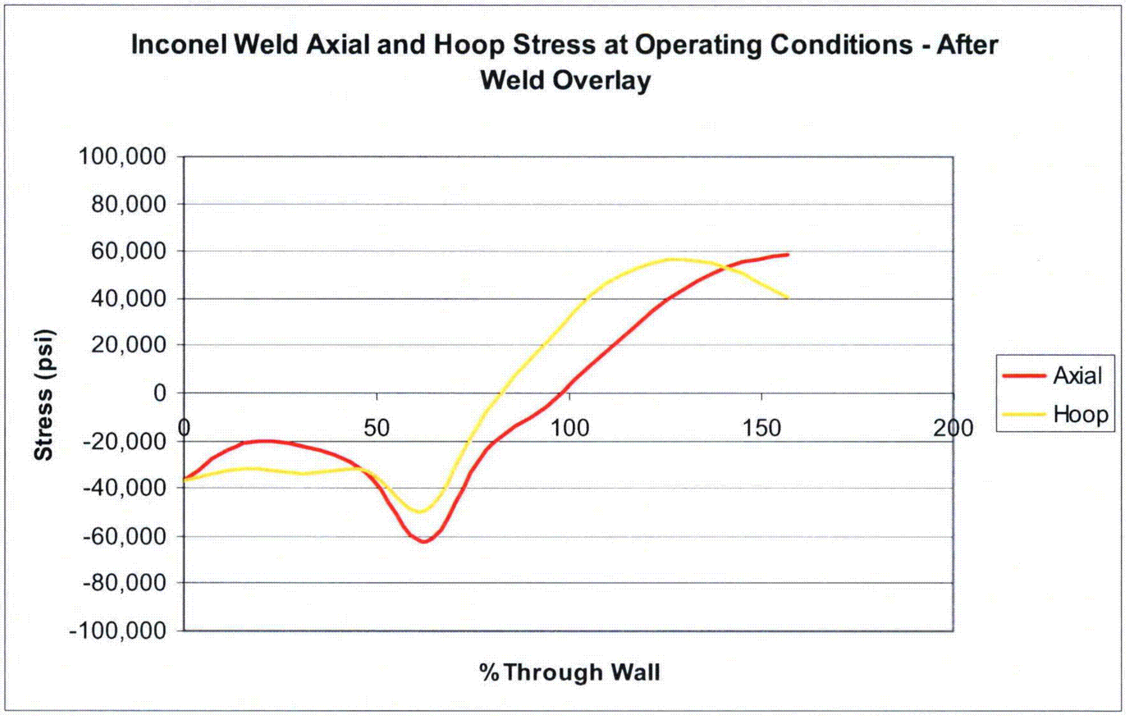

Figure 6-4: Axial and Hoop Residual Stresses in the Alloy 82/182 Weld at Operating Conditions*

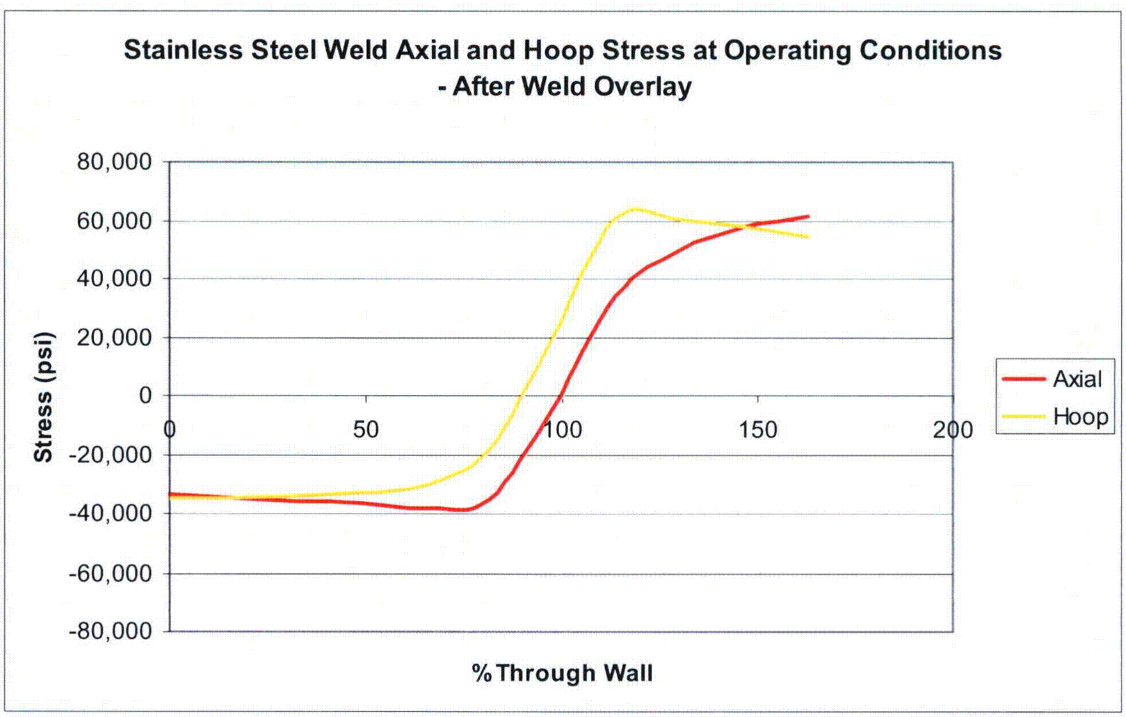

Figure 6-5: Axial and Hoop Residual Stresses in the SS Weld at Operating Conditions*

*Note: The percent through-wall indicated on the horizontal axis is expressed in terms of the original pipe wall thickness. The weld overlay region is the region beyond 100% wall thickness.

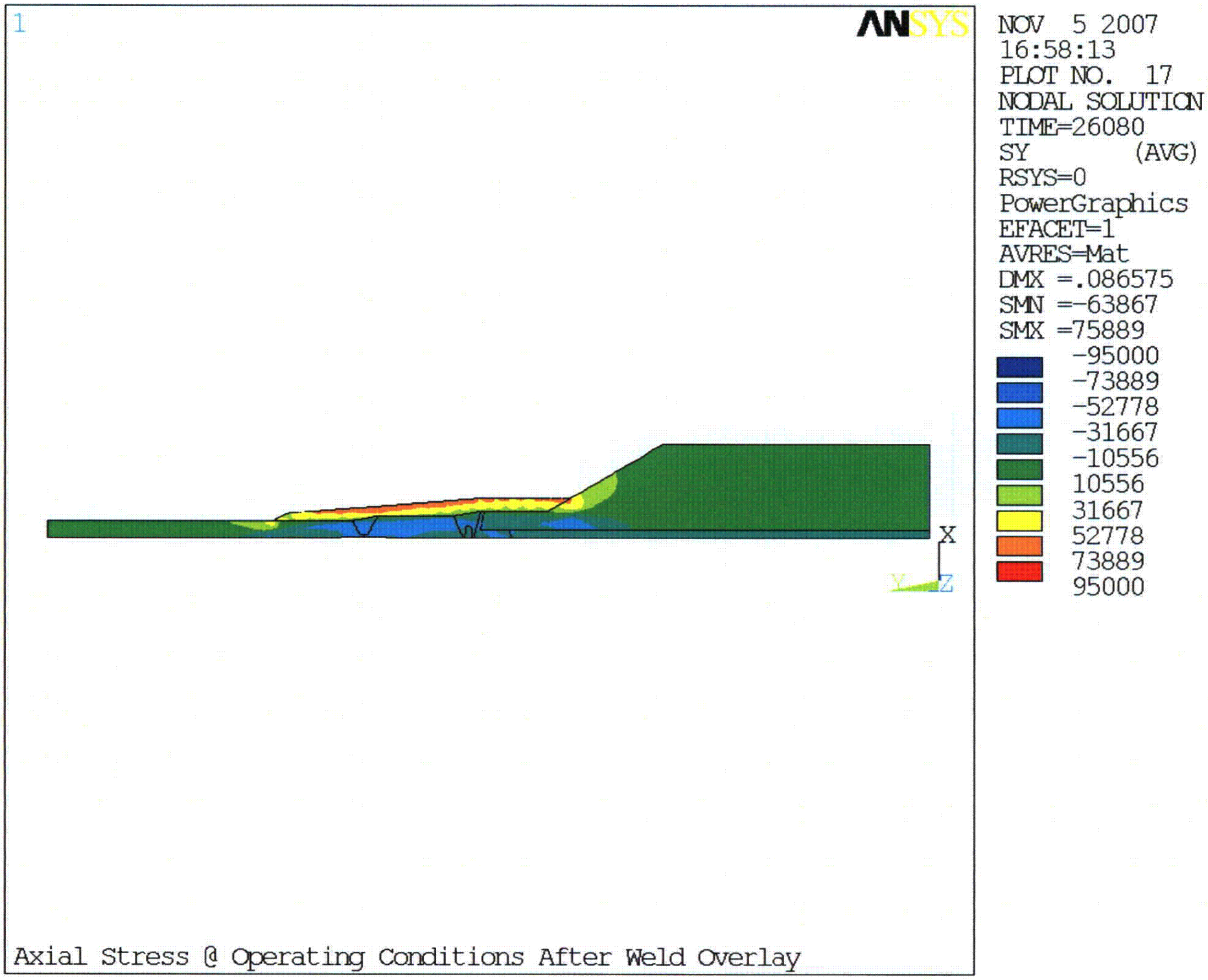

Figure 6-6: Axial Stress (psi) Contour Plot at Operating Condition after Weld Overlay

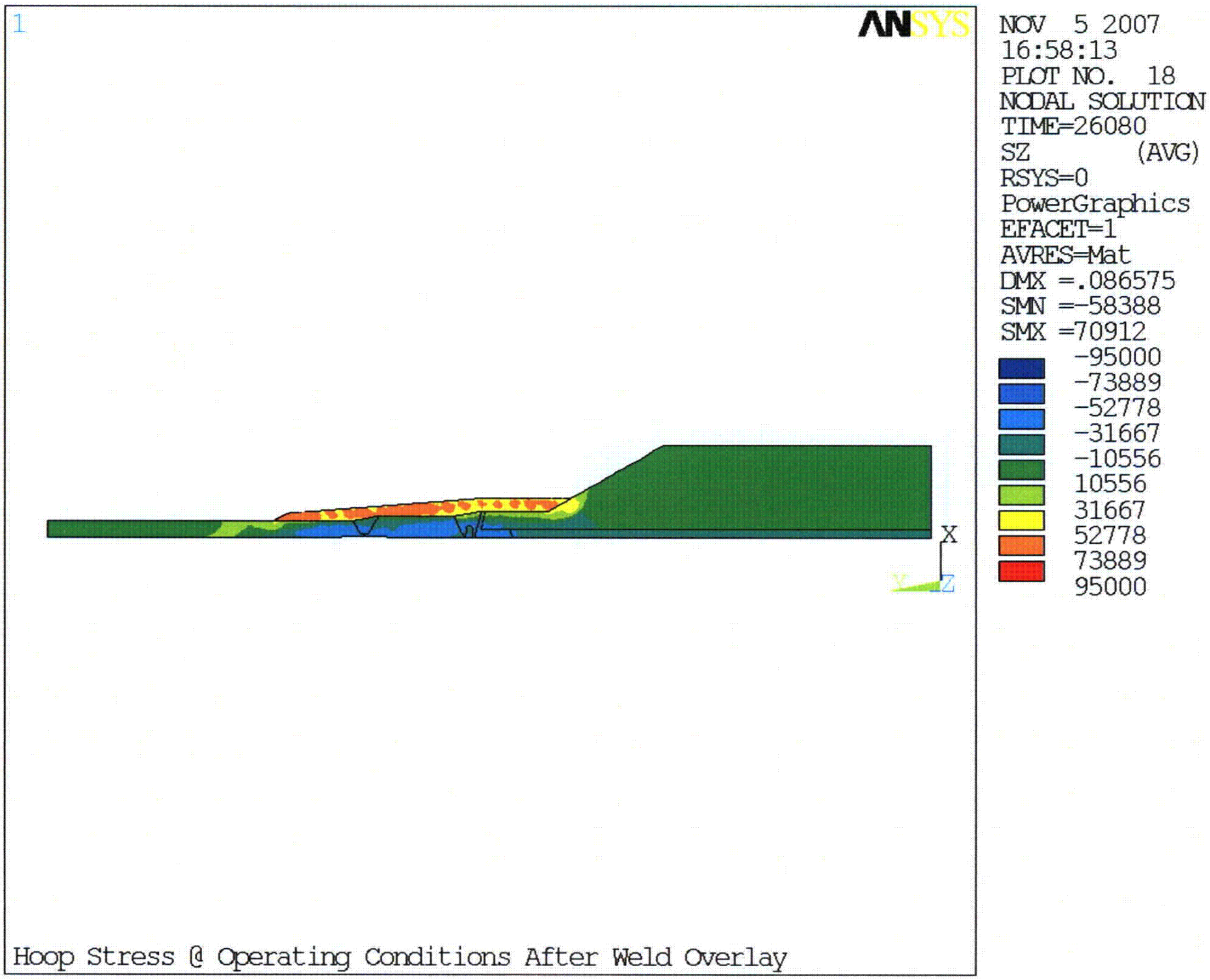

Figure 6-7: Hoop Stress (psi) Contour Plot at Operating Condition after Weld Overlay

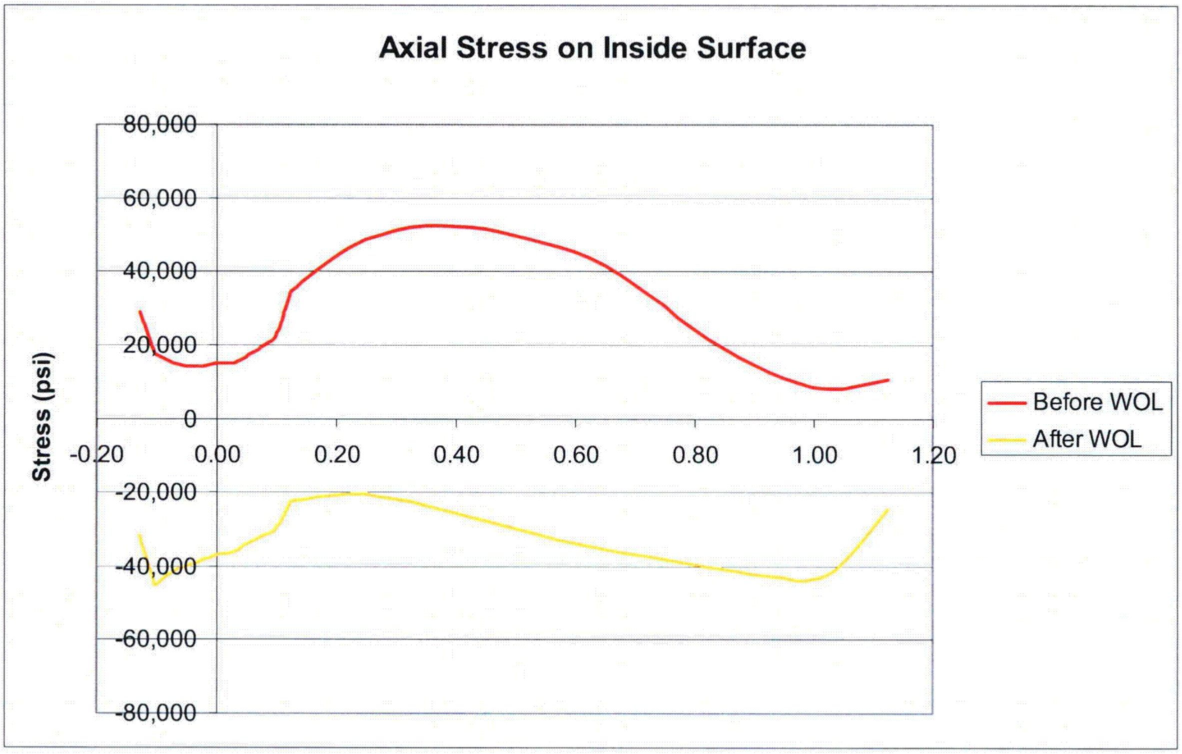

Figure 6-8: Axial Residual Stress along the Inside Surface at Operating Condition*

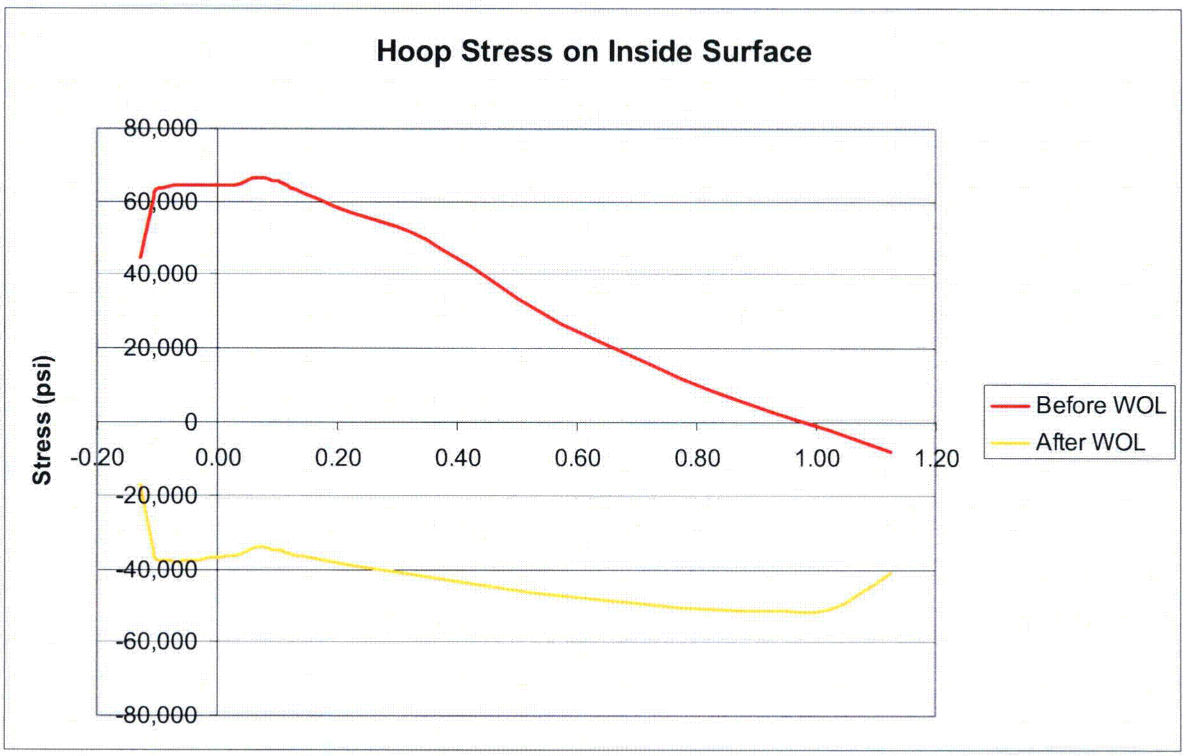

Figure 6-9: Hoop Residual Stress along the Inside Surface at Operating Condition*

*Note: X-axis is the location (inch) along the inside surface path. Zero is the center of alloy weld. See Figure 6-2.

6.5 FATIGUE CRACK GROWTH RESULTS AND ESTIMATE OF WELD OVERLAY DESIGN LIFE: RCS SPRAY NOZZLE REGION

The methodology used to determine fatigue crack growth is described in Section 4.4. Fatigue crack growth analyses were performed for the RCS spray nozzle using the through-wall stress distribution including residual stresses generated from the weld overlay mitigation/repair process and the thermal transient stresses.

The weld overlay service life is a function of the flaw depth found in the region being overlaid, and the projected growth of that flaw. The allowable maximum flaw depth is 75% of the piping wall thickness (including the weld overlay thickness), per Section XI, IWB-3640 [6].

A range of possible flaw sizes, from 0 to 100% of the original wall thickness, was postulated in the fatigue crack growth evaluations. The results of these evaluations for the flaw depths less than the original design wall thickness are plotted in Figures 6-10 and 6-11, in the form of expected time for these flaws to reach the interface between the original wall and the newly laid weld overlay material. Figure 6-10 shows results for the Alloy 82/182 weld, and Figure 6-11 shows results for the SS weld. For the maximum possible flaw depths of 100% of the original design wall thickness propagating into the Alloy 52/52M weld overlay material, results are shown in Figure 6-12. This figure shows the estimated flaw depth with time for the design cycles spread over either the original design life or the extended life of the plant.

Figures 6-10 and 6-11 summarize the expected service life (based on transients cycles spread evenly for either 40 years or 60 years of plant life) for a given initial flaw depth to reach 100% of the original wall thickness at the Alloy 82/182 weld and the SS weld locations, respectively. Based on the results shown in Figures 6-10 and 6-11, it can be concluded that if no flaws are detected during the post-SWOL inspection, a conservatively assumed flaw, 75% through the original wall would not grow to 100% of the original wall thickness for 40 years FCG due to transient cycles. This is based on the assumption that the current 40-year design transient cycles are spread evenly over 40 years of plant life. If flaws are detected during the post-SWOL inspection, the as-found flaw size can be used to determine the design life of the SWOL using the crack growth results shown in Figures 6-10 and 6-11.

For the case of an initial flaw depth of 100% of the original wall thickness, i.e., a through-wall flaw, Table 6-9 shows that the total flaw growth into the newly laid Alloy 52/52M welds material in one 10-year inspection interval is 0.0022 inch, based on design cycles spread over a 60-year extended life. The final flaw depth after the 10-year period with the fatigue crack growth considered is still within 75% of the total post-WOL wall thickness, as required by SWOL criteria.

Two examination scenarios exist: a pre-overlay examination and a post-overlay examination. If an examination found no flaws, the overlay service life would be governed by the largest flaw that might have been missed by the examination. For an examination performed prior to the weld overlay installation, a conservative approach would be to assume that the flaw depth is 10% of the original wall thickness. Alternatively, this would be 75% of the original wall for an examination performed after the weld overlay installation. This is because the area required to be inspected after the overlay is only the outer 25% of the original pipe thickness plus the overlay thickness itself. The PDI qualification blocks do not contain any flaws in the inner 75% of the pipe wall. Therefore, it would be conservative to assume

such a flaw for the qualification. As shown in Figure 6-10, an initial flaw as deep as 75% would result in a remaining service life of 100% of the original design cycles. If the design cycles are assumed to be spread over 40 years of plant operation, the remaining life of the SWOL would be 40 years. This is well beyond the required 10-year in-service inspection (ISI) interval. If, after the next ISI, no flaws are detected in the outer 25% of the original welds, the SWOL life is 40 years from the time of the latest inspection.

In the unlikely event that the post-overlay inspection detected a flaw as large as the full depth of the original design wall thickness, the expected service life of the weld overlay would be at least one 10-year inspection interval period. For the RCS spray nozzle, flaw growth rate into the weld overlay material is small or negligible, which indicates the expected service life of the repair would be 40 years if the transient cycles are spread over original design life of 40 years.

For example, if an axial flaw that is 99% through the original Alloy 82/182 wall thickness is detected as a result of the post-WOL inspection, and assuming conservatively that the current 40-year design transient cycles are spread evenly for only 40 years, the expected service life from Figure 6-10 for this flaw to reach 100% of the original wall thickness is approximately 40 years. This indicates the fatigue crack growth is insignificant. If it is assumed that the design transient cycles are spread evenly for 60 years, the remaining service life would be 60 years. This can also be determined by applying a factor of 1.5 to the service life based on the 40-year design cycles. For a similar-size circumferential flaw, the expected service life is about 40 years, based on current 40-year design transient cycles assumed to be spread evenly over 40 years. Since the typical in-service inspection interval is 10 years for this initial flaw depth of 99%, it can be concluded that the sizing of the SWOL is adequate up to the next inspection period based on the current 40-year design transient cycles spread evenly over the next 40 years.

Another case of a 100% original design wall thickness through-wall flaw in the alloy weld was hypothesized assuming a total post-WOL wall of 0.993 inch. This included an extra allowance of 0.1 inch for the FCG in the Alloy 690 material. This 100% original wall axial flaw was evaluated for the FCG results shown in Table 6-9 and Figure 6-12. Results demonstrate that the total growth in 10 years is insignificant (0.0022 inch). The final flaw depth after 10 years FCG is within 75% of the total post-WOL wall thickness, as required by SWOL criteria. Therefore, the 0.1 inch SWOL thickness increase provided in the SWOL design is adequate to address the issue of PWSCC for an almost through-wall flaw.

The actual time required to use the remaining design cycles depends on plant operating practice.

Table 6-9: RCS Spray Nozzle Alloy 52/52M FCG Data – Axial Flaw [35]

Nozzle Thickness (in)	Initial Flaw Depth (in)	Final Flaw Depth in 10 years (in)	Total Flaw Growth in 10 years (in)
0.993(1,2)	0.632	0.6342	0.0022

Notes:

1. This thickness is due to a 0.100-inch increase in SWOL thickness.
2. A review of transient stresses indicates that a rise time of 5,000 seconds is conservative for use in Alloy 52/52M FCG rate.

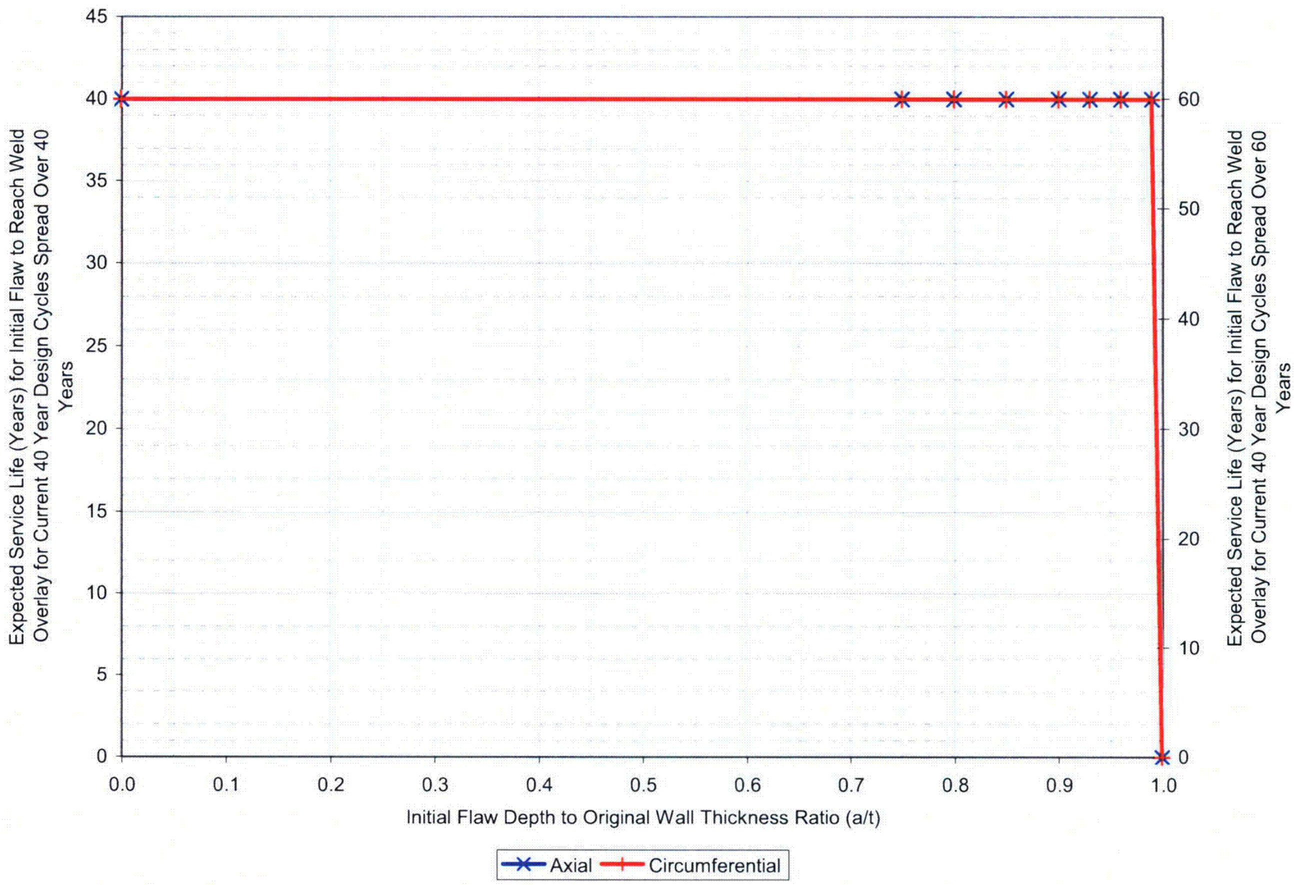

Figure 6-10: Expected Time for the Initial Flaw Depth to Reach the Weld Metal Interface for RCS Spray Nozzle Alloy 82/182 Weld [35]

Note: Curves for axial and circumferential flaw estimated life coincide with each other. Hence, only one curve is visible in the figure above.

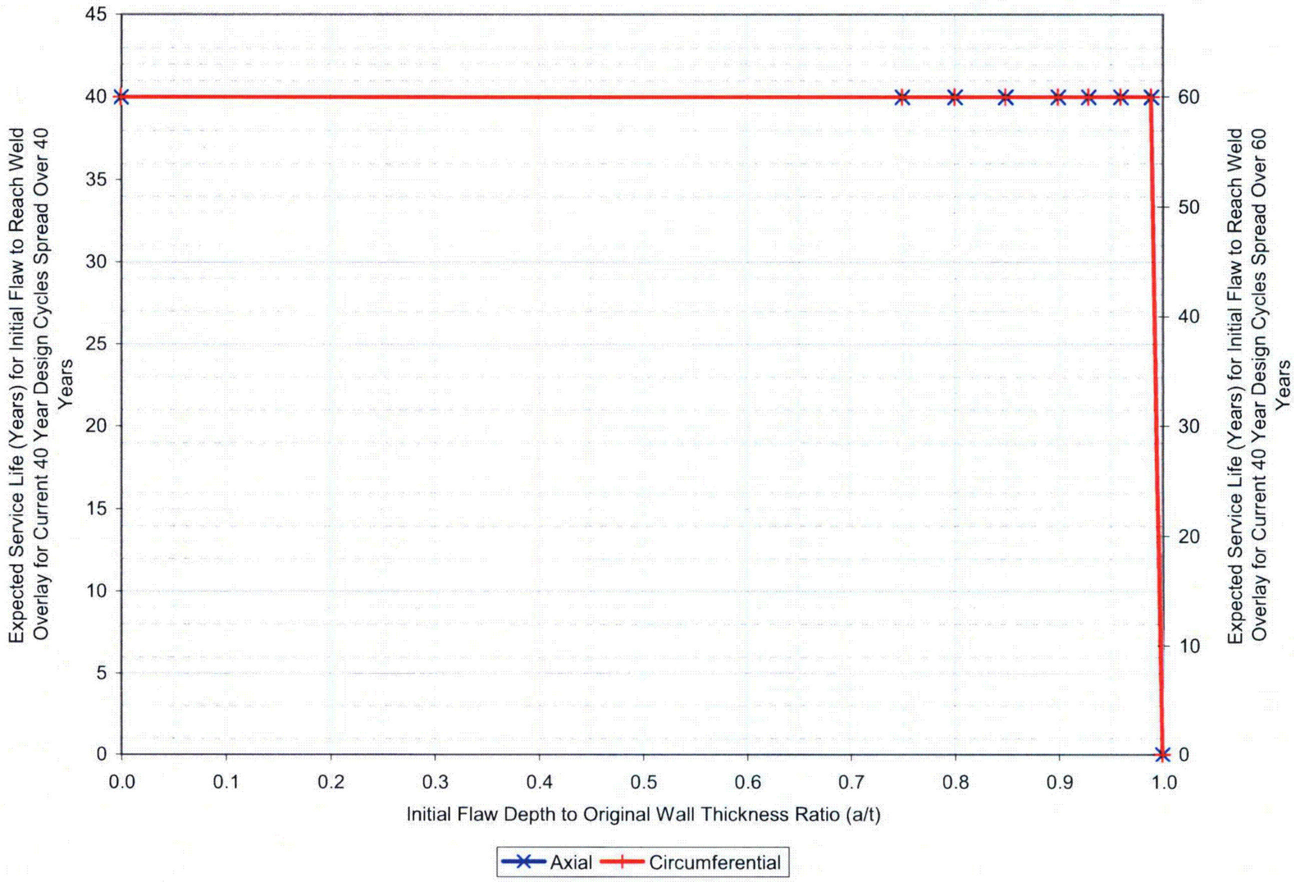

Figure 6-11: Expected Time for the Initial Flaw Depth to Reach the Weld Metal Interface for RCS Spray Nozzle SS Weld [35]

Note: Curves for axial and circumferential flaw estimated life coincide with each other. Hence, only one curve is visible in the figure above.

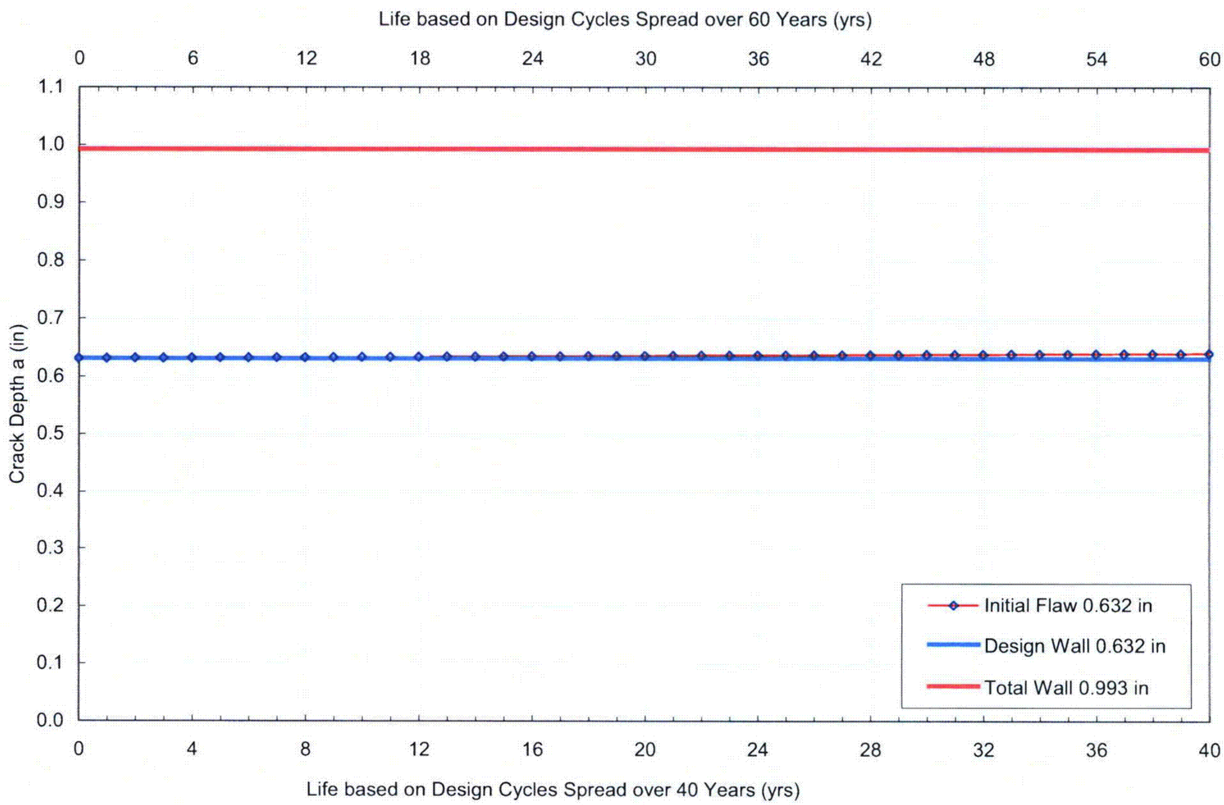

Figure 6-12: Flaw Growth for 100% Original Wall Thickness Initial Flaw versus Service Period in Alloy 52/52M at RCS Spray Nozzle Alloy Weld [35]

6.6 IMPACT ON DESIGN QUALIFICATION OF NOZZLE AND PIPE

The SWOL was evaluated to demonstrate that the presence of the weld overlay repair does not have any adverse impact on the existing stress qualification of the RCS spray nozzle with respect to the Code of Construction [33].

Effects of SWOL on Transient Stress and Fatigue Analysis

Since the intention of the structural weld overlay is to mitigate/repair the potentially cracked dissimilar-metal butt-weld at the RCS spray nozzle safe-end, the crack growth analyses discussed in Section 6.5 using the ASME Code Section XI methodology are acceptable bases to address the fatigue qualification of the weld overlay region for the RCS spray nozzle.

The original analysis was performed in accordance with the ANSI Code [33]. The analysis offers protection against membrane or catastrophic failure, and protection against fatigue or leak type failure. The SWOL does not influence the reinforced region of the spray nozzle. Therefore, the existing analysis [34] remains applicable for this region, provided the loading used in [34] remains applicable. The transient stresses and structural evaluation for the weld overlay spray nozzle were documented in [7]. The primary stress for the RCS spray nozzle was evaluated by hand calculations in accordance with ANSI B31.7 [33]. Addition of the SWOL does not affect the B indices of the loads from the piping, but it increases the section modulus in the overlay region. The applicable primary loads (pressure and mechanical loads) used in [34] are not changed by the SWOL. Therefore, the primary stresses in the structures with SWOL are, by definition, less than or equal to those without SWOL. The previous qualifications [34] performed for the RCS spray nozzle apply to this calculation.

The fatigue for the RCS spray nozzle was evaluated using finite element techniques. Cut locations are illustrated in Figure 6-13. Table 6-10 shows that all stress, thermal ratcheting, and fatigue results meet the requirements specified in ANSI B31.7 [33]. Therefore, it is concluded that the existing ANSI B31.7 analysis of the RCS spray nozzle is not adversely affected by the addition of the SWOL.

Effects of Additional Mass on Piping/Support System

The impact of the addition of weld overlay material on the existing primary stress qualification, which considers deadweight and dynamic loadings (such as those due to earthquake), was evaluated in [36], and found to be insignificant.

Table 6-10: Spray Nozzle with SWOL Result Summary

Loading Condition	Stress Category	Cut No.	Stress (psi) or Usage	Stress Limit	Allowable Stress (psi) or Usage	Margin
Design	$P_m + P_b$	--	11,313	$1.5S_m$	25,500	55.64%
Level A/B	P + Q	7	24,088	$3S_m$	51,000	52.77%
	Linear Thermal Ratchet	7	0.308	N/A	1.0	69.20%
	Parabolic Thermal Ratchet	7	0.287	N/A	1.0	71.31%
	Fatigue	10	0.029	N/A	1.0	97.08%
Level C/D	$P_m + P_b$	--	14,362	$2.25S_m$	38,250	62.45%

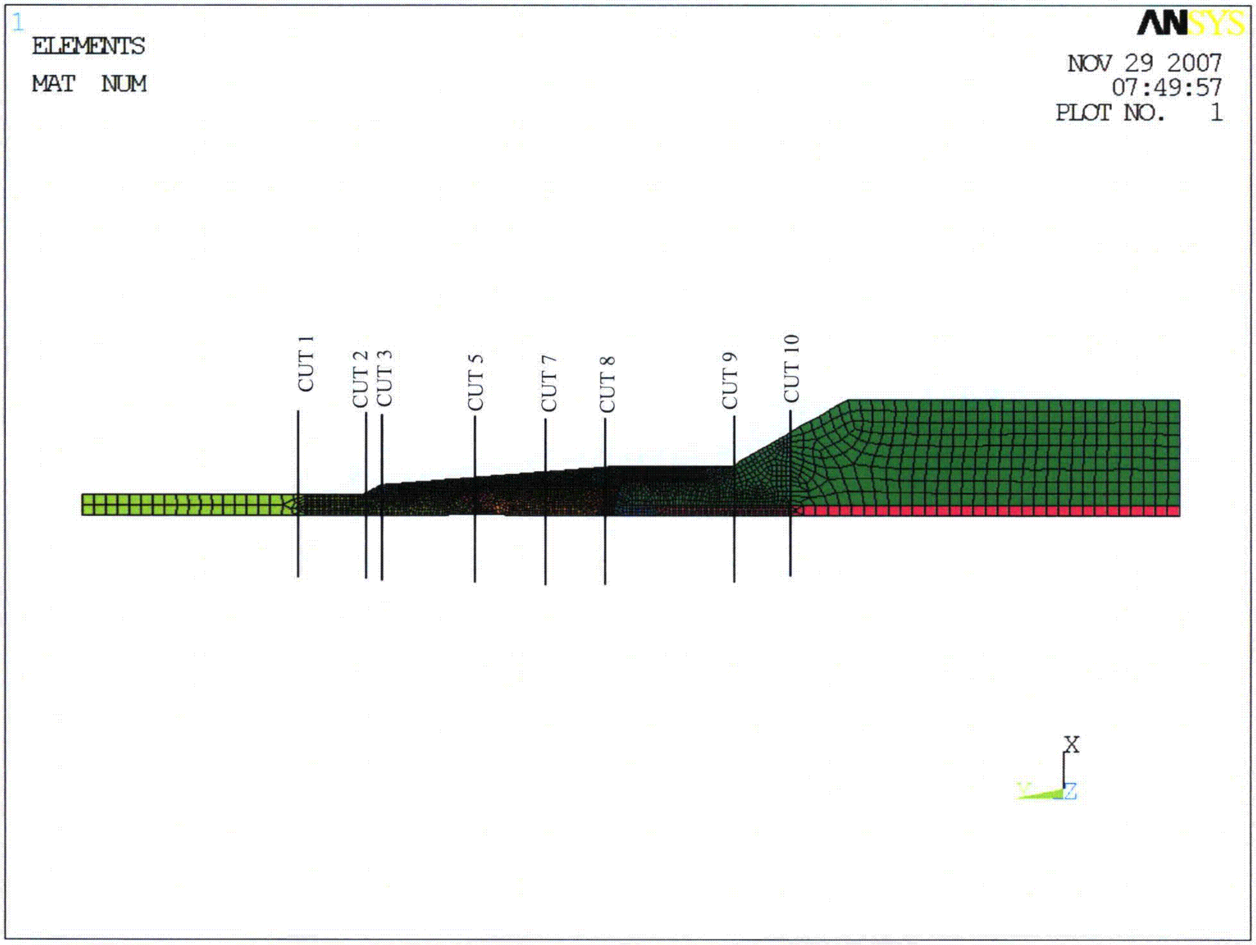

Figure 6-13: Spray Nozzle Cut/Path Locations

7 WELD OVERLAY DESIGN QUALIFICATION ANALYSIS: RCS SURGE NOZZLE

7.1 INTRODUCTION

This section provides the SWOL design qualification analysis to demonstrate the adequacy of the SWOL design for the RCS surge nozzle. The effectiveness of a WOL with Alloy 52/52M weld material is demonstrated using crack growth analysis, per IWB-3640 of [6], to ensure that the SWOL does not deteriorate during service. Using the residual weld stresses developed by the finite element model of the WOL process, future crack growth was evaluated at the surge nozzle safe-end weld locations using the operational design transients affecting the WOL region. The advantage of the Alloy 52/52M material is its high resistance to PWSCC, which minimizes the possibility for future PWSCC crack growth. Since the purpose of the SWOL is to mitigate/repair a potentially cracked dissimilar-metal butt-weld, performing crack growth analyses using the ASME Code Section XI methodology is the accepted method used to address the fatigue qualification of the WOL region for the RCS surge nozzle.

The effect of the SWOL on the existing fatigue qualification of the RCS surge nozzle outside the WOL region is addressed in accordance with the ANSI B31.7 requirements, considering the effect of the applicable thermal transient stresses, structural discontinuities, and bimetallic effects resulting from the SWOL.

7.2 LOADS

The loads used for the design of the surge nozzle weld overlay are listed in Table 7-1. These loads are considered in [2] and specified in [31]. The load combinations considered in the design are listed in Table 7-2. The transients considered in the surge nozzle fatigue and FCG evaluations are shown in Table 7-4. The pipe end loads used for fatigue and FCG evaluations are listed in Table 7-3. Theses loads are considered in [7] and specified in [31]. The nozzle loads and transients used for the design and FCG analysis are bounding for the actual nozzle loads and the plant-specific transients [7, 31, and 30].

Table 7-1: Enveloping RCS Surge Nozzle Loads Used for Weld Overlay [31]

Load Type	Axial Force F_a (kips)	Bending Moment M_b (in-kips)
DW	-1.000	20.248
OBE	4.000	367.234
SSE	8.000	734.469

Notes:
DW = Deadweight Loads
OBE = Operating Basis Earthquake Loads
SSE = Safe Shutdown Earthquake Loads

Table 7-2: Load Combinations

Condition	Load Combination	Service Level
Design	DP + DW + DS	Design
Normal/Upset	TR[1] + DW + NT[(1)]	Level A/B
Emergency	DP + DW + MS + NT[(1)]	Level C
Test	TP + DW	Test

Notes:
1. Not applicable to WOL design sizing.
DW = Deadweight
DP = Design Pressure
TP = Test Pressure
TR = Level A/B Transient Loadings (Thermal and Pressure)
NT = Thermal Expansion
DS = Design Seismic
MS = Maximum Seismic

Table 7-3: Enveloping RCS Surge Nozzle Loads for Fatigue and FCG Evaluations

Condition	Force (kips)			Moment (in-kips)		
	F_x	F_y	F_z	M_x	M_y	M_z
Deadweight	0.000	-1.000	0.000	19.000	-1.000	-7.000
Thermal	11.000	-4.000	-24.000	7.000	-448.000	-47.000
Design Seismic	6.000	4.000	4.000	269.000	290.000	250.000
Maximum Seismic	12.000	8.000	8.000	538.000	580.000	500.000
Stratification (Δ320°F Low Pressure)	2.530	-0.040	-7.270	-2,407.340	-257.410	-548.220
Stratification (Δ250°F Low Pressure)	4.850	-0.900	-10.970	-1,996.510	-257.170	-508.220
Stratification (Δ200°F Low Pressure)	6.510	-1.510	-13.610	-1,703.060	-257.000	-479.650
Stratification (Δ150°F Low Pressure)	8.170	-2.120	-16.250	-1,409.610	-256.820	-451.080
Stratification (Δ320°F High Pressure)	6.770	-1.280	-15.150	-2,482.080	-343.450	-653.730
Stratification (Δ250°F High Pressure)	7.800	-1.760	-16.450	-2,048.500	-317.020	-581.620
Stratification (Δ200°F High Pressure)	8.540	-2.100	-17.380	-1,738.800	-298.140	530.110
Stratification (Δ150°F High Pressure)	9.270	-2.450	-18.310	-1,429.110	-279.270	-478.600
Stratification (Δ90°F High Pressure)	10.150	-2.860	-19.430	-1,057.470	-256.610	-416.790

Notes:

Axial force = F_y
Shear force = $\sqrt{(F_x^2 + F_z^2)}$
Torsion moment = M_y
Bending moment = $\sqrt{(M_x^2 + M_z^2)}$

Table 7-4: Summary of Design Transients for Reference Surge Nozzle

ID	Transient Title	Cycles	Level
1	Plant Heatup, 100°F / hr	500	A
2	Plant Cooldown, 100°F / hr	500	A
3	Plant Loading, 5% / min	15,000	A
4	Plant Unloading, 5% / min	15,000	A
5	Step Load Increase 10%	2,000	A
6	Step Load Decrease 10%	2,000	A
7	Reactor Trip	400	B
8	Loss of Turbine Generator Load / Loss of Reactor Coolant Flow	80(3)	B
9	Loss of Secondary Pressure	5	C
10	Hydrostatic Test	10	Test
11	Leak Test	200	Test
12	Stratification Heatup Δ320°F Low Pressure	75	A
13	Stratification Heatup Δ250°F Low Pressure	375	A
14	Stratification Heatup Δ200°F Low Pressure	400	A
15	Stratification Heatup Δ150°F Low Pressure	500	A
16	Stratification Heatup Δ320°F High Pressure	75	A
17	Stratification Heatup Δ250°F High Pressure	375	A
18	Stratification Heatup Δ200°F High Pressure	400	A
19	Stratification Heatup Δ150°F High Pressure	500	A
20	Stratification Heatup Δ90°F High Pressure	87,710	A
21	Stratification Cooldown Δ90°F High Pressure	87,710	A
22	Stratification Cooldown Δ150°F High Pressure	500	A
23	Stratification Cooldown Δ200°F High Pressure	400	A
24	Stratification Cooldown Δ250°F High Pressure	375	A
25	Stratification Cooldown Δ320°F High Pressure	75	A
26	Stratification Cooldown Δ150°F Low Pressure	500	A
27	Stratification Cooldown Δ200°F Low Pressure	400	A
28	Stratification Cooldown Δ250°F Low Pressure	375	A
29	Stratification Cooldown Δ320°F Low Pressure	75	A
30(1)	Seismic (Positive)	200	B
31(1)	Seismic (Negative)	200	B
32	Zero Load	710(2)	-

Notes:

1. The design specification [30] states 200 cycles of OBE and 200 cycles of design basis earthquake. For this analysis, 400 cycles of design basis earthquake will be used.
2. The total cycles for this transient consist of 500 heatup and cooldown cycles, 10 hydrostatic test cycles and 200 Leak Test cycles.
3. The total cycles for this transient consist of 40 Loss of Turbine Generator Load Cycles and 40 Loss of Reactor Coolant Flow Cycles.

7.3 WELD OVERLAY DESIGN SIZING

The minimum WOL thickness was determined based on a through-wall flaw in the original pipe. The methodology used to determine the WOL design thickness and length is discussed in Section 3. Using that methodology, radii from the design geometry, as shown in Table 7-5, are used to design the minimum SWOL parameters. As-designed inside and outside radii at the thickest portion of the Alloy 82/182 and SS welds are presented here. The thickest portion results from considering the smallest inner radius ($R_{i\text{-}min}$) and the largest outer radius ($R_{o\text{-}max}$). By using the maximum wall thickness of the design geometry, a conservative SWOL design thickness and length are achieved. The WOL length was based conservatively on the recommended length, per Code Case N-740:

$$L_{WOL} = 0.75\sqrt{Rt}$$

where,

R = $R_{o\text{-}max}$ = outside radius

t = $R_{o\text{-}max} - R_{i\text{-}min}$ = wall thickness at the location of indication

The WOL length (L_{WOL}) will extend from the weld/base metal interface on either side of the Alloy 82/182 and SS welds, as shown in Figure 7-1. The WOL thickness (t_{WOL}) was determined by the following equation:

$$t_{WOL} = t/0.75 - t$$

The minimum design WOL dimensions are shown in Table 7-6.

In accordance with ASME Section XI IWB-3640, the criterion from Section XI, Appendix C is used to evaluate the maximum resulting post-WOL stresses from the actual applied loadings. To determine the applied post-WOL stresses, the minimum post-WOL thicknesses are considered. This results in a conservative method to determine stresses for comparison to the allowable stress criterion. The thinnest portion of the Alloy 82/182 and SS welds results from considering the largest inner radius ($R_{i\text{-}max}$) and the smallest outer radius post-WOL ($R_{o\text{-}min\text{-}WOL}$). These parameters and the resulting geometric section properties are presented in Table 7-7.

The applied bending stresses were calculated by:

$$\sigma_b = \frac{M_b}{Z}$$

M_b is per Table 7-1 and Z is per Table 7-7.

$$Z = \frac{\pi(R_{o-\min-wol}{}^4 - R_{i-\max}{}^4)}{4(R_{o-\min-wol})}$$

$R_{i\text{-}max}$ and $R_{o\text{-}min\text{-}wol}$ are per Table 7-7.

The applied membrane stresses were calculated by:

$$\sigma_m = \sigma_p + \frac{F_a}{A_x}$$

where,

$$\sigma_p = \frac{\pi R_{i-\max}^2}{\pi\left(R_{o-\min-wol}^2 - R_{i-\max}^2\right)} P$$

F_a is per Table 7-1.

A_x is per Table 7-7.

$A_x = \pi\ (R_{o\text{-}min\text{-}wol}^2 - R_{i\text{-}max}^2)$

$R_{i\text{-}max}$ and $R_{o\text{-}min\text{-}wol}$ are per Table 7-7.

P = 2,235 psig [2]

The allowable stress intensity S_m (at 650°F) used in the sizing of the Alloy 52/52M (N06690) overlay is 23.3 ksi [9]. This allowable is based on the annealed condition of SB-166/SB-167. The normal operating pressure, 2,235 psig, was used for the calculation.

The resulting bending stresses, determined by using the previous equations, as well as the loads and load combinations from Tables 7-2 and 7-3, respectively, are listed and compared to the Code allowables in Table 7-8.

Table 7-5: RCS Surge Nozzle Geometry for SWOL Design Calculations [2]

Alloy 82/182 Weld			Stainless Steel Weld		
Inside Radius $R_{i\text{-}min}$ (in)	**Outside Radius $R_{o\text{-}max}$ (in)**	**Wall Thickness t_{design} (in)**	**Inside Radius $R_{i\text{-}min}$ (in)**	**Outside Radius $R_{o\text{-}max}$ (in)**	**Wall Thickness t_{design} (in)**
5.063	6.790	1.728	5.063	6.375	1.312

Table 7-6: RCS Surge Nozzle Minimum Structural Weld Overlay Design Dimensions [2]

Alloy 82/182 Weld		Stainless Steel Weld	
t_{WOL} (in)	**L_{WOL} (in)**	**t_{WOL} (in)**	**L_{WOL} (in)**
0.78	2.57	0.44	2.17

Table 7-7: RCS Surge Nozzle Geometry for Stress Check in Post-Weld-Overlay Condition [2]

Alloy 82/182 Weld				Stainless Steel Weld			
Inside Radius $R_{i\text{-}max}$ (in)	Outside Radius $R_{o\text{-}min\text{-}WOL}$ (in)	Cross-Sectional Area A_x (in^2)	Section Modulus Z (in^3)	Inside Radius $R_{i\text{-}max}$ (in)	Outside Radius $R_{o\text{-}min\text{-}WOL}$ (in)	Cross-Sectional Area A_x (in^2)	Section Modulus Z (in^3)
5.063	6.955	71.450	190.055	5.207	6.815	60.748	163.907

Table 7-8: RCS Surge Nozzle Post-SWOL Stress Comparison [2]

	Normal/Upset		Emergency/Faulted	
Location	Applied Stress σ_b (ksi)	Allowable Stress P_b (ksi)	Applied Stress σ_b (ksi)	Allowable Stress P_b (ksi)
Alloy Weld	2.039	8.648	3.971	19.719
SS Weld	2.364	7.847	4.605	18.729

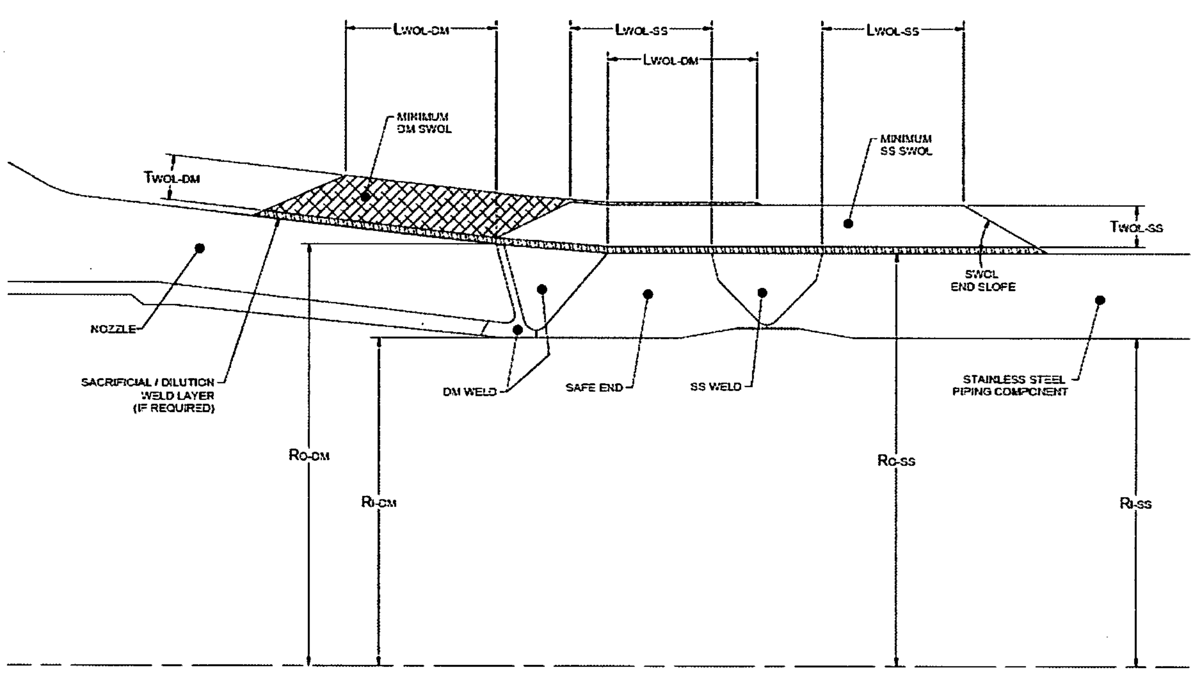

Figure 7-1: Weld Overlay Design Parameters for the RCS Surge Nozzle
(Not drawn to scale.)

7.4 WELD OVERLAY RESIDUAL WELD STRESS RESULTS

The finite element model was developed to capture the parts of the structure in the vicinity of the RCS surge nozzle safe-end with the SWOL repair/mitigation. This includes a portion of the surge nozzle attached to the nozzle safe-end and a length of SS pipe attached to the safe-end. An ID weld repair was considered in the finite element model as discussed in Section 5.3. The finite element model and boundary conditions are shown in Figure 7-2. The nozzle is fixed in the axial direction to simulate the rest of the nozzle. The SS piping is coupled in the axial direction to simulate the remaining portion of the SS piping not included in the model. The model assumes that a 50% through-wall weld repair was performed from the inside surface of the surge nozzle to safe-end Alloy 82/182 butt-weld.

The final residual weld stresses, including normal operating pressure and temperature conditions, are shown in Figures 7-4 and 7-5 for selected stress cuts in the Alloy 82/182 and SS welds. The locations of the stress cuts at the alloy and SS welds are shown in Figure 7-3. The axial and hoop stress contours in the RCS surge nozzle after the weld overlay application are provided in Figures 7-6 and 7-7, respectively.

Figure 7-4 shows the axial and hoop residual stresses for the Alloy 82/182 weld, at normal operating condition after the SWOL. These stresses are compressive up to about 95% of the original pipe wall thickness. This stress distribution minimizes the potential for crack growth in the dissimilar-metal weld region. Similarly, Figure 7-5 shows both the axial and hoop residual weld stresses for the SS weld. The stresses remain compressive at normal operating conditions up to about 95% of the original pipe wall thickness. Therefore, the potential for FCG is minimized.

Acceptable post-weld-overlay residual stresses (i.e., stresses that satisfy the requirements for mitigating PWSCC) are those that are sufficiently compressive over the entire length and circumference of the inside surface of the Alloy 82/182 weld (at operating temperature, but prior to applying operating pressure and loads) that the resulting total stress, after application of operating pressure and loads, remains less than 10 ksi tensile [28]. This target level has been selected as a conservatively safe value, below which PWSCC initiation, or growth of small initiated cracks, is very unlikely. Additionally, the residual plus operating stresses must remain compressive through some portion of the weld thickness away from the inside surface. The residual stresses in the Alloy 82/182 weld of the RCS surge nozzle, resulting from the weld overlay, are well below this stress level through at least 95% of the original weld thickness.

Figures 7-8 and 7-9 show that the axial and hoop stresses on the inside surface (in the vicinity of the alloy weld and buttering) remain compressive after SWOL. The maximum resultant bending moment for normal operating condition is 452.9 in-kips. The resulting maximum bending stress in the Alloy 82/182 weld and SS weld are 1.734 ksi and 2.197 ksi, respectively [32]. Therefore, the pipe bending stress would have a negligible effect on the residual weld stress results.

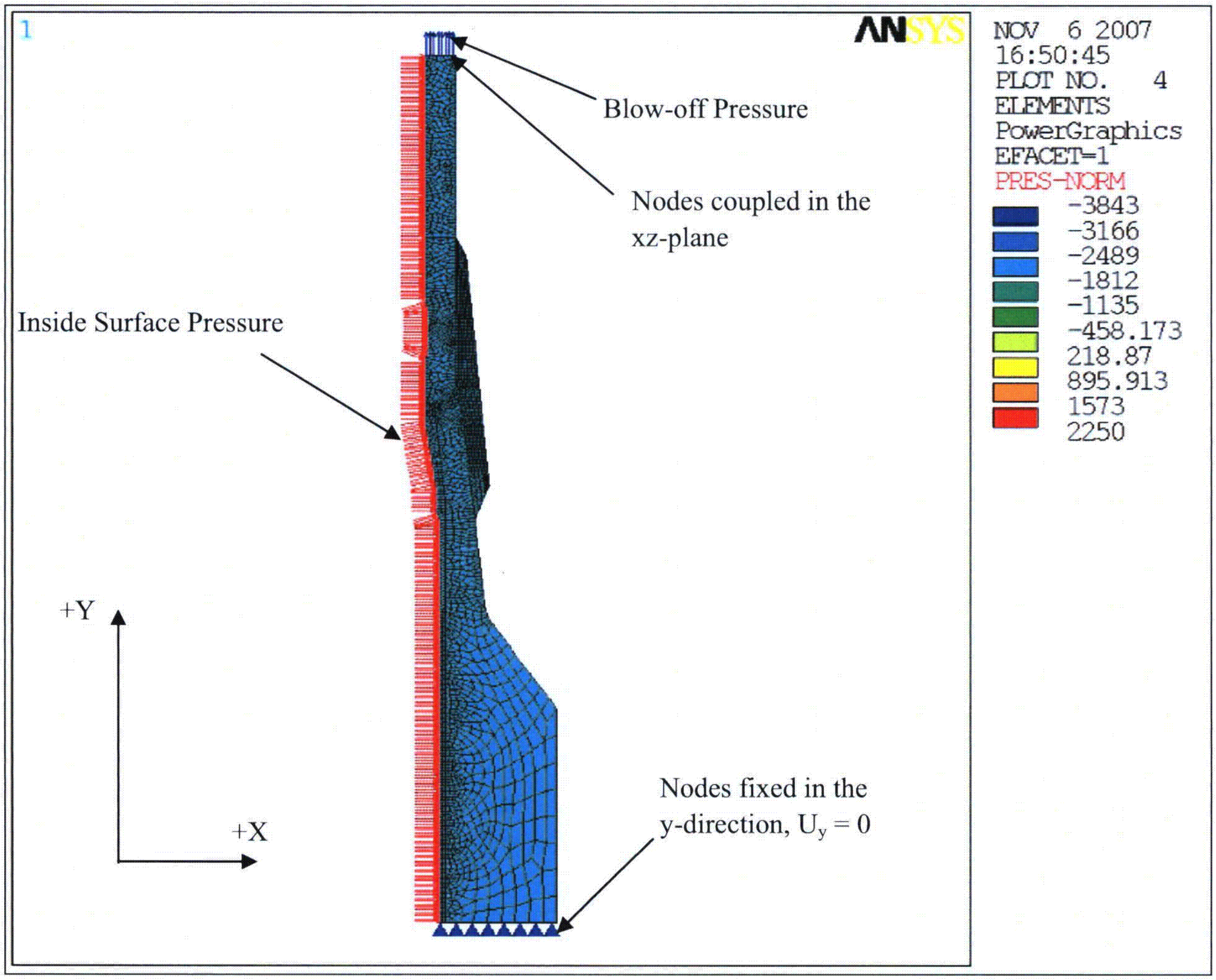

Figure 7-2: Axisymmetric Finite Element Model Used for Surge Nozzle Weld Overlay Analysis

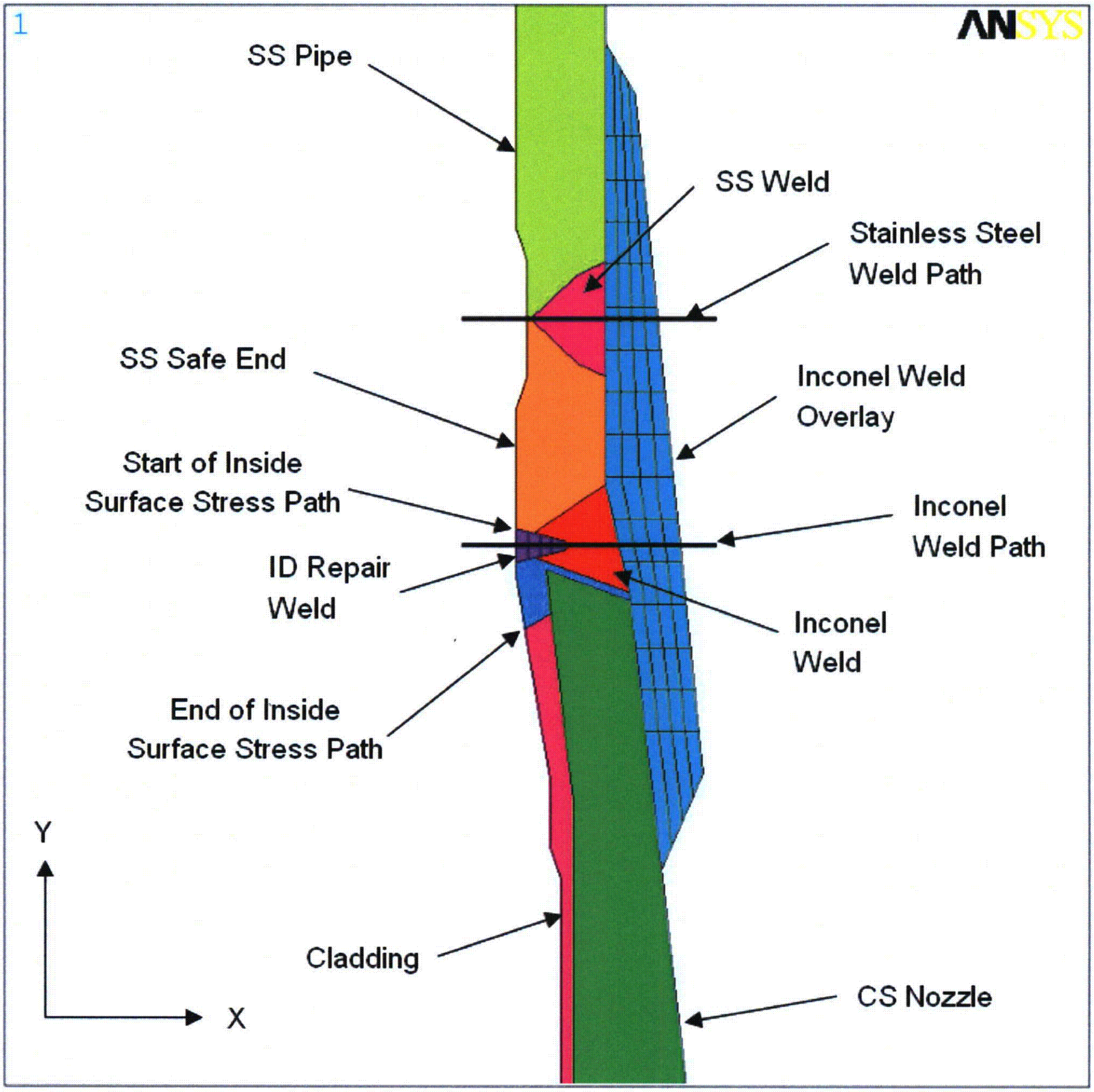

Figure 7-3: Surge Nozzle Structural Weld Overlay Stress Cut Locations

Note: CS = Carbon Steel

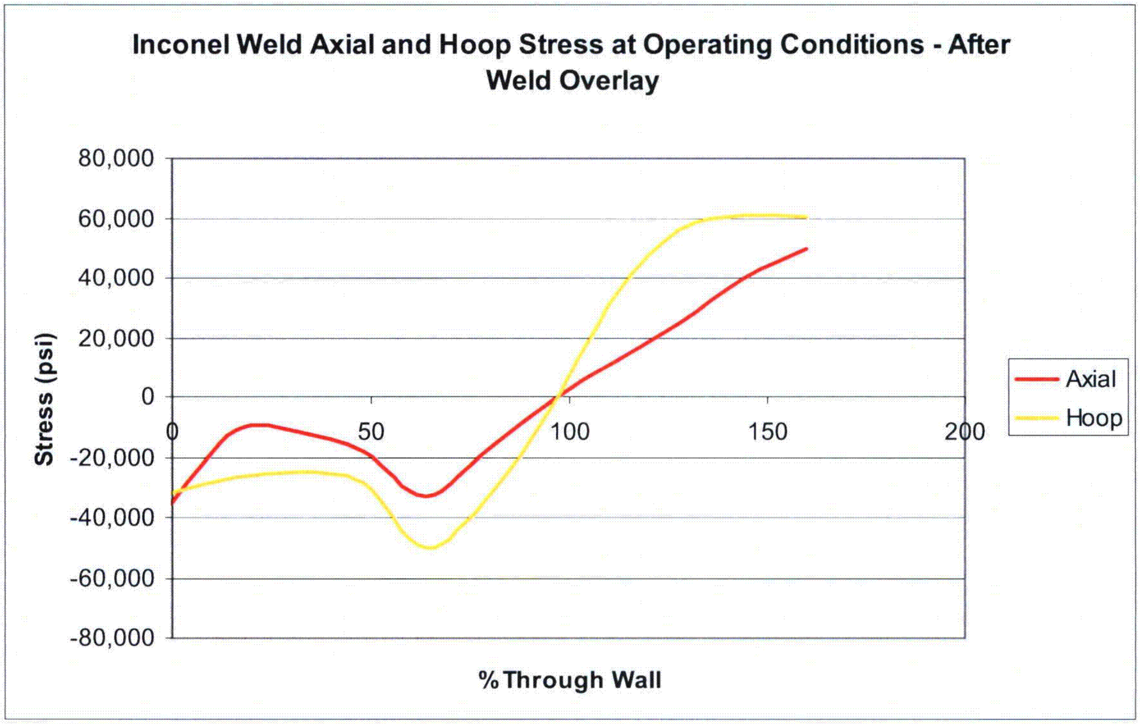

Figure 7-4: Axial and Hoop Residual Stress Distribution for Alloy 82/182 Inconel Weld at Normal Operating Condition*

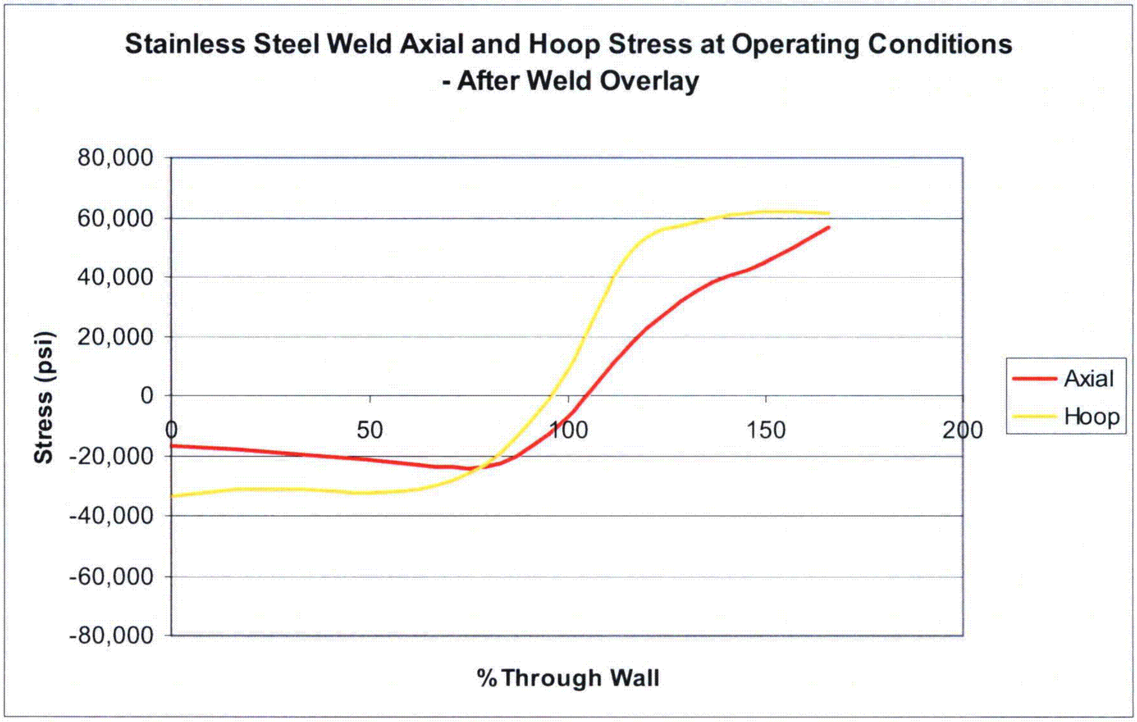

Figure 7-5: Axial and Hoop Residual Stress Distribution for SS Weld at Normal Operating Condition*

*Note: The percent through-wall indicated on the horizontal axis is expressed in terms of the original pipe wall thickness. The weld overlay region is the region beyond 100% wall thickness.

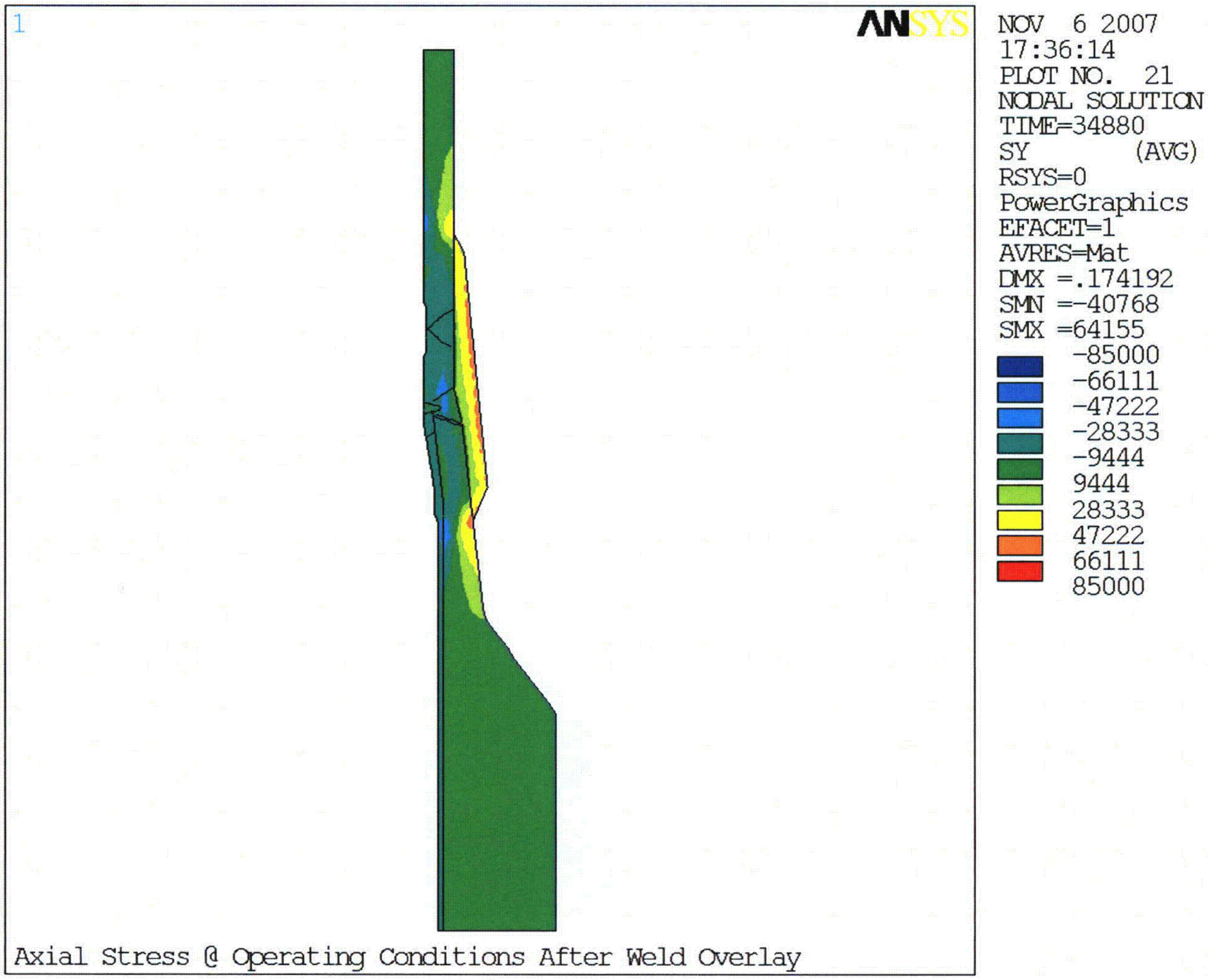

Figure 7-6: Axial Stress (psi) Contour Plot at Normal Operating Condition

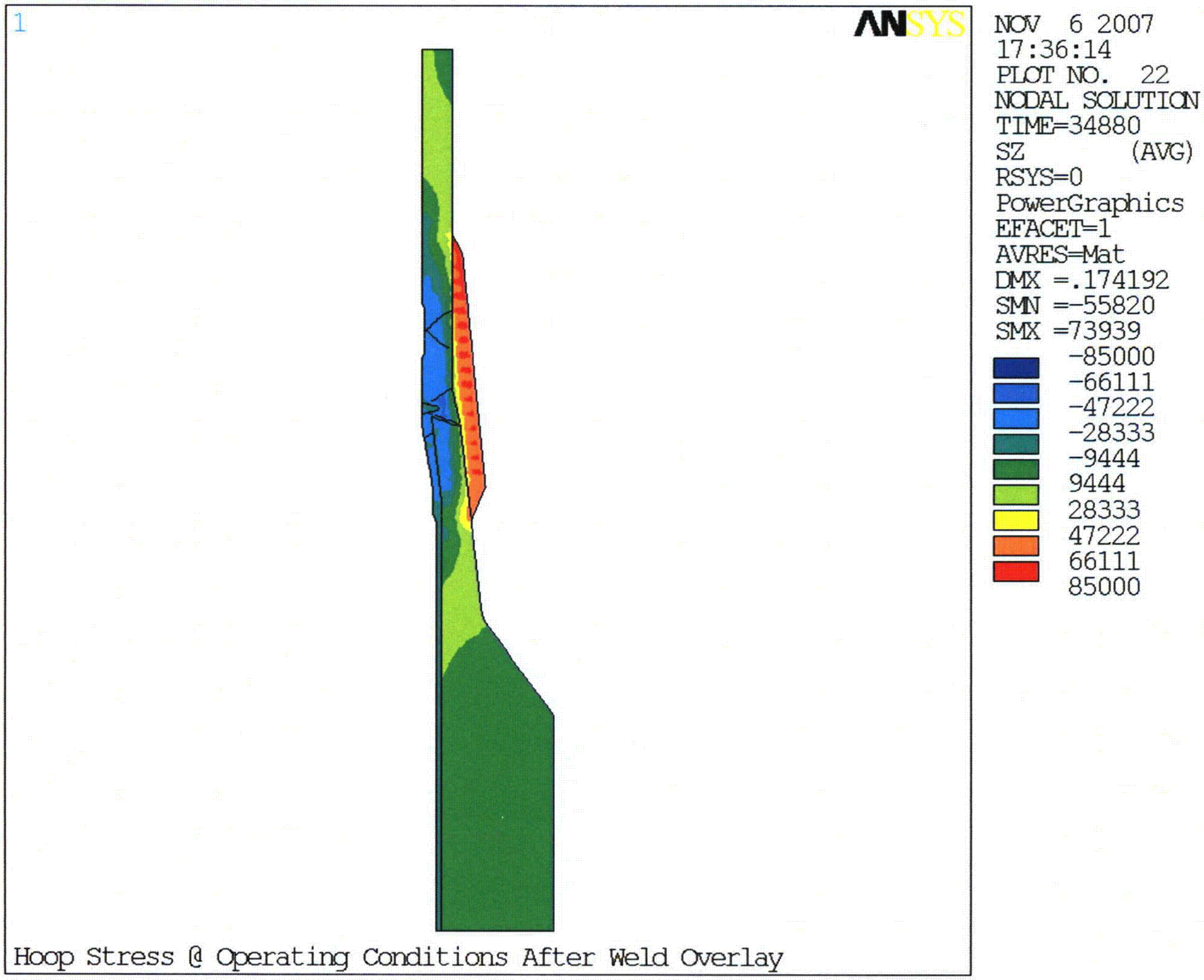

Figure 7-7: Hoop Stress (psi) Contour Plot at Normal Operating Condition

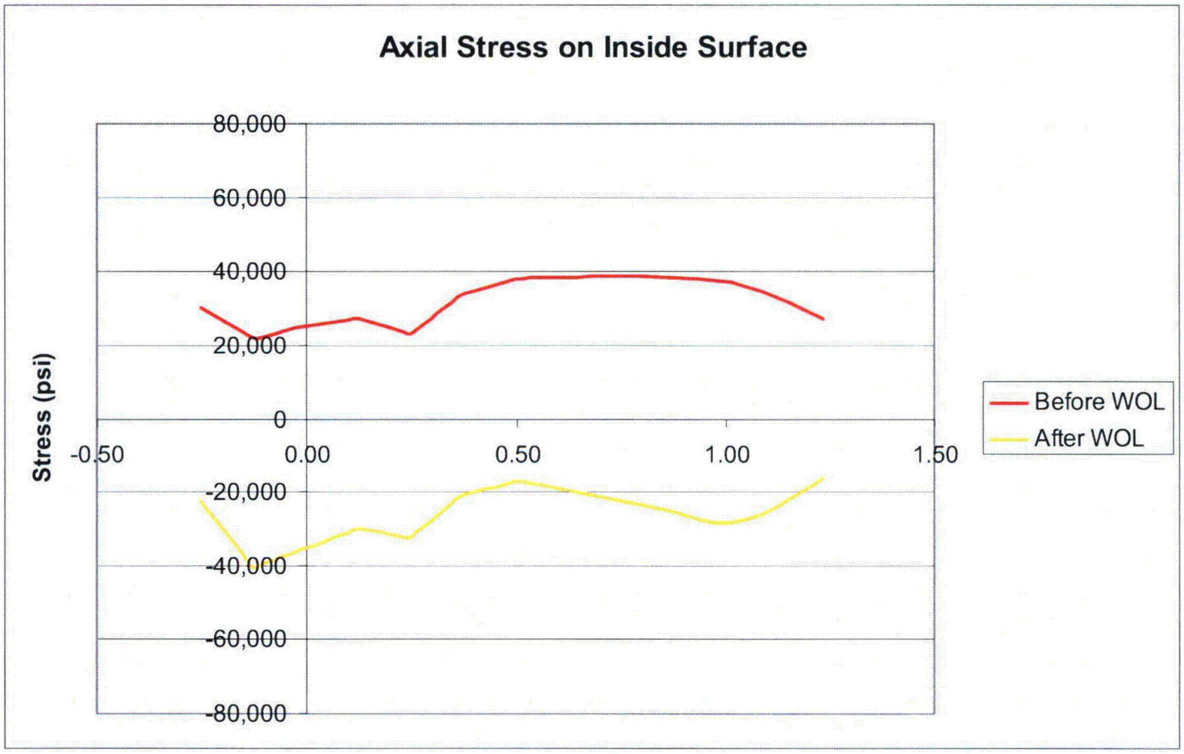

Figure 7-8: Axial Residual Stress along the Inside Surface at Operating Condition*

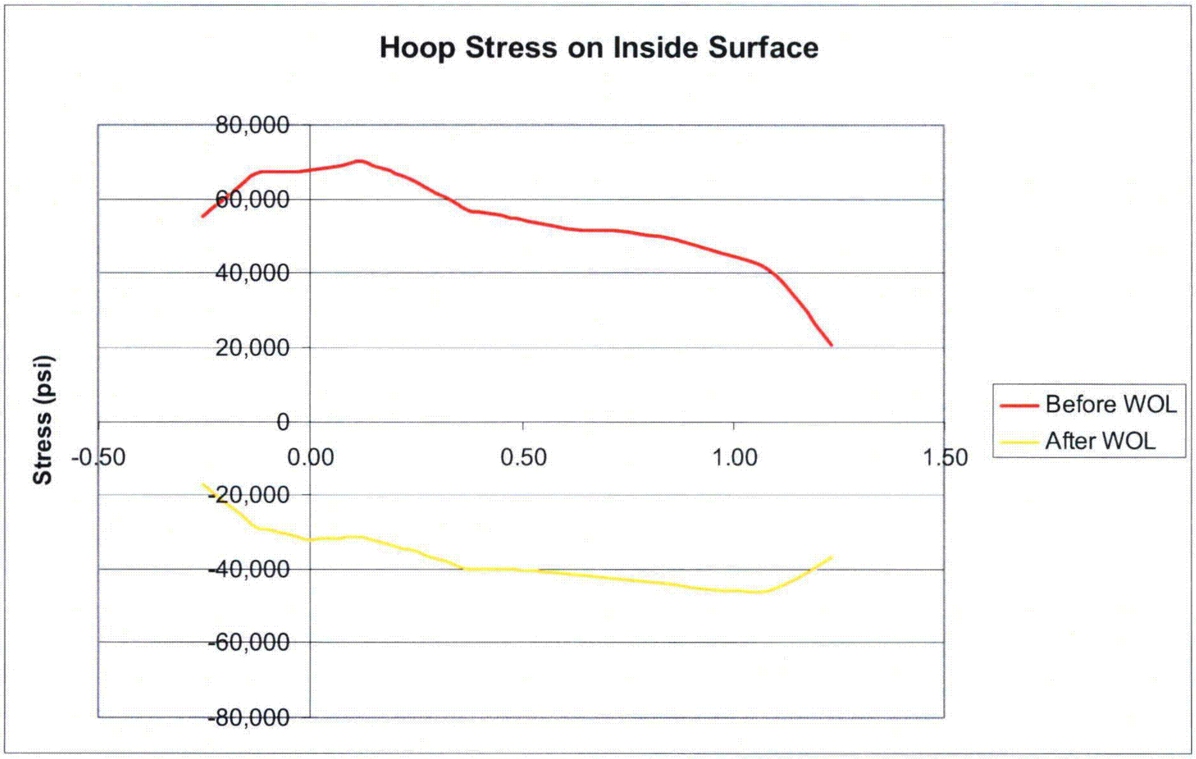

Figure 7-9: Hoop Residual Stress along the Inside Surface at Operating Condition*

*Note: X-axis is the location (inch) along the inside surface path. Zero is the center of alloy weld. See Figure 7-3.

7.5 FATIGUE CRACK GROWTH RESULTS AND ESTIMATE OF WELD OVERLAY DESIGN LIFE: RCS SURGE NOZZLE REGION

The methodology used to determine fatigue crack growth is described in Section 4.4. Fatigue crack growth analyses were performed for the RCS surge nozzle using the through-wall stress distribution including residual stresses generated from the weld overlay mitigation/repair process and the thermal transient stresses.

The weld overlay service life is a function of the flaw depth found in the region being overlaid, and the projected growth of that flaw. The limitation on the maximum flaw depth is 75% of the piping wall thickness (including the weld overlay thickness), per Section XI, IWB-3640 [6].

A range of possible flaw sizes, from 0 to 100% of the original design wall thickness, was postulated in the fatigue crack growth evaluations. The results of these evaluations for the flaw depths less than the original design wall thickness are plotted in Figures 7-10 and 7-11, in the form of expected time for these flaws to reach the interface between the original wall and the newly laid weld overlay material. Figure 7-10 shows results for the Alloy 82/182 weld, and Figure 7-11 shows results for the SS weld. For the maximum possible flaw depths of 100% of the original design wall thickness propagating into the Alloy 52/52M weld overlay material, results are shown in Figure 7-12. This figure shows the estimated flaw depth with time for the design cycles spread over either the original design life or the extended life of the plant.

Figures 7-10 and 7-11 summarize the expected service life (based on transient cycles spread evenly for either 40 years or 60 years of plant life) for a given initial flaw depth to reach 100% of the original wall thickness at the Alloy 82/182 weld and the SS weld locations, respectively. Based on the results shown in Figures 7-10 and 7-11, it can be concluded that if no flaws are detected during the post-SWOL inspection, a conservatively assumed flaw extending 75% through the original wall would not grow to 100% of the original wall thickness for 40 years FCG due to transient cycles. This is based on the assumption that the current 40-year design transient cycles are spread evenly over 40 years of plant life. If flaws are detected during the post-SWOL inspection, the as-found flaw size can be used to determine the design life of the SWOL using the crack growth results shown in Figures 7-10 and 7-11.

For the case of an initial flaw depth of 100% of the original wall thickness, i.e., a through-wall flaw, Table 7-9 shows that the total flaw growth into the newly laid Alloy 52/52M welds material in one 10-year inspection interval is 0.005 inch, based on design cycles spread over a 60-year extended life. The final flaw depth after the 10-year period with the fatigue crack growth considered is still within 75% of the total post-WOL wall thickness, as required by SWOL criteria.

Two examination scenarios exist: a pre-overlay examination and a post-overlay examination. If an examination found no flaws, the overlay service life would be governed by the largest flaw that might have been missed by the examination. For an examination performed prior to the weld overlay installation, a conservative approach would be to assume that the flaw depth is 10% of the original wall thickness. Alternatively, this would be 75% of the original wall for an examination performed after the weld overlay installation. This is because the area required to be inspected after the overlay is only the outer 25% of the original pipe thickness plus the overlay thickness itself. The PDI qualification blocks do not contain any flaws in the inner 75% of the pipe wall. Therefore, it would be conservative to assume

such a flaw for the qualification. As shown in Figure 7-10, an initial flaw as deep as 75% would result in a remaining service life of 100% of the original design cycles. If the design cycles are assumed to be spread over 40 years of plant operation, the remaining life of the SWOL would be 40 years. This is well beyond the required 10-year in-service inspection (ISI) interval. If, after the next ISI, no flaws are detected in the outer 25% of the original welds, the SWOL life is at 40 years from the time of the latest inspection.

In the unlikely event that the post-overlay inspection detected a flaw as large as the full depth of the original design wall thickness, expected service life of the weld overlay would be at least one 10-year inspection interval period. For the RCS surge nozzle, flaw growth rate into the weld overlay material is small or negligible, which indicates the expected service life of the repair would be 40 years if the transient cycles are spread over original design life of 40 years.

For example, if an axial flaw that is 90% through the original Alloy 82/182 wall thickness is detected as a result of the post-SWOL inspection, and assuming conservatively that the current 40-year design transient cycles are spread evenly for only 40 years, the expected service life from Figure 7-10 for this flaw to reach 100% of the original wall thickness is about 24 years. If it is assumed that the design transient cycles are spread evenly for 60 years, the remaining service life would be 36 years. This can also be determined by applying a factor of 1.5 to the service life based on the 40-year design cycles. For a similar-size circumferential flaw, the expected service life is about 40 years, based on current 40-year design transient cycles assumed to be spread evenly over 40 years. Since the typical in-service inspection interval is 10 years for this initial flaw depth of 90%, it can be concluded that the sizing of the structural weld overlay is adequate up to the next inspection period based on the current 40-year design transient cycles spread evenly over the next 40 years.

Another case of 100% original design wall thickness through-wall flaw in the alloy weld was hypothesized assuming the total post-WOL wall of 2.43 inches. This included an extra allowance of 0.20 inch for the FCG into the Alloy 690 material. This 100% original wall axial flaw was evaluated for the FCG results, shown in Table 7-9 and Figure 7-12. Results demonstrate that the total growth in 10 years is insignificant (0.005 inch). The final flaw depth after 10 years FCG is within 75% of the total post-WOL wall thickness, as required by SWOL criteria. Therefore, the 0.2 inch SWOL thickness increase provided in the SWOL design is adequate to address the issue of PWSCC for an almost through-wall flaw.

The actual time required to use the remaining cycles depends on plant operating practice.

Table 7-9: Surge Nozzle Alloy 52/52M FCG Data – Axial Flaw [35]

Nozzle Thickness (in)	Initial Flaw Depth (in)	Final Flaw Depth in 10 years (in)	Total Flaw Growth in 10 years (in)
2. 43^(1,2)	1.520	1.525	0.005

Notes:
1. This thickness is due to a 0.2 inch increase in SWOL thickness.
2. A review of transient stresses indicates that a rise time of 5,000 seconds is conservative for use in Alloy 52/52M FCG rate.

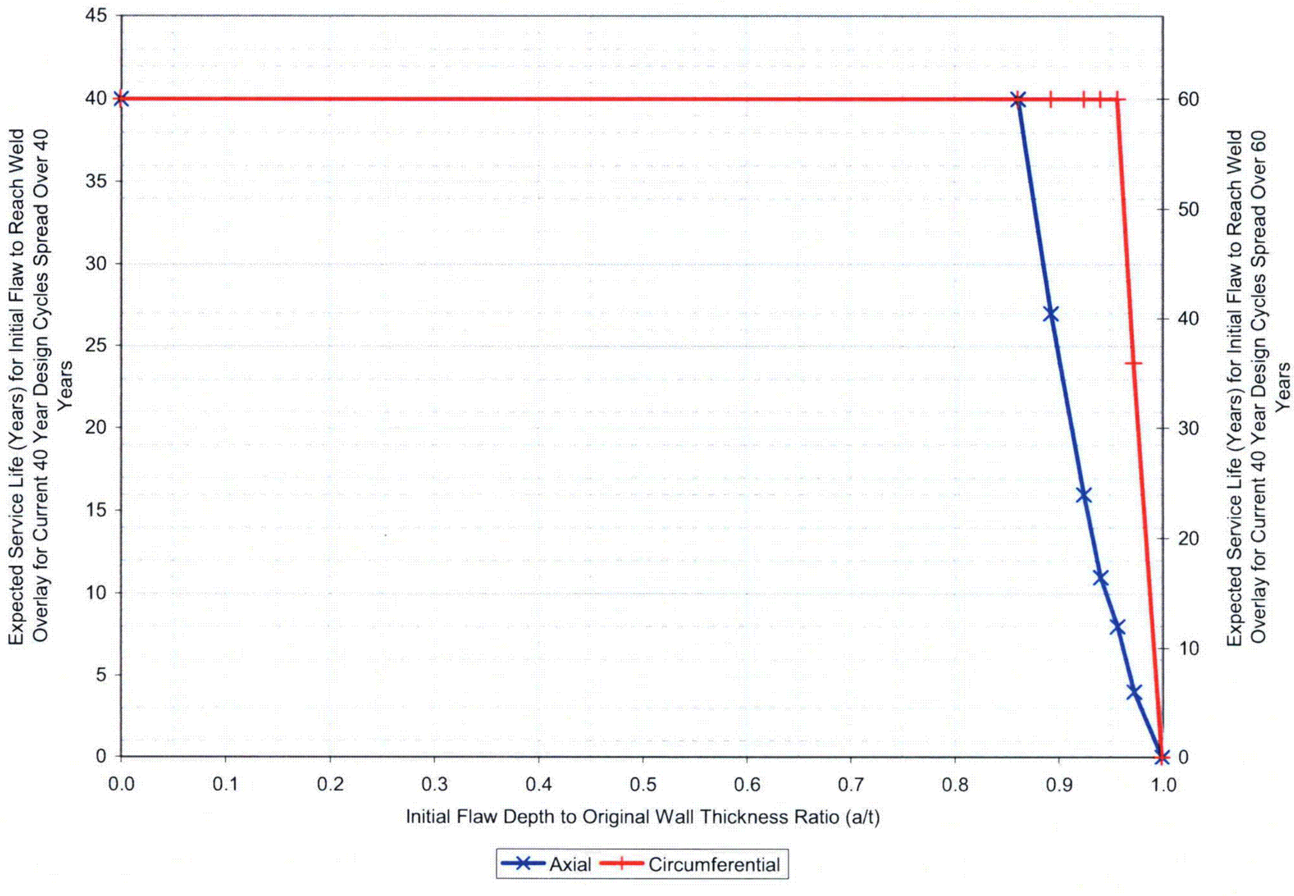

Figure 7-10: Expected Time for the Initial Flaw Depth to Reach the Weld Metal Interface for RCS Surge Nozzle Safe-End Alloy 82/182 Weld [35]

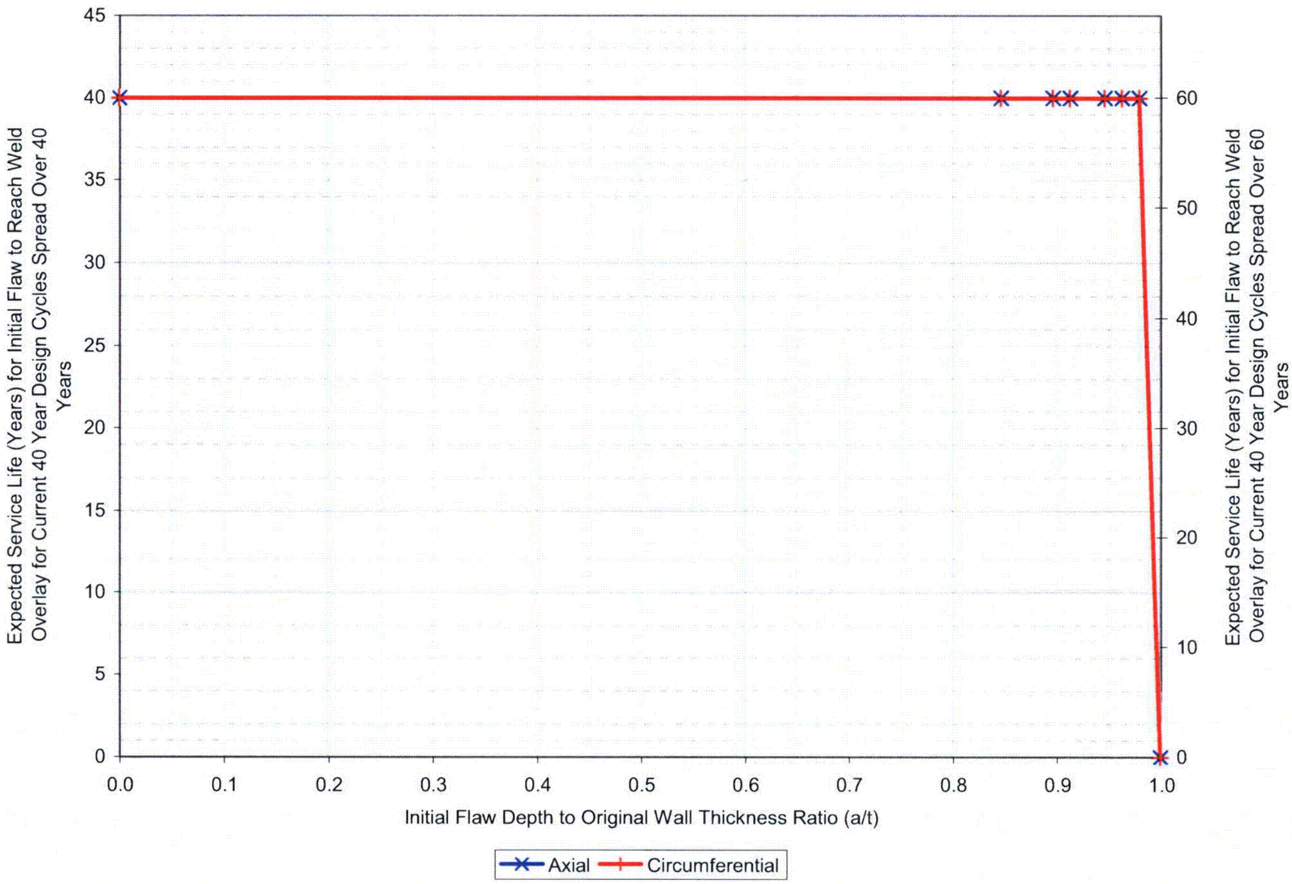

Figure 7-11: Expected Time for the Initial Flaw Depth to Reach the Weld Metal Interface for RCS Surge Nozzle Safe-End SS Weld [35]

Note: Curves for axial and circumferential flaw estimated life coincide with each other. Hence, only one curve is visible in the figure above.

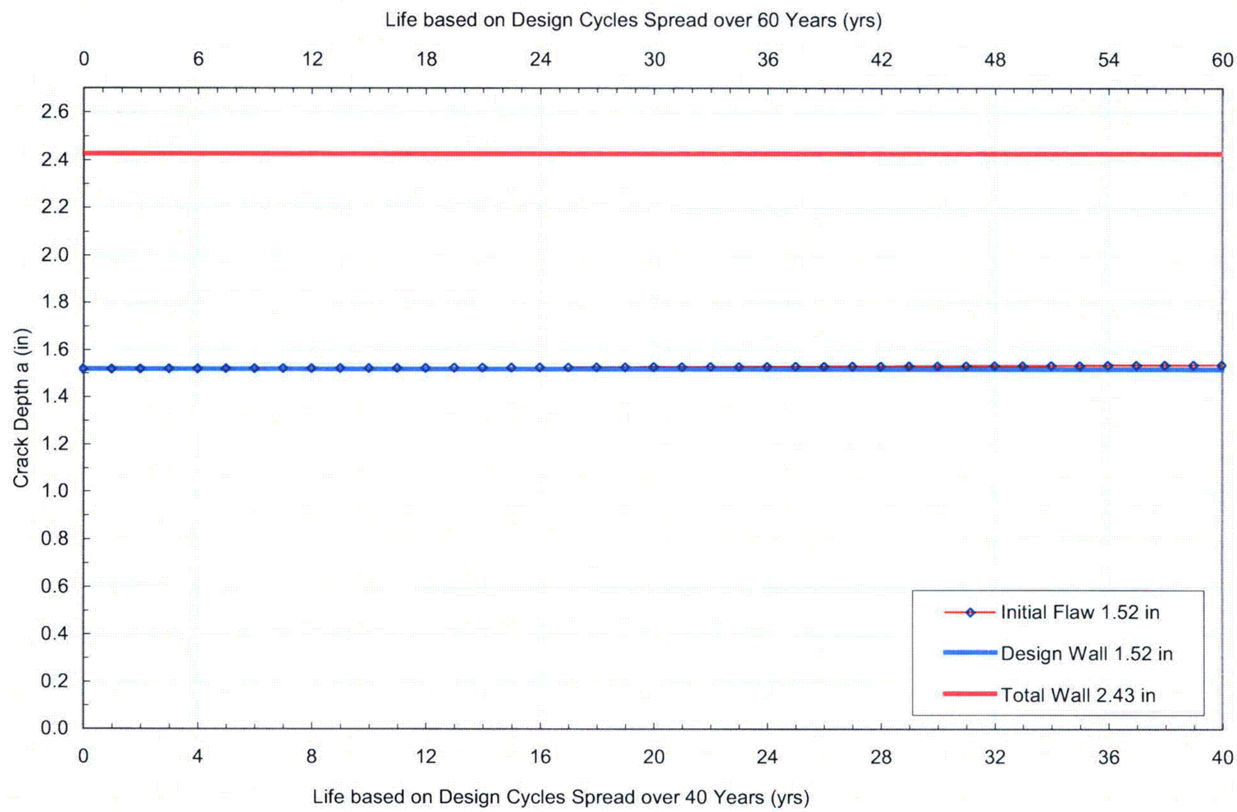

Figure 7-12: Flaw Growth for 100% Original Wall Thickness Initial Flaw versus Service Period in Alloy 52/52M at RCS Surge Nozzle Alloy Weld [35]

7.6 IMPACT ON DESIGN QUALIFICATIONS OF NOZZLE AND PIPE

The impact of the structural weld overlay was evaluated to demonstrate that the presence of the structural weld overlay repair does not have any adverse impact on the existing stress qualification of the RCS surge nozzle with respect to the Code of Construction [33].

Effects of SWOL on Transient Stress and Fatigue Analysis

Since the intention of the SWOL is to mitigate/repair the potentially cracked dissimilar-metal butt-weld at the RCS surge nozzle safe-end, the crack growth analyses discussed in Section 7.5 using the ASME Code Section XI methodology are acceptable bases to address the fatigue qualification of the weld overlay region for the RCS surge nozzle.

The original analysis was performed in accordance with the ANSI Code [33]. It offers protection against membrane or catastrophic failure, and protection against fatigue or leak type failure. The SWOL does not influence the reinforced region of the surge nozzle. Therefore, the existing analysis [34] remains applicable for this region, provided the loading used in [34] remains applicable. The transient stresses and structural evaluation for the weld overlay surge nozzle were documented in [7]. The primary stress for the RCS surge nozzle was evaluated by hand calculations in accordance with ANSI B31.7 [33]. Addition of the SWOL does not affect the B indices of the loads from the piping, but increases the section modulus in the overlay region. The applicable primary loads (pressure and mechanical loads) used in [34] are not changed by the SWOL. Therefore, the primary stresses in the structures with SWOL are, by definition, less than or equal to those without SWOL. The previous qualifications [34] performed for the surge line weld to nozzle safe-end applies to this calculation.

The fatigue for the RCS surge nozzle was evaluated with finite element techniques. Cut locations are illustrated in Figure 7-13. As Table 7-10 shows, all stress, thermal ratcheting, and fatigue results meet the requirements specified in ANSI B31.7 [33]. Therefore, it is concluded that the existing ANSI B31.7 analysis of the RCS surge nozzle is not adversely affected by the addition of the SWOL.

Table 7-10: RCS Surge Nozzle with SWOL Result Summary

Loading Condition	Stress Category	Cut No.	Stress (psi) or Usage	Stress Limit	Allowable Stress (psi) or Usage	Margin
Design	$P_L + P_b$	--	12,888	$1.5S_m$	28,050	54.05%
Level A/B	P + Q	2	32,985	$3S_m$	56,100	41.20%
	Linear Thermal Ratchet	7	0.477	N/A	1.000	52.26%
	Parabolic Thermal Ratchet	7	0.446	N/A	1.000	55.41%
	Fatigue	2	0.124	N/A	1.000	87.60%
Level C/D	$P_L + P_b$	--	16,484	$2.25S_m$	42,075	60.82%

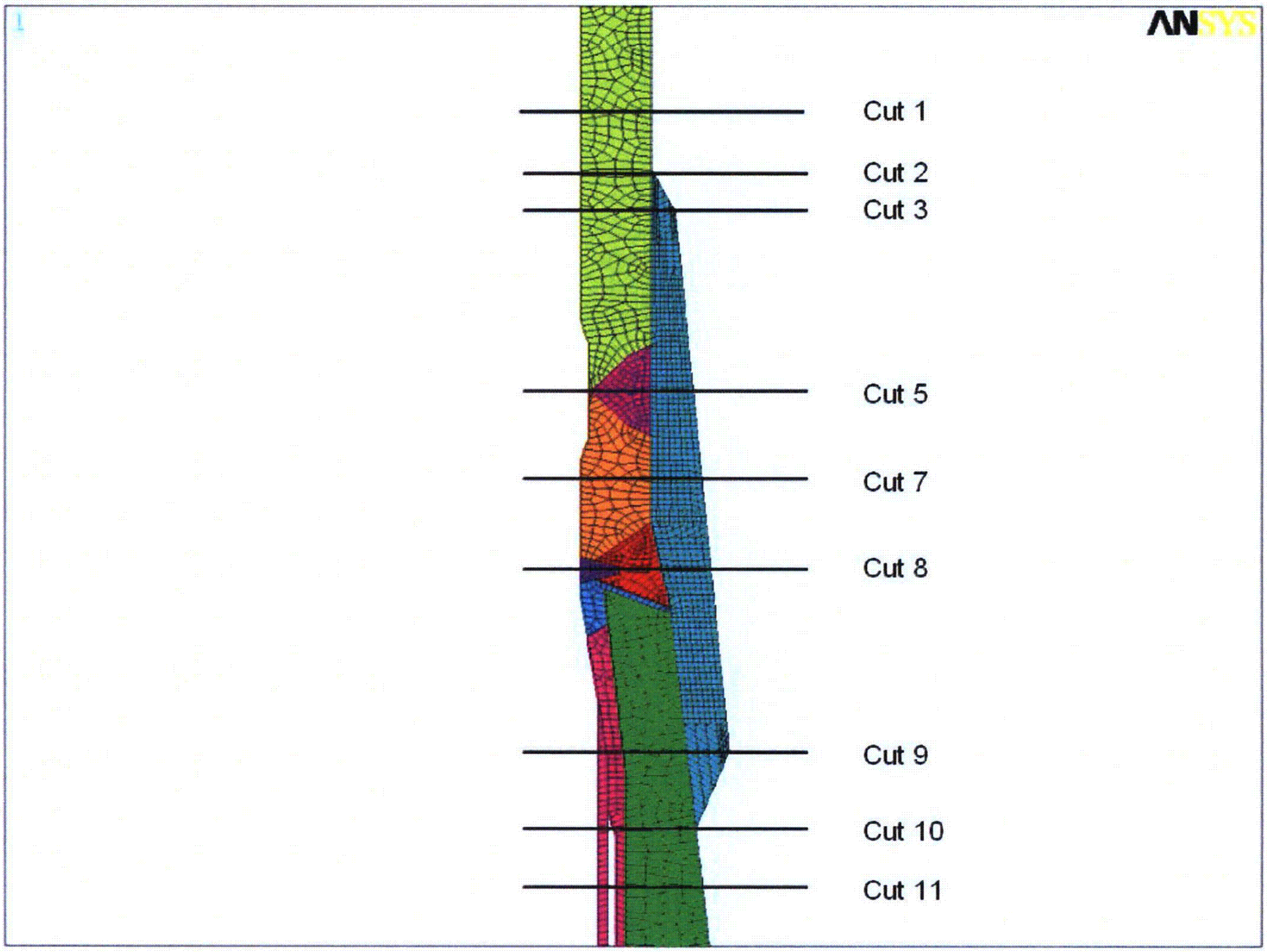

Figure 7-13: RCS Surge Nozzle Cut/Path Locations

Effects of Structural Weld Overlay on the Thermal Sleeve

The effect of the SWOL on the surge nozzle thermal sleeve is judged insignificant. The nozzle has a thermal sleeve welded on the inside diameter of the nozzle that shields the nozzle body. The thermal sleeve is not a pressure-retaining component, nor is it a load path for the piping forces and moments imposed on the nozzle. However, the impact of the weld overlay on the thermal sleeve partial fillet weld attachment to the nozzle is addressed in this section.

From a structural standpoint, the weld between the thermal sleeve and the nozzle is affected by pressure in the nozzle and thermal transients, and may displace relative to the nozzle. This has the potential to result in stresses that are expected to maximize near the attachment weld. The SWOL on the outside of the nozzle is not expected to have a significant detrimental effect on the stresses at the thermal sleeve attachment weld for the following reasons:

- If there is any effect, the relative displacement between the sleeve and the safe-end due to pressure loading is expected to be less with a SWOL because the whole nozzle is more restricted from expansion due to pressure.
- The response to a thermal transient is expected to be dominated by the differential temperature gradient through the sleeve thickness and its corresponding relative displacement to the internal nozzle surface responding to the same transient. Thermal stress in the sleeve thickness due to shock effects of the transient is not expected to change because the sleeve thickness has not changed. Thermal stress in the sleeve due to differential expansion of the sleeve and the nozzle inside surface is not expected to be significant. This is due to the large difference in stiffness of the sleeve and the nozzle, essentially making the nozzle a fixed attachment point. Therefore, thermal stresses in the sleeve attachment are not expected to be effected by the SWOL material on the outside surface of the nozzle.

These reasons are supported by the stress results taken from the analysis at the thermal sleeve location shown in Figure 7-14. The stresses were evaluated for the design condition and the thermal transients. Then, these stresses were compared to the limits of the ANSI Code for basic stress intensity limits. Table 7-11 shows the stresses for the primary membrane (P_m), primary membrane plus bending (P_L + P_b), and primary plus secondary stresses (P + Q), and compares these stresses against the limits of ANSI Code [33]. The primary stresses, P_m and $P_L + P_b$, are the maximum stresses from the Design and Level C condition. The primary plus secondary stresses, P + Q, are the maximum stresses from the thermal transients.

Effects of Additional Mass on Piping/Support System

The impact of the addition of weld overlay material on the existing primary stress qualification, which considers deadweight and dynamic loadings (such as those due to earthquake), was evaluated in [36], and found to be insignificant.

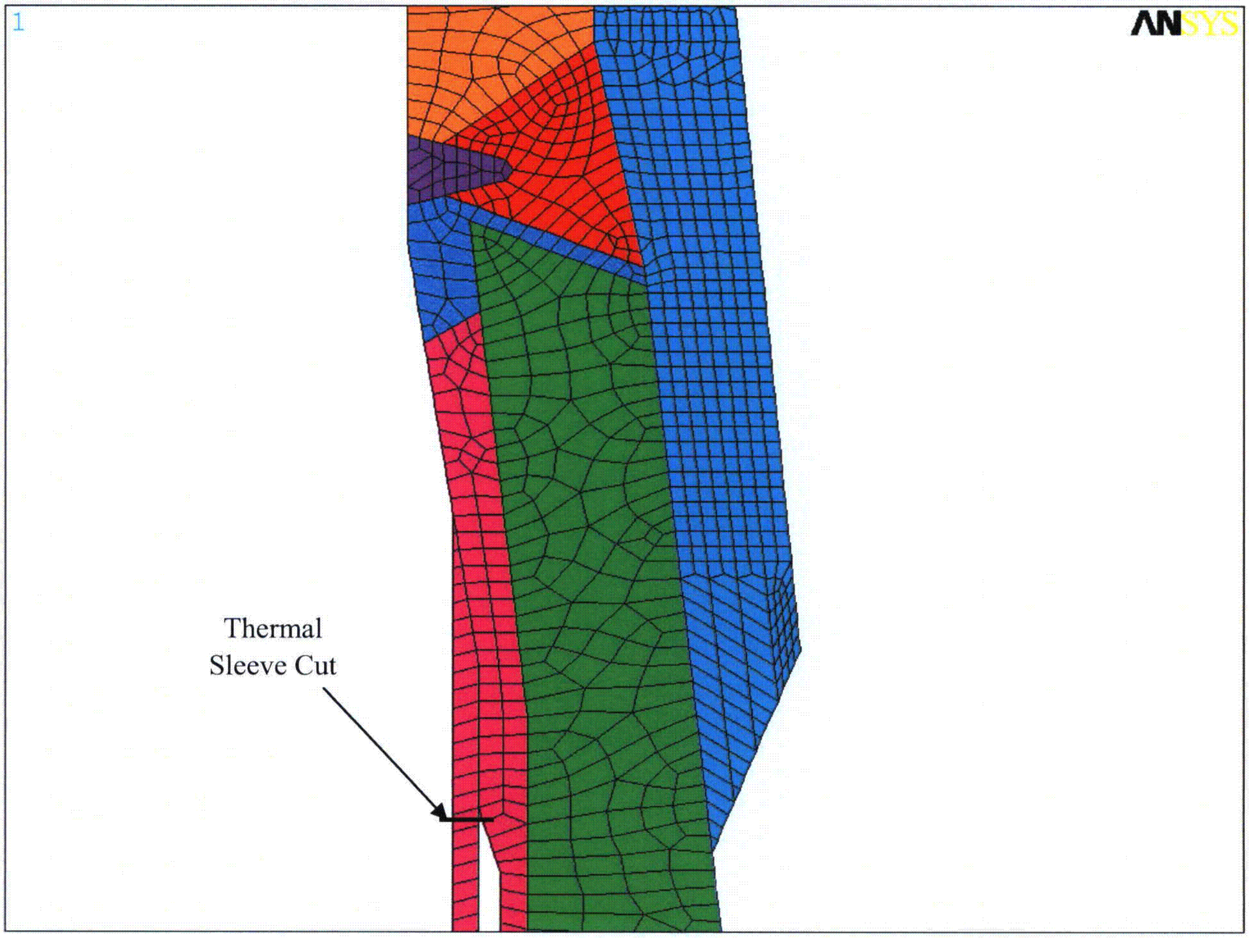

Figure 7-14: Thermal Sleeve Cut Location

Table 7-11: Thermal Sleeve Stresses

Stress Category	Stresses (psi)	Allowable Stress (psi)	Margin[(1)]
P_m	10,934	15,300	28.54%
$P_L + P_b$	15,991	22,950	30.32%
P + Q	27,743	45,900	39.56%

Notes: [(1)] Margin = [1 – (Actual/Allowable)] x 100%

8 WELD OVERLAY DESIGN QUALIFICATION ANALYSIS: RCS SHUTDOWN COOLING NOZZLE

8.1 INTRODUCTION

This section provides the WOL design qualification analysis to demonstrate the adequacy of the SWOL design for the RCS shutdown cooling nozzle. The effectiveness of a WOL with Alloy 52/52M weld material is demonstrated using crack growth analysis, per IWB-3640 [6], to ensure that the WOL does not deteriorate during service. Using the residual weld stresses developed by the finite element model of the WOL process, future crack growth was evaluated at the shutdown cooling nozzle safe-end weld locations using the operational design transients affecting the WOL region. The advantage of the Alloy 52/52M material is its high resistance to PWSCC, which minimizes the possibility for future PWSCC crack growth. Since the purpose of the SWOL is to mitigate/repair a potentially cracked dissimilar-metal butt-weld, performing crack growth analyses using the ASME Code Section XI methodology is the accepted method to address the fatigue qualification of the WOL region for the RCS shutdown cooling nozzle.

The effect of the SWOL on the existing fatigue qualification of the RCS shutdown cooling nozzle outside the WOL region is addressed in accordance with ANSI B31.7 [33] requirements, considering the effect of the applicable thermal transient stresses, structural discontinuities, and bimetallic effects resulting from the SWOL.

8.2 LOADS

The loads used for the design of the shutdown cooling nozzle weld overlay are listed in Table 8-1. These loads are considered in [2] and specified in [31]. The load combinations considered in the design are listed in Table 8-2. The transients considered in the shutdown cooling nozzle FCG evaluation are shown in Table 8-3. The pipe end loads used for fatigue and FCG evaluations are listed in Table 8-4. These loads are considered in [7] and specified in [31]. The nozzle loads and transients used for the design and FCG analysis are bounding for the actual nozzle loads and the plant-specific transients [7, 31, and 30].

Table 8-1: Enveloping Shutdown Cooling Nozzle Loads Used for Weld Overlay Design [31]

Load Type	Axial Force F_a (kips)	Bending Moment M_b (in-kips)
DW	2.123	83.223
OBE	7.840	367.350
SSE	15.679	734.701

Notes:
DW = Deadweight Loads
OBE = Operating Basis Earthquake Loads
SSE = Safe Shutdown Earthquake Loads

Table 8-2: Load Combinations

Condition	Load Combination	Service Level
Design	DP + DW + DS	Design
Normal/Upset	TR[1] + DW + NT[1]	Level A/B
Emergency	DP + DW + MS + NT[1]	Level C
Test	TP + DW	Test

Notes:
1. Not applicable to WOL design sizing
DW = Deadweight
DP = Design Pressure
TP = Test Pressure
TR = Level A/B Transient Loadings (Thermal and Pressure)
NT = Thermal Expansion
DS = Design Seismic
MS = Maximum Seismic

Table 8-3: Applicable Thermal Transients for RCS Shutdown Cooling Nozzle

Number	Transient	Cycles	Level
1	Plant Heatup, 100°F / hr	500	A
2	Plant Cooldown, 100°F / hr	500	A
3	Plant Loading, 5% / min	15,000	A
4	Plant Unloading 5% / min	15,000	A
5	Step Load Increase 10%	2,000	A
6	Step Load Decrease 10%	2,000	A
7	Reactor Trip	400	B
8	Loss of Turbine Generator Load	40	B
9	Loss of Secondary Pressure	5	C
10	Hydrostatic Test	10	TEST
11	Leak Test	200	TEST
12(1)	Seismic (Positive)	200	B
13(1)	Seismic (Negative)	200	B
14	Zero Load	710(2)	-

Notes:
(1) The design specification [30] states 200 cycles of operational basis earthquake and 200 cycles of design basis earthquake. For this analysis, 400 cycles of design basis earthquake will be used.
(2) The total cycles for this transient consist of 500 Heatup and Cooldown cycles, 10 Hydrostatic Test cycles, and 200 Leak Test cycles.

Table 8-4: Enveloping Shutdown Cooling Nozzle Loads for Fatigue and FCG Evaluations

Load Conditions	Force (kips)			Moment (in-kips)		
	Fx	Fy	Fz	Mx	My	Mz
Deadweight	-0.047	-2.664	-0.369	-76.660	-15.004	46.068
Thermal	-3.942	8.516	11.125	-421.617	-558.828	-543.156
Design Seismic	2.534	7.842	2.097	302.464	150.998	153.552
Maximum Seismic	5.068	15.684	4.194	604.928	301.996	307.104

Note:

Axial force = $-0.866*F_y+0.5*F_y$
Shear force = SQRT $[F_x^2+(0.5*F_y+0.866*F_z)^2]$
Torsion moment = $-0.866*M_y+0.5*M_z$
Bending moment = SQRT $[(M_x^2+(0.866*M_z+0.5*M_y)^2)]$

8.3 WELD OVERLAY DESIGN SIZING

The minimum WOL thickness was determined based on a through-wall flaw in the original pipe. The methodology used to determine the WOL design thickness and length is discussed in Section 3. Using that methodology, radii from the design geometry, shown in Table 8-5, are used to design the minimum SWOL parameters. As-designed inside and outside radii at the thickest portion of the Alloy 82/182 and SS welds are presented here. The thickest portion results from considering the smallest inner radius (R_{i-min}) and the largest outer radius (R_{o-max}). By using the maximum wall thickness of the design geometry, a conservative SWOL design thickness and length is achieved. The WOL length was based conservatively on the recommended length, per Code Case N-740:

$$L_{WOL} = 0.75\sqrt{Rt}$$

where,

$R = R_{o-max}$ = outside radius
$t = R_{o-max} - R_{i-min}$ = wall thickness at the location of indication

The WOL length (L_{WOL}) will extend from the weld/base metal interface on either side of the Alloy 82/182 and SS welds, as shown in Figure 8-1. The WOL thickness (t_{WOL}) was determined using the following equation:

$$t_{WOL} = t/0.75 - t$$

The minimum WOL design dimensions are shown in Table 8-6.

In accordance with ASME Section XI IWB-3640, the criterion from Section XI, Appendix C is used to evaluate the maximum post-WOL stresses resulting from the actual applied loadings. To determine the applied post-WOL stresses, the minimum post-WOL thicknesses are considered. This produces a conservative method to determine stresses for comparison to the allowable stress criterion. The thinnest portion of the Alloy 82/182 and SS welds results from considering the largest inner radius (R_{i-max}) and the smallest outer radius post-WOL ($R_{o-min-WOL}$). These parameters and the resulting geometric section properties are presented in Table 8-7.

The applied bending stresses were calculated by:

$$\sigma_b = \frac{M_b}{Z}$$

M_b is per Table 8-1, and Z is per Table 8-7.

$$Z = \frac{\pi(R_{o-\min-wol}^{\ 4} - R_{i-\max}^{\ 4})}{4(R_{o-\min-wol})}$$

$R_{i\text{-max}}$ and $R_{o\text{-min-wol}}$ are per Table 8-7

The applied membrane stresses were calculated by:

$$\sigma_m = \sigma_p + \frac{F_a}{A_x}$$

where,

$$\sigma_p = \frac{\pi R_{i-\max}^{\ 2}}{\pi\left(R_{o-\min-wol}^{\ 2} - R_{i-\max}^{\ 2}\right)} P$$

F_a is per Table 8-1.

A_x is per Table 8-7.

$A_x = \pi\ (R_{o\text{-min-wol}}^2 - R_{i\text{-max}}^2)$

$R_{i\text{-max}}$ and $R_{o\text{-min-wol}}$ are per Table 8-7.

P = 2,235 psig [2]

The allowable stress intensity S_m (at 650°F) used in the sizing of the Alloy 52/52M (N06690) overlay is 23.3 ksi [9]. This allowable is based on the annealed condition of SB-166/SB-167. The normal operating pressure of 2,235 psig was used for the calculation.

The resulting stresses, determined by using the previous equations, as well as the loads and load combinations from Tables 8-1 and 8-2, respectively, are listed and compared to the Code allowable in Table 8-8.

Table 8-5: Shutdown Cooling Nozzle Geometry for WOL Design Calculations [2]

Alloy 82/182 Weld			Stainless Steel Weld		
Inside Radius $R_{i\text{-min}}$ (in)	**Outside Radius $R_{o\text{-max}}$ (in)**	**Wall Thickness t_{design} (in)**	**Inside Radius $R_{i\text{-min}}$ (in)**	**Outside Radius $R_{o\text{-max}}$ (in)**	**Wall Thickness t_{design} (in)**
5.063	6.547	1.485	5.250	6.375	1.125

Table 8-6: Shutdown Cooling Nozzle Minimum Weld Overlay Repair Design Dimensions [2]

Alloy 82/182 Weld		Stainless Steel Weld	
t_{WOL} (in)	L_{WOL} (in)	t_{WOL} (in)	L_{WOL} (in)
0.70	2.34	0.38	2.01

Table 8-7: Shutdown Cooling Nozzle Geometry for Stress Check in Post-Weld-Overlay Condition [2]

Alloy 82/182 Weld				Stainless Steel Weld			
Inside Radius $R_{i\text{-}max}$ (in)	Outside Radius $R_{o\text{-}min\text{-}WOL}$ (in)	Cross-Sectional Area A_x (in^2)	Section Modulus Z (in^3)	Inside Radius $R_{i\text{-}max}$ (in)	Outside Radius $R_{o\text{-}min\text{-}WOL}$ (in)	Cross-Sectional Area A_x (in^2)	Section Modulus Z (in^3)
5.063	6.875	67.974	180.179	5.370	6.755	52.757	145.398

Table 8-8: RCS Shutdown Cooling Nozzle Post-SWOL Stress Comparison [2]

	Normal/Upset		Emergency/Faulted	
Location	Applied Stress σ_b (ksi)	Allowable Stress P_b (ksi)	Applied Stress σ_b (ksi)	Allowable Stress P_b (ksi)
Alloy Weld	2.501	8.416	4.540	19.369
SS Weld	3.099	6.876	5.625	17.469

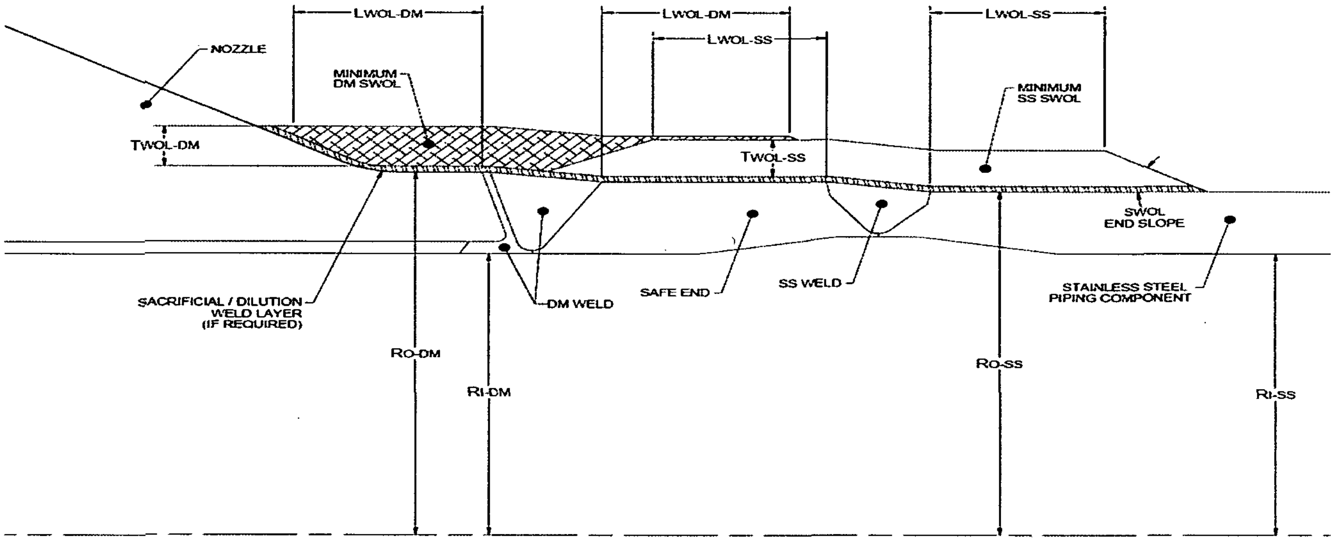

Figure 8-1: Weld Overlay Design Parameters for the Shutdown Cooling Nozzle

(Not drawn to scale.)

8.4 WELD OVERLAY RESIDUAL WELD STRESS RESULTS

As described in Section 5.3, the finite element model was developed to capture the parts of the structure in the vicinity of the shutdown cooling nozzle safe-end with the SWOL. This includes a portion of the shutdown cooling nozzle attached to the nozzle safe-end and a length of SS pipe attached to the safe-end. An ID weld repair was considered in the finite element model. The finite element model and boundary conditions are shown in Figures 8-2 and 8-3. The nozzle is fixed in the axial direction to simulate the rest of the nozzle. The end of the SS piping is coupled in the axial direction to simulate the remaining portion of the SS piping not included in the model. The model assumes that a 50% through-wall weld was preformed from the inside surface of the shutdown cooling nozzle to the safe-end Alloy 82/182 butt-weld.

The final residual weld stresses, including normal operating pressure and temperature conditions, are shown in Figures 8-4 and 8-5 for selected stress cuts in the Alloy 82/182 and SS welds. The locations of the stress cuts are provided in Figure 8-2. The axial and hoop stress contours in the RCS shutdown cooling nozzle after the WOL application are provided in Figures 8-6 and 8-7.

Figure 8-4 shows the axial and hoop residual stresses for the Alloy 82/182 weld at normal operating conditions after the SWOL. The stresses are compressive up to about 88% of the original pipe wall thickness. This stress distribution is favorable due to the generally compressive stress field, which minimizes the potential for crack growth in the DM weld region. Figure 8-5 shows the axial and hoop stresses for the stainless weld, which remain compressive for about 86% of the original pipe wall at normal operating conditions. Therefore, the potential for FCG in the SS weld is also minimized.

Acceptable post-WOL residual stresses (i.e., stresses that satisfy the requirements for mitigating PWSCC) are sufficiently compressive over the entire length and circumference of the inside surface of the Alloy 82/182 weld (at operating temperature, but prior to applying operating pressure and loads). Acceptable post-WOL residual stresses have a resulting total stress, after application of operating pressure and loads, that remains less than 10 ksi tensile [28]. This target level has been selected as a conservatively safe value, below which PWSCC initiation, or growth of small initiated cracks, is unlikely. Additionally, the residual plus operating stresses must remain compressive through some portion of the weld thickness away from the inside surface. The residual stresses in the Alloy 82/182 weld of the RCS shutdown cooling nozzle, resulting from the WOL, are well below this stress level through 88% of the original weld thickness.

Figures 8-8 and 8-9 show the axial and hoop stresses on the inside surface (in the vicinity of the alloy weld and buttering) remain compressive after SWOL. The maximum resultant bending moment for the normal operating condition is 908 in-kips. The resulting maximum bending stresses in the Alloy 82/182 weld and SS weld are 4.0 ksi and 5.2 ksi, respectively [32]. The pipe bending stresses are low, and are considered to have a negligible effect on the residual weld stress results

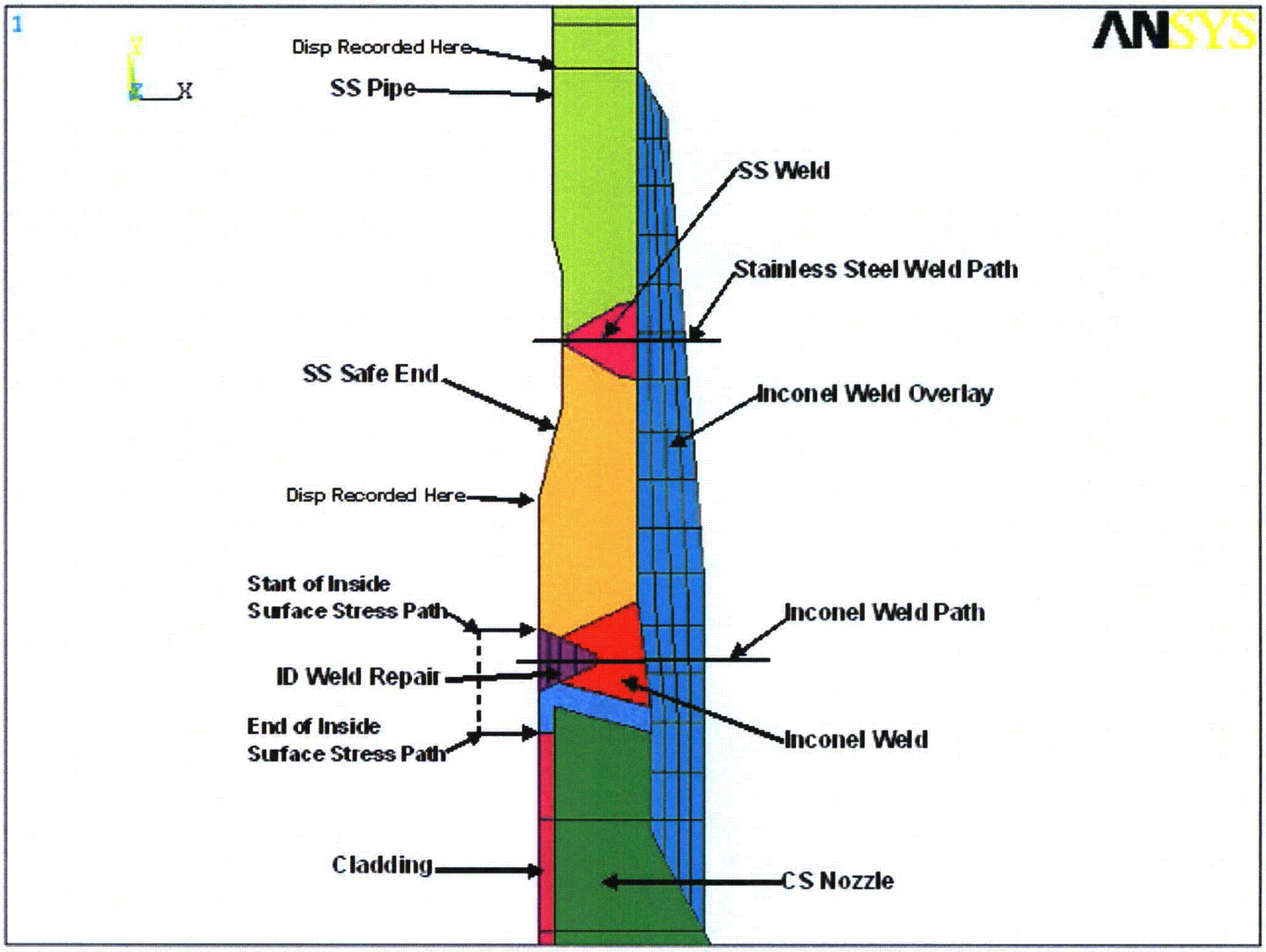

Figure 8-2: ANSYS Model of Shutdown Cooling Nozzle

Note: CS = Carbon Steel

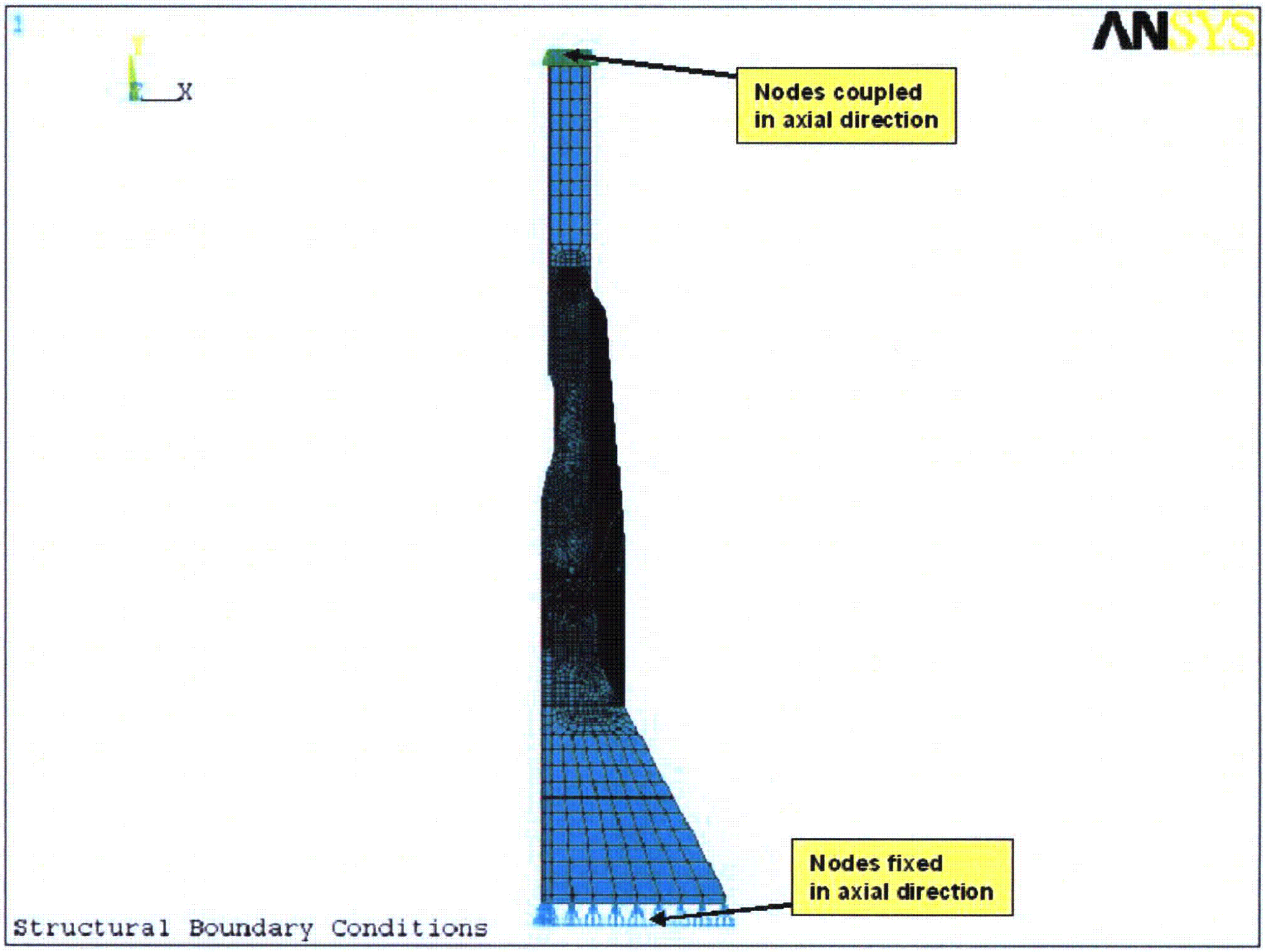

Figure 8-3: Finite Element Model and Structural Boundary Conditions

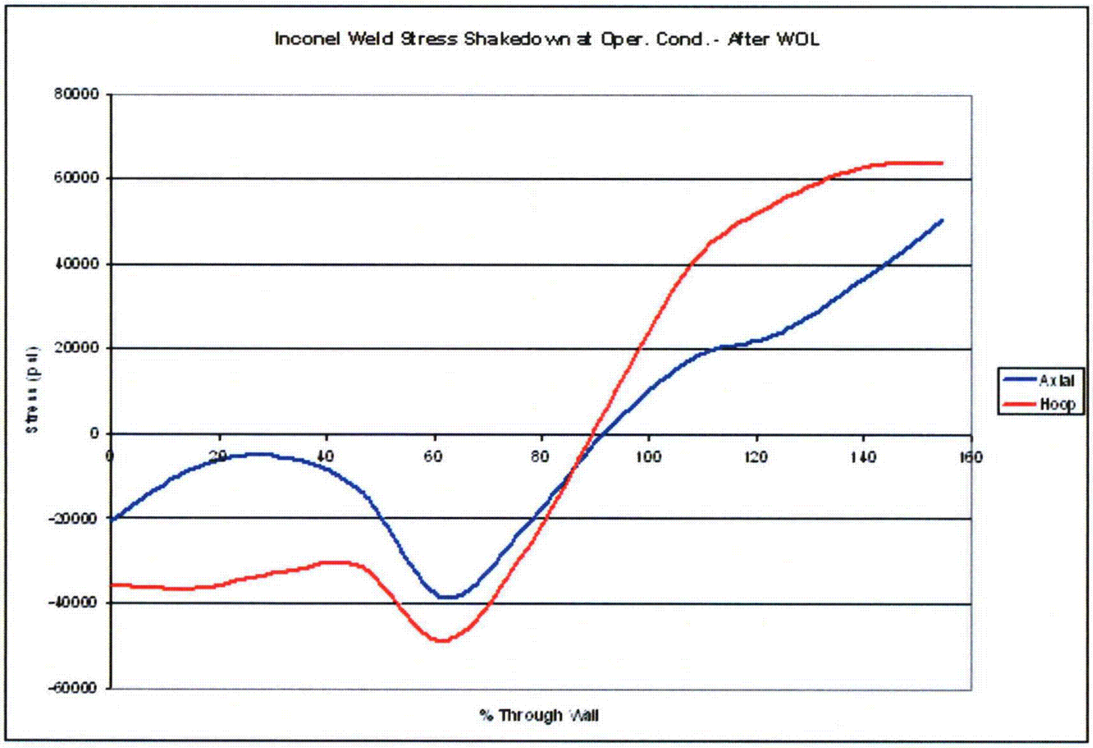

Figure 8-4: Axial and Hoop Residual Stresses in the Alloy 82/182 Weld at Operating Conditions*

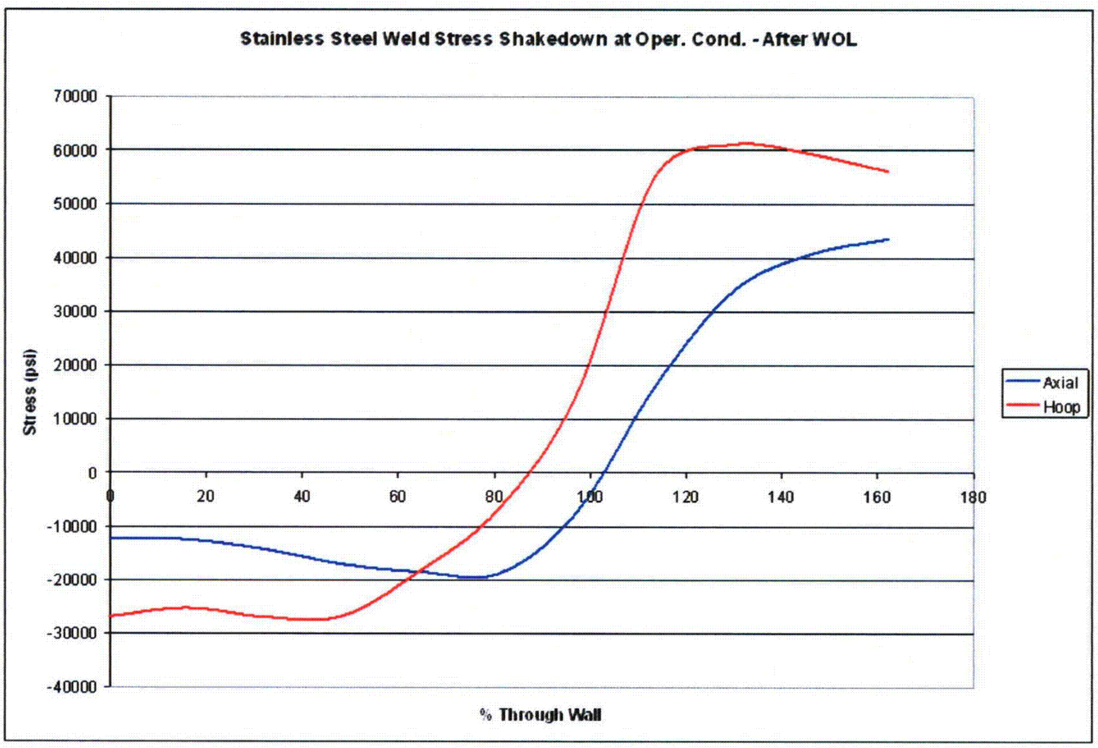

Figure 8-5: Axial and Hoop Residual Stresses in the SS Weld at Operating Conditions*

*Note: The percent through-wall indicated on the horizontal axis is expressed in terms of the original pipe wall thickness. The WOL region is the region beyond 100% wall thickness.

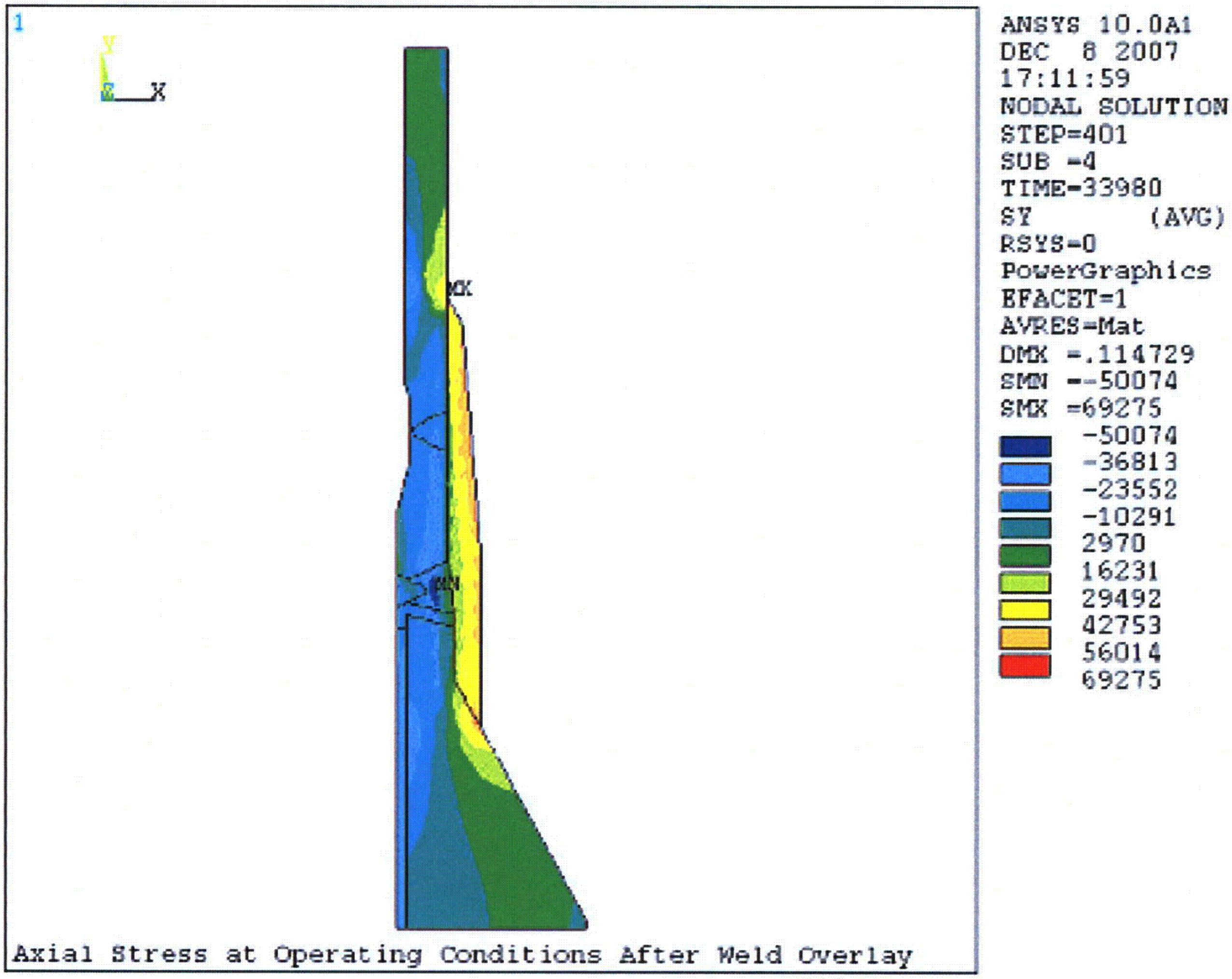

Figure 8-6: Axial Stress (psi) Contour Plot at Operating Condition after the Weld Overlay

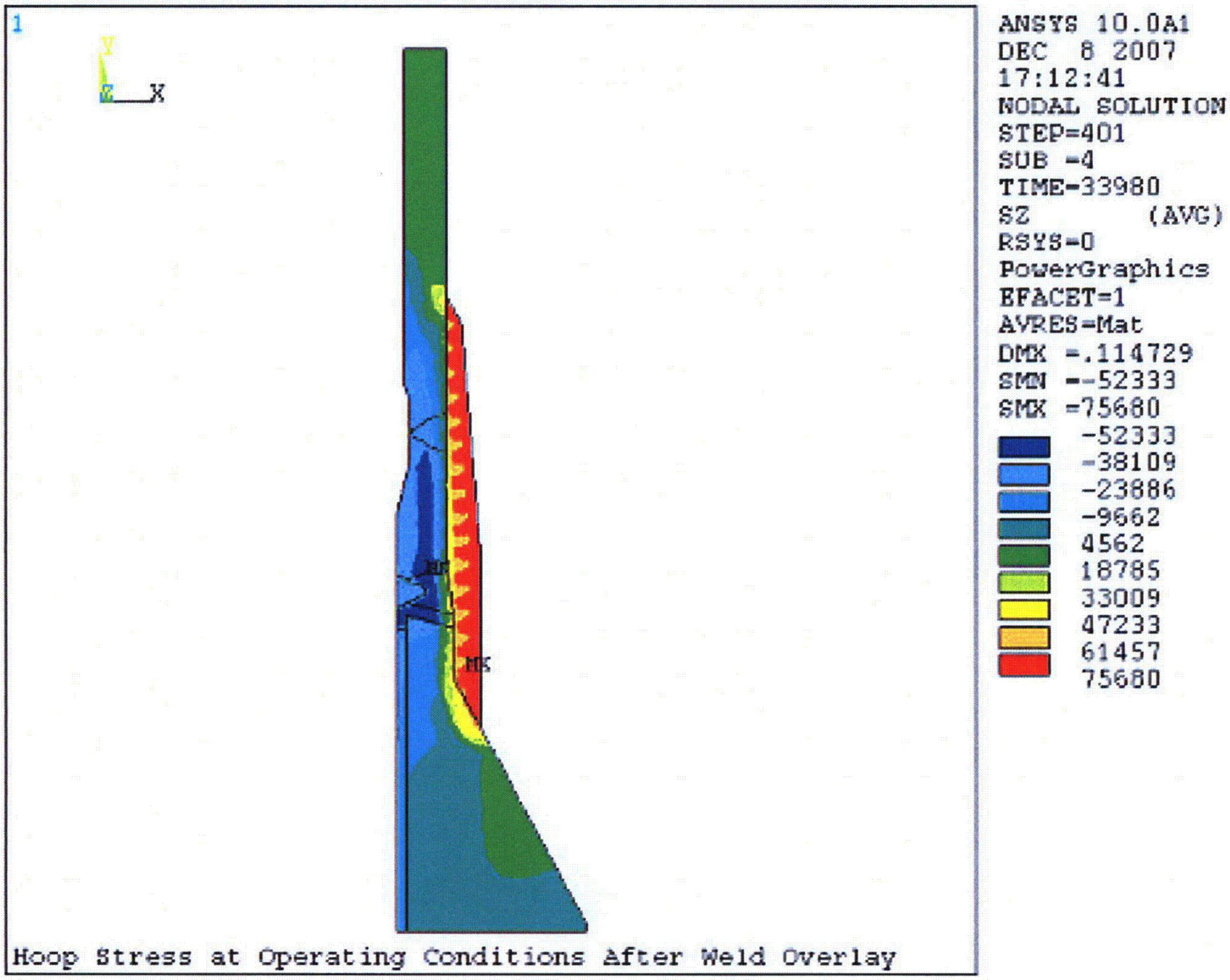

Figure 8-7: Hoop Stress (psi) Contour Plot at Operating Condition after the Weld Overlay

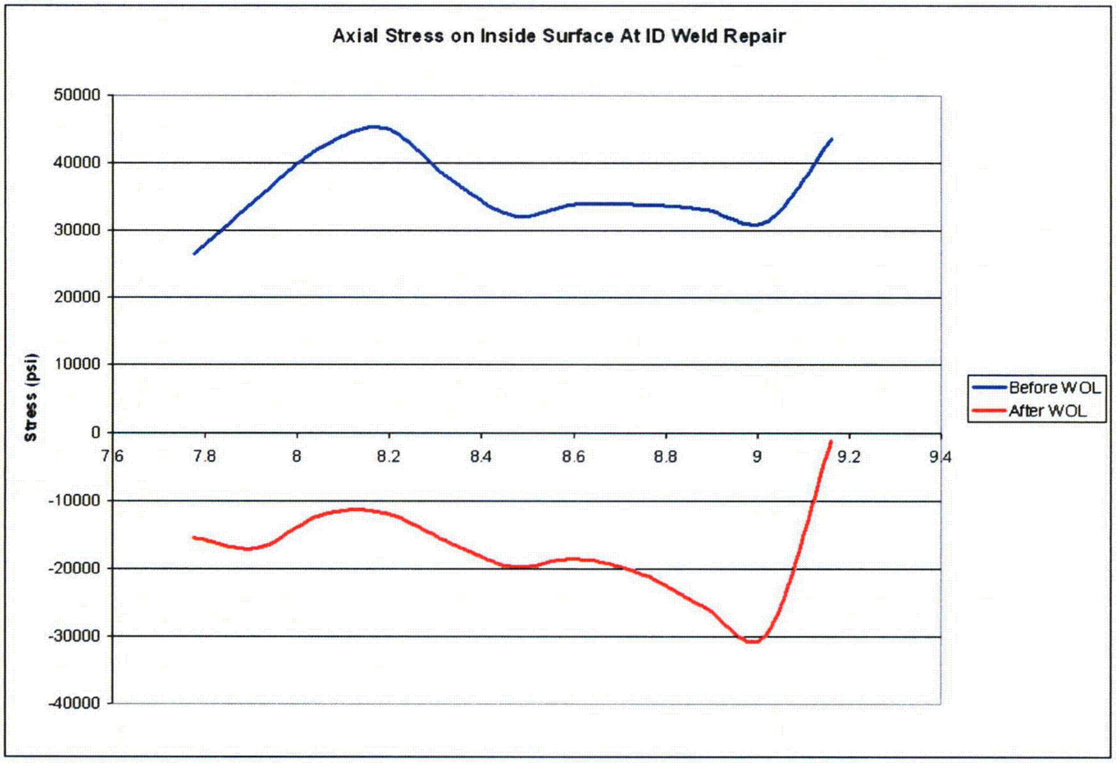

Figure 8-8: Axial Residual Stress along the Inside Surface at Operating Condition*

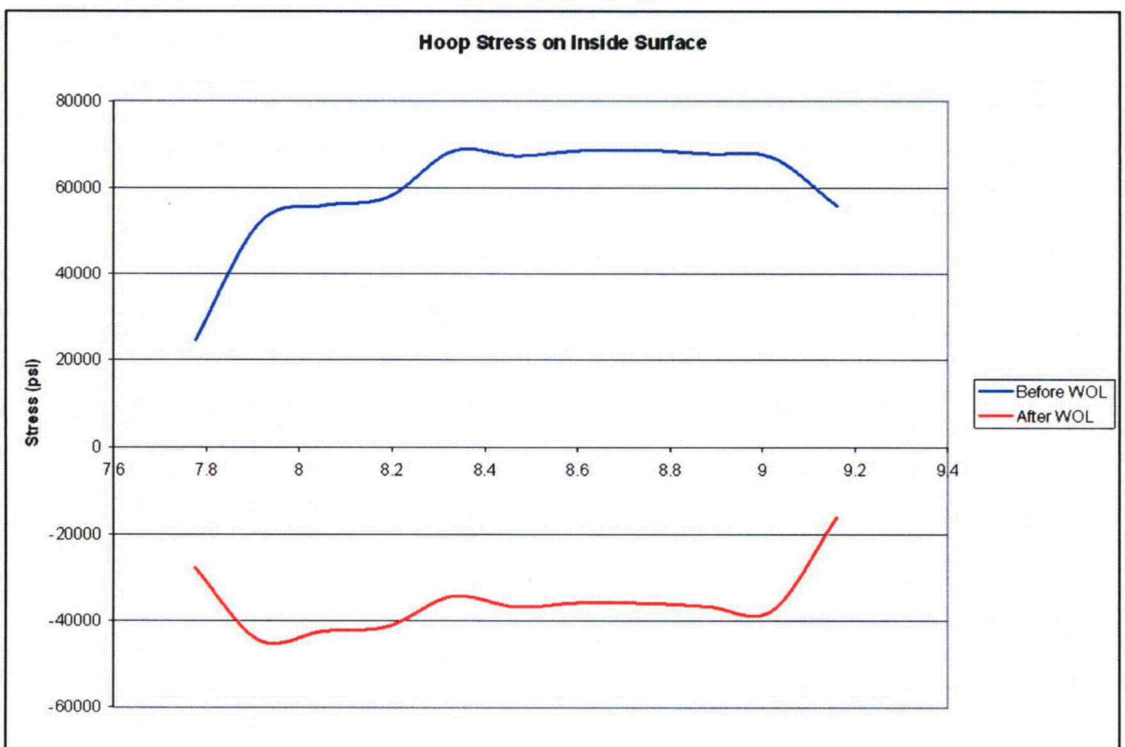

Figure 8-9: Hoop Residual Stress along the Inside Surface at Operating Condition*

*Note: X-axis is the FEA model axial location (inch). See Figure 8-2.

8.5 FATIGUE CRACK GROWTH RESULTS AND ESTIMATE OF WELD OVERLAY DESIGN LIFE: SHUTDOWN COOLING NOZZLE REGION

The methodology used to determine fatigue crack growth is described in Section 4.4. Fatigue crack growth analyses were performed for the RCS shutdown cooling nozzle using the through-wall stress distribution including residual stresses generated from the weld overlay mitigation/repair process and the thermal transient stresses.

The weld overlay service life is a function of the flaw depth found in the region being overlaid, and the projected growth of that flaw. The allowable maximum flaw depth is 75% of the piping wall thickness (including the weld overlay thickness), per Section XI, IWB-3640 [6].

A range of possible flaw sizes, from 0 to 100% of the original design wall thickness, were postulated in the fatigue crack growth evaluations. The results of these evaluations for the flaw depths less than the original design wall thickness are plotted in figure 8-10 and 8-11, in the form of expected time for these flaws to reach the interface between the original wall and the newly laid weld overlay material. Figure 8-10 shows results for the Alloy 82/182 weld, and Figure 8-11 shows results for the SS weld. For the maximum possible flaw depths of 100% of the original design wall thickness propagating into the Alloy 52/52M weld overlay material, results are show in Figure 8-12. This figure shows the estimated flaw depth with time for the design cycles spread over either the original design life or the extended life of the plant.

Figures 8-10 and 8-11 summarize the expected service life (based on transient cycles spread evenly for either 40 years or 60 years of plant life) for a given initial flaw depth to reach 100% of the original wall thickness at the Alloy 82/182 weld and the SS weld locations, respectively. Based on the results shown in Figures 8-10 and 8-11, it can be concluded that if no flaws are detected during the post-SWOL inspection, a conservatively assumed flaw extending 75% through the original wall would not grow to 100% of the original wall thickness for 40 years FCG due to transient cycles. This is based on the assumption that the current 40-year design transient cycles are spread evenly over 40 years of plant life. If flaws are detected during the post-SWOL inspection, the as-found flaw size can be used to determine the design life of the SWOL using the crack growth results shown in Figures 8-10 and 8-11.

For the case of an initial flaw depth of 100% of the original wall thickness, i.e., a through-wall flaw, Table 8-9 shows that the total flaw growth into the newly laid Alloy 52/52M welds material in 40-year is 0.043 inch. The final flaw depth after the 40-year period with the fatigue crack growth considered is still within 75% of the total post-WOL wall thickness, as required by SWOL criteria.

Two examination scenarios exist: a pre-overlay examination and a post-overlay examination. If an examination found no flaws, the overlay service life would be governed by the largest flaw that might have been missed by the examination. For an examination performed prior to the weld overlay installation, a conservative approach would be to assume that the flaw depth is 10% of the original wall thickness. Alternatively, this would be 75% of the original wall for an examination performed after the weld overlay installation. This is because the area required to be inspected after the overlay is only the outer 25% of the original pipe thickness plus the overlay thickness itself. The PDI qualification blocks do not contain any flaws in the inner 75% of the pipe wall; therefore, it would be conservative to assume such a flaw for the qualification. As shown in Figure 8-10, an initial flaw as deep as 75% would result in a remaining service life of 100% of the original design cycles. If the design cycles are assumed to be spread over 40 years of plant operation, the remaining life of the SWOL would be 40 years. This is well beyond the required 10-year in-service inspection (ISI) interval. If, after the next ISI, no flaws are detected in the outer 25% of the original welds, the SWOL life is 40 years from the time of the latest inspection.

In the unlikely event that the post-overlay inspection detected a flaw that is as large as the full depth of the original design wall thickness, the expected service life of the weld overlay is at least one 10-year inspection interval period. For the shutdown cooling nozzle, flaw growth rate into the weld overlay material is small or negligible, which indicates the expected service life of the repair would be 40 years if the transient cycles are spread over original design life of 40 years.

For example, if an axial flaw that is 95% through the original Alloy 82/182 wall thickness is detected as a result of the post weld overlay inspection, and assuming conservatively that the current 40-year design transient cycles are spread evenly for only 40 years, the expected service life from Figure 8-10 for this flaw to reach 100% of the original wall thickness is about 28 years. If it is assumed that the design transient cycles are spread evenly for 60 years, the remaining service life would be 42 years. This can also be determined by applying a factor of 1.5 to the service life based on the 40-year design cycles. For a similar size circumferential flaw, the expected service life is about 40 years, based on current 40-year design transient cycles assumed to be spread evenly over 40 years. Since the typical in-service inspection interval is 10 years for this initial flaw depth of 95%, it can be concluded that the sizing of the structural weld overlay is adequate up to the next inspection period based on the current 40-year design transient cycles spread evenly over the next 40 years.

Another case of 100% original design wall thickness through-wall flaw was hypothesized assuming the total post-WOL wall of 2.184 inches. This included an extra allowance of 0.2 inch for the FCG in the Alloy 690 material. This 100% original wall axial flaw was evaluated for the FCG results, shown in Table 8-9 and in Figure 8-12. Results demonstrate that the total growth in 40 years is approximately 0.043 inch. The final flaw depth after 40 years FCG is within 75% of the total post-WOL wall thickness, as required by SWOL criteria. Therefore, the 0.2 inch SWOL thickness increase provided in the SWOL design is adequate to address the issue of PWSCC for an almost through-wall flaw.

The actual time required to use the remaining design cycles depends on plant operating practice.

Table 8-9: Shutdown Cooling Nozzle Alloy 52/52M FCG Data – Axial Flaw [35]

Nozzle Thickness (in)	Initial Flaw Depth (in)	Final Flaw Depth in 40 years (in)	Total Flaw Growth in 40 years (in)
2.184	1.409	1.452	0.043

Notes:
(1) This thickness is due to a 0.2 inch increase in SWOL thickness.
(2) A review of transient stresses indicates that a rise time of 5,000 seconds is conservative for use in Alloy 52/52M FCG rate.

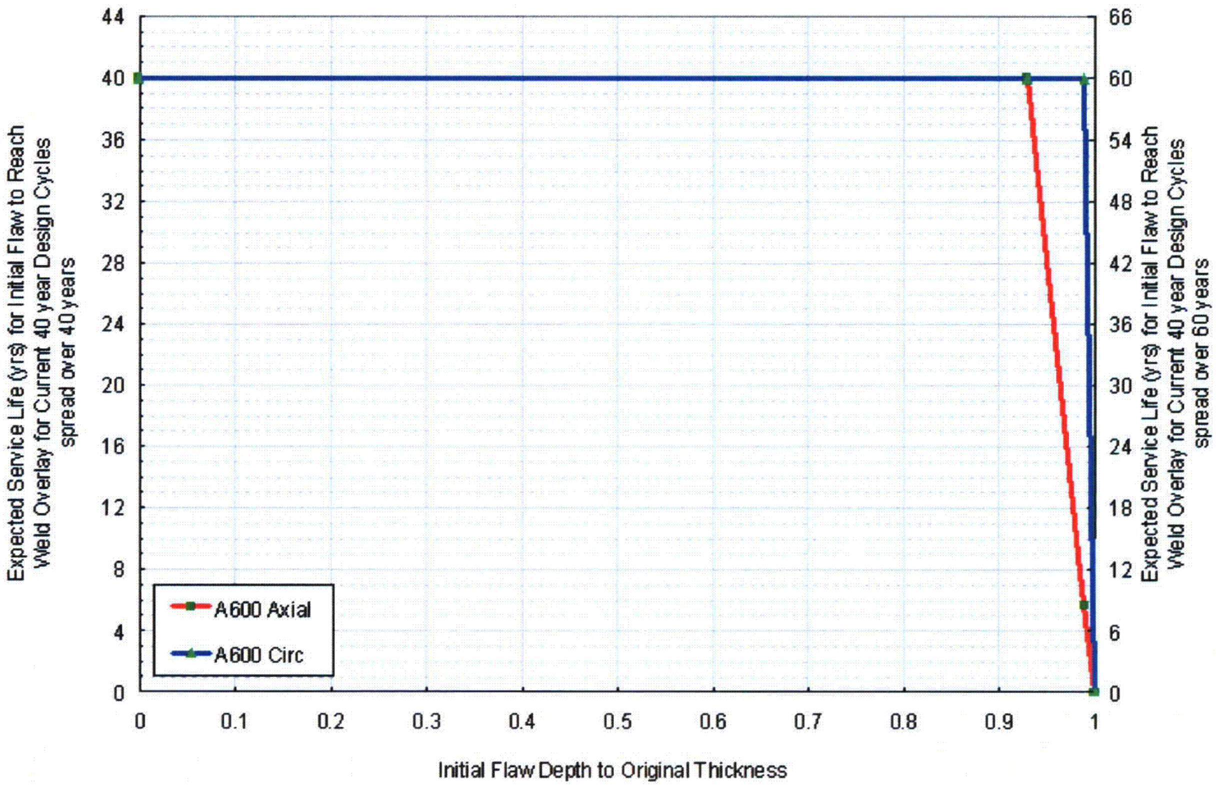

Figure 8-10: Expected Time for the Initial Flaw Depth to Reach the Weld Metal Interface for SDC Nozzle Alloy 82/182 Weld [35]

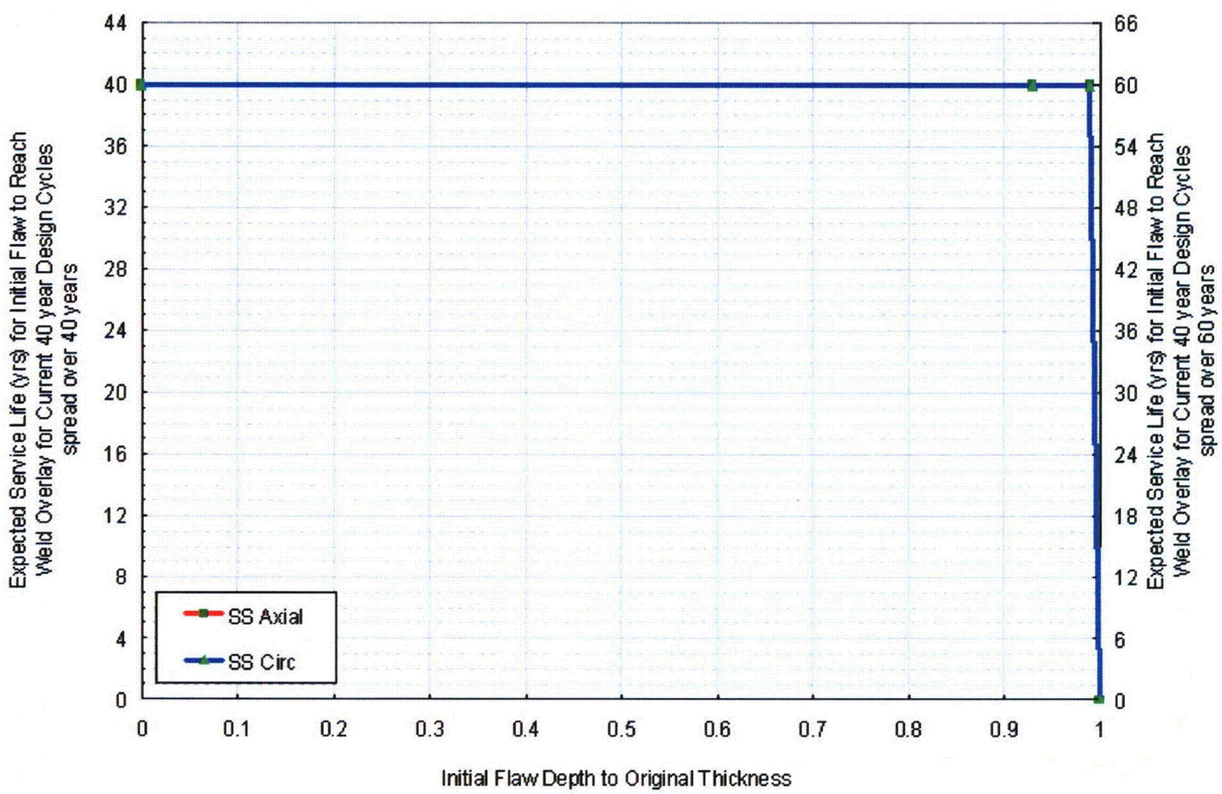

Figure 8-11: Expected Time for the Initial Flaw Depth to Reach the Weld Metal Interface for SDC Nozzle SS Weld [35]

Note: Curves for axial and circumferential flaw estimated life coincide with each other. Hence, only one curve is visible in the figure above.

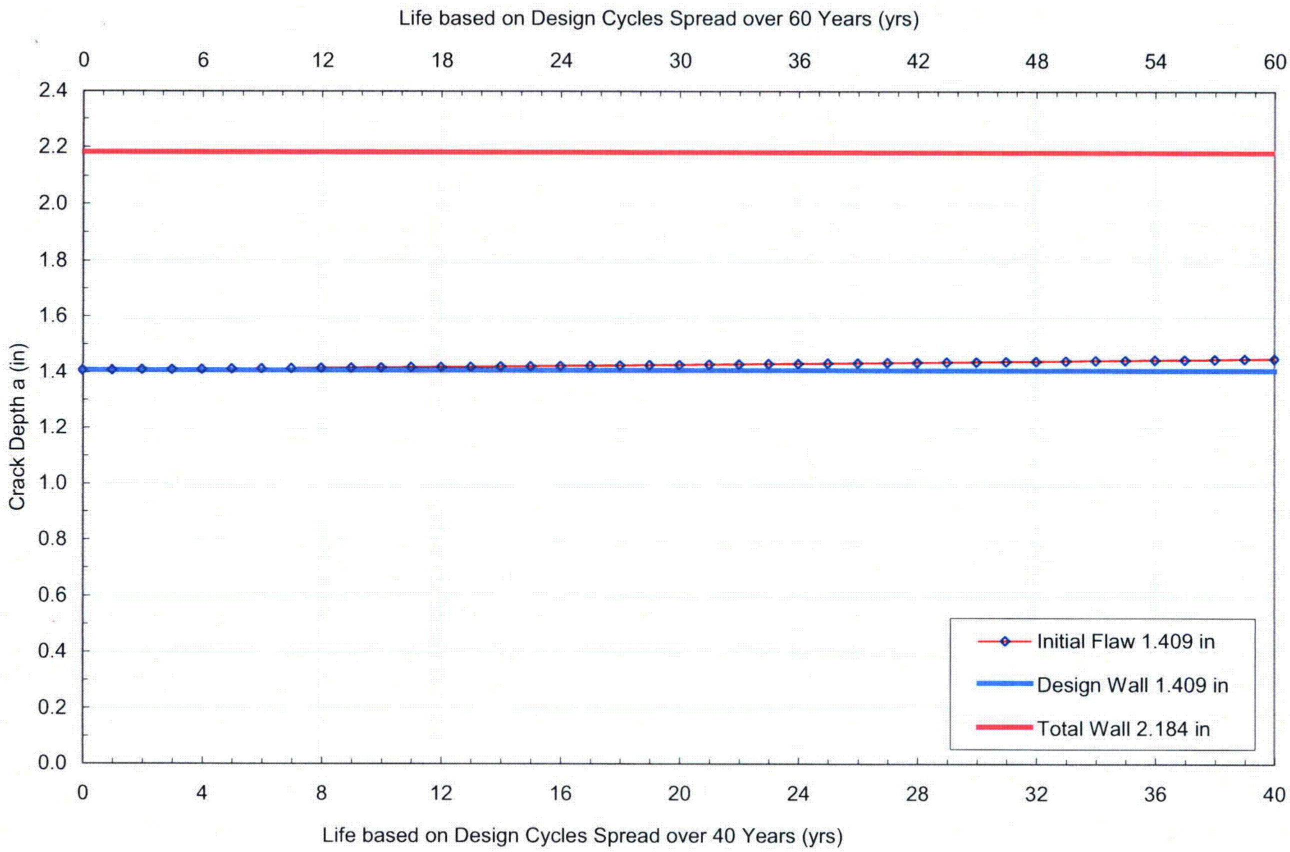

Figure 8-12: Axial Flaw Growth for 100% Original Wall Thickness Initial Flaw versus Service Period in Alloy 52/52M at SDC Nozzle Alloy Weld [35]

8.6 IMPACT ON DESIGN QUALIFICATIONS OF NOZZLE AND PIPE

The SWOL was evaluated to demonstrate that the presence of the SWOL repair does not have any adverse impact on the existing stress qualification of the RCS shutdown cooling nozzle with respect to the Code of Construction [33].

Effects of SWOL on Transient Stress and Fatigue Analysis

Since the intention of the SWOL is to mitigate/repair the potentially cracked dissimilar-metal butt-weld at the RCS shutdown cooling nozzle safe-end, the crack growth analyses discussed in Section 8.5 using the ASME Code Section XI methodology are acceptable bases to address the fatigue qualification of the WOL for the RCS shutdown cooling nozzle.

The original analysis was performed in accordance with the ANSI Code [33]. The analysis offers protection against membrane or catastrophic failure, and protection against fatigue or a leak-type failure. The SWOL does not influence the reinforced region of the shutdown cooling nozzle. Therefore, the existing analysis [34] remains applicable for this region, provided the loading used in [34] remains applicable. The transient stresses and structural evaluation for the WOL on the shutdown cooling nozzle were documented in [7]. This primary stress for the shutdown cooling nozzle was evaluated by hand calculations in accordance with ANSI B31.7 [33]. Addition of the SWOL does not affect the B indices of the loads from the piping, but it increases the section modulus in the overlay region. The applicable primary loads (pressure and mechanical loads) used in [34] are not changed by the SWOL. Therefore, the primary stresses in the structures with SWOL are, by definition, less than or equal to those without SWOL. The previous qualifications [34] performed for the shutdown cooling nozzle applies to this calculation.

The fatigue for the shutdown cooling nozzle was evaluated using finite element techniques. Cut locations are illustrated in Figure 8-13. Table 8-10 shows that all stress, thermal ratcheting, and fatigue results meet the requirements specified in ANSI B31.7 [33]. Therefore, it is concluded that the existing ANSI B31.7 analysis of the RCS surge nozzle is not adversely affected by the addition of the SWOL.

Table 8-10: Shutdown Cooling Nozzle with SWOL Result Summary

Loading Condition	Stress Category	Cut No.	Stress (ksi) or Usage	Stress Limit	Allowable Stress (ksi) or Usage	Margin
Design	$P_m + P_b$	-	16.55	1.5 S_m	25.05	33.93%
Level A/B	P + Q	7	31.73	3 S_m	56.10	43.44%
	Linear Thermal Ratchet	4	0.473	N/A	1.00	52.70%
	Parabolic Thermal Ratchet	8	0.413	N/A	1.00	58.70%
	Fatigue	3	0.127	N/A	1.00	87.30%
Level C/D	$P_m + P_b$	-	19.74	2.25 S_m	37.58	47.47%

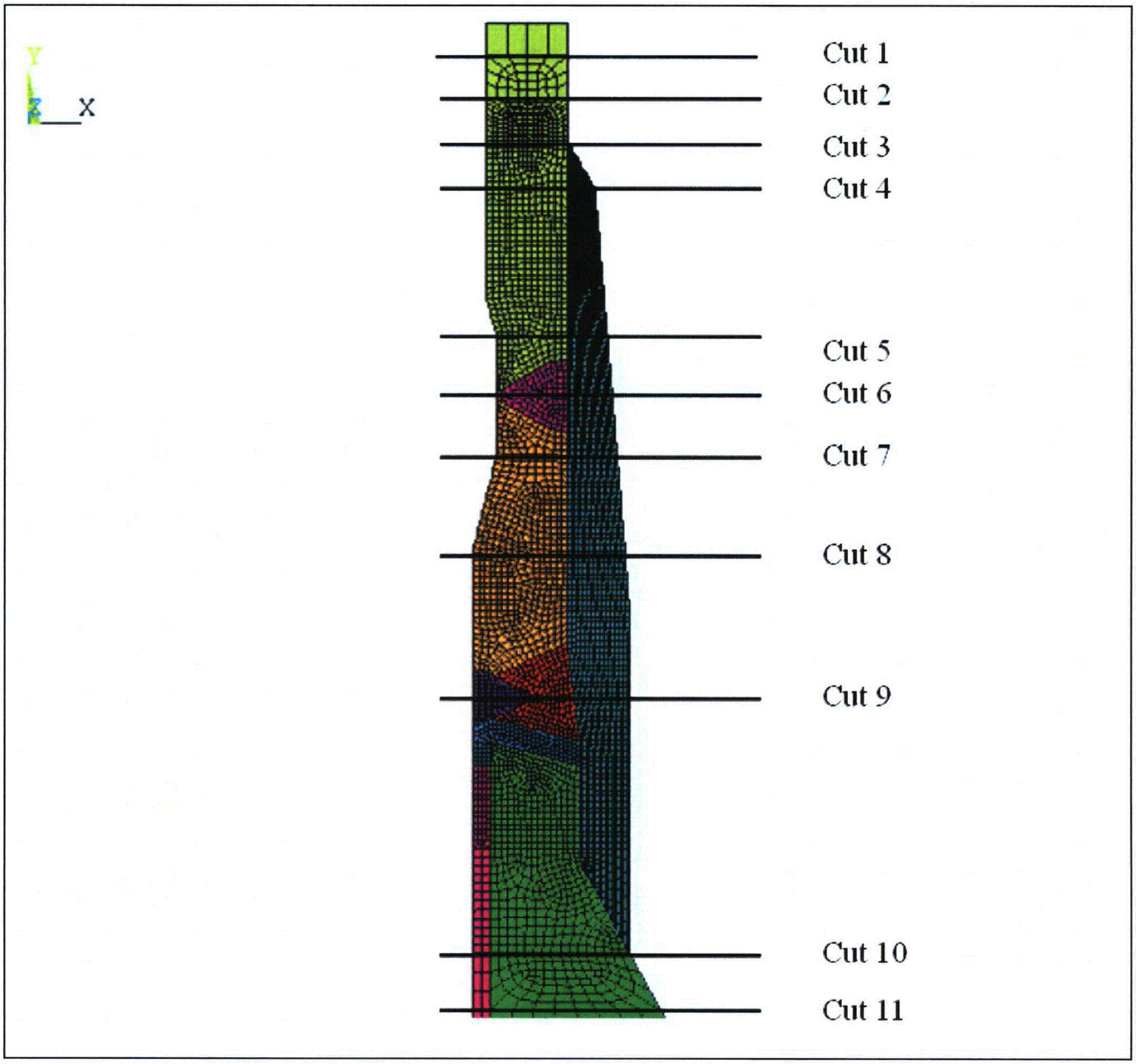

Figure 8-13: Shutdown Cooling Nozzle Cut/Path Locations

Effects of Additional Mass on Piping/Support System

The impact of the addition of weld overlay material on the existing primary stress qualification, which considers deadweight and dynamic loadings (such as those due to earthquake), was evaluated in [36], and found to be insignificant.

9 WELD OVERLAY DESIGN QUALIFICATION ANALYSIS: SAFETY INJECTION NOZZLE

9.1 INTRODUCTION

This section provides the WOL design qualification analysis to demonstrate the adequacy of the SWOL design for the RCS safety injection nozzle. The effectiveness of a WOL with Alloy 52/52M weld material is demonstrated using crack growth analysis, per IWB-3640 [6], to ensure that the WOL does not deteriorate during service. Using the residual weld stresses developed by the finite element model of the WOL process, future crack growth was evaluated at the safety injection nozzle safe-end weld locations using the operational design transients affecting the WOL region. The advantage of the Alloy 52/52M material is its high resistance to PWSCC, which minimizes the possibility for future PWSCC crack growth. Since the purpose of the SWOL is to mitigate/repair a potentially cracked dissimilar-metal butt-weld, performing crack growth analyses using ASME Code Section XI methodology is the accepted method to address the fatigue qualification of the WOL region for the RCS safety injection nozzle.

The effect of the SWOL on the existing fatigue qualification of the RCS safety injection nozzle outside the WOL region is addressed in accordance with ASME Section III requirements, considering the effect of the applicable thermal transient stresses, structural discontinuities, and bimetallic effects resulting from the SWOL.

9.2 LOADS

The loads used for the design of the safety injection nozzle weld overlay and FCG evaluation are listed in Table 9-1. These loads are considered in [2] and specified in [31]. The load combinations considered in the design are listed in Table 9-2. The transients considered in the safety injection nozzle FCG evaluation are shown in Table 9-3. The pipe end loads used for fatigue reconciliation are calculated using the equation in Table 9-4. These equations for axial and shear forces, as well as torsion and bending moments, were created based on orientation of the particular nozzle on the main loop pipe [31].

Table 9-1: Enveloping Safety Injection Nozzle Loads Used for Weld Overlay Design [31]

Load Type	Axial Force F_a (kips)	Bending Moment M_b (in-kips)
DW	-2.369	72.998
OBE	13.775	1648.978
SSE	27.549	3297.956

Notes:
DW = Deadweight Loads
OBE = Operating Basis Earthquake Loads
SSE = Safe Shutdown Earthquake Loads

Table 9-2: Load Combinations

Condition	Load Combination	Service Level
Design	DP + DW + DS	Design
Normal/Upset	TR[1] + DW + NT[1]	Level A/B
Emergency	DP + DW + MS + NT[1]	Level C
Test	TP + DW	Test

Notes:
1. Not applicable to WOL design sizing
DW = Deadweight
DP = Design Pressure
TP = Test Pressure
TR = Level A/B Transient Loadings (Thermal and Pressure)
NT = Thermal Expansion
DS = Design Seismic
MS = Maximum Seismic

Table 9-3: Applicable Thermal Transients for RCS Safety Injection Nozzles

#	Transient	Cycles	Level
1	Plant Heatup, 100°F / hr	500	A
2	Plant Cooldown, 100°F / hr	500	A
3	Plant Loading, 5% / min	15,000	A
4	Plant Unloading, 5% / min	15,000	A
5	Step Load Increase 10%	2,000	A
6	Step Load Decrease 10%	2,000	A
7	Reactor Trip	400	B
8	Loss of Turbine Generator Load / Loss of Reactor Coolant Flow	80[(3)]	B
9	Loss of Secondary Pressure	5	C
10	Hydrostatic Test	10	Test
11	Leak Test	200	Test
12	Large Break Loss of Coolant Accident	1	D
13	Shut Down Cooling	500	A
14	Secondary Side Break	5	C
15[(1)]	Seismic (Positive)	200	B
16[(1)]	Seismic (Negative)	200	B
17	Zero Load	710[(2)]	-

Notes:

(1) The design specification [31] states 200 cycles of operational basis earthquake and 200 cycles of design basis earthquake. For this analysis, 400 cycles of design basis earthquake will be used.

(2) The total cycles for this transient consist of 500 Heat-Up and Cool-Down cycles, 10 Hydro Static Test cycles and 200 Leak Test cycles.

(3) The total cycles for this transient consist of 40 Loss of Turbine Generator Load Cycles and 40 Loss of Reactor Coolant Flow Cycles

Table 9-4: Eveloping Safety Injection Nozzle Loads for Fatigue and FCG Evaluations

Condition	Force (kips)			Moment (in-kips)		
	F_X	F_Y	F_Z	M_X	M_Y	M_Z
Deadweight	-0.019	-2.254	0.005	-22.140	3.336	-70.068
Thermal	4.032	-4.526	0.830	-187.908	35.052	70.180
Design Seismic	5.333	2.667	13.300	1,242.322	224.587	531.061
Maximum Seismic	10.666	5.334	26.600	2,484.644	449.174	1,062.122

Note:

Axial force = $0.866*F_y+0.5*(0.889*F_x+0.457*F_z)$
Shear force = $SQRT\{[0.866*(0.889*F_x+0.457*F_z)+0.5*F_y]^2+(0.889*F_z+0.457*F_x)^2\}$
Torsion moment = $0.866*M_y+0.5*(0.889*M_x+0.457*M_z)$
Bending moment = $SQRT\{[0.866*(0.889*M_x+0.457*M_z)+0.5*M_y]^2+(0.889*M_z+0.457*M_x)^2\}$

9.3 WELD OVERLAY DESIGN SIZING

The minimum WOL thickness was determined based on a through-wall flaw in the original pipe. The methodology used to determine the WOL design thickness and length is discussed in Section 3. Using this methodology, radii from the design geometry, shown in Table 9-5, are used to design the minimum SWOL parameters. As-designed inside and outside radii at the thickest portion of the Alloy 82/182 and SS welds are presented here. The thickest portion results from considering the smallest inner radius ($R_{i\text{-}min}$) and the largest outer radius ($R_{o\text{-}max}$). By using the maximum wall thickness of the design geometry, a conservative SWOL design thickness and length is achieved. The WOL length was based conservatively on the recommended length, per Code Case N-740:

$$L_{WOL} = 0.75\sqrt{Rt}$$

where,

$R = R_{o\text{-}max}$ = outside radius
$t = R_{o\text{-}max} - R_{i\text{-}min}$ = wall thickness at the location of indication

The WOL length (L_{WOL}) will extend from the weld/base metal interface on either side of the Alloy 82/182 and SS welds, as shown in Figure 9-1. The WOL thickness (t_{WOL}) was determined using the following equation:

$$t_{WOL} = t/0.75 - t$$

The minimum WOL design dimensions are shown in Table 9-6.

In accordance with ASME Section XI IWB-3640, the criterion from Section XI, Appendix C is used to evaluate the maximum post-WOL stresses resulting from the actual applied loadings. To determine the applied post-WOL stresses, the minimum post-WOL thicknesses are considered, which produces a conservative method to determine stresses for comparison to the allowable stress criterion. The thinnest portion of the Alloy 82/182 and SS welds results from considering the largest inner radius ($R_{i\text{-}max}$) and the smallest outer radius post-WOL ($R_{o\text{-}min\text{-}WOL}$). These parameters and the resulting geometric section properties are presented in Table 9-7.

The applied bending stresses were calculated by:

$$\sigma_b = \frac{M_b}{Z}$$

M_b is per Table 9-1, and Z is per Table 9-7

$$Z = \frac{\pi(R_{o-\min-wol}{}^4 - R_{i-\max}{}^4)}{4(R_{o-\min-wol})}$$

$R_{i\text{-max}}$ and $R_{o\text{-min-wol}}$ are per Table 9-7

The applied membrane stresses were calculated by:

$$\sigma_m = \sigma_p + \frac{F_a}{A_x}$$

where,

$$\sigma_p = \frac{\pi R_{i-\max}{}^2}{\pi\left(R_{o-\min-wol}{}^2 - R_{i-\max}{}^2\right)} P$$

F_a is per Table 9-1.

A_x is per Table 9-7.

$A_x = \pi\ (R_{o\text{-min-wol}}{}^2 - R_{i\text{-max}}{}^2)$

$R_{i\text{-max}}$ and $R_{o\text{-min-wol}}$ are per Table 9-7.

P = 2,235 psig [2]

The allowable stress intensity S_m (at 650°F) used in the sizing of the Alloy 52/52M (N06690) overlay is 23.3 ksi [9]. This allowable is based on the annealed condition of SB-166/SB-167. The normal operating pressure, 2,235 psig, was used for the calculation.

The resulting stresses, determined by using the previous equations and the loads and load combinations from Tables 9-1 and 9-2, respectively, are listed and compared to the Code allowable in Table 9-8.

Table 9-5: Safety Injection Nozzle Geometry for WOL Design Calculations [2]

Alloy 82/182 Weld			**Stainless Steel Weld**		
Inside Radius $R_{i\text{-min}}$ (in)	**Outside Radius $R_{o\text{-max}}$ (in)**	**Wall Thickness t_{design} (in)**	**Inside Radius $R_{i\text{-min}}$ (in)**	**Outside Radius $R_{o\text{-max}}$ (in)**	**Wall Thickness t_{design} (in)**
5.094	6.780	1.686	5.250	6.375	1.125

Table 9-6: Safety Injection Nozzle Minimum Weld Overlay Repair Design Dimensions [2]

Alloy 82/182 Weld		Stainless Steel Weld	
t_{WOL} (in)	L_{WOL} (in)	t_{WOL} (in)	L_{WOL} (in)
0.82	2.54	0.54(1)	2.01(1)

Note (1): At the piping toe of the SS weld, the 0.54-inch thickness decreases linearly to a thickness of 0.45 inch at a distance of 2.01 inches onto the piping component. Linear interpolation is permitted to determine thicknesses along the 2.01-inch length.

Table 9-7: Safety Injection Nozzle Geometry for Stress Check in Post-Weld-Overlay Condition [2]

Alloy 82/182 Weld				Stainless Steel Weld			
Inside Radius $R_{i\text{-}max}$ (in)	Outside Radius $R_{o\text{-}min\text{-}WOL}$ (in)	Cross-Sectional Area A_x (in^2)	Section Modulus Z (in^3)	Inside Radius $R_{i\text{-}max}$ (in)	Outside Radius $R_{o\text{-}min\text{-}WOL}$ (in)	Cross-Sectional Area A_x (in^2)	Section Modulus Z (in^3)
5.094	6.985	71.758	191.952	5.370	6.915	59.628	165.248

Table 9-8: Safety Injection Nozzle Post-SWOL Stress Comparison [2]

	Normal/Upset		Emergency/Faulted	
Location	Applied Stress σ_b (ksi)	Allowable Stress P_b (ksi)	Applied Stress σ_b (ksi)	Allowable Stress P_b (ksi)
Alloy Weld	8.971	9.057	17.561	20.505
SS Weld	10.421	10.447	20.399	24.127

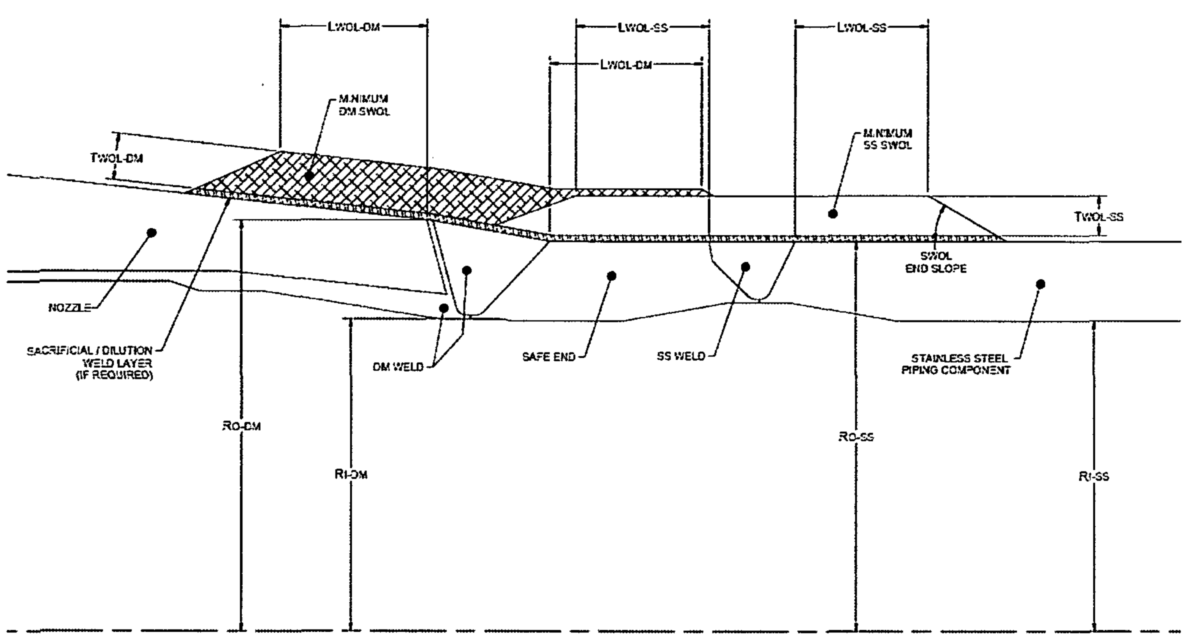

Figure 9-1: Weld Overlay Design Parameters for the Safety Injection Nozzles
(Not drawn to scale.)

9.4 WELD OVERLAY RESIDUAL WELD STRESS RESULTS

As described in Section 5.3, the finite element model was developed to capture the parts of the structure in the vicinity of the safety injection nozzle safe-end with the SWOL. This includes a portion of the safety injection nozzle attached to the nozzle safe-end and a length of SS pipe attached to the safe-end. An ID weld repair was considered in the finite element model. The finite element model and boundary conditions are shown in Figures 9-2 and 9-3. The nozzle is fixed in the axial direction to simulate the rest of the nozzle. The end of the SS piping is coupled in the axial direction to simulate the reaming portion of the SS piping not included in the model. The model assumes that a 50% through-wall weld repair was performed from the inside surface of the safety injection nozzle to safe-end Alloy 82/182 butt-weld.

The final residual weld stresses, including normal operating pressure and temperature conditions, are shown in Figures 9-4 and 9-5 for selected stress cuts in the Alloy 82/182 and SS welds. The locations of the stress cuts are provided in Figure 9-2. The stress contours in the RCS safety injection nozzle after the weld overlay application are provided in Figures 9-6 and 9-7.

Figure 9-4 shows the axial and hoop residual stress for Alloy 82/182 weld, at normal operating conditions after the SWOL. The stresses are compressive up to about 80% of the original pipe wall thickness. This stress distribution is favorable due to the generally compressive stress field. It minimizes the potential for crack growth in the dissimilar-metal weld region. Similarly, Figure 9-5 shows the axial and hoop stresses for the stainless weld. They remain compressive for 80% of the original pipe wall at normal operating conditions. Therefore, the potential for FCG is minimized.

Acceptable post-weld-overlay residual stresses (i.e., stresses that satisfy the requirements for mitigating PWSCC) are those that are sufficiently compressive over the entire length and circumference of the inside surface of the Alloy 82/182 weld (at operating temperature, but prior to applying operating pressure and loads) that the resulting total stress, after application of operating pressure and loads, remains less than 10 ksi tensile [28]. This target level has been selected as a conservatively safe value, below which PWSCC initiation, or growth of small initiated cracks, is very unlikely. Additionally, the residual plus operating stresses must remain compressive through some portion of the weld thickness away from the inside surface. The residual stresses in the Alloy 82/182 weld of the safety injection nozzle, resulting from the weld overlay, are well below this level through 80% of the original weld thickness.

Figures 9-8 and 9-9 show the axial and hoop stresses on the inside surface (in the vicinity of the alloy weld and buttering) remain compressive after SWOL. The maximum resultant bending moment for normal operating condition is 870.443 in-kips. The resulting maximum bending stress in the Alloy 82/182 weld and SS weld are 3.177 ksi and 4.508 ksi, respectively [32]. The pipe bending stresses are low, and considered to have negligible effect on the residual weld stress results.

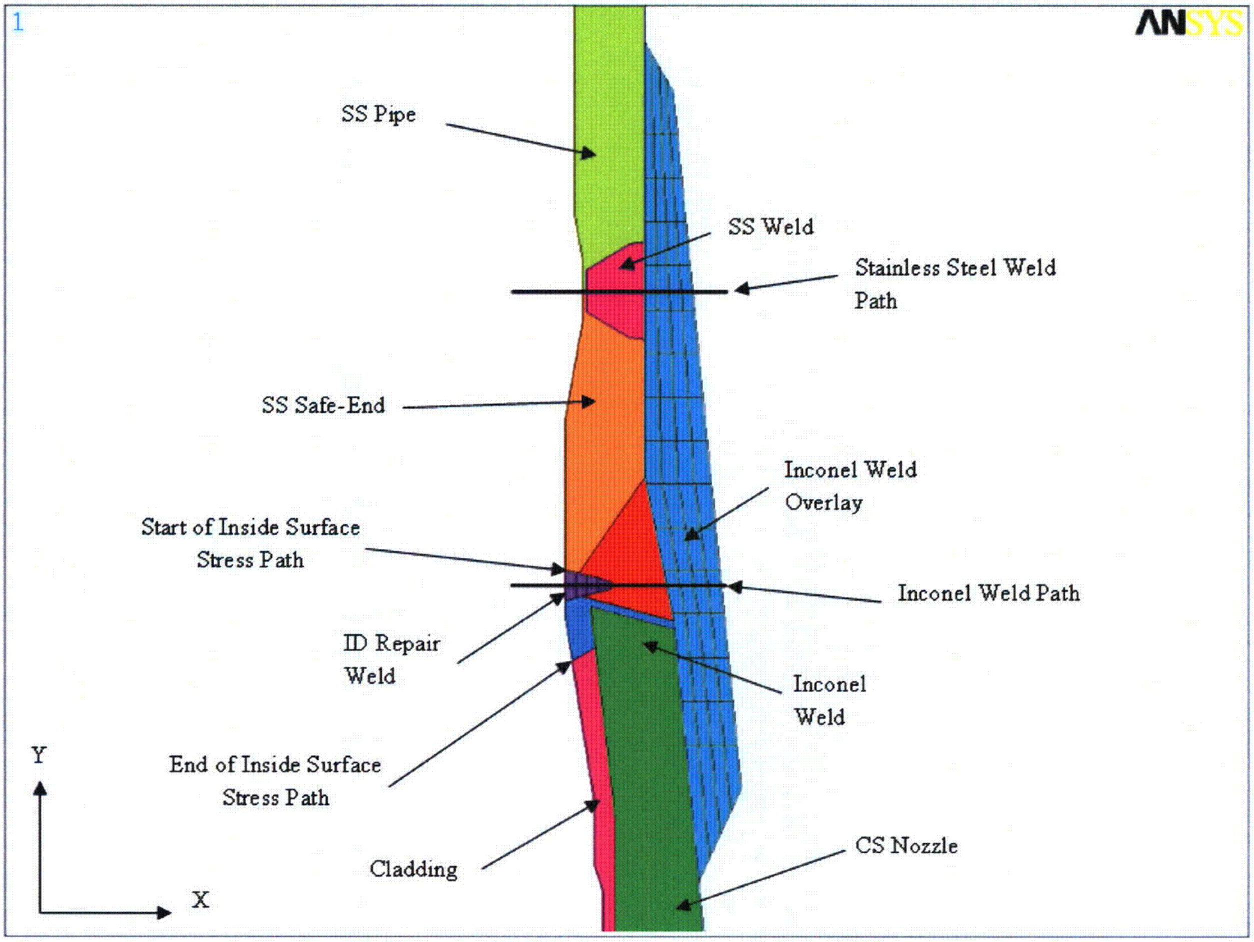

Figure 9-2: ANSYS Model of Safety Injection Nozzle

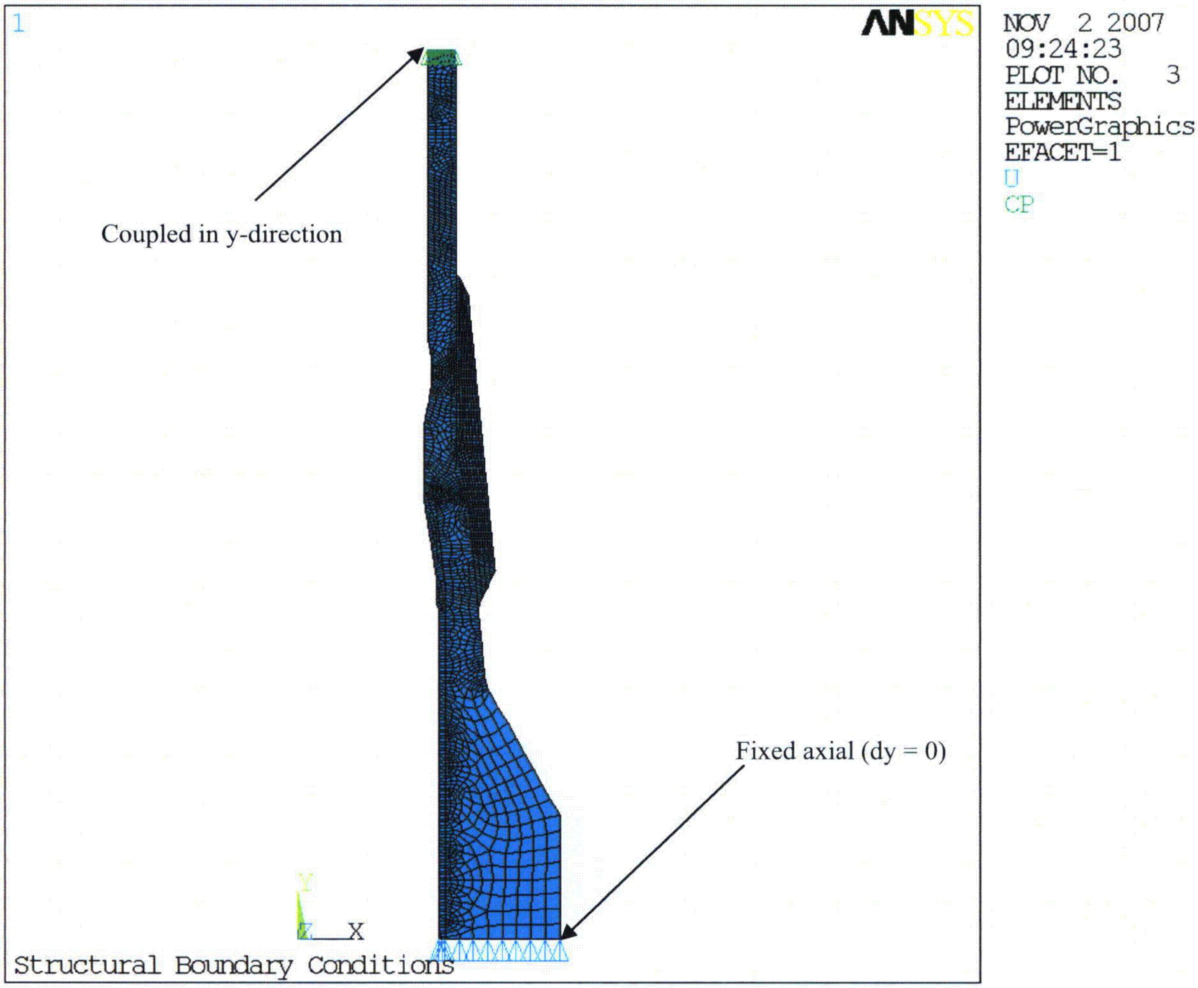

Figure 9-3: Finite Element Model and Structural Boundary Conditions

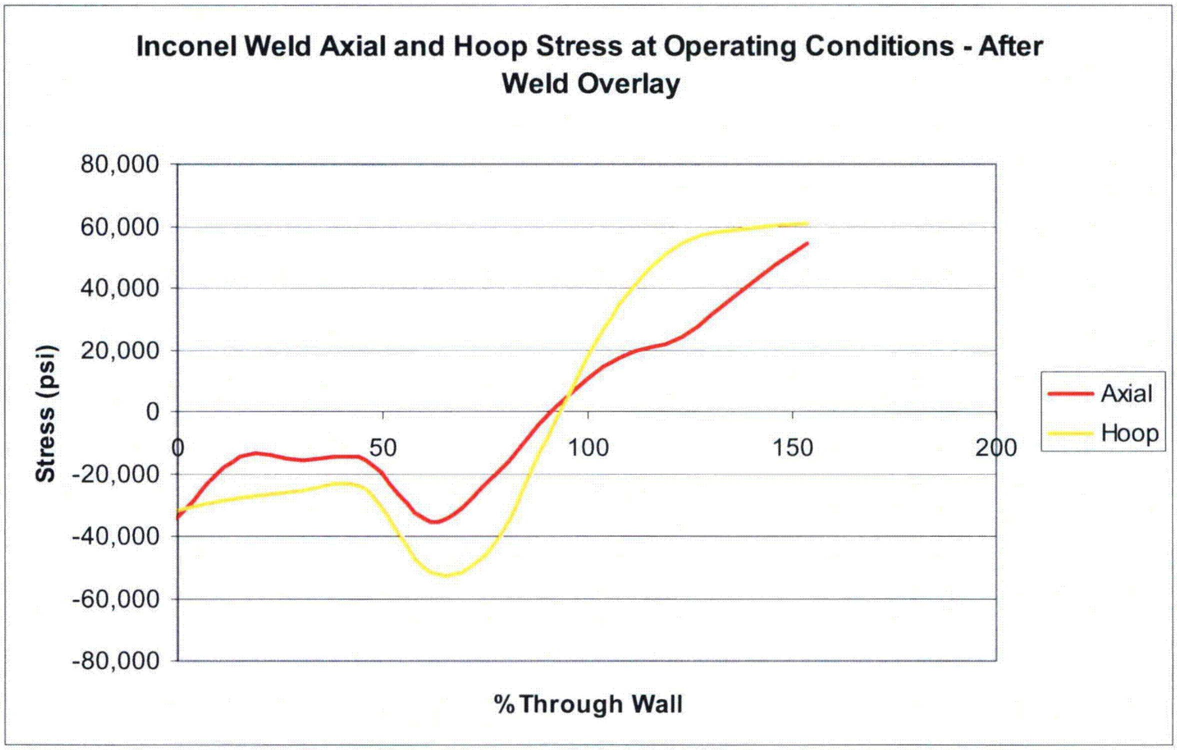

Figure 9-4: Axial and Hoop Residual Stresses in the Alloy 82/182 Weld at Operating Conditions*

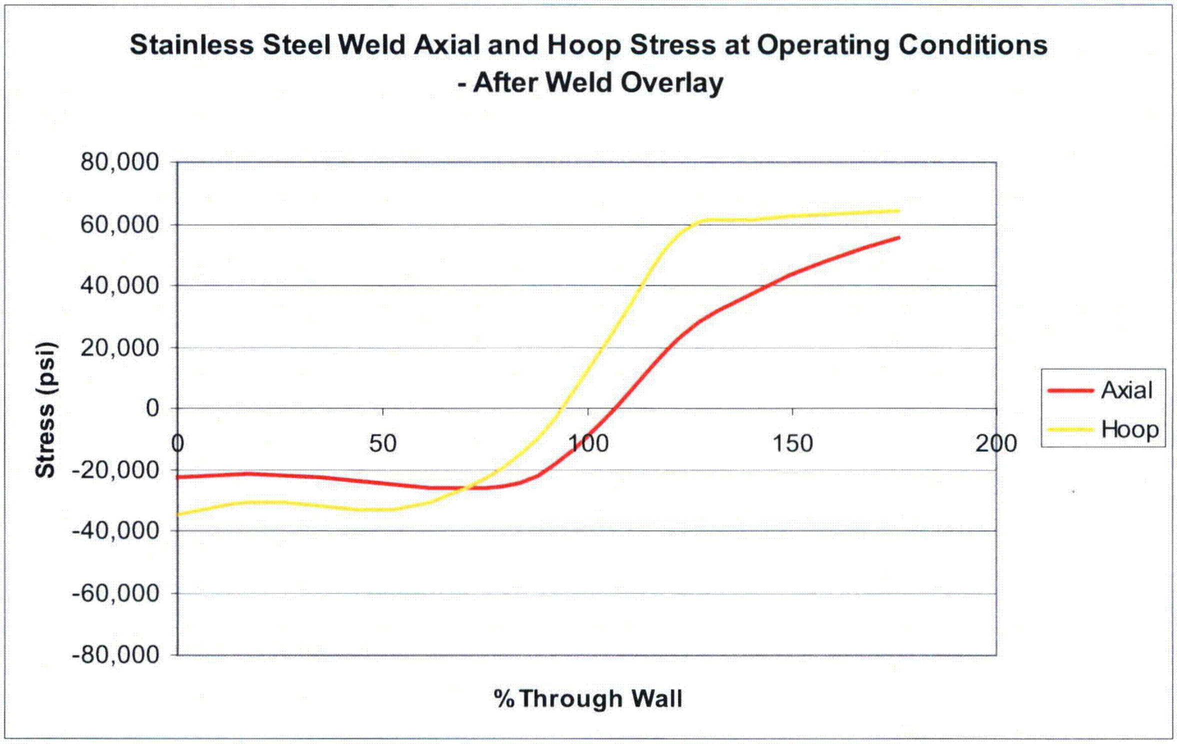

Figure 9-5: Axial and Hoop Residual Stresses in the SS Weld at Operating Conditions*

*Note: The percent through-wall indicated on the horizontal axis is expressed in terms of the original pipe wall thickness. The weld overlay region is the region beyond 100% wall thickness.

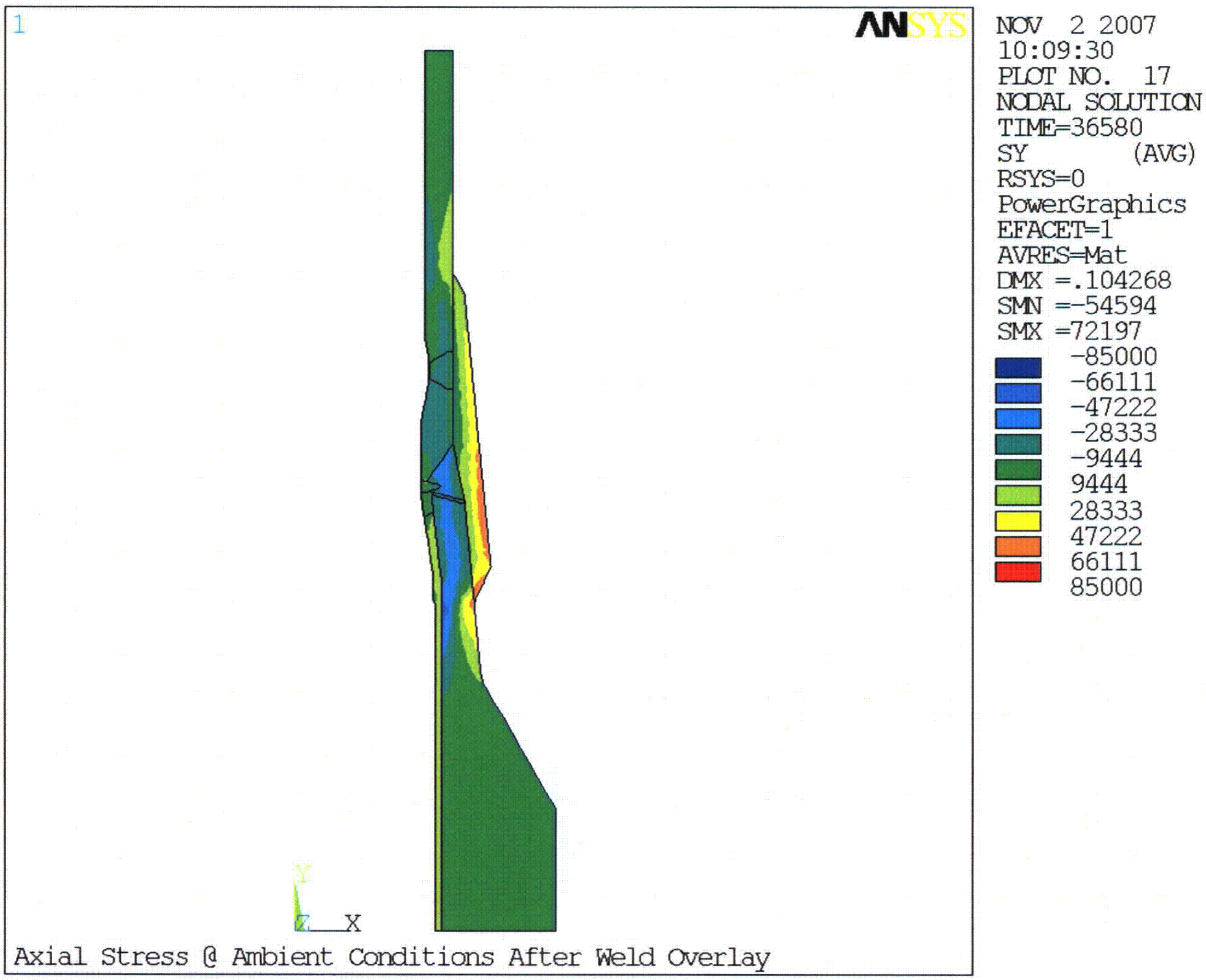

Figure 9-6: Axial Stress (psi) Contour Plot at Operating Condition after Weld Overlay

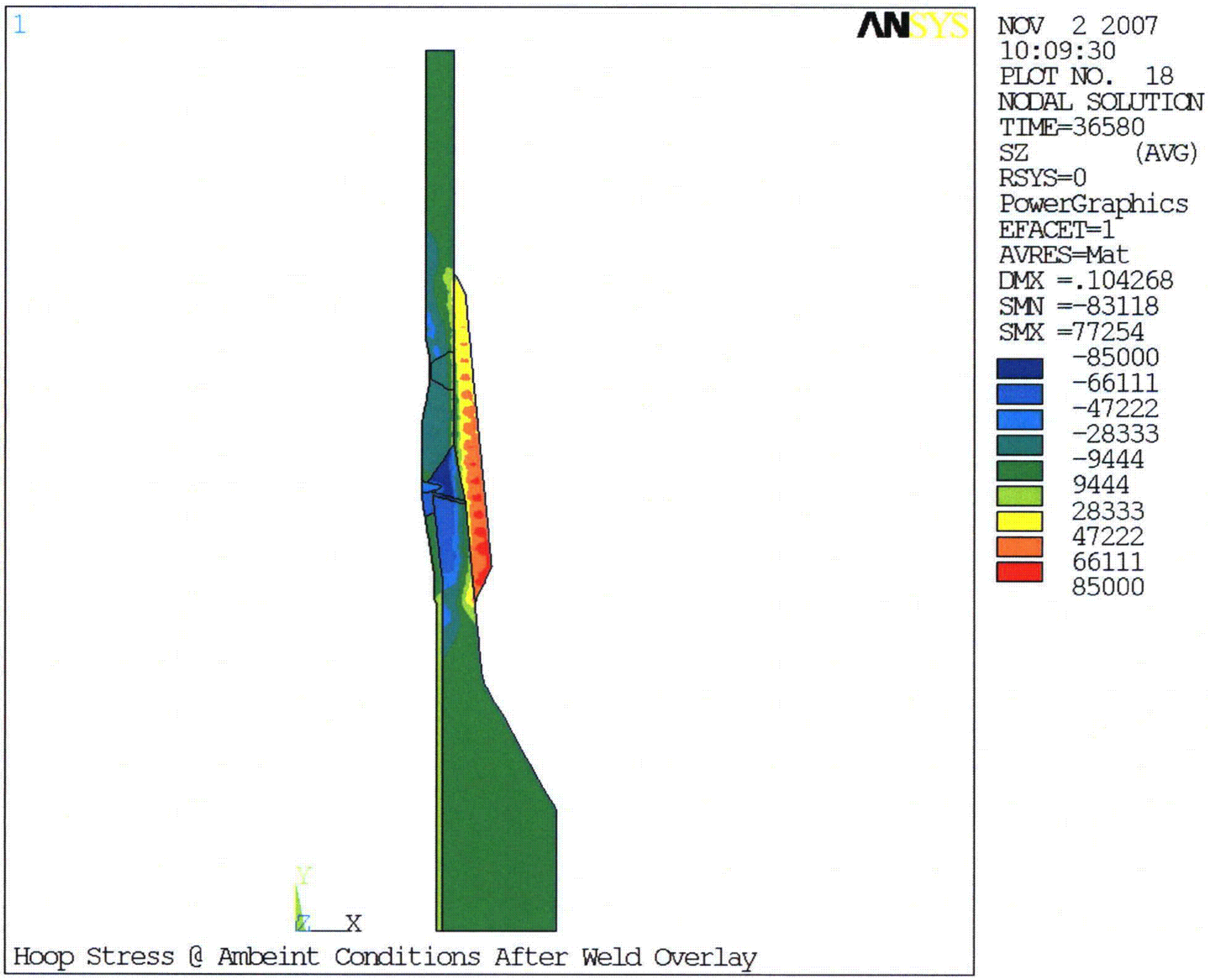

Figure 9-7: Hoop Stress (psi) Contour Plot at Operating Condition after Weld Overlay

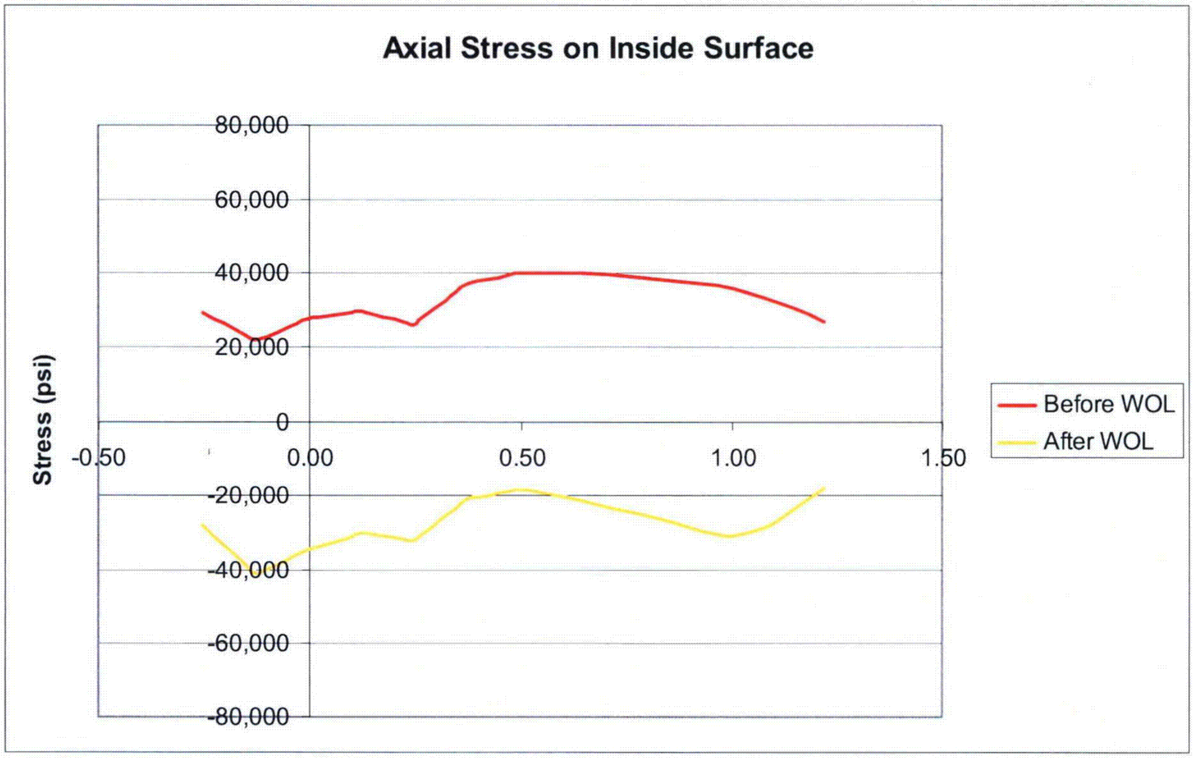

Figure 9-8: Axial Residual Stress along the Inside Surface at Operating Condition*

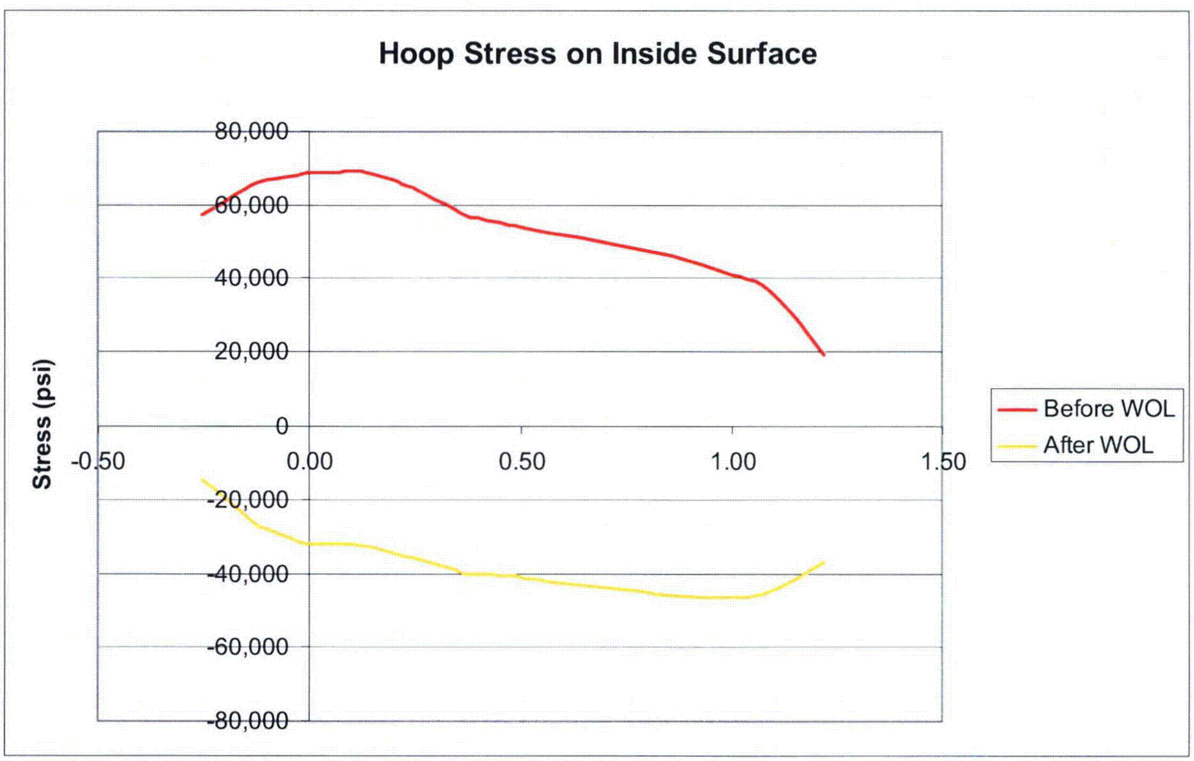

Figure 9-9: Hoop Residual Stress along the Inside Surface at Operating Condition*

*Note: X-axis is the location (inch) along the inside surface path. Zero is the center of alloy weld. See Figure 9-2.

9.5 FATIGUE CRACK GROWTH RESULTS AND ESTIMATE OF WELD OVERLAY DESIGN LIFE: SAFETY INJECTION NOZZLE REGION

The methodology used to determine fatigue crack growth is described in Section 4.4. Fatigue crack growth analyses were performed for the safety injection nozzles using the through-wall stress distribution including residual stresses generated from the weld overlay mitigation/repair process and the thermal transient stresses.

The weld overlay service life is a function of the flaw depth found in the region being overlaid, and the projected growth of that flaw. The allowable maximum flaw depth is 75% of the piping wall thickness (including the weld overlay thickness), per Section XI, IWB-3640 [6].

A range of possible flaw sizes, from 0 to 100% of the original wall thickness, were postulated in the fatigue crack growth evaluations. The results of these evaluations for the flaw depths less than the original design wall thickness are plotted in Figures 9-10 and 9-11, in the form of expected time for these flaws to reach the interface between the original wall and the newly laid weld overlay material. Figure 9-10 shows results for the Alloy 82/182 weld, and Figure 9-11 shows results for the SS weld. For the maximum possible flaw depths of 100% of the original design wall thickness propagating into the Alloy 52/52M weld overlay material, results are shown in Figure 9-12. This figure shows the estimated flaw depth with time for the design cycles spread over either the original design life or the extended life of the plant.

Figures 9-10 and 9-11 summarize the expected service life (based on transients cycles spread evenly for either 40 years or 60 years of plant life) for a given initial flaw depth to reach 100% of the original wall thickness at the Alloy 82/182 weld and the SS weld locations, respectively. Based on the results shown in Figures 9-10 and 9-11, it can be concluded that if no flaws are detected during the post-SWOL inspection, a conservatively assumed 75% through the original wall flaw would not grow to 100% of the original wall thickness for 40 years FCG due to transient cycles. This is based on the assumption that the current 40-year design transient cycles are spread evenly over 40 years of plant life. If flaws are detected during the post-SWOL inspection, the as-found flaw size can be used to determine the design life of the SWOL using the crack growth results shown in Figures 9-10 and 9-11.

For the case of an initial flaw depth of 100% of the original wall thickness, i.e., a through-wall flaw, Table 9-9 shows that the total flaw growth into the newly laid Alloy 52/52M welds material in one 10-year inspection interval is 0.001 inch, based on the design cycles spread over a 60-year extended life. The final flaw depth after the 10-year period with the fatigue crack growth considered is well within 75% of the total post-WOL wall thickness, as required by SWOL criteria.

Two examination scenarios exist: a pre-overlay examination and a post-overlay examination. If an examination found no flaws, the overlay service life would be governed by the largest flaw that might have been missed by the examination. For an examination performed prior to the weld overlay installation, a conservative approach would be to assume that the flaw depth is 10% of the original wall thickness. Alternatively, this would be 75% of the original wall for an examination performed after the weld overlay installation. This is because the area required to be inspected after the overlay is only the outer 25% of the original pipe thickness plus the overlay thickness itself. The PDI qualification blocks do not contain any flaws in the inner 75% of the pipe wall. Therefore, it would be conservative to assume

such a flaw for the qualification. As shown in Figure 9-10, an initial flaw as deep as 75% would result in a remaining service life of 100% of the original design cycles. If the design cycles are assumed to be spread over 40 years of plant operation, the remaining life of the SWOL would be 40 years. This is well beyond the required 10-year in-service inspection (ISI) interval. If, after the next ISI, no flaws are detected in the outer 25% of the original welds, the SWOL life is 40 years from the time of the latest inspection.

In the unlikely event that the post-overlay inspection detected a flaw that is as large as the full depth of the original design wall thickness, the expected service life of the weld overlay is at least one 10-year inspection interval period. For the safety injection nozzle, flaw growth rate into the weld overlay material is small or negligible, indicates that the expected service life of the repair would be 40 years if the transient cycles are spread over original design life of 40 years.

For example, if an axial flaw that is 96% through the original Alloy 82/182 wall thickness is detected as a result of the post WOL inspection, and assuming conservatively that the current 40-year design transient cycles are spread evenly for only 40 years, the expected service life from Figure 9-10 for this flaw to reach 100% of the original wall thickness is about 40 years. If it is assumed that the design transient cycles are spread evenly for 60 years, the remaining service life would be 60 years. This can also be determined by applying a factor of 1.5 to the service life based on the 40-year design cycles. For a similar size circumferential flaw, the expected service life is about 40 years, based on current 40-year design transient cycles assumed to be spread evenly over 40 years. Since the typical in-service inspection interval is 10 years for this initial flaw depth of 96%, it can be concluded that the sizing of the SWOL is adequate up to the next inspection period based on the current 40-year design transient cycles spread evenly over the next 40 years.

Another case of 100% original design wall thickness through-wall flaw in the alloy weld was hypothesized assuming the total post-WOL wall of 2.501 inches. This included an extra allowance of 0.21 inch for the FCG in to the Alloy 690 material. This 100% original wall axial flaw was evaluated for the FCG results, shown in Table 9-9 and Figure 9-12. Results demonstrate that the total growth in 10 years is insignificant (0.001 inch). The final flaw depth after 10 years FCG is within 75% of the total post-WOL wall thickness, as required by SWOL criteria. Therefore, the 0.21 inch SWOL thickness increase provided in the SWOL design is adequate to address the issue of PWSCC for an almost through-wall flaw.

The actual time required to use the remaining design cycles depends on plant operating practice.

Table 9-9: Safety Injection Nozzle Alloy 52/52M FCG Data – Axial Flaw [35]

Nozzle Thickness (in)	Initial Flaw Depth (in)	Final Flaw Depth in 10 years (in)	Total Flaw Growth in 10 years (in)
2.501(1,2)	1.623	1.624	0.001

Notes:
(1) This thickness is due to a 0.21 inch increase in SWOL thickness.
(2) A review of transient stresses indicates that a rise time of 5,000 seconds is conservative for use in Alloy 52/52M FCG rate.

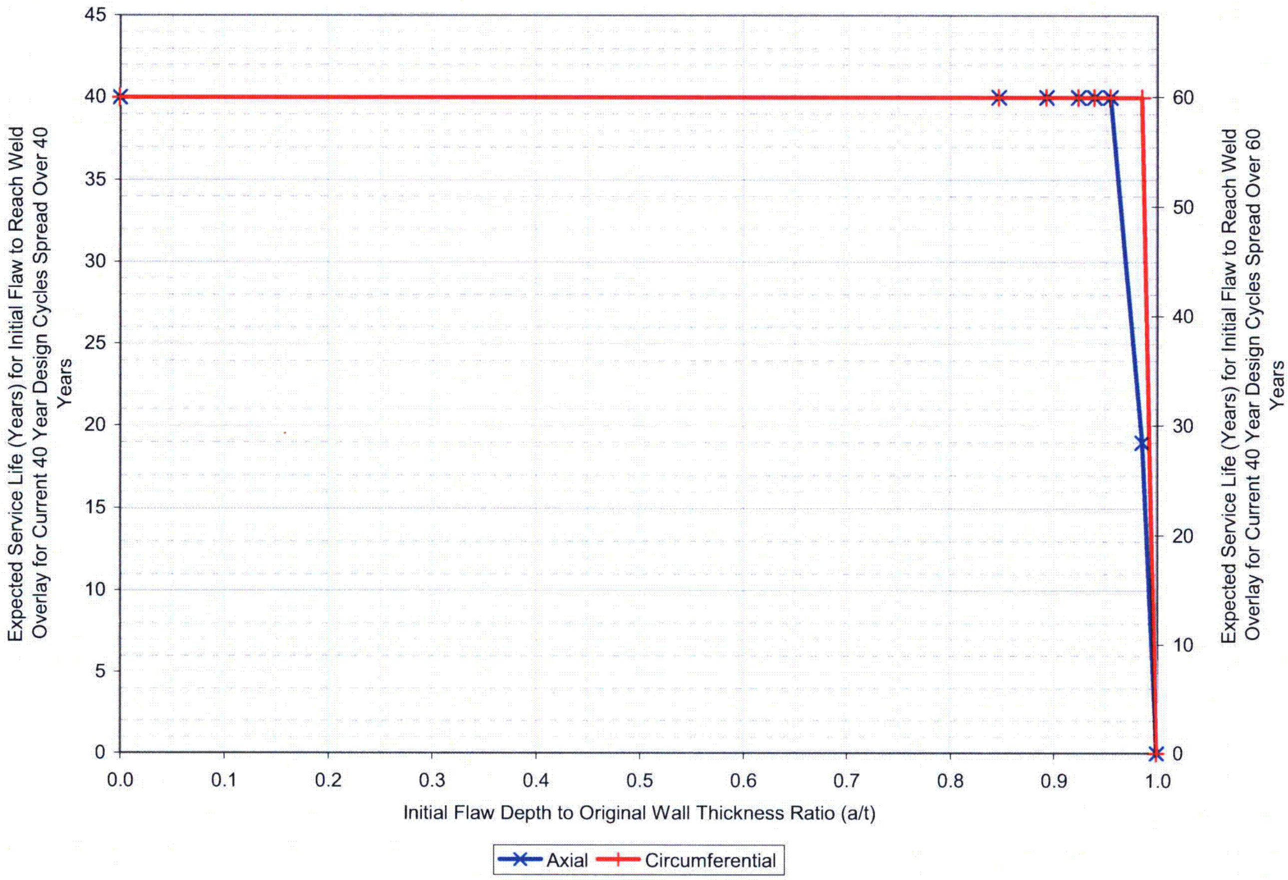

Figure 9-10: Expected Time for the Initial Flaw Depth to Reach the Weld Metal Interface for SI Nozzle Alloy 82/182 Weld [35]

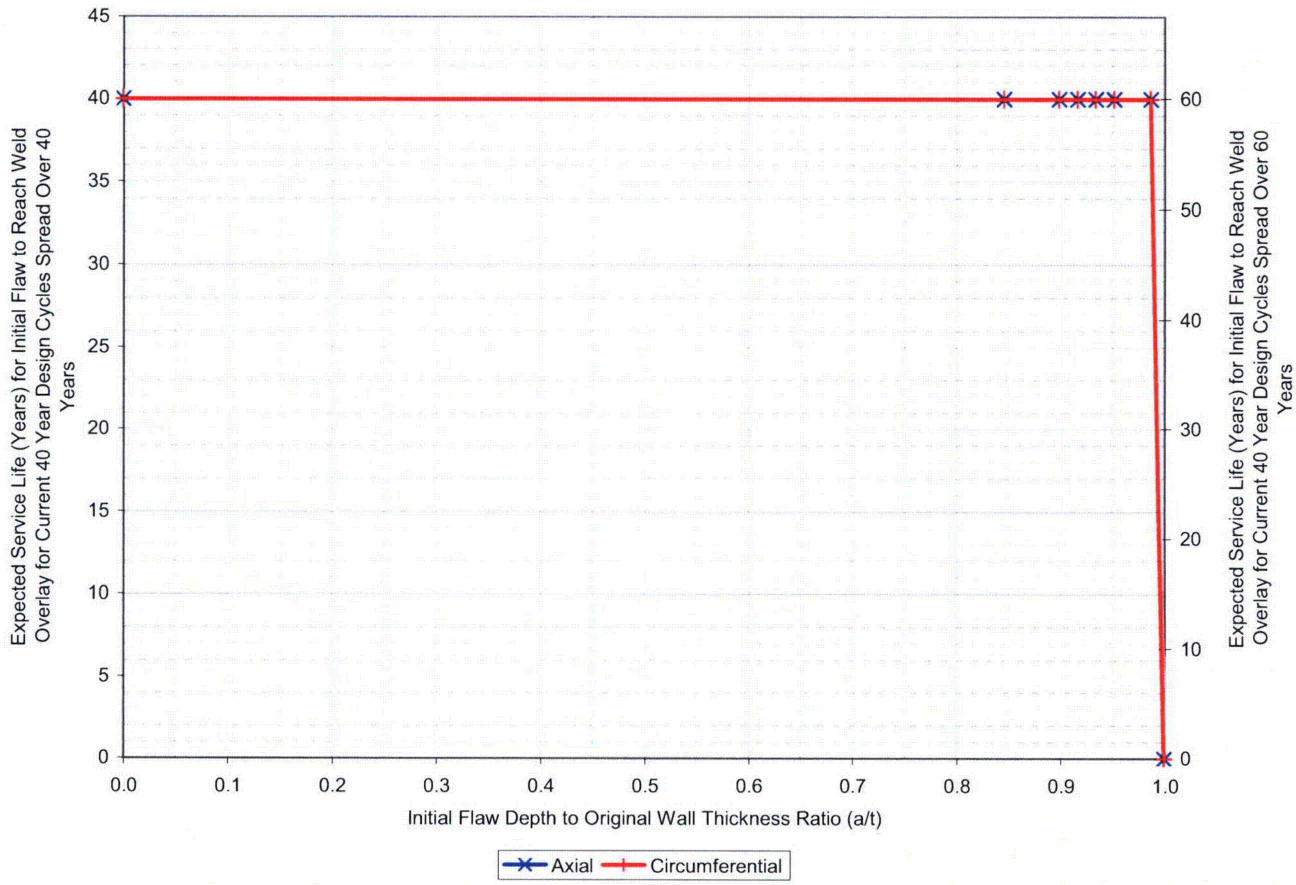

Figure 9-11: Expected Time for the Initial Flaw Depth to Reach the Weld Metal Interface for SI Nozzle SS Weld [35]

Note: Curves for axial and circumferential flaw estimated life coincide with each other. Hence, only one curve is visible in the figure above.

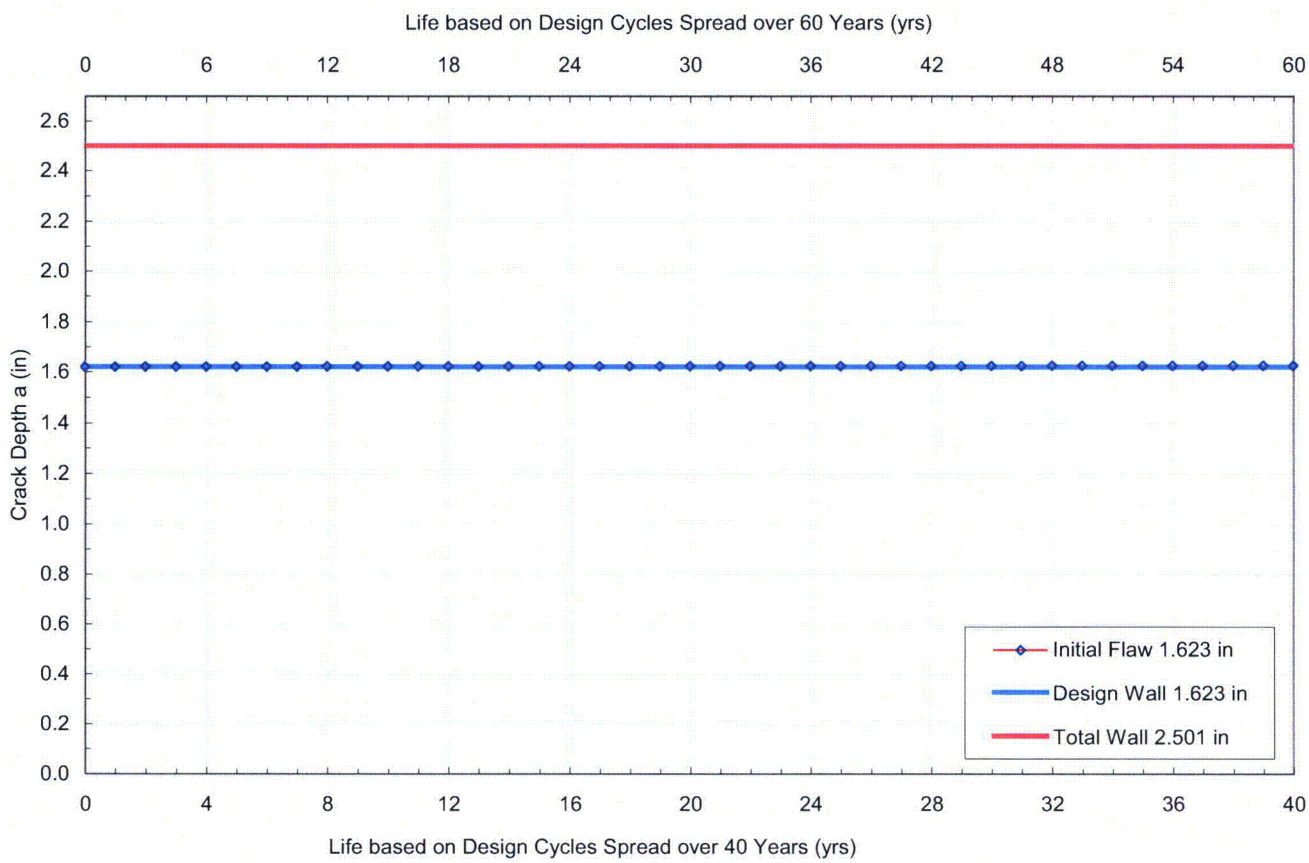

Figure 9-12: Flaw Growth for 100% Original Wall Thickness
Initial Flaw versus Service Period in Alloy 52/52M at SI Nozzle Alloy Weld [35]

9.6 IMPACT ON DESIGN QUALIFICATIONS OF NOZZLE AND PIPE

The impact of the weld overlay is evaluated to demonstrate that the presence of the weld overlay repair does not have any adverse impact on the existing stress qualification of the safety injection nozzle with respect to the Code of Construction [33].

Effects of SWOL on Transient Stress and Fatigue Analysis

Since the intention of the structural weld overlay is to mitigate/repair the potentially cracked dissimilar-metal butt-weld at the RCS safety injection nozzle safe-end, the crack growth analyses discussed in Section 9.5 using the ASME Code Section XI methodology are acceptable bases to address the fatigue qualification of the weld overlay region for the safety injection nozzle.

The original analysis was performed in accordance with the ANSI Code [33]. It offers protection against membrane or catastrophic failure, and protection against fatigue or leak type failure. The SWOL does not influence the reinforced region of the safety injection nozzle. Therefore, the existing analysis [34] remains applicable for this region, provided the loading used in [34] remains applicable. The transient stresses and structural evaluation for the weld overlay safety injection nozzle were documented in [7]. The primary stress for the safety injection nozzle was evaluated by hand calculations in accordance with ANSI B31.7 [33]. Addition of the SWOL does not affect the B indices of the loads from the piping, but increases the section modulus in the overlay region. The applicable primary loads (pressure and mechanical loads) used in [34] are not changed by the SWOL. Therefore, the primary stresses in the structures with SWOL are, by definition, less than or equal to those without SWOL. The previous qualifications [34] performed for the safety injection nozzle applies to this calculation.

The fatigue for the safety injection nozzle was evaluated with finite element techniques. Cut locations are illustrated in Figure 9-13. As Table 9-10 shows, all stress, thermal ratcheting, and fatigue results meet the requirements specified in ANSI B31.7 [33]. It is concluded that the existing ANSI B31.7 analysis of the safety injection nozzle is not adversely affected by the addition of the SWOL.

Table 9-10: Safety Injection Nozzle with SWOL Result Summary

Loading Condition	Stress Category	Cut No.	Stress (psi) or Usage	Stress Limit	Allowable Stress (psi) or Usage	Margin
Design	$P_L + P_b$	-	21,196	1.5 S_m	25,500	16.88%
Level A/B	P + Q	1	69,536	3 S_m	50,100	-38.79%(1)
	Linear Thermal Ratchet	2	0.509	N/A	1.000	49.15%
	Parabolic Thermal Ratchet	2	0.425	N/A	1.000	57.55%
	Fatigue	2	0.159	N/A	1.000	84.10%
Level C/D	$P_L + P_b$	-	33,622	2.25 S_m	38,250	12.10%

Note: (1) A simplified elastic-plastic analysis was performed [7] in accordance with ANSI B31.7 [33] to justify $P + Q > 3S_m$.

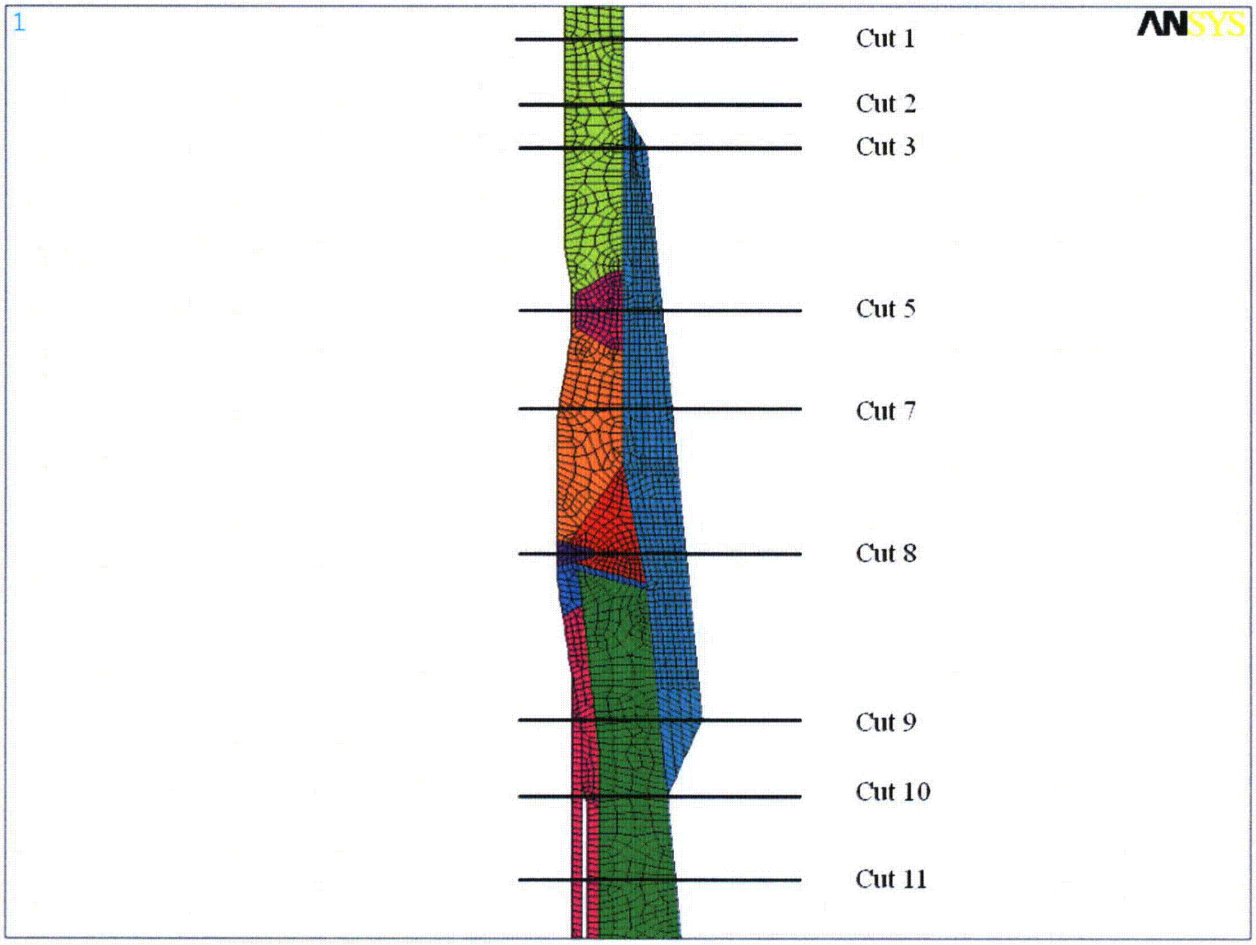

Figure 9-13: Safety Injection Nozzle Cut/Path Locations

Effects of Structural Weld Overlay on the Thermal Sleeve

The effect of the SWOL on the safety injection nozzle thermal sleeve is judged insignificant. The nozzle has a thermal sleeve welded on the ID of the nozzle that shields the nozzle body. The thermal sleeve is not a pressure-retaining component, nor is it a load path for the piping forces and moments imposed on the nozzle. However, the impact of the WOL on the thermal sleeve partial fillet weld attachment to the nozzle is addressed in this section.

From a structural standpoint, the weld between the thermal sleeve and the nozzle is affected by pressure in the nozzle and thermal transients, and may displace relative to the nozzle. This has the potential to result in stresses that are expected to maximize near the attachment weld. The SWOL on the outside of the nozzle is not expected to have a significant detrimental effect on the stresses at the thermal sleeve attachment weld for the following reasons:

- If there is any effect, the relative displacement between the sleeve and the safe-end due to pressure loading is expected to be less with a SWOL because the whole nozzle is more restricted from expansion due to pressure.

- The response to a thermal transient is expected to be dominated by the differential temperature gradient through the sleeve thickness and its corresponding relative displacement to the internal nozzle surface responding to the same transient. Thermal stress in the sleeve thickness due to shock effects of the transient is not expected to change because the sleeve thickness has not changed. Thermal stress in the sleeve due to differential expansion of the sleeve and the nozzle inside surface is not expected to be significant. This is due to the large difference in stiffness of the sleeve and the nozzle, essentially making the nozzle a fixed attachment point. Therefore, thermal stresses in the sleeve attachment are not expected to be affected by the SWOL material on the outside surface of the nozzle.

These reasons are supported by the stress results taken from the analysis at the thermal sleeve location shown in Figure 9-14. The stresses were evaluated for the design condition and the thermal transients. Then, these stresses were compared to the limits of the ANSI code for basic stress intensity limits. Table 9-11 shows the stresses for the primary membrane (P_m), primary membrane plus bending ($P_L + P_b$), and primary plus secondary stresses (P + Q), and compares these stresses against the limits of the ANSI Code [33]. The primary stresses, P_m and $P_L + P_b$, are the maximum stresses from the Design and Level C condition. The primary plus secondary stresses, P + Q, are the maximum stress from the thermal transients.

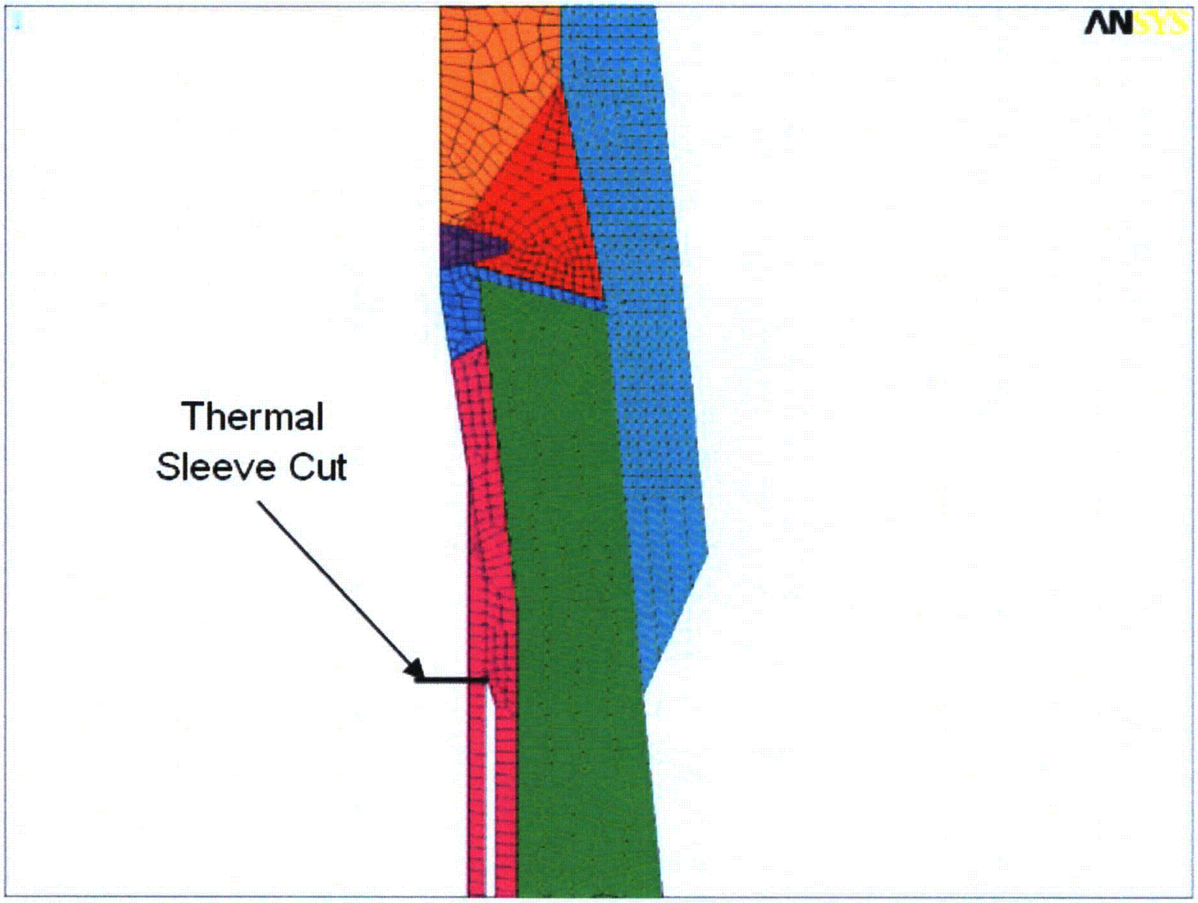

Figure 9-14: Thermal Sleeve Cut Location

Table 9-11: Thermal Sleeve Stresses

Stress Category	Stresses (psi)	Allowable Stress (psi)	Margin(1)
P_m	506	15,300	96.69%
$P_L + P_b$	3,556	22,950	84.51%
P + Q	35,519	45,900	22.62%

Notes: (1) Margin = [1 – (Actual/Allowable)] x 100%

Effects of Additional Mass on Piping/Support System

The impact of the addition of weld overlay material on the existing primary stress qualification, which considers deadweight and dynamic loadings (such as those due to earthquake), was evaluated in [36], and found to be insignificant.

10 WELD OVERLAY DESIGN QUALIFICATION ANALYSIS: CHARGING INLET NOZZLE

10.1 INTRODUCTION

This section provides the WOL design qualification analysis to demonstrate the adequacy of the SWOL design for the RCS charging inlet (CI) nozzle. The effectiveness of a WOL with Alloy 52/52M weld material is demonstrated using crack growth analysis, per IWB-3640 [6], to ensure that the WOL does not deteriorate during service. Using the residual weld stresses developed by the finite element model of the WOL process, future crack growth was evaluated at the charging inlet nozzle safe-end weld locations using the operational design transients affecting the WOL region. The advantage of the Alloy 52/52M material is its high resistance to PWSCC, which minimizes the possibility for future PWSCC crack growth. Since the purpose of the SWOL is to mitigate/repair a potentially cracked dissimilar-metal butt-weld, performing crack growth analyses using ASME Code Section XI methodology is the accepted method to address the fatigue qualification of the WOL region for the RCS charging inlet nozzle.

The effect of the SWOL on the existing fatigue qualification of the RCS charging inlet nozzle outside the WOL region is addressed in accordance with ANSI B31.7 [33] requirements, considering the effect of the applicable thermal transient stresses, structural discontinuities, and bimetallic effects resulting from the SWOL.

10.2 LOADS

The loads used for the design of the charging inlet nozzle weld overlay are listed in Table 10-1. These loads are considered in [2] and specified in [31]. The load combinations considered in the design are listed in Table 10-2. The transients considered in the shutdown cooling nozzle FCG evaluation are shown in Table 10-3. The pipe end loads used for fatigue and FCG evaluations are listed in Table 10-4. These loads are considered in [7] and specified in [31]. The nozzle loads and transients used for the design and FCG analysis are bounding for the actual nozzle loads and the plant-specific transients [7, 31, and 30].

Table 10-1: Enveloping Charging Inlet Nozzle Loads Used for Weld Overlay Design [31]

Load Type	Axial Force F_a (kips)	Bending Moment M_b (in-kips)
DW	0.000	0.414
OBE	0.103	6.659
SSE	0.206	13.318

Notes:
DW = Deadweight Loads
OBE = Operating Basis Earthquake Loads
SSE = Safe Shutdown Earthquake Loads

Table 10-2: Load Combinations

Condition	Load Combination	Service Level
Design	DP + DW + DS	Design
Normal/Upset	TR(1) + DW + NT(1)	Level A/B
Emergency	DP + DW + MS + NT(1)	Level C
Test	TP + DW	Test

Notes:
1. Not applicable to WOL design sizing.
DW = Deadweight
DP = Design Pressure
TP = Test Pressure
TR = Level A/B Transient Loadings (Thermal and Pressure)
NT = Thermal Expansion
DS = Design Seismic
MS = Maximum Seismic

Table 10-3: Applicable Thermal Transients for RCS Charging Inlet Nozzles

#	Transient	Cycles	Level
1	Plant Heatup, 100°F / hr	500	A
2	Plant Cooldown, 100°F / hr	500	A
3	Plant Loading, 5% / min	15,000	A
4	Plant Unloading, 5% / min	15,000	A
5	Step Load Increase 10%	2,000	A
6	Step Load Decrease 10%	2,000	A
7	Reactor Trip	400	B
8	Loss of Flow	40	B
9	Loss of Load	40	B
10	Loss of Secondary Pressure	5	C
11	Purification	1,000	A
12	Low Volume Control	2,000	A
13	Boric Acid Dilution	8,000	A
14	Loss of Charging Flow	200	B
15	Loss of Letdown	50	B
16	Reg. HX Isolation (Short Term)	400	B
17	Hydro Test	10	Test
18	Leak Test	200	Test
19(1)	Seismic (Positivie)	200	B
20(1)	Seismic (Negative)	200	B
21	Zero Load	710(2)	-

Notes:

(1) The design specification[31] states 200 cycles of operational basis earthquake and 200 cycles of design basis earthquake. For this analysis, 400 cycles of design basis earthquake will be used.

(2) The total cycles for this transient consist of 500 Heat-Up and Cool-Down cycles, 10 Hydro Static Test cycles and 200 Leak Test cycles.

Table 10-4: Enveloping Charging Inlet Nozzle Loads for Fatigue and FCG Evaluations

Condition	Force (kips)			Moment (in-kips)		
	F_X	F_Y	F_Z	M_X	M_Y	M_Z
Deadweight	0.000	-0.036	0.000	-0.456	0.024	0.018
Thermal	0.039	0.017	-0.040	1.044	1.860	-1.776
Design Seismic	0.077	0.210	0.076	4.512	2.797	4.441
Maximum Seismic	0.154	0.420	0.152	9.024	5.594	8.882

Notes:

Axial force = $0.457*F_x+0.889*F_z$
Shear force = SQRT $[Fy^2+(0.889*F_x+0.457*F_z)^2]$
Torsion moment = $0.457*M_x+0.889*M_z$
Bending moment = SQRT $[M_y^2+(0.889*M_x+0.457*M_z)^2]$

10.3 WELD OVERLAY DESIGN SIZING

The minimum WOL thickness was determined based on a through-wall flaw in the original pipe. The methodology used to determine the WOL design thickness and length is discussed in Section 3. Using this methodology, radii from the design geometry, shown in Table 10-5, are used to design the minimum SWOL parameters. As-designed inside and outside radii at the thickest portion of the Alloy 82/182 and SS welds are presented here. The thickest portion results from considering the smallest inner radius (R_{i-min}) and the largest outer radius (R_{o-max}). By using the maximum wall thickness of the design geometry, a conservative SWOL design thickness and length is achieved. The WOL length was based conservatively on the recommended length, per Code Case N-740:

$$L_{WOL} = 0.75\sqrt{Rt}$$

where,

$R = R_{o-max}$ = outside radius
$t = R_{o-max} - R_{i-min}$ = wall thickness at the location of indication

The WOL length (L_{WOL}) will extend from the weld/base metal interface on either side of the Alloy 82/182 and SS welds, as shown in Figure 10-1. The WOL thickness (t_{WOL}) was determined using the following equation:

$$t_{WOL} = t/0.75 - t$$

The minimum WOL design dimensions are shown in Table 10-6.

In accordance with ASME Section XI IWB-3640, the criterion from Section XI, Appendix C is used to evaluate the maximum post-WOL stresses resulting from the actual applied loadings. To determine the applied post-WOL stresses, the minimum post-WOL thicknesses are considered, which produces a conservative method to determine stresses for comparison to the allowable stress criterion. The thinnest portion of the Alloy 82/182 and SS welds results from considering the largest inner radius (R_{i-max}) and the smallest outer radius post-WOL ($R_{o-min-WOL}$). These parameters and the resulting geometric section properties are presented in Table 10-7.

The applied bending stresses were calculated by:

$$\sigma_b = \frac{M_b}{Z}$$

M_b is per Table 10-1, and Z is per Table 10-7.

$$Z = \frac{\pi(R_{o-\min-wol}{}^4 - R_{i-\max}{}^4)}{4(R_{o-\min-wol})}$$

R_{i-max} and $R_{o-min-wol}$ are per Table 10-7.

The applied membrane stresses were calculated by:

$$\sigma_m = \sigma_p + \frac{F_a}{A_x}$$

where,

$$\sigma_p = \frac{\pi R_{i-\max}{}^2}{\pi\left(R_{o-\min-wol}{}^2 - R_{i-\max}{}^2\right)} P$$

F_a is per Table 10-1.

A_x is per Table 10-7.

$A_x = \pi \ (R_{o\text{-}min\text{-}wol}{}^2 - R_{i\text{-}max}{}^2)$

R_{i-max} and $R_{o-min-wol}$ are per Table 10-7.

P = 2,235 psig [2]

The allowable stress intensity S_m (at 650°F) used in the sizing of the Alloy 52/52M (N06690) overlay is 23.3 ksi [9]. This allowable is based on the annealed condition of SB-166/SB-167. The normal operating pressure, 2,235 psig, was used for the calculation.

The resulting stresses, determined by using the previous equations and the loads and load combinations from Tables 10-1 and 10-2, respectively, are listed and compared to the Code allowable in Table 10-8.

Table 10-5: Charging Inlet Nozzle Geometry for WOL Design Calculations [2]

Alloy 82/182 Weld			Stainless Steel Weld		
Inside Radius R_{i-min} (in)	Outside Radius R_{o-max} (in)	Wall Thickness t_{design} (in)	Inside Radius R_{i-min} (in)	Outside Radius R_{o-max} (in)	Wall Thickness t_{design} (in)
0.844	1.438	0.594	0.844	1.188	0.344

Table 10-6: Charging Inlet Nozzle Minimum Weld Overlay Repair Design Dimensions [2]

Alloy 82/182 Weld		Stainless Steel Weld	
t_{WOL} (in)	L_{WOL} (in)	t_{WOL} (in)	L_{WOL} (in)
0.30	0.69	0.12	0.48

Table 10-7: Charging Inlet Nozzle Geometry for Stress Check in Post-Weld-Overlay Condition [2]

Alloy 82/182 Weld				Stainless Steel Weld			
Inside Radius $R_{i\text{-}max}$ (in)	Outside Radius $R_{o\text{-}min\text{-}WOL}$ (in)	Cross-Sectional Area A_x (in^2)	Section Modulus Z (in^3)	Inside Radius $R_{i\text{-}max}$ (in)	Outside Radius $R_{o\text{-}min\text{-}WOL}$ (in)	Cross-Sectional Area A_x (in^2)	Section Modulus Z (in^3)
0.844	1.575	5.555	2.816	0.867	1.308	3.009	1.416

Table 10-8: Charging Inlet Nozzle Post-SWOL Stress Comparison [2]

	Normal/Upset		Emergency/Faulted	
Location	Applied Stress σ_b (ksi)	Allowable Stress P_b (ksi)	Applied Stress σ_b (ksi)	Allowable Stress P_b (ksi)
Alloy Weld	2.512	10.761	4.877	22.329
SS Weld	4.995	9.967	9.697	21.586

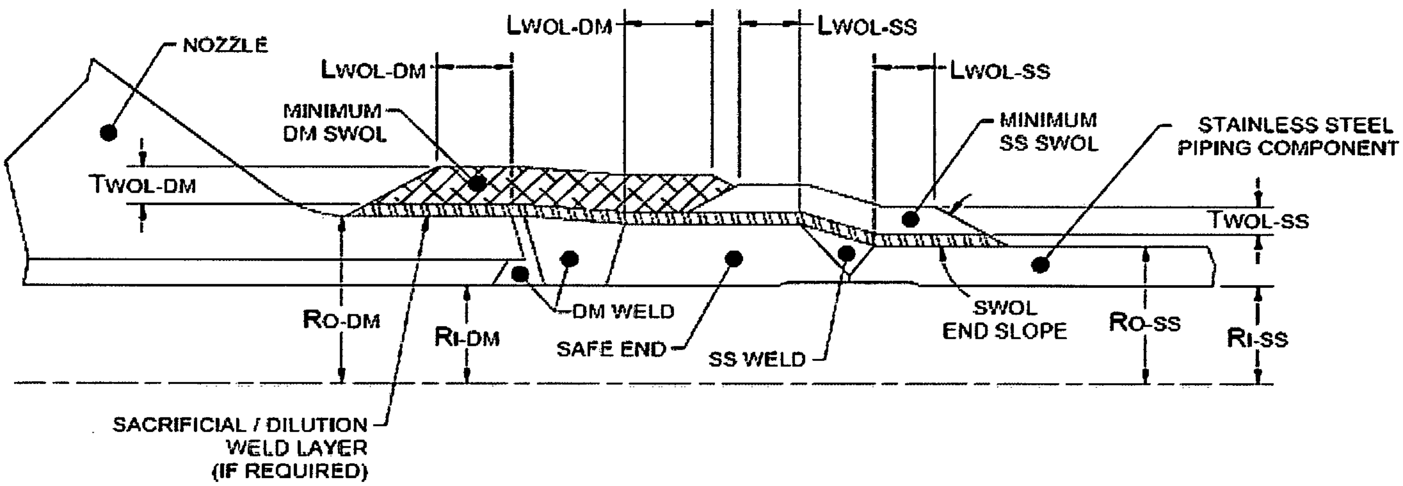

Figure 10-1: Weld Overlay Design Parameters for the Charging Inlet Nozzle

(Not drawn to scale.)

10.4 WELD OVERLAY RESIDUAL WELD STRESS RESULTS

As described in Section 5.3, the finite element model was developed to capture the parts of the structure in the vicinity of the charging inlet nozzle safe-end with the SWOL. This includes a portion of the charging inlet nozzle attached to the nozzle safe-end and a length of SS pipe attached to the safe-end. An ID weld repair was considered in the finite element model. The finite element model and boundary conditions are shown in Figures 10-2 and 10-3. The nozzle is fixed in the axial direction to simulate the rest of the nozzle. The end of the SS piping is coupled in the axial direction to simulate the remaining portion of the SS piping not included in the model. The model assumes that a 50% through-wall weld repair was performed from the inside surface of the charging inlet nozzle to safe-end Alloy 82/182 butt-weld.

The final residual weld stresses, including normal operating pressure and temperature conditions, are shown in Figures 10-4 and 10-5 for selected stress cuts in the Alloy 82/182 and SS welds. The locations of the stress cuts are provided in Figure 10-2. The axial and hoop stress contours in the RCS spray nozzle after the WOL application are provided in Figures 10-6 and 10-7.

Figure 10-4 shows the axial and hoop residual stresses for the Alloy 82/182 weld at normal operating conditions after the SWOL. The stresses are compressive up to about 80% of the original pipe wall thickness. This stress distribution is favorable due to the generally compressive stress field because it minimizes the potential for crack growth in the DM weld region. Similarly, Figure 10-5 shows the axial and hoop stresses for the stainless weld, which remain compressive for more than 80% of the original pipe wall at normal operating conditions. Therefore, the potential for FCG is minimized.

Acceptable post-WOL residual stresses (i.e., stresses that satisfy the requirements for mitigating PWSCC) are those that are sufficiently compressive over the entire length and circumference of the inside surface of the Alloy 82/182 weld (at operating temperature, but prior to applying operating pressure and loads). Acceptable post-WOL residual stresses also have a total stress, after application of operating pressure and loads, that remains less than 10 ksi tensile [28]. This target level has been selected as a conservatively safe value, below which PWSCC initiation, or growth of small initiated cracks, is unlikely. Additionally, the residual plus operating stresses must remain compressive through some portion of the weld thickness away from the inside surface. The residual stresses in the Alloy 82/182 weld of the charging inlet nozzle, resulting from the WOL, are well below this stress level through 80% of the original weld thickness.

Figures 10-8 and 10-9 show that the axial and hoop stresses on the inside surface (in the vicinity of the alloy weld and buttering) remain compressive after SWOL. The maximum resultant bending moment for a normal operating condition is 3.209 in-kips. The resulting maximum bending stresses in the Alloy 82/182 weld and SS weld are 0.825 ksi and 1.005 ksi, respectively [32]. The pipe bending stresses are low, and are considered to have a negligible effect on the residual weld stress results.

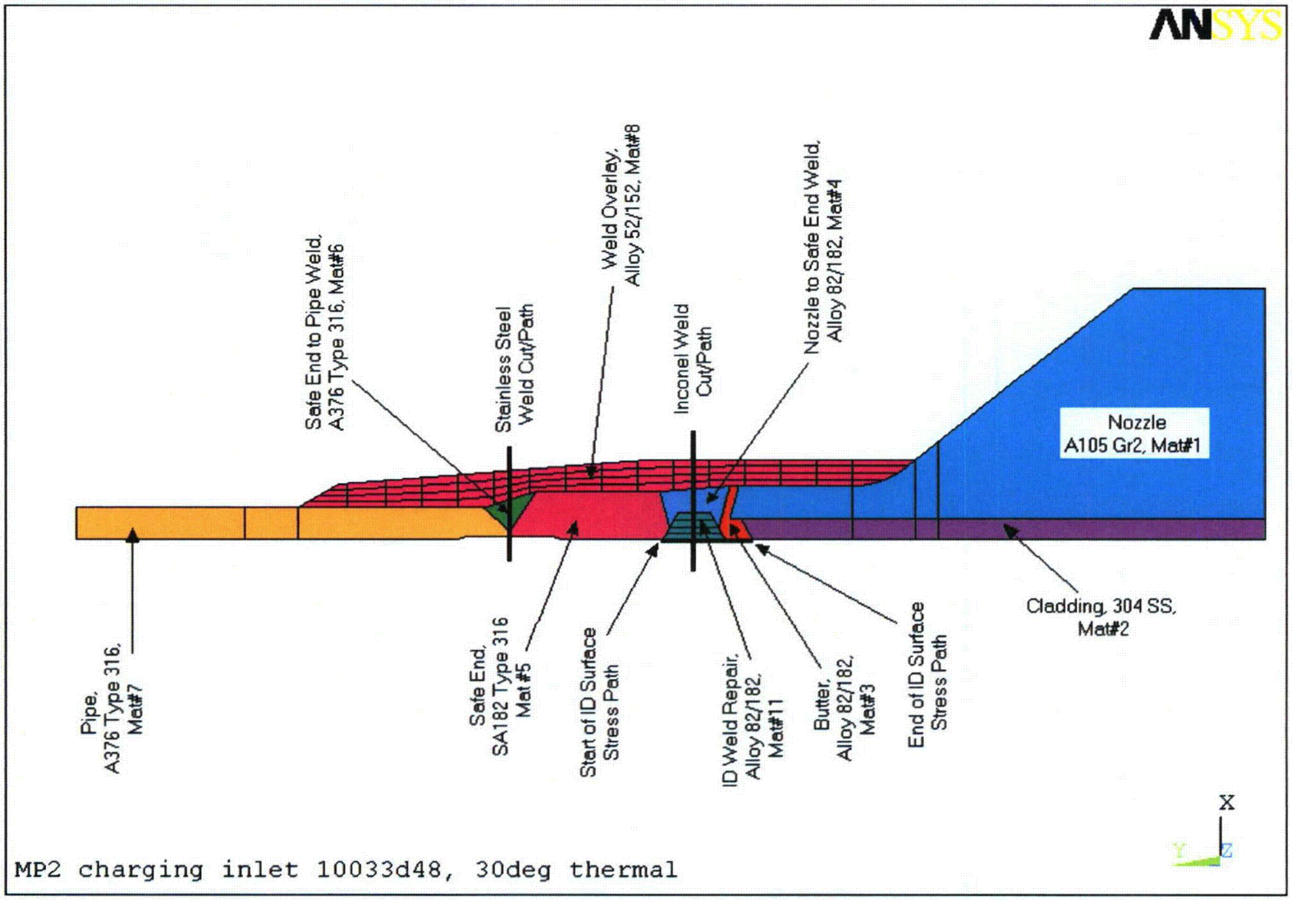

Figure 10-2: ANSYS Model of Charging Inlet Nozzle

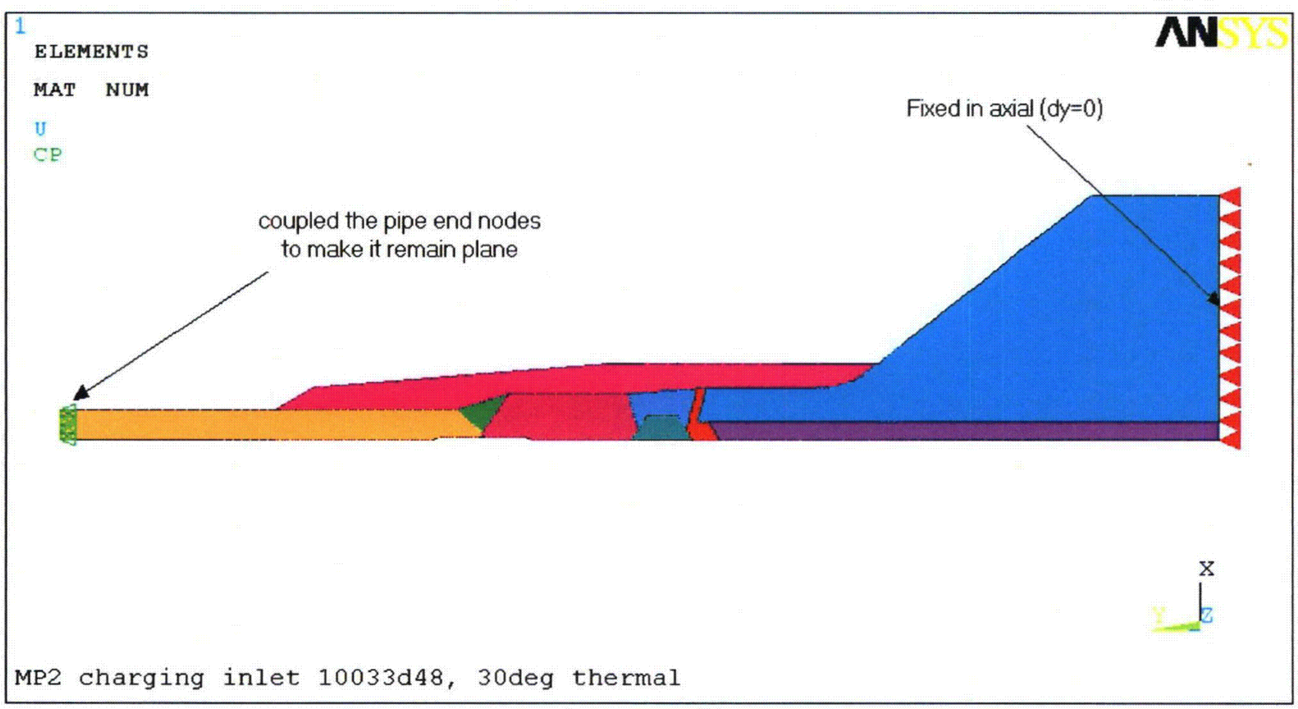

Figure 10-3: Finite Element Model and Structural Boundary Conditions

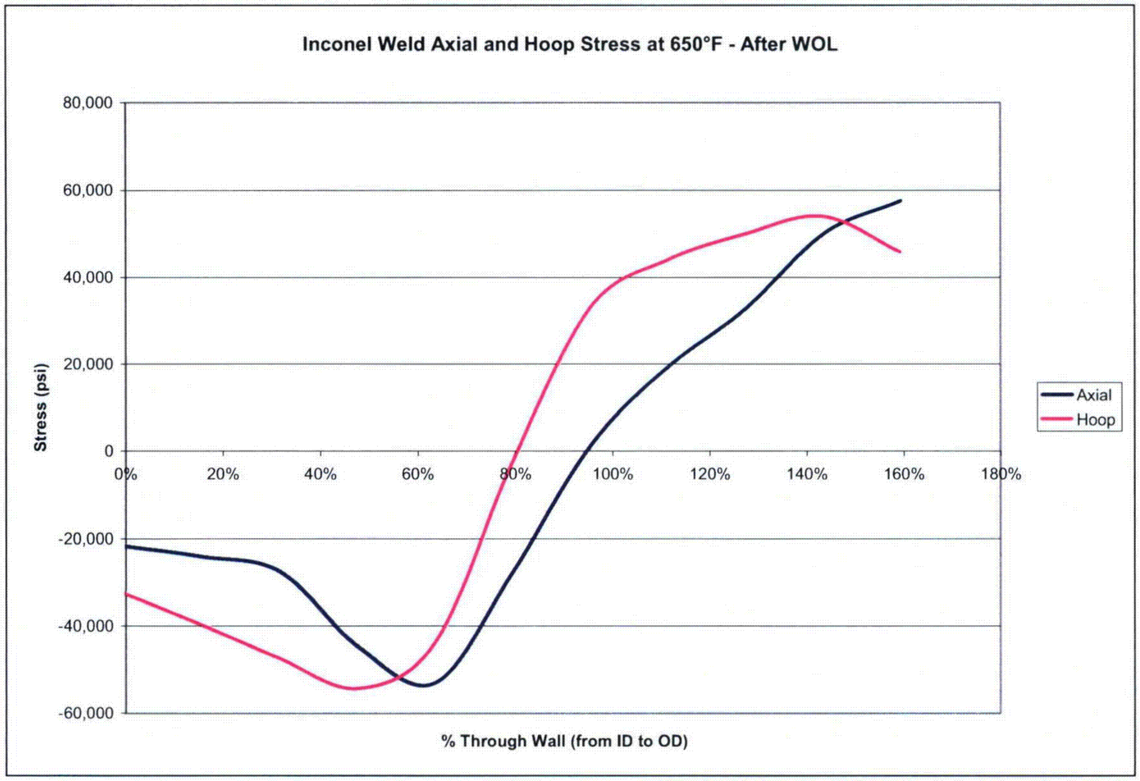

Figure 10-4: Axial and Hoop Residual Stresses in the Alloy 82/182 Weld at Operating Conditions*

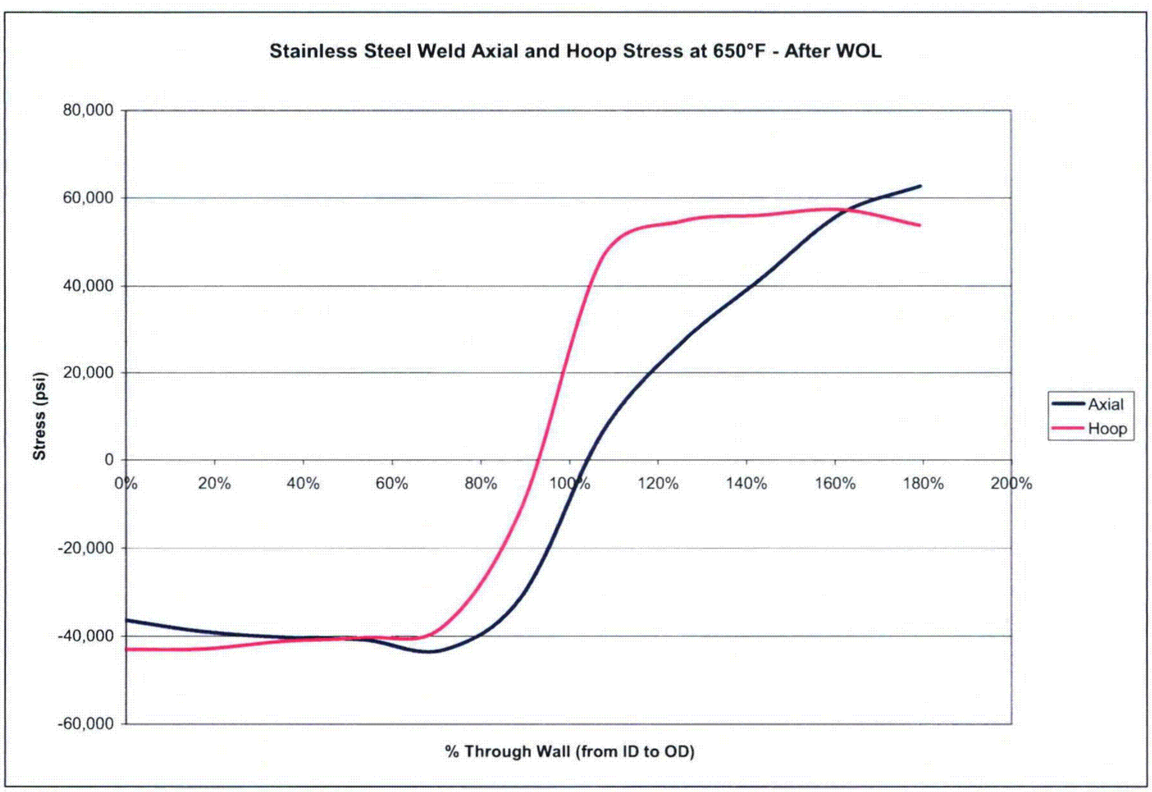

Figure 10-5: Axial and Hoop Residual Stresses in the SS Weld at Operating Conditions*

*Note: The percent through-wall indicated on the horizontal axis is expressed in terms of the original pipe wall thickness. The WOL region is the region beyond 100% wall thickness.

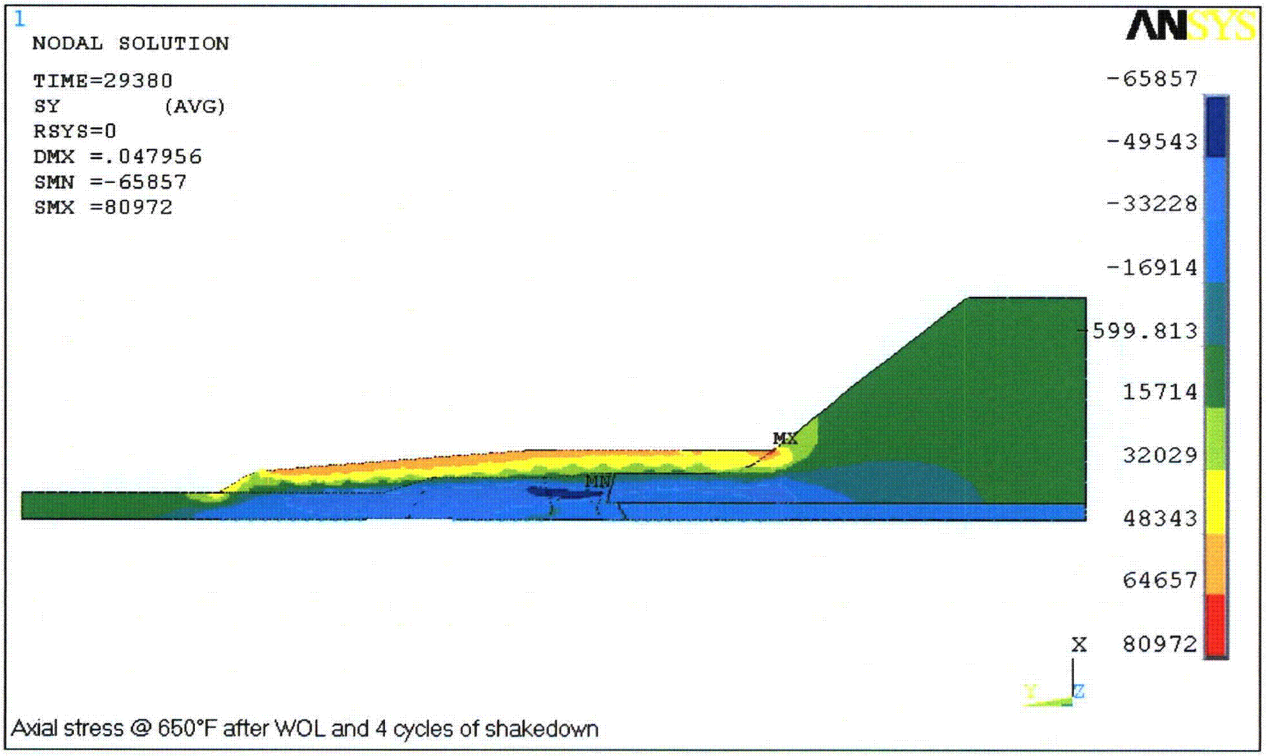

Figure 10-6: Axial Stress (psi) Contour Plot at Operating Condition after Weld Overlay

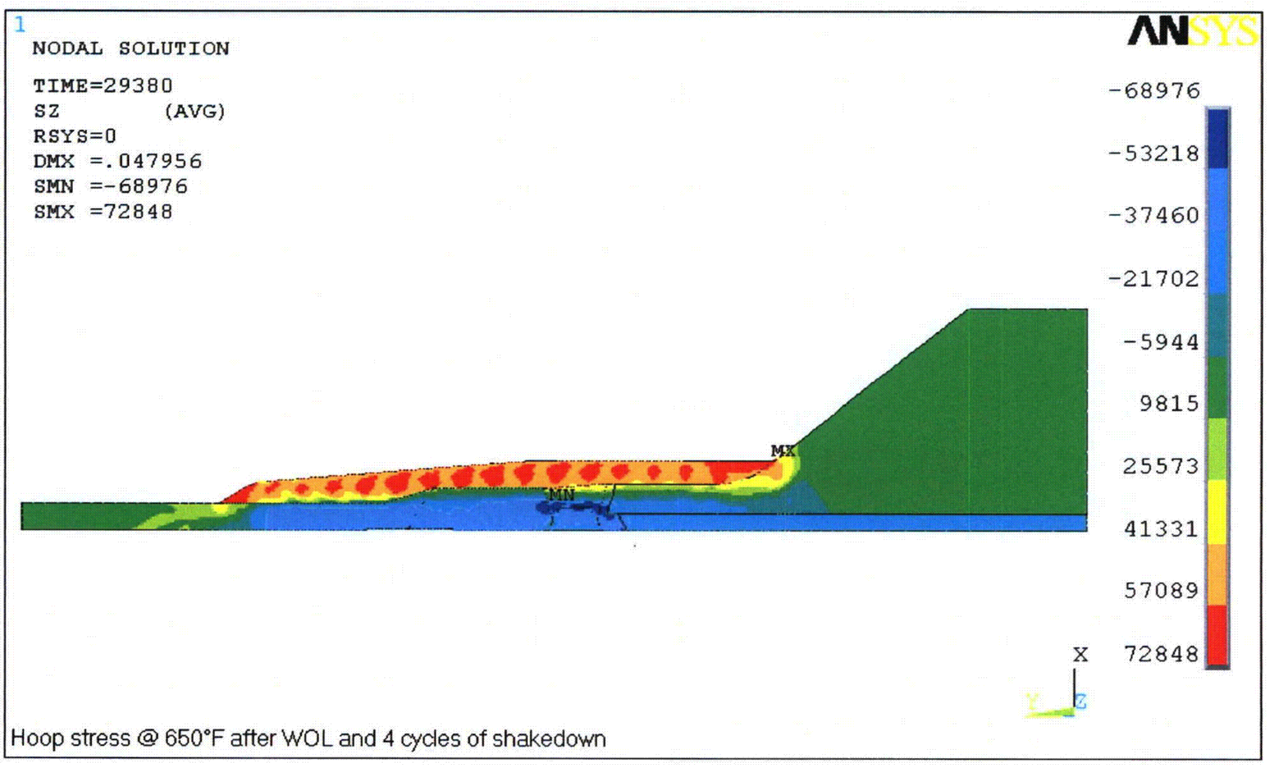

Figure 10-7: Hoop Stress (psi) Contour Plot at Operating Condition after Weld Overlay

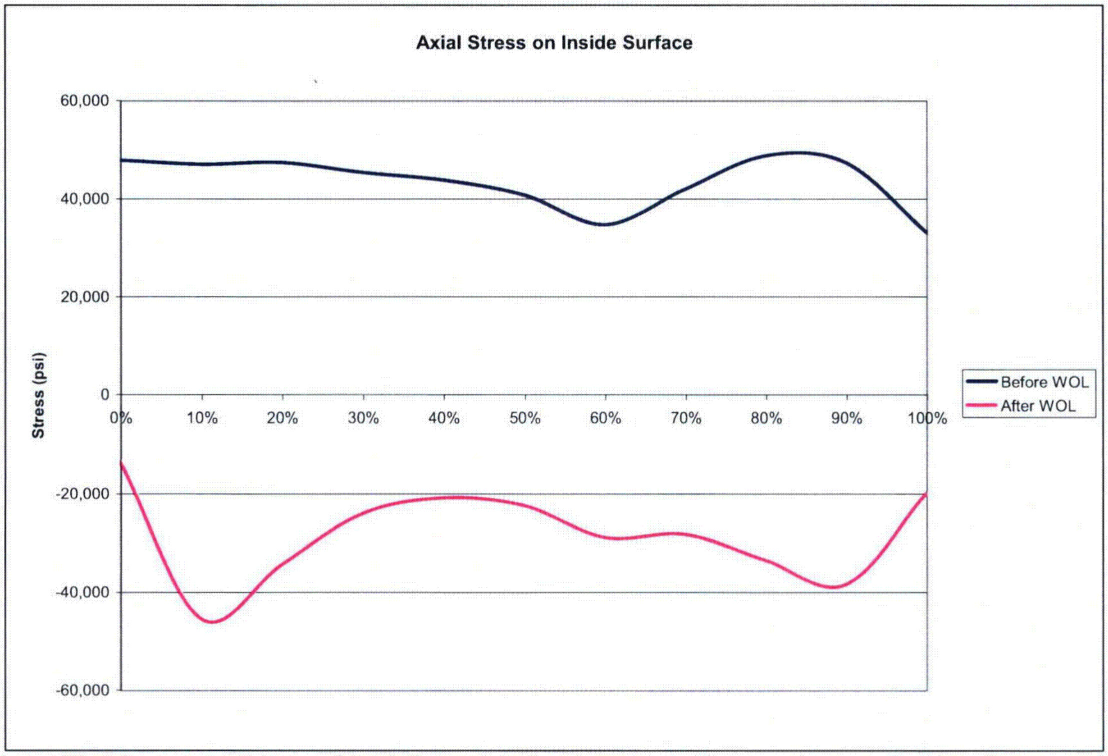

Figure 10-8: Axial Residual Stress along the ID Surface at Operating Condition*

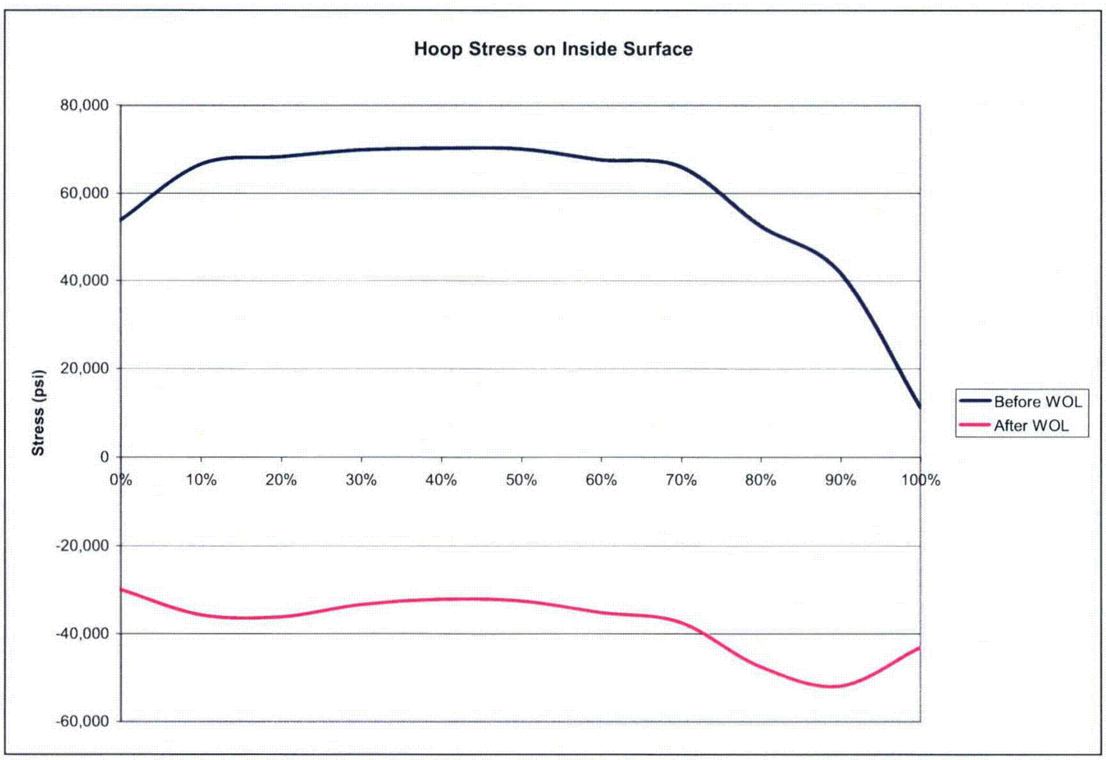

Figure 10-9: Hoop Residual Stress along the ID Surface at Operating Condition*

*Note: X-axis is % along the ID path. See Figure 10-2.

10.5 FATIGUE CRACK GROWTH RESULTS AND ESTIMATE OF WELD OVERLAY DESIGN LIFE: CHARGING INLET NOZZLE REGION

The methodology used to determine fatigue crack growth is described in Section 4.4. Fatigue crack growth analyses were performed for the charging inlet nozzles using the through-wall stress distribution including residual stresses generated from the weld overlay mitigation/repair process and the thermal transient stresses.

The weld overlay service life is a function of the flaw depth found in the region being overlaid, and the projected growth of that flaw. The limitation on the maximum flaw depth is 75% of the piping wall thickness (including the weld overlay thickness), per Section XI, IWB-3640 [6].

A range of possible flaw sizes, from 0 to 100% of the original wall thickness, was postulated in the fatigue crack growth evaluations. The results of these evaluations for the flaw depths less than the original design wall thickness are plotted in Figures 10-10 and 10-11, in the form of expected time for these flaws to reach the interface between the original wall and the newly laid weld overlay material. Figure 10-10 shows results for the Alloy 82/182 weld, and Figure 10-11 shows results for the SS weld. For the maximum possible flaw depths of 100% of the original design wall thickness propagating into the Alloy 52/52M weld overlay material, results are shown in Figure 10-12. This figure shows the estimated flaw depth with time for the design cycles spread over either the original design life or the extended life of the plant.

Figures 10-10 and 10-11 summarize the expected service life (based on transients cycles spread evenly for either 40 years or 60 years of plant life) for a given initial flaw depth to reach 100% of the original wall thickness at the Alloy 82/182 weld and the SS weld locations, respectively. Based on the results shown in Figures 10-10 and 10-11, it can be concluded that if no flaws are detected during the post-SWOL inspection, a conservatively assumed flaw, 75% through the original wall would not grow to 100% of the original wall thickness for 40 years FCG due to transient cycles. This is based on the assumption that the current 40-year design transient cycles are spread evenly over 40 years of plant life. If flaws are detected during the post-SWOL inspection, the as-found flaw size can be used to determine the design life of the SWOL using the crack growth results shown in Figures 10-10 and 10-11.

For the case of an initial flaw depth of 100% of the original wall thickness, i.e., a through-wall flaw, Table 10-9 shows that the total flaw growth into the newly laid Alloy 52/52M welds material in one 10-year inspection interval is 0.016 inch, based on the design cycles spread over a 60-year extended life. The final flaw depth after the 10-year period with the fatigue crack growth considered is still within 75% of the total post-WOL wall thickness, as required by SWOL criteria.

Two examination scenarios exist: a pre-overlay examination and a post-overlay examination. If an examination found no flaws, the overlay service life would be governed by the largest flaw that might have been missed by the examination. For an examination performed prior to the weld overlay installation, a conservative approach would be to assume that the flaw depth is 10% of the original wall thickness. Alternatively, this would be 75% of the original wall for an examination performed after the weld overlay installation. This is because the area required to be inspected after the overlay is only the outer 25% of the original pipe thickness plus the overlay thickness itself. The PDI qualification blocks do not contain any flaws in the inner 75% of the pipe wall. Therefore, it would be conservative to assume

such a flaw for the qualification. As shown in Figure 9-10, an initial flaw as deep as 75% would result in a remaining service life of 100% of the original design cycles. If the design cycles are assumed to be spread over 40 years of plant operation, the remaining life of the SWOL would be 40 years. This is well beyond the required 10-year in-service inspection (ISI) interval. If, after the next ISI, no flaws are detected in the outer 25% of the original welds, the SWOL life is 40 years from the time of the latest inspection.

In the unlikely event that the post-overlay inspection detected a flaw as large as the full depth of the original design wall thickness, the expected service life of the weld overlay would be at least one 10-year inspection interval period. For the charging inlet nozzle, flaw growth rate into the weld overlay material is small during the 10 year period and with the 75% of the total post-WOL wall thickness.

For example, if an axial flaw that is 91% through the original Alloy 82/182 wall thickness is detected as a result of the post-weld-overlay inspection, and assuming conservatively that the current 40-year design transient cycles are spread evenly for only 40 years, the expected service life from Figure 10-10 for this flaw to reach 100% of the original wall thickness is about 11 years. If it is assumed that the design transient cycles are spread evenly for 60 years, the remaining service life would be approximately 16 years. This can also be determined by applying a factor of 1.5 to the service life based on the 40-year design cycles. For a similar-size circumferential flaw, the expected service life is about 40 years, based on current 40-year design transient cycles assumed to be spread evenly over 40 years. Since the typical in-service inspection interval is 10 years for this initial flaw depth of 91%, it can be concluded that the sizing of the structural weld overlay is adequate up to the next inspection period based on the current 40-year design transient cycles spread evenly over the next 40 years.

Another case of 100% original design wall thickness through-wall flaw was hypothesized assuming the total post-weld-overlay wall of 0.8935 inch. This included an extra allowance of 0.1 inch for the FCG in to the Alloy 690 material. The 100% original wall axial flaw of 0.5605 inch was evaluated for the fatigue crack growth results, shown in Table 10-9 and in Figure 10-12. Results demonstrate that the total growth in 10 years is approximately 0.016 inch. The final flaw depth after a 10 years of fatigue crack growth is within 75% of the total post-WOL wall thickness, as required by SWOL criteria. Also, for the 100% design wall thickness initial flaw depth to reach the 75% of the post-WOL total wall thickness would take 36.7 years based on the design cycles spread over a 60-years life. Therefore, the 0.21 inch SWOL thickness increase provided in the SWOL design is adequate to address the issue of PWSCC for an almost through-wall flaw.

The actual time required to use the remaining design cycles depends on plant operating practice.

Table 10-9: Charging Inlet Nozzle Alloy 52/52M FCG Data – Axial Flaw [35]

Nozzle Thickness (in)	Initial Flaw Depth (in)	Final Flaw Depth in 10 years (in)	Total Flaw Growth in 10 years (in)
0.8935(1,2)	0.560	0.576	0.016

Notes:

(1) This thickness is due to a 0.1-inch increase in SWOL thickness. The final flaw depth in 10 years results in approximately 75% of the total thickness including SWOL.
(2) A rise time of 5,000 seconds is conservatively used in the Alloy 52/52M FCG rate.

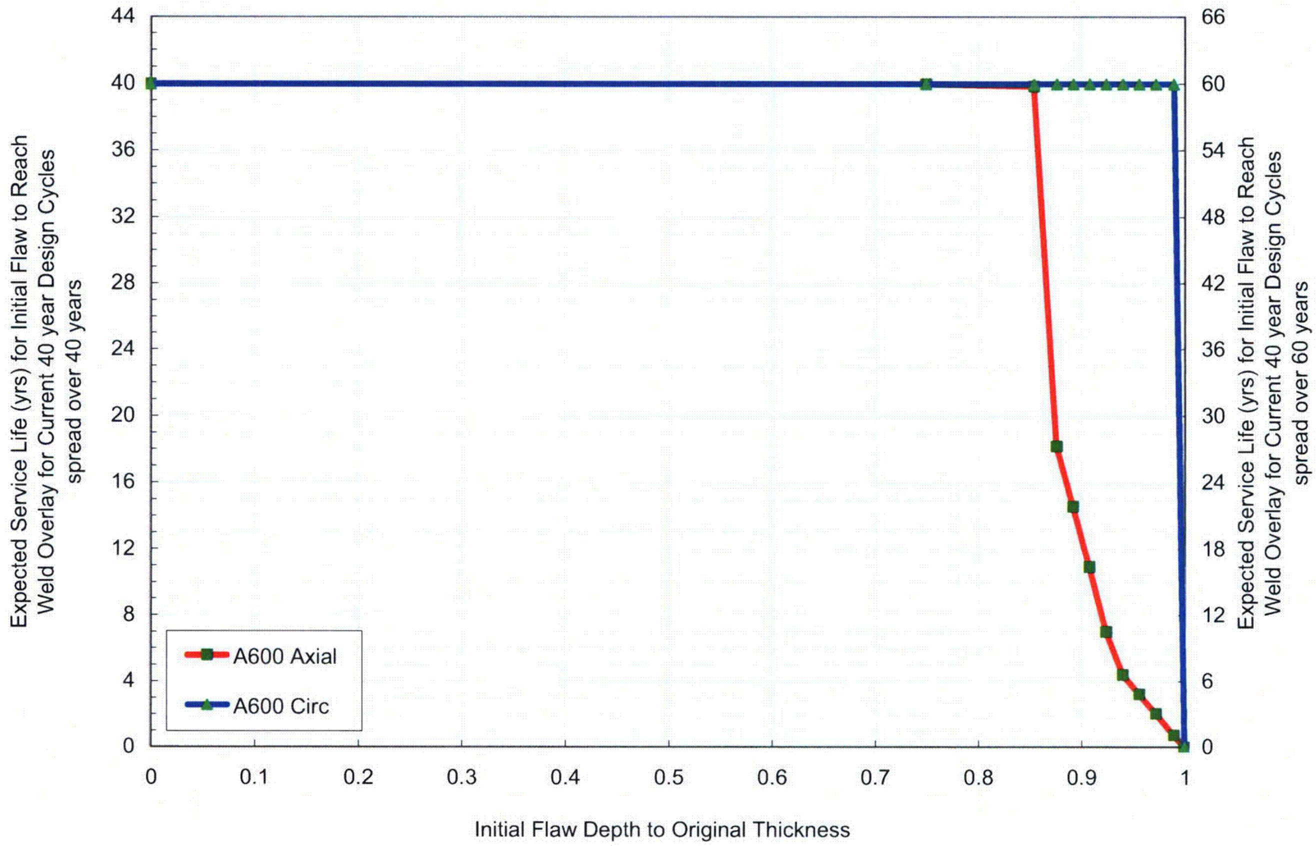

Figure 10-10: Expected Time for the Initial Flaw Depth to Reach the Weld Metal Interface for CI Nozzle Alloy 82/182 Weld [35]

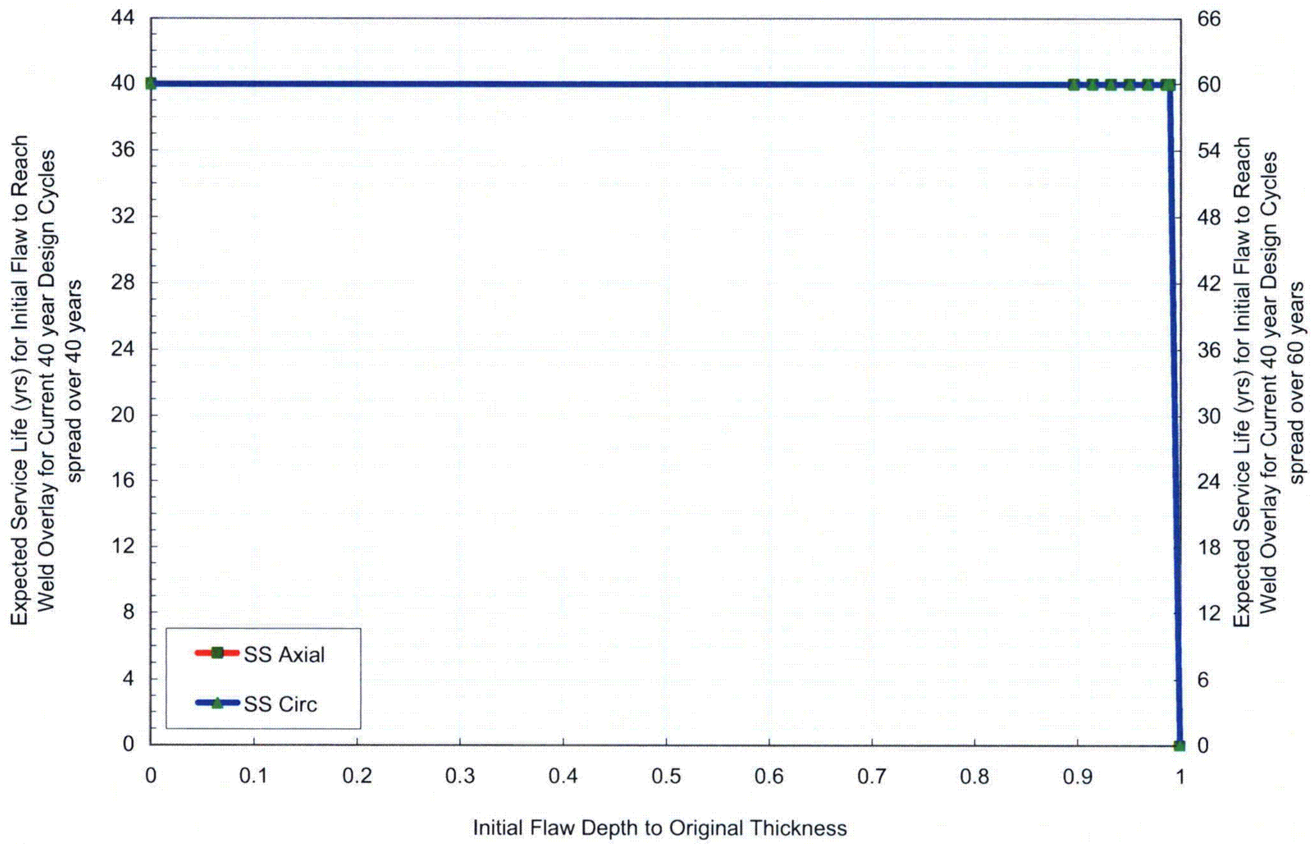

Figure 10-11: Expected Time for the Initial Flaw Depth to Reach the Weld Metal Interface for CI Nozzle SS Weld [35]

Note: Curves for axial and circumferential flaw estimated life coincide with each other. Hence, only one curve is visible in the figure above.

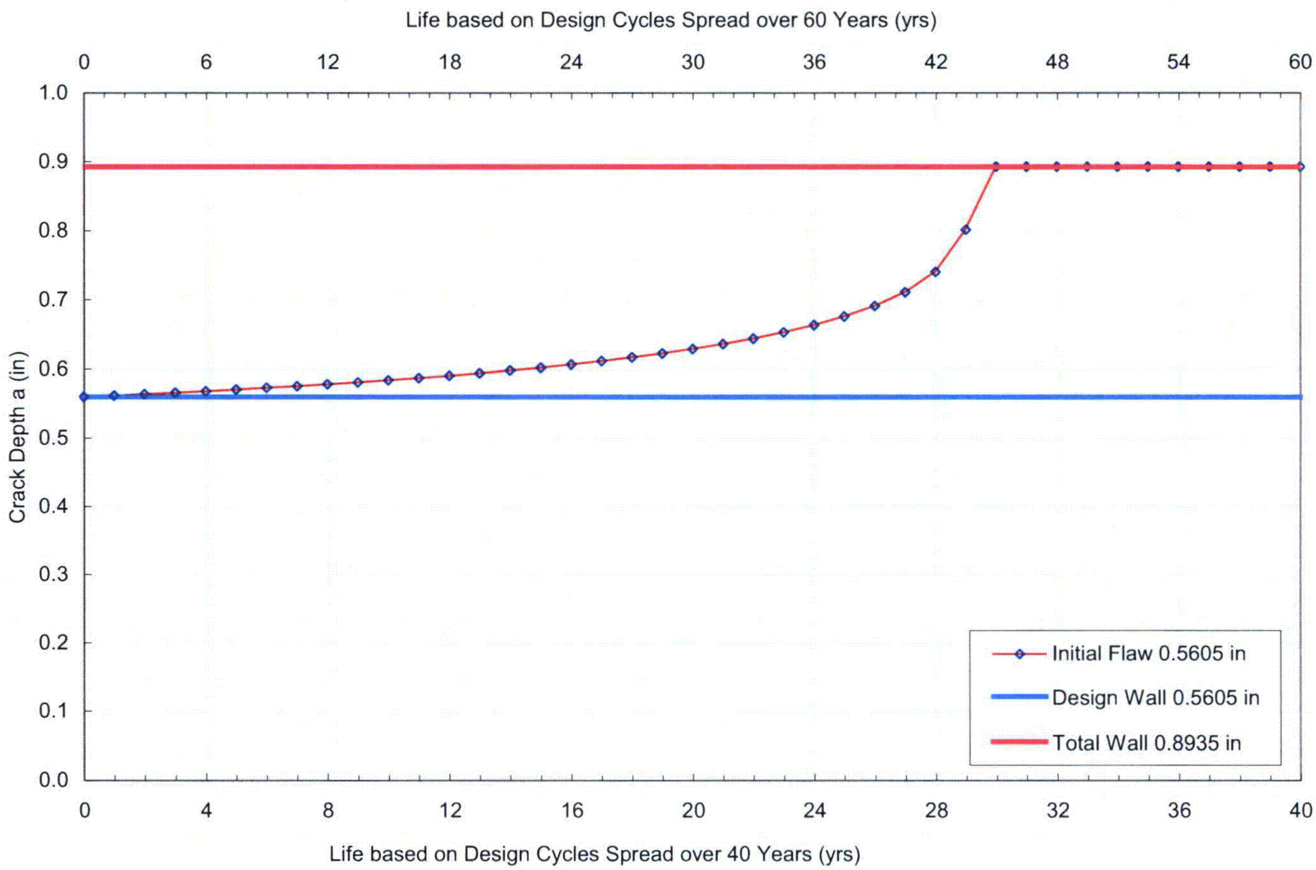

Figure 10-12: Flaw Growth for 100% Original Wall Thickness Initial Flaw versus Service Period in Alloy 52/52M at CI Nozzle Alloy Weld [35]

10.6 IMPACT ON DESIGN QUALIFICATIONS OF NOZZLE AND PIPE

The impact of the weld overlay is evaluated to demonstrate that the presence of the weld overlay repair does not have any adverse impact on the existing stress qualification of the charging inlet nozzle with respect to the Code of Construction [33].

Effects of SWOL on Transient Stress and Fatigue Analysis

Since the intention of the structural weld overlay is to mitigate/repair the potentially cracked dissimilar-metal butt-weld at the charging inlet nozzle safe-end, the crack growth analyses discussed in Section 10.5 using the ASME Code Section XI methodology are acceptable bases to address the fatigue qualification of the weld overlay region for the RCS charging inlet nozzle.

The original analysis was performed in accordance with the ANSI Code [33]. It offers protection against membrane or catastrophic failure, and protection against fatigue or leak type failure. The SWOL does not influence the reinforced region of the charging inlet nozzle. Therefore, the existing analysis [34] remains applicable for this region, provided the loading used in [34] remains applicable. The transient stresses and structural evaluation for the weld overlay charging inlet nozzle were documented in [7]. The primary stress for the charging inlet nozzle was evaluated by hand calculations in accordance with ANSI B31.7 [33]. Addition of the SWOL does not affect the B indices of the loads from the piping, but increases the section modulus in the overlay region. The applicable primary loads (pressure and mechanical loads) used in [34] are not changed by the SWOL. Therefore, the primary stresses in the structures with SWOL are, by definition, less than or equal to those without SWOL. The previous qualifications [34] performed for the charging inlet nozzle applies to this calculation.

The fatigue for the charging inlet nozzle was evaluated with finite element techniques. Cut locations are illustrated in Figure 10-13. As Table 10-10 shows, all stress, thermal ratcheting, and fatigue results meet the requirements specified in ANSI B31.7 [33]. Therefore, it is concluded that the existing ANSI B31.7 analysis of the charging inlet nozzle is not adversely affected by the addition of the SWOL.

Table 10-10: Charging Inlet Nozzle with SWOL Result Summary

Loading Condition	Stress Category	Cut No.	Stress (psi) or Usage	Stress Limit	Allowable Stress (psi) or Usage	Margin
Design	$P_L + P_b$	-	11,911	1.5 S_m	25,500	53.29%
Level A/B	P + Q	1	55,428	3 S_m	50,100	-10.63%(1)
	Linear Thermal Ratchet	1	0.676	N/A	1.000	32.44%
	Parabolic Thermal Ratchet	3	0.563	N/A	1.000	43.68%
	Fatigue	3	0.849	N/A	1.000	15.10%
Level C/D	$P_L + P_b$	-	18,738	2.25 S_m	38,250	51.01%

Note: (1) A simplified elastic-plastic analysis was performed [7] in accordance with ANSI B31.7 [33] to justify $P + Q > 3S_m$.

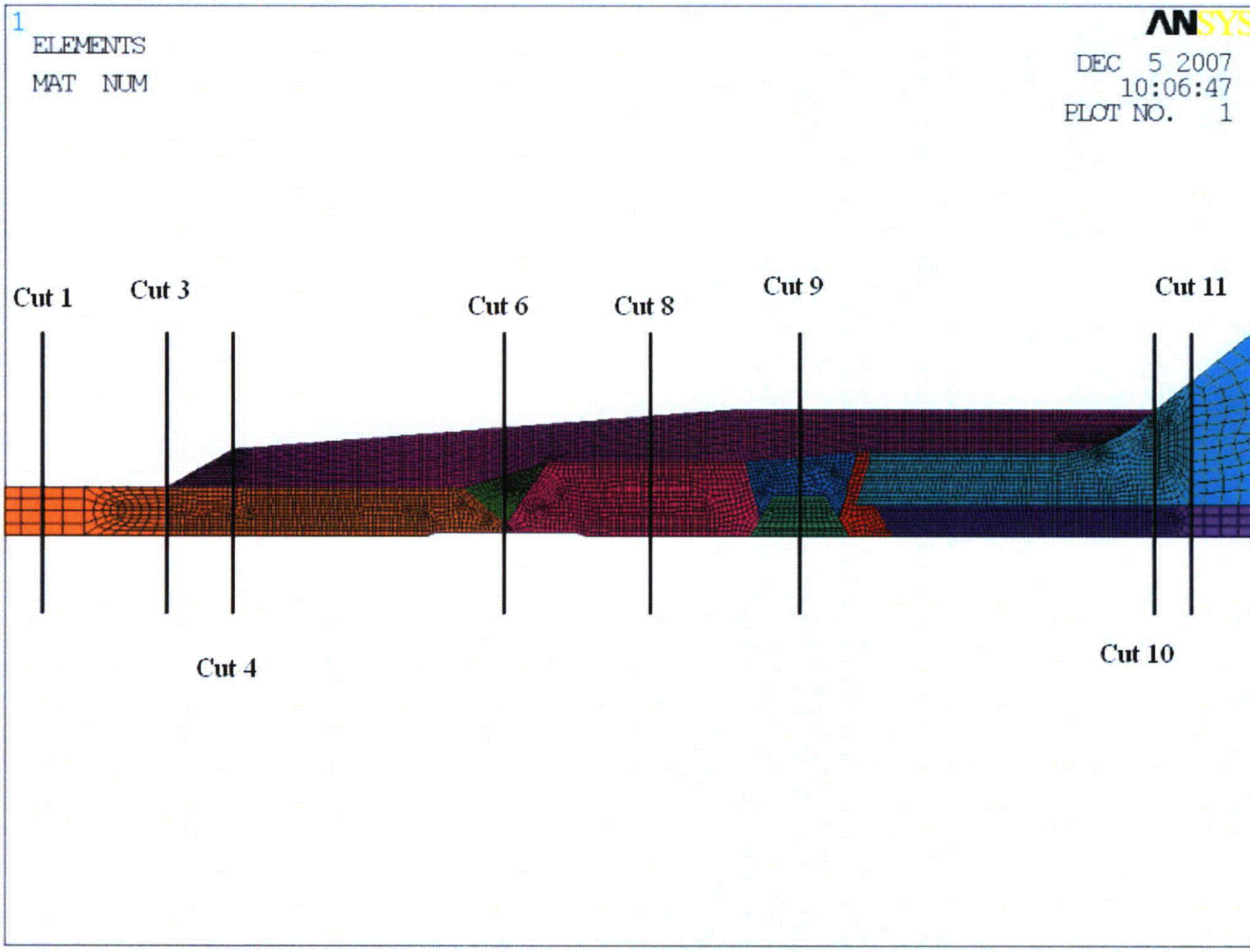

Figure 10-13: Charging Inlet Nozzle Cut/Path Locations

Effects of Additional Mass on Piping/Support System

The impact of the addition of weld overlay material on the existing primary stress qualification, which considers deadweight and dynamic loadings (such as those due to earthquake), was evaluated in [36], and found to be insignificant.

11 WELD OVERLAY DESIGN QUALIFICATION ANALYSIS: LETDOWN/DRAIN NOZZLE

11.1 INTRODUCTION

This section provides the WOL design qualification analysis to demonstrate the adequacy of the SWOL design for the RCS letdown/drain nozzle. The effectiveness of a WOL with Alloy 52/52M weld material is demonstrated using crack growth analysis, per IWB-3640 [6], to ensure that the WOL does not deteriorate during service. Using the residual weld stresses developed by the finite element model of the WOL process, future crack growth was evaluated at the letdown/drain nozzle safe-end weld locations using the operational design transients affecting the WOL region. The advantage of the Alloy 52/52M material is its high resistance to PWSCC, which minimizes the possibility for future PWSCC crack growth. Since the purpose of the SWOL is to mitigate/repair a potentially cracked DM butt-weld, performing crack growth analyses using ASME Code Section XI methodology is the accepted method to address the fatigue qualification of the WOL region for the RCS letdown/drain nozzle.

The effect of the SWOL on the existing fatigue qualification of the RCS letdown/drain nozzle outside the WOL region is addressed in accordance with ANSI B31.7 requirements, considering the effect of the applicable thermal transient stresses, structural discontinuities, and bimetallic effects resulting from the SWOL.

11.2 LOADS

The loads used for the design of the letdown/drain nozzle weld overlay are listed in Table 11-1. These loads are considered in [2] and specified [31]. The load combinations considered in the design are listed in Table 11-2. The transients considered in the letdown/drain nozzle FCG evaluation are shown in Table 11-3. The pipe end loads used for fatigue and FCG evaluations are listed in Table 11-4. These loads are considered in [7] and specified in [31]. The nozzle loads and transients used for the design and FCG analysis are bounding for the actual nozzle loads and the plant-specific transients [7, 31, and 30].

Table 11-1: Enveloping Letdown/Drain Nozzle Loads Used for Weld Overlay Design [31]

Load Type	Axial Force F_a (kips)	Bending Moment M_b (in-kips)
DW	0.084	1.750
OBE	0.376	18.557
SSE	0.752	37.114

Notes:
DW = Deadweight Loads
OBE = Operating Basis Earthquake Loads
SSE = Safe Shutdown Earthquake Loads

Table 11-2: Load Combinations

Condition	Load Combination	Service Level
Design	DP + DW + DS	Design
Normal/Upset	TR(1) + DW + NT(1)	Level A/B
Emergency	DP + DW + MS + NT(1)	Level C
Test	TP + DW	Test

Notes:
1. Not applicable to WOL design sizing.
DW = Deadweight
DP = Design Pressure
TP = Test Pressure
TR = Level A/B Transient Loadings (Thermal and Pressure)
NT = Thermal Expansion
DS = Design Seismic
MS = Maximum Seismic

Table 11-3: Applicable Thermal Transients for RCS Letdown/Drain Nozzles

#	Transient	Cycles	Level
1	Plant Heatup, 100°F / hr	500	A
2	Plant Cooldown, 100°F / hr	500	A
3	Plant Loading, 5% / min	15,000	A
4	Plant Unloading 5% / min	15,000	A
5	Step Load Increase 10%	2,000	A
6	Step Load Decrease 10%	2,000	A
7	Reactor Trip	400	B
8	Loss of Turbine Generator Load/ Loss of Reactor Coolant Flow	80(3)	B
9	Loss of Secondary Pressure	5	C
10	Hydrostatic Test	10	TEST
11	Leak Test	200	TEST
12(1)	Seismic (Positive)	200	B
13(1)	Seismic (Negative)	200	B
14	Zero Load	710(2)	-

Notes:

(1) The design specification [31] states 200 cycles of operational basis earthquake and 200 cycles of design basis earthquake. For this analysis, 400 cycles of design basis earthquake will be used.

(2) The total cycles for this transient consist of 500 Heatup and Cooldown cycles, 10 Hydrostatic Test cycles, and 200 Leak Test cycles.

(3) The total cycles for this transient consist of 40 Loss of Turbine Generator Load cycles and 40 Loss of Reactor Coolant Flow cycles.

Table 11-4: Equations for Pipe End Loads

Condition	Force (kips)			Moment (in-kips)		
	F_x	F_y	F_z	M_x	M_y	M_z
Deadweight	-0.003	-0.062	0.000	0.156	0.192	0.588
Thermal	0.273	0.361	0.268	-4.090	6.946	5.814
Design Seismic	0.483	0.376	0.422	13.895	7.630	12.300
Maximum Seismic	0.966	0.752	0.844	27.790	15.260	24.600

Notes:

Axial force = $-F_y$
Shear force = $\sqrt{(F_x^2 + F_z^2)}$
Torsion moment = M_y
Bending moment = $\sqrt{(M_x^2 + M_z^2)}$

11.3 WELD OVERLAY DESIGN SIZING

The minimum WOL thickness was determined based on a through-wall flaw in the original pipe. The methodology used to determine the WOL design thickness and length is discussed in Section 3. Using this methodology, radii from the design geometry, shown in Table 11-5, are used to design the minimum SWOL parameters. As-designed inside and outside radii at the thickest portion of the Alloy 82/182 and SS welds are presented here. The thickest portion results from considering the smallest inner radius ($R_{i\text{-}min}$) and the largest outer radius ($R_{o\text{-}max}$). By using the maximum wall thickness of the design geometry, conservative SWOL design thickness and length are achieved. The WOL length was based conservatively on the recommended length, per Code Case N-740:

$$L_{WOL} = 0.75\sqrt{Rt}$$

where,

$R = R_{o\text{-}max}$ = outside radius
$t = R_{o\text{-}max} - R_{i\text{-}min}$ = wall thickness at the location of indication

The WOL length (L_{WOL}) will extend from the weld/base metal interface on either side of the Alloy 82/182 and SS welds, as shown in Figure 11-1. The WOL thickness (t_{WOL}) was determined using the following equation:

$$t_{WOL} = t/0.75 - t$$

The minimum WOL design dimensions are shown in Table 11-6.

In accordance with ASME Section XI IWB-3640, the criterion from Section XI, Appendix C is used to evaluate the maximum post-WOL stresses resulting from the actual applied loadings. To determine the applied post-WOL stresses, the minimum post-WOL thicknesses are considered, which produces a conservative method to determine stresses for comparison to the allowable stress criterion. The thinnest portion of the Alloy 82/182 and SS welds results from considering the largest inner radius ($R_{i\text{-}max}$) and the smallest outer radius post-WOL ($R_{o\text{-min-WOL}}$). These parameters and the resulting geometric section properties are presented in Table 11-7.

The applied bending stresses were calculated by:

$$\sigma_b = \frac{M_b}{Z}$$

M_b is per Table 11-1, and Z is per Table 11-7.

$$Z = \frac{\pi(R_{o-\min-wol}^{\ 4} - R_{i-\max}^{\ 4})}{4(R_{o-\min-wol})}$$

$R_{i\text{-max}}$ and $R_{o\text{-min-wol}}$ are per Table 11-7.

The applied membrane stresses were calculated by:

$$\sigma_m = \sigma_p + \frac{F_a}{A_x}$$

where,

$$\sigma_p = \frac{\pi R_{i-\max}^{\ 2}}{\pi\left(R_{o-\min-wol}^{\ 2} - R_{i-\max}^{\ 2}\right)} P$$

F_a is per Table 11-1.

A_x is per Table 11-7.

$A_x = \pi\ (R_{o\text{-min-wol}}^2 - R_{i\text{-max}}^2)$

$R_{i\text{-max}}$ and $R_{o\text{-min-wol}}$ are per Table 11-7.

P = 2,235 psig [2]

The allowable stress intensity S_m (at 650°F) used in the sizing of the Alloy 52/52M (N06690) overlay is 23.3 ksi [9]. This allowable is based on the annealed condition of SB-166/SB-167. The normal operating pressure, 2,235 psig, was used for the calculation.

The resulting stresses, determined by using the previous equations and the loads and load combinations from Tables 11-1 and 11-2, respectively, are listed and compared to the Code allowable in Table 11-8.

Table 11-5: Letdown/Drain Nozzle Geometry for WOL Design Calculations [2]

Alloy 82/182 Weld			Stainless Steel Weld		
Inside Radius $R_{i\text{-min}}$ (in)	**Outside Radius $R_{o\text{-max}}$ (in)**	**Wall Thickness t_{design} (in)**	**Inside Radius $R_{i\text{-min}}$ (in)**	**Outside Radius $R_{o\text{-max}}$ (in)**	**Wall Thickness t_{design} (in)**
0.844	1.438	0.594	0.844	1.188	0.344

Table 11-6: Letdown/Drain Nozzle Minimum Weld Overlay Repair Design Dimensions [2]

Alloy 82/182 Weld		Stainless Steel Weld	
t_{WOL} (in)	L_{WOL} (in)	t_{WOL} (in)	L_{WOL} (in)
0.30	0.69	0.17	0.48

Table 11-7: Letdown/Drain Nozzle Geometry for Stress Check in Post-Weld-Overlay Condition [2]

Alloy 82/182 Weld				Stainless Steel Weld			
Inside Radius R_{i-max} (in)	Outside Radius $R_{o-min-WOL}$ (in)	Cross-Sectional Area A_x (in^2)	Section Modulus Z (in^3)	Inside Radius R_{i-max} (in)	Outside Radius $R_{o-min-WOL}$ (in)	Cross-Sectional Area A_x (in^2)	Section Modulus Z (in^3)
0.844	1.575	5.555	2.816	0.867	1.358	3.428	1.638

Table 11-8: Letdown/Drain Nozzle Post-SWOL Stress Comparison [2]

	Normal/Upset		Emergency/Faulted	
Location	Applied Stress σ_b (ksi)	Allowable Stress P_b (ksi)	Applied Stress σ_b (ksi)	Allowable Stress P_b (ksi)
Alloy Weld	7.213	10.681	13.804	22.163
SS Weld	12.399	13.095	23.729	27.609

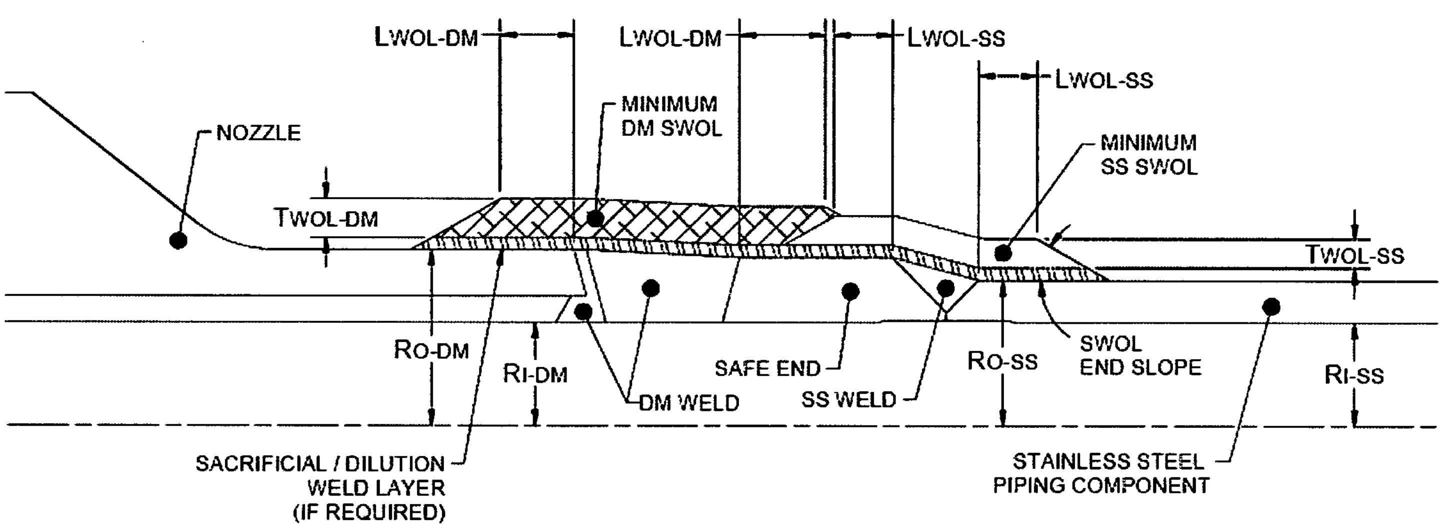

Figure 11-1: Weld Overlay Design Parameters for the Letdown/Drain Nozzle

(Not drawn to scale.)

11.4 WELD OVERLAY RESIDUAL WELD STRESS RESULTS

As described in Section 5.3, the finite element model was developed to capture the parts of the structure in the vicinity of the RCS letdown/drain nozzles safe-end with the SWOL. This includes a portion of the letdown/drain nozzle attached to the nozzle safe-end and a length of SS pipe attached to the safe-end. An ID weld repair was considered in the finite element model. The finite element model and boundary conditions are shown in Figures 11-2 and 11-3. The nozzle is fixed in the axial direction to simulate the rest of the nozzle. The end of the SS piping is coupled in the axial direction to simulate the remaining portion of the SS piping not included in the model. The model assumes that a 50% through-wall weld repair was performed from the inside surface of the letdown/drain nozzle to safe-end Alloy 82/182 butt-weld.

The final residual weld stresses, including normal operating pressure and temperature conditions, are shown in Figures 11-4 and 11-5 for selected stress cuts in the Alloy 82/182 and SS welds. The locations of the stress cuts are provided in Figure 11-2. The stress contours in the RCS letdown/drain nozzle after the weld overlay application are provided in Figures 11-6 and 11-7.

Figures 11-4 shows the axial and hoop residual stresses for the Alloy 82/182 weld, at normal operating conditions after the SWOL. The stresses are compressive up to about 80% of the original pipe wall thickness. This stress distribution is favorable due to the generally compressive stress field. It minimizes the potential for crack growth in the dissimilar-metal weld region. Similarly, Figure 11-5 shows the axial and hoop stress for the stainless weld. They remain compressive for more then 80% of the original pipe wall at normal operating conditions. Therefore, the potential for FCG is minimized.

Acceptable post-weld-overlay residual stresses (i.e., stresses that satisfy the requirements for mitigating PWSCC) are those that are sufficiently compressive over the entire length and circumference of the inside surface of the Alloy 82/182 weld (at operating temperature, but prior to applying operating pressure and loads) that the resulting total stress, after application of operating pressure and loads, remains less than 10 ksi tensile [28]. This target level has been selected as a conservatively safe value, below which PWSCC initiation, or growth of small initiated cracks, is very unlikely. Additionally, the residual plus operating stresses must remain compressive through some portion of the weld thickness away from the inside surface. The residual stresses in the Alloy 82/182 weld of the RCS letdown/drain nozzle, resulting from the weld overlay, are well below this stress level through 80% of the original weld thickness.

Figure 11-8 and 11-9 show that the axial and hoop stresses on the inside surface (in the vicinity of the alloy weld and buttering) remain compressive after SWOL. The maximum resultant bending moment for normal operating condition is 11.319 in-kips. The resulting maximum bending stresses in the Alloy 82/182 weld and SS weld are only 2.652 ksi and 3.76 ksi, respectively [32]. The pipe bending stresses are low, and considered to have negligible effects on the residual weld stress results.

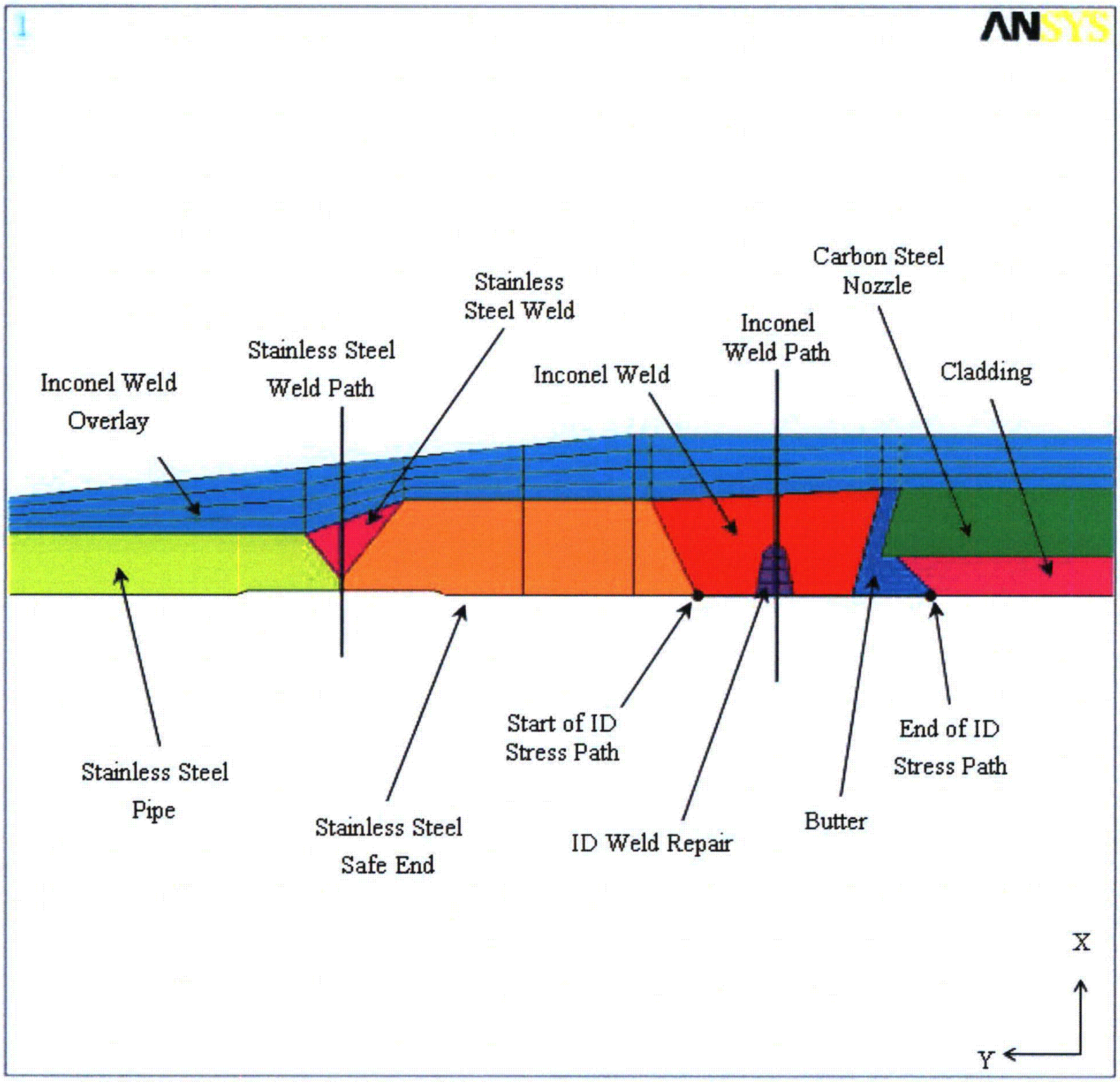

Figure 11-2: ANSYS Model of Letdown/Drain Nozzle

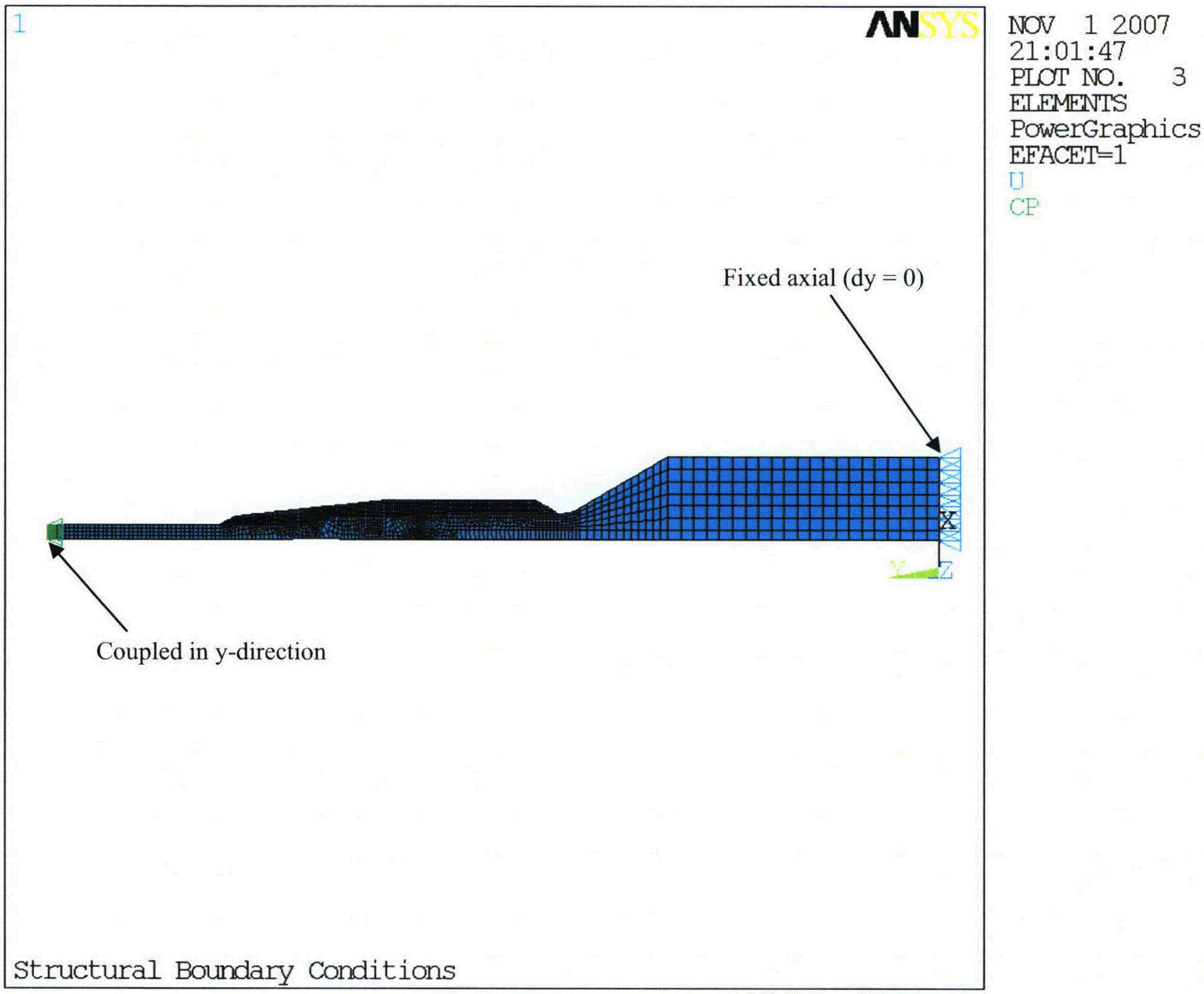

Figure 11-3: Finite Element Model and Structural Boundary Conditions

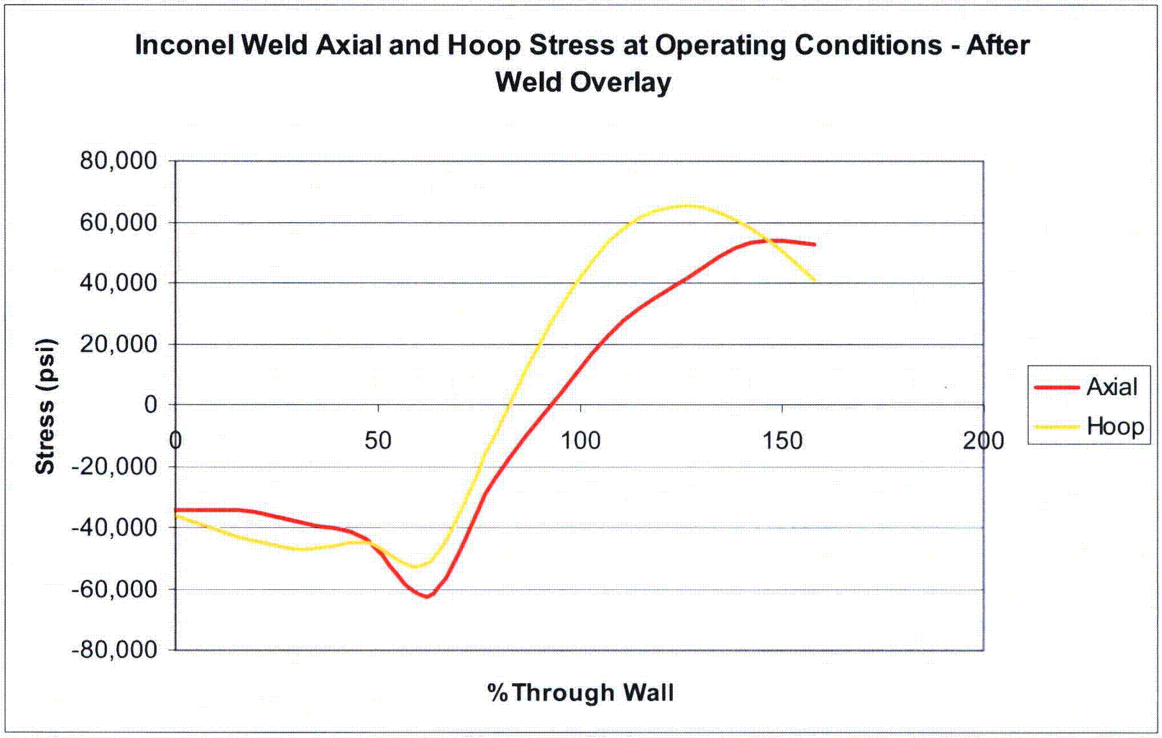

Figure 11-4: Axial and Hoop Residual Stresses in the Alloy 82/182 Weld at Operating Conditions*

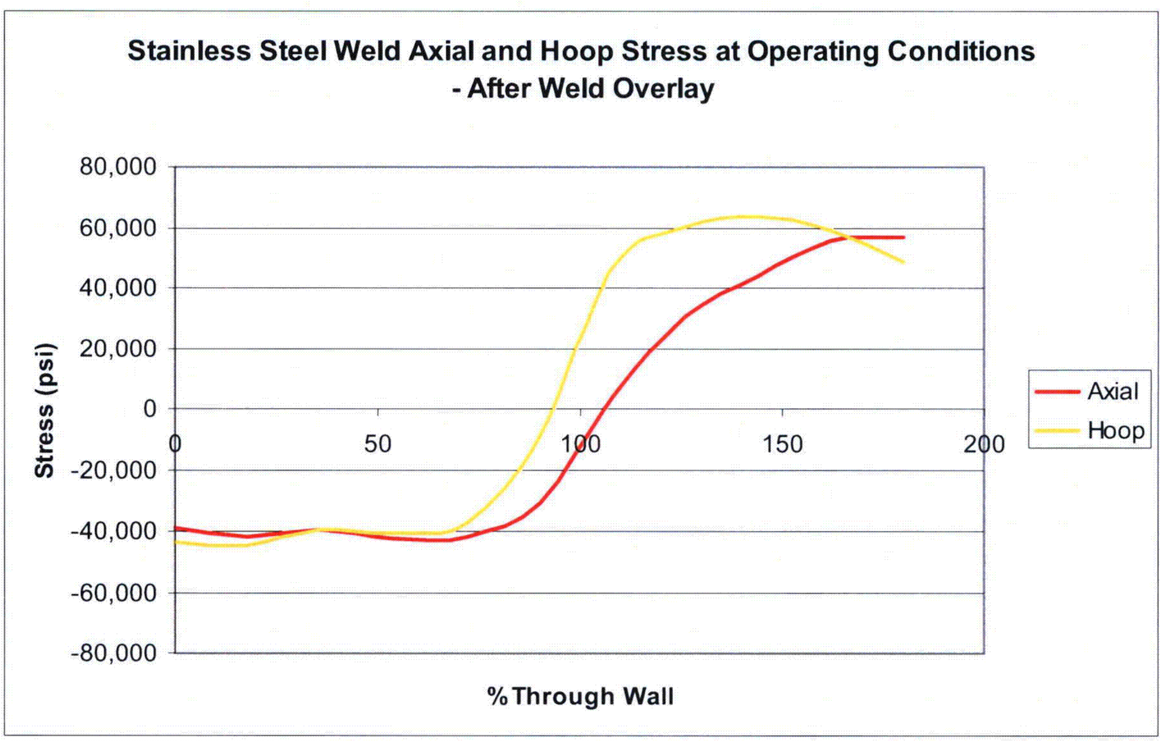

Figure 11-5: Axial and Hoop Residual Stresses in the SS Weld at Operating Conditions*

*Note: The percent through-wall indicated on the horizontal axis is expressed in terms of the original pipe wall thickness. The weld overlay region is the region beyond 100% wall thickness.

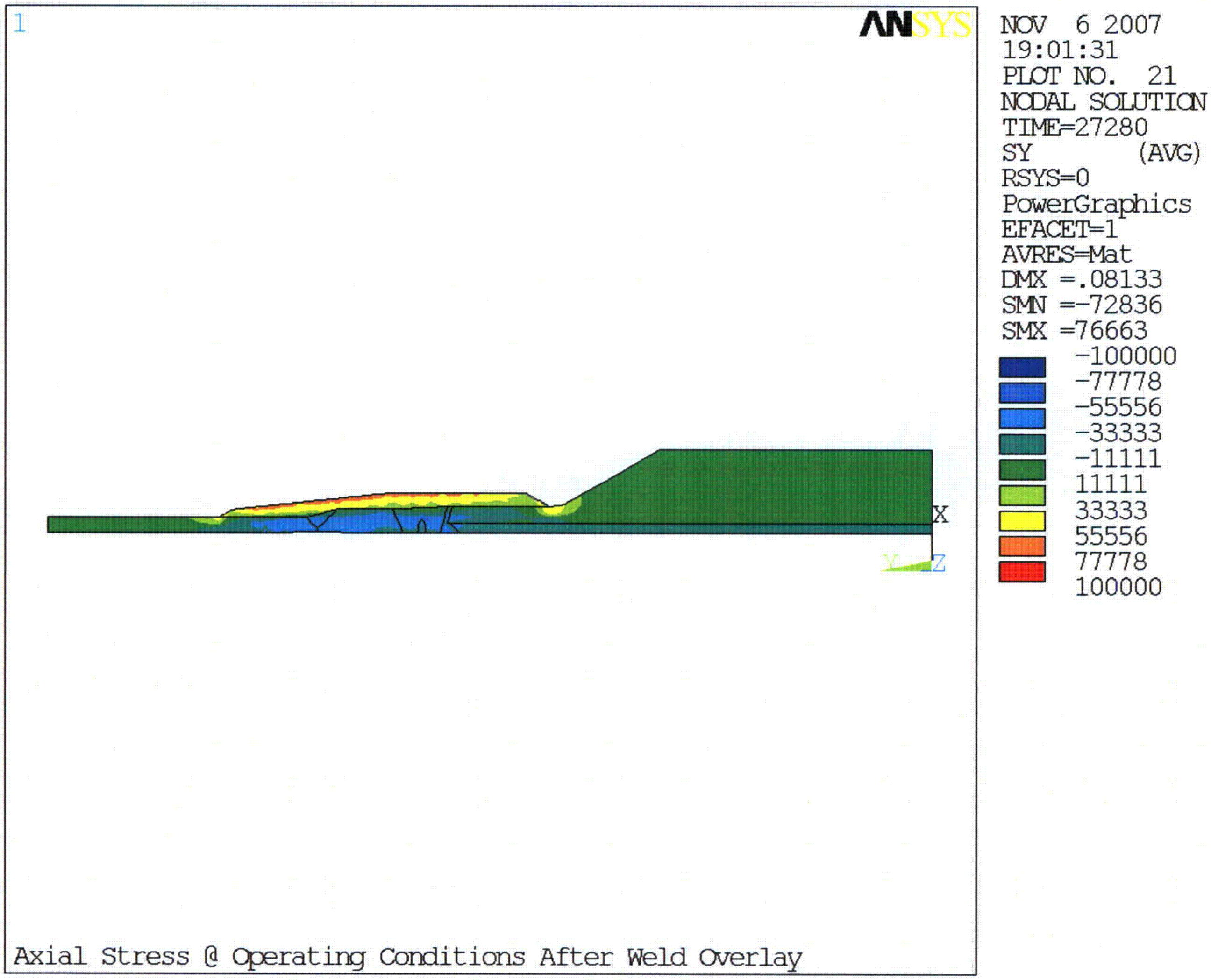

Figure 11-6: Axial Stress (psi) Contour Plot at Operating Condition after Weld Overlay

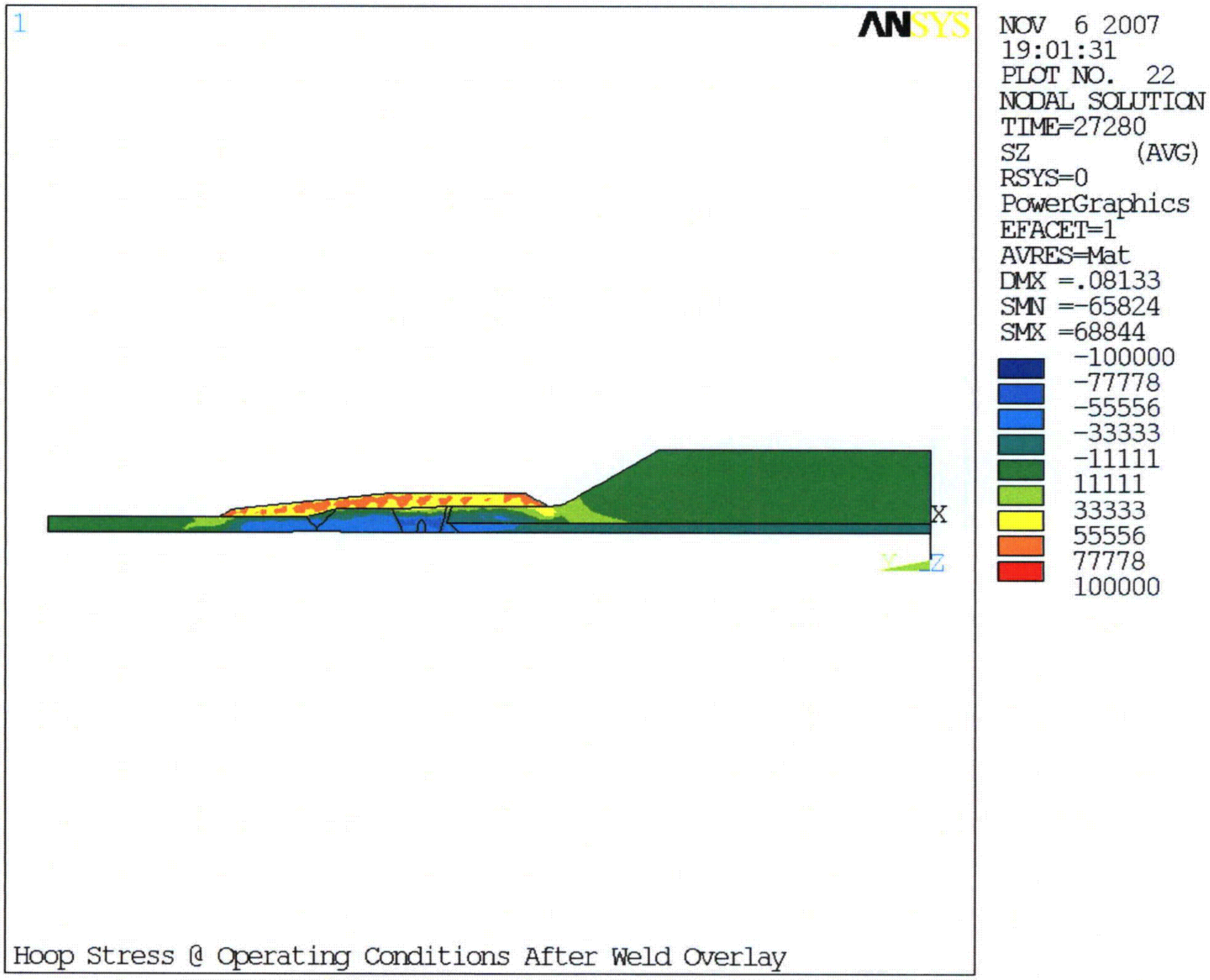

Figure 11-7: Hoop Stress (psi) Contour Plot at Operating Condition after Weld Overlay

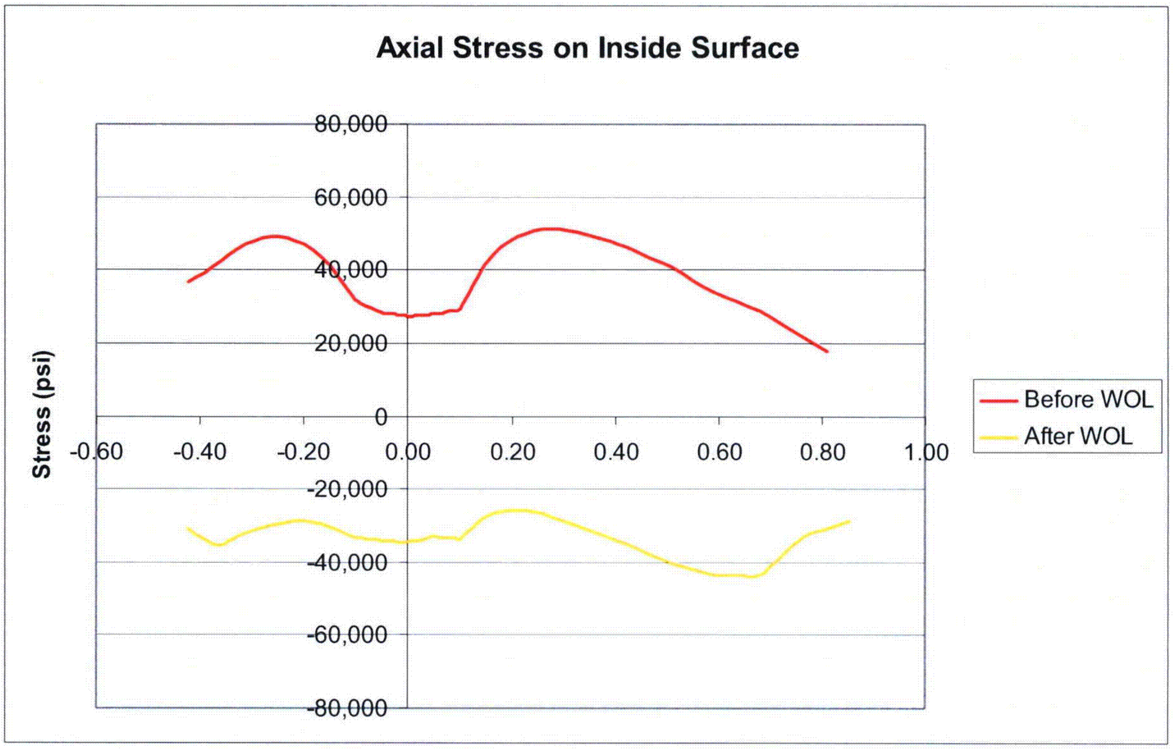

Figure 11-8: Axial Residual Stress along the Inside Surface at Operating Condition*

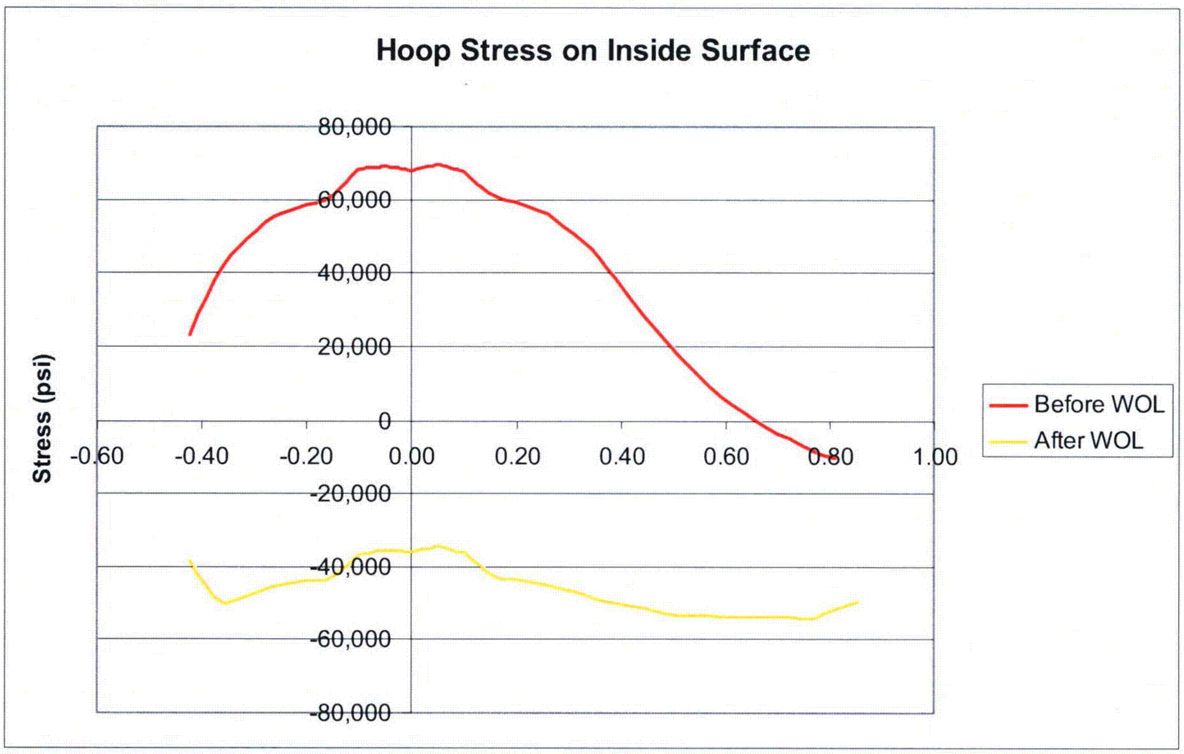

Figure 11-9: Hoop Residual Stress along the Inside Surface at Operating Condition*

*Note: X-axis is the location (inch) along the inside surface path. Zero is the center of alloy weld. See Figure 6-2.

11.5 FATIGUE CRACK GROWTH RESULTS AND ESTIMATE OF WELD OVERLAY DESIGN LIFE: LETDOWN/DRAIN NOZZLE REGION

The methodology used to determine fatigue crack growth is described in Section 4.4. Fatigue crack growth analyses were performed for the letdown/drain nozzles using the through-wall stress distribution including residual stresses generated from the weld overlay mitigation/repair process and the thermal transient stresses.

The weld overlay service life is a function of the flaw depth found in the region being overlaid, and the projected growth of that flaw. The allowable maximum flaw depth is 75% of the piping wall thickness (including the weld overlay thickness), per Section XI, IWB-3640 [6].

A range of possible flaw sizes, from 0 to 100% of the original wall thickness, was postulated in the fatigue crack growth evaluations. The results of these evaluations for the flaw depths less than the original design wall thickness are plotted in Figures 11-10 and 11-11, in the form of expected time for these flaws to reach the interface between the original wall and the newly laid weld overlay material. Figure 11-10 shows results for the Alloy 82/182 weld, and Figure 11-11 shows results for the SS weld. For the maximum possible flaw depths of 100% of the original design wall thickness propagating into the Alloy 52/52M weld overlay material, results are shown in Figure 11-12. This figure shows the estimated flaw depth with time for the design cycles spread over either the original design life or the extended life of the plant.

Figures 11-10 and 11-11 summarize the expected service life (based on transients cycles spread evenly for either 40 years or 60 years of plant life) for a given initial flaw depth to reach 100% of the original wall thickness at the Alloy 82/182 weld and the SS weld locations, respectively. Based on the results shown in Figures 11-10 and 11-11, it can be concluded that if no flaws are detected during the post-SWOL inspection, a conservatively assumed flaw, 75% through the original wall would not grow to 100% of the original wall thickness for 40 years FCG due to transient cycles. This is based on the assumption that the current 40-year design transient cycles are spread evenly over 40 years of plant life. If flaws are detected during the post-SWOL inspection, the as-found flaw size can be used to determine the design life of the SWOL using the crack growth results shown in Figures 11-10 and 11-11.

For the case of an initial flaw depth of 100% of the original wall thickness, i.e., a through-wall flaw, Table 11-9 shows that the total flaw growth into the newly laid Alloy 52/52M welds material in one 10-year inspection interval is 0.004 inch, which is considered small. The final flaw depth after the 10-year period with the fatigue crack growth considered is well within 75% of the total post-WOL wall thickness, as required by SWOL criteria.

Two examination scenarios exist: a pre-overlay examination and a post-overlay examination. If an examination found no flaws, the overlay service life would be governed by the largest flaw that might have been missed by the examination. For an examination performed prior to the weld overlay installation, a conservative approach would be to assume that the flaw depth is 10% of the original wall thickness. Alternatively, this would be 75% of the original wall for an examination performed after the weld overlay installation. This is because the area required to be inspected after the overlay is only the outer 25% of the original pipe thickness plus the overlay thickness itself. The PDI qualification blocks do not contain any flaws in the inner 75% of the pipe wall. Therefore, it would be conservative to assume such a flaw for the qualification. As shown in Figure 11-10, an initial flaw as deep as 75% would result in a remaining service life of 100% of the original design cycles. If the design cycles are assumed to be spread over 40 years of plant operation, the remaining life of the SWOL would be 40 years. This is well beyond the required 10-year in-service inspection (ISI) interval. If, after the next ISI, no flaws are detected in the outer 25% of the original welds, the SWOL life is 40 years from the time of the latest inspection.

In the unlikely event that the post-overlay inspection detected a flaw as large as the full depth of the original design wall thickness, the expected service life of the weld overlay would be at least one 10-year inspection interval period. For the RCS letdown/drain nozzles, flaw growth rate into the weld overlay material is small or negligible, which indicates the expected service life of the repair would be 40 years if the transient cycles are spread over original design life of 40 years.

For example, if an axial flaw that is 96% through the original Alloy 82/182 wall thickness is detected as a result of the post-WOL inspection, and assuming conservatively that the current 40-year design transient cycles are spread evenly for only 40 years, the expected service life from Figure 11-10 for this flaw to reach 100% of the original wall thickness is approximately 20 years. If it is assumed that the design transient cycles are spread evenly for 60 years, the remaining service life would be 30 years. This can also be determined by applying a factor of 1.5 to the service life based on the 40-year design cycles. For a similar-size circumferential flaw, the expected service life is about 40 years, based on current 40-year design transient cycles assumed to be spread evenly over 40 years. Since the typical in-service inspection interval is 10 years, for this initial flaw depth of 96%, it can be concluded that the sizing of the SWOL is adequate up to the next inspection period based on the current 40-year design transient cycles spread evenly over the next 40 years.

Another case of 100% original design wall thickness through-wall flaw in the alloy weld was hypothesized assuming the total post-WOL wall of 0.894 inch. This included an extra allowance of 0.1 inch for the FCG in the Alloy 690 material. This 100% original wall axial flaw was evaluated for the FCG results shown in Table 11-9 and Figure 11-12. Results demonstrate that the total growth in 10 years is insignificant (0.004 inch). The final flaw depth after 10 years of FCG is well within 75% of the total post-WOL wall thickness, as required by SWOL criteria. Therefore, the 0.1 inch SWOL thickness increase provided in the SWOL design is adequate to address the issue of PWSCC for an almost through-wall flaw.

The actual time required to use the remaining design cycles depends on plant operating practice.

Table 11-9: Letdown/Drain Nozzle Alloy 52/52M FCG Data – Axial Flaw [35]

Nozzle Thickness (in)	Initial Flaw Depth (in)	Final Flaw Depth in 10 years (in)	Total Flaw Growth in 10 years (in)
0.894(1,2)	0.565	0.5688	0.0038

Notes:
(1) This thickness is due to a 0.100-inch increase in SWOL thickness.
(2) A review of transient stresses indicates that a rise time of 5,000 seconds is conservative for use in the Alloy 52/52M FCG rate.

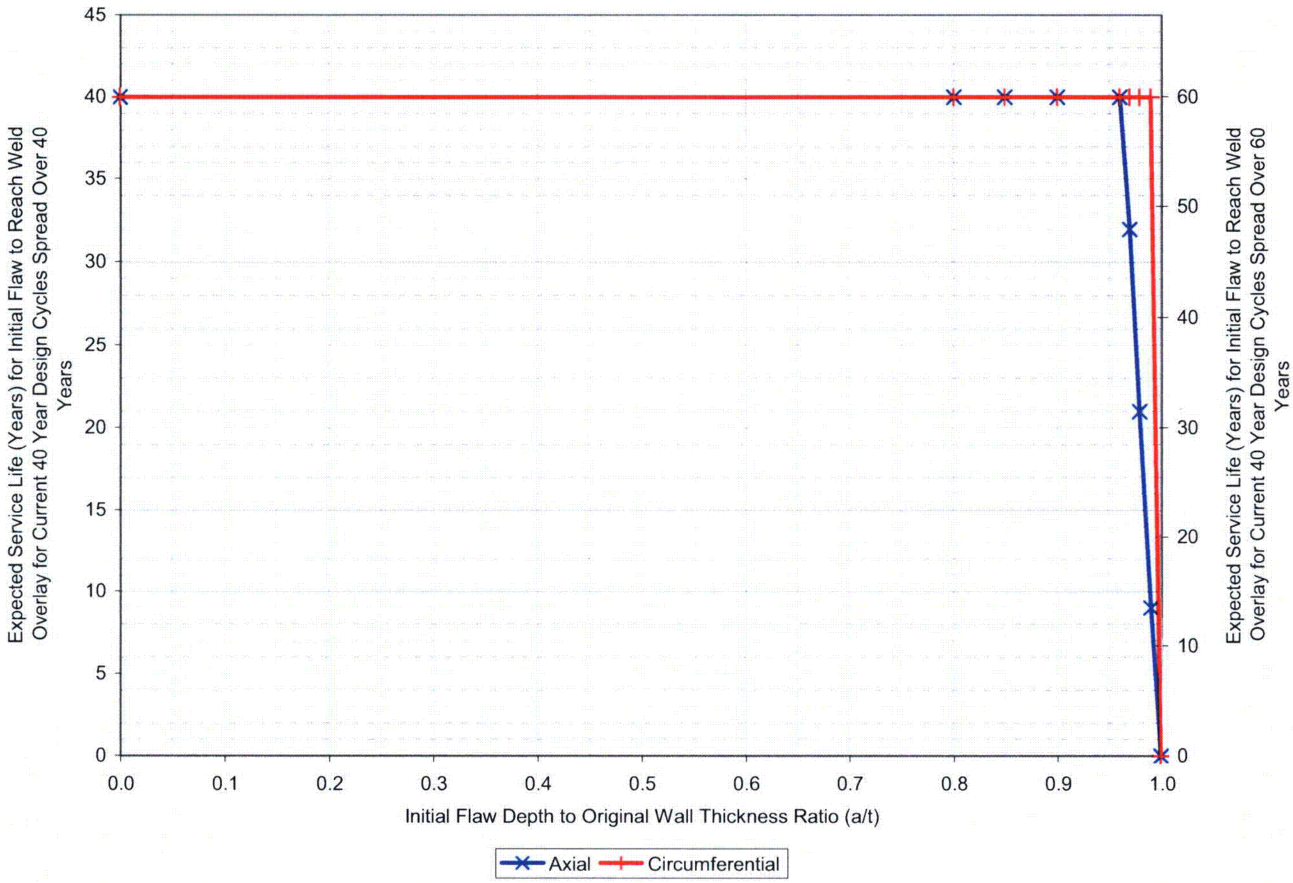

Figure 11-10: Expected Time for the Initial Flaw Depth to Reach the Weld Metal Interface for Letdown/Drain Nozzles Alloy 82/182 Weld [35]

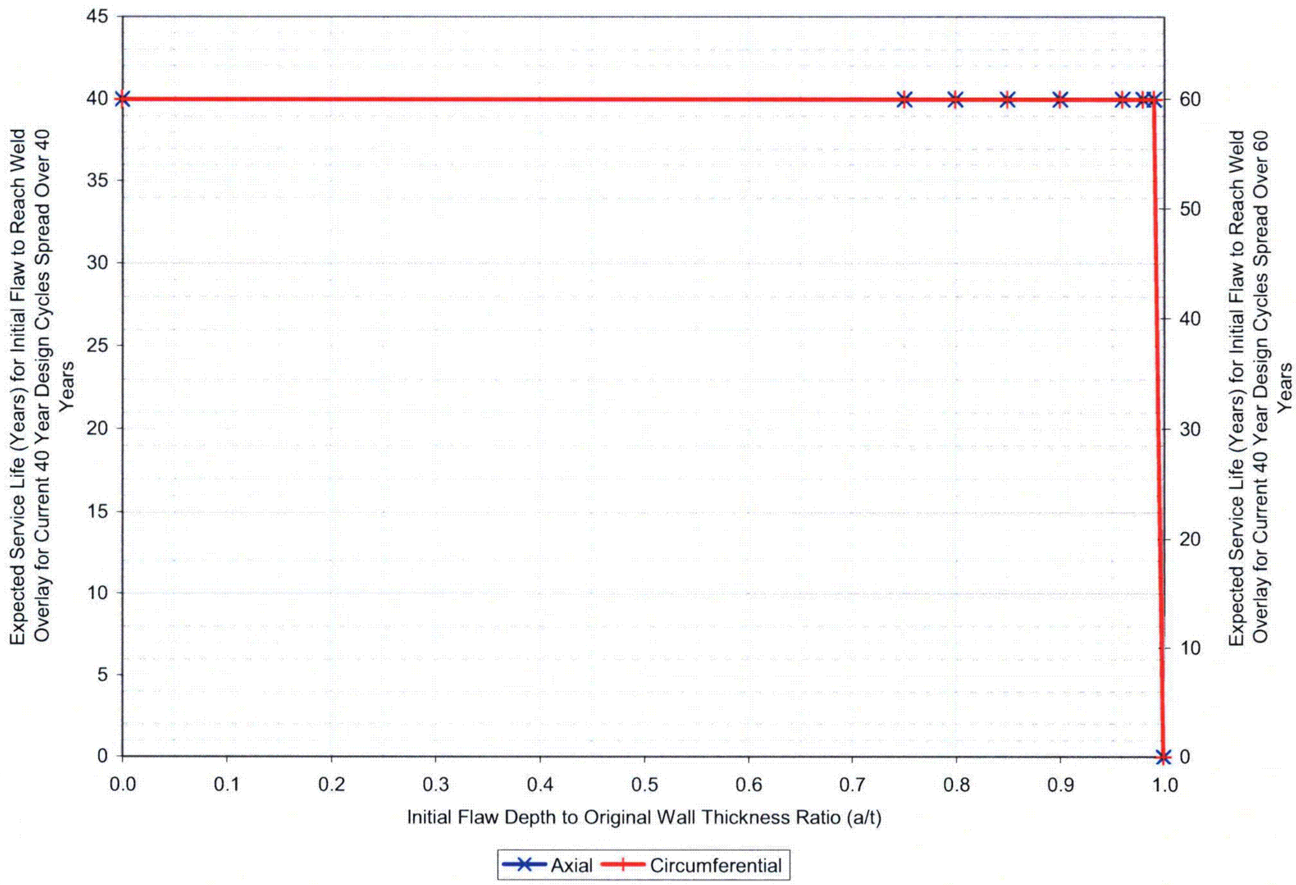

Figure 11-11: Expected Time for the Initial Flaw Depth to Reach the Weld Metal Interface for Letdown/Drain Nozzles SS Weld [35]

Note: Curves for axial and circumferential flaw estimated life coincide with each other. Hence, only one curve is visible in the figure above.

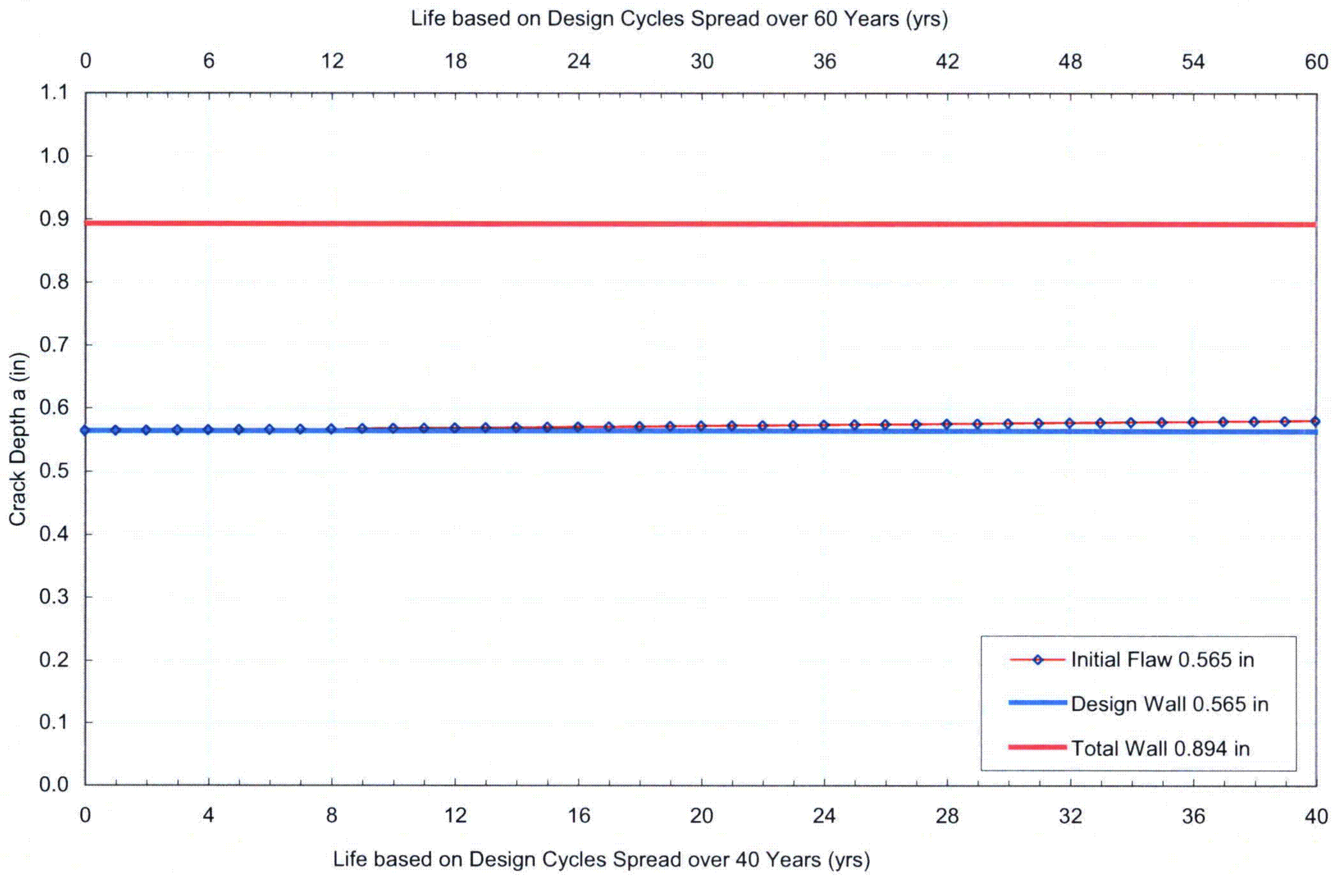

Figure 11-12: Flaw Growth for 100% Original Wall Thickness Initial Flaw versus Service Period in Alloy 52/52M at Letdown/Drain Nozzles Alloy Weld [35]

11.6 IMPACT ON DESIGN QUALIFICATIONS OF NOZZLE AND PIPE

The impact of the weld overlay is evaluated to demonstrate that the presence of the weld overlay repair does not have any adverse impact on the existing stress qualification of the RCS letdown/drain nozzle with respect to the Code of Construction [33].

Effects of SWOL on Transient Stress and Fatigue Analysis

Since the intention of the structural weld overlay is to mitigate/repair the potentially cracked dissimilar-metal butt-weld at the RCS letdown/drain nozzle safe-end, the crack growth analyses discussed in Section 11.5 using the ASME Code Section XI methodology are acceptable bases to address the fatigue qualification of the weld overlay region for the RCS letdown/drain nozzle.

The original analysis was performed in accordance with the ANSI Code [33]. It offers protection against membrane or catastrophic failure, and protection against fatigue or leak type failure. The SWOL does not influence the reinforced region of the letdown/drain nozzle. Therefore, the existing analysis [34] remains applicable for this region, provided the loading used in [34] remains applicable. The transient stresses and structural evaluation for the weld overlay letdown/drain nozzle were documented in [7]. The primary stress for the RCS letdown/drain nozzle was evaluated by hand calculations in accordance with ANSI B31.7 [33]. Addition of the SWOL does not affect the B indices of the loads from the piping, but increases the section modulus in the overlay region. The applicable primary loads (pressure and mechanical loads) used in [34] are not changed by the SWOL. Therefore, the primary stresses in the structures with SWOL are, by definition, less than or equal to those without SWOL. The previous qualifications [34] performed for the RCS letdown/drain nozzle applies to this calculation.

The fatigue for the letdown/drain nozzle was evaluated with finite element techniques. Cut locations are illustrated in Figure 11-13. As Table 11-10 shows, all stress, thermal ratcheting, and fatigue results meet the requirements specified in ANSI B31.7 [33]. Therefore, it is concluded that the existing ANSI B31.7 analysis of the letdown/drain nozzle is not adversely affected by the addition of the SWOL.

Table 11-10: Letdown/Drain Nozzle with SWOL Result Summary

Loading Condition	Stress Category	Cut No.	Stress (psi) or Usage	Stress Limit	Allowable Stress (psi) or Usage	Margin
Design	$P_m + P_b$	-	21,946	1.5 S_m	25,500	13.94%
Level A/B	P + Q	10	34,897	3 S_m	49,800	29.93%
	Linear Thermal Ratchet	2	0.364	N/A	1.000	63.57%
	Parabolic Thermal Ratchet	7	0.355	N/A	1.000	64.54%
	Fatigue	2	0.022	N/A	1.000	97.80%
Level C/D	$P_m + P_b$	-	31,890	2.25 S_m	38,250	16.63%

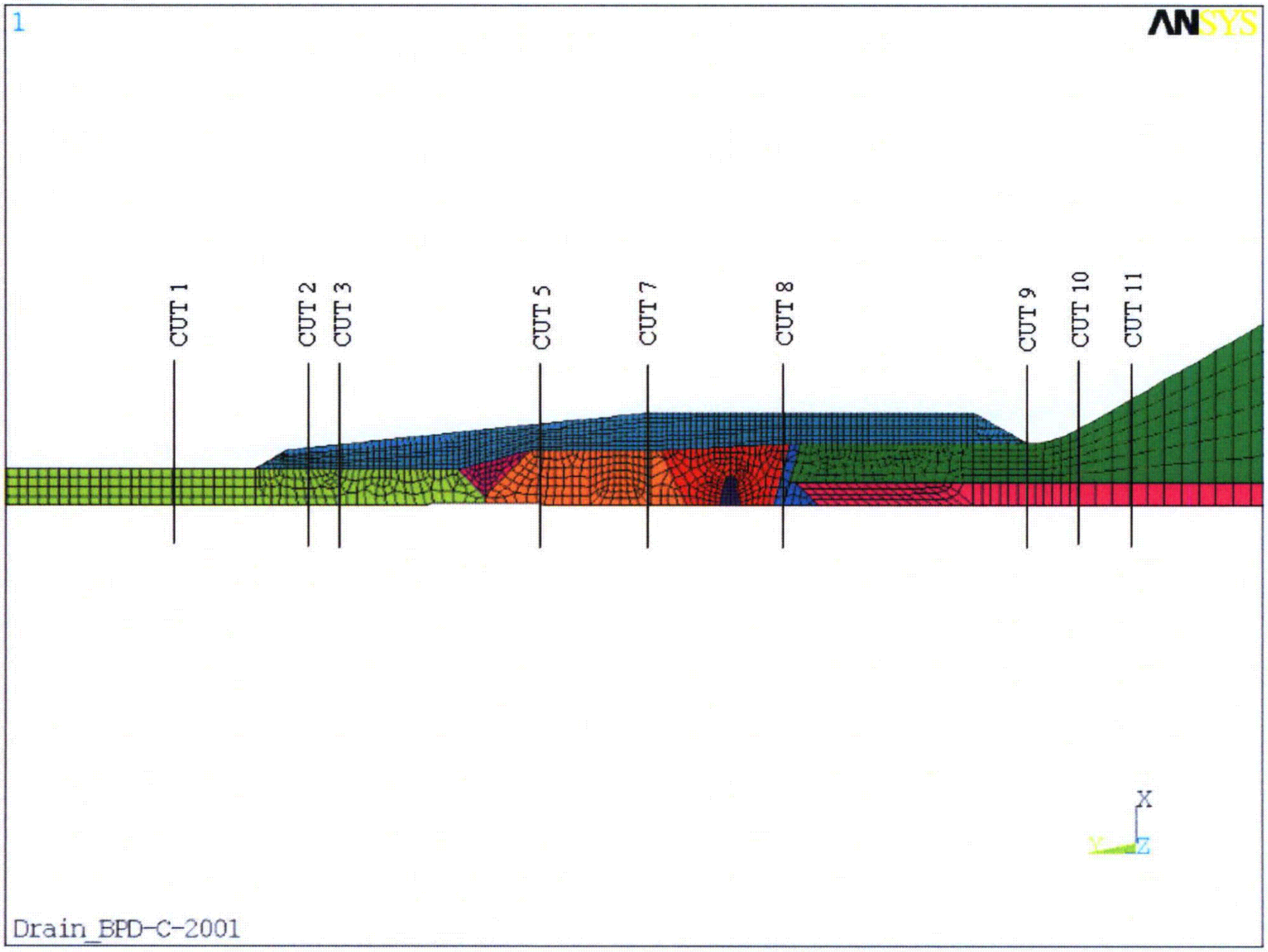

Figure 11-13: Letdown/Drain Nozzle Cut/Path Locations

Effects of Additional Mass on Piping/Support System

The impact of the addition of weld overlay material on the existing primary stress qualification, which considers deadweight and dynamic loadings (such as those due to earthquake), was evaluated in [36], and found to be insignificant.

12 SUMMARY AND CONCLUSIONS

The RCS nozzle weld overlay designs have been demonstrated to meet the intent of the requirements in ASME Code Case N-740 and Section XI IWB-3640 through FEA and fracture mechanics evaluations. In accordance with ASME Code Case N-740, the minimum SWOL thicknesses and lengths for the dissimilar-metal butt-welds and the SS welds are listed in Table 12-1.

The minimum thickness does not include any dilution or sacrificial layers [29]. Additional weld passes or a larger weld overlay thickness will not invalidate the results of the analysis and qualification. The weld overlay design values given in this report are considered the minimum acceptable values. The resulting weld overlay designs shown in Figures 3-1 through 3-6 have also considered the issues of weldability and future UT inspectability, such that the weld overlay for the SS weld is also a SWOL. Therefore, the length of the weld overlay exceeds the minimum length required for a full SWOL in accordance with ASME Code Case N-740.

Alloy 52/52M or equivalent weld material is widely accepted in the industry for its stress corrosion resistance, along with the GTAW process that will further reinforce the effectiveness of a SWOL repair. The FEA results for the SWOL design of the Millstone Unit 2 RCS nozzles, as discussed in Sections 6 through 11, show that the weld overlay repair will create a favorable compressive stress field to mitigate PWSCC on the inner portion of the pipe, thereby minimizing the potential for any future PWSCC crack initiation and/or future crack propagation.

Fatigue crack growth analyses using the ASME Code Section XI methodology were performed to address the fatigue qualification at the weld overlay regions. Once the post-weld-overlay examination has been completed, the remaining service life of the weld overlay can be determined from Figures 6-10 and 6-11 for the spray nozzle; Figures 7-10 and 7-11 for the surge nozzle; Figures 8-10 and 8-11 for the shutdown cooling nozzle; Figures 9-10 and 9-11 for the safety injection nozzle; Figures 10-10 and 10-11 for the charging inlet nozzle; and Figures 11-10 and 11-11 for the letdown/drain nozzles.

An evaluation of the impact of the SWOL on the stress qualification of the RCS nozzles was performed in accordance with the existing Code of Construction. The impact of the addition of weld overlay material on the existing primary stress qualification, which considers deadweight and dynamic loadings (such as those due to earthquake), was found to be insignificant [36]. Reconciliation of the existing fatigue evaluation was performed for the limiting locations outside the SWOL and it was demonstrated that the RCS nozzles with the SWOL would still meet the applicable ANSI B31.7 requirements.

Since the intent of the requirements of ASME Code Case N-740, Section XI IWB-3640, and ANSI B31.7 is met, the structural integrity of the nozzle dissimilar-metal weld region is maintained with the SWOL repair. It should be noted that the weld overlay design is developed based on the assumptions that a 360° through-wall flaw exists and the crack growth mechanism is PWSCC. The use of Alloy 52/52M PWSCC-resistant weld material for the weld overlay will prevent any future PWSCC crack growth into the weld overlay even if any indications grew through the existing pipe wall thickness. Consequently, the SWOL repair implemented for the Millstone Unit 2 RCS nozzles will mitigate future PWSCC crack initiation and/or propagation and therefore maintain structural integrity of the dissimilar-metal weld region.

Table 12-1: Minimum Structural Weld Overlay Thicknesses and Lengths [2]

Weld	Nozzle	SWOL Thickness(1) t_{WOL} (in)	SWOL Length(2) L_{WOL} (in)
DM	RCS Surge	0.78	2.57
	Shutdown Cooling	0.70	2.34
	Charging Inlet	0.30	0.69
	Safety Injection	0.82	2.54
	RCS Spray	0.33	0.88
	Drain/Letdown	0.30	0.69
SS	RCS Surge	0.44	2.17
	Shutdown Cooling	0.38	2.01
	Charging Inlet	0.12	0.48
	Safety Injection	0.54(3)	2.01(3)
	RCS Spray	0.15	0.66
	Drain/Letdown	0.17	0.48

Notes:

1. t_{wol} excludes any sacrificial weld layer but includes an allowance for fatigue crack growth.
2. L_{wol} is the length of extension of the overlay weld beyond the toes of the original weld.
3. At the piping toe of the SS weld, the 0.54-inch thickness decreases linearly to a thickness of .45 inch at a distance of 2.01 inches onto the piping component. Linear interpolation is permitted to determine thicknesses along the 2.01 inch length.

13 REFERENCES

1. ASME Section XI Code Case N-740, "Dissimilar Metal Weld Overlay for Repair of Class 1, 2, and 3 Items," October 12, 2006 (as modified by [3]).
2. Westinghouse Calculation Note, CN-MRCDA-07-72, Rev. 1, "Millstone Unit 2 RCS Nozzle Structural Weld Overlay Design Sizing," January 17, 2008.
3. Dominion Nuclear Connecticut, Inc Letter Submitting 10CFR50.55a Relief Request, "Dominion Nuclear Connecticut, Inc. Millstone Power Station Unit 2 Alternative Request RR-89-61, Use of Weld Overlays as an Alternative Repair and Mitigation Technique," October 4, 2007.
4. NUREG-0313, Rev. 2, "Technical Report on Material Selection and Processing Guidelines for BWR Coolant Pressure Boundary Piping," January 1988.
5. NRC Information Notice, 2004-11, "Cracking in Pressurizer Safety and Relief Nozzle and in Surge Line Nozzle," May 6, 2004.
6. ASME Boiler and Pressure Vessel Code, Section XI, "Rules for Inservice Inspection of Nuclear Power Plant Components," 1998 Edition, No Addenda.
7. Transient Stress Analysis Reports:
   a. Westinghouse Calculation Note, CN-MRCDA-07-110, Rev. 0, "Millstone Unit 2 Weld Overlay RCS Spray Nozzle Transient Stress Analysis and Structural Evaluation," February 21, 2008.
   b. Westinghouse Calculation Note, CN-MRCDA-07-108, Rev. 0, "Millstone Unit 2 Weld Overlay RCS Surge Nozzle Transient Stress Analysis and Structural Evaluation," February 21, 2008.
   c. Westinghouse Calculation Note, CN-MRCDA-07-114, Rev. 1, "Millstone Unit 2 Weld Overlay RCS Shutdown Cooling Nozzle Transient Stress Analysis and Structural Evaluation," February 22, 2008.
   d. Westinghouse Calculation Note, CN-MRCDA-07-109, Rev. 0, "Millstone Unit 2 Weld Overlay RCS Safety Injection Nozzle Transient Stress Analysis and Structural Evaluation," February 21, 2008.
   e. Westinghouse Calculation Note, CN-MRCDA-07-112, Rev. 0, "Millstone Unit 2 Weld Overlay RCS Charging Inlet Nozzle Transient Stress Analysis and Structural Evaluation", February 22, 2008.
   f. Westinghouse Calculation Note, CN-MRCDA-07-111, Rev. 0, "Millstone Unit 2 Weld Overlay RCS Letdown/Drain Nozzle Transient Stress Analysis and Structural Evaluation", February 21, 2008.
8. Westinghouse Weld Overlay Design Drawings:
   a. 10033D57, Rev. 0, "Millstone Unit 2 RCS Spray Nozzle SWOL Design & Field Implementation (BPY-C-3000)."
   b. 10027E43, Rev. 0, "Millstone Unit 2 RCS Surge Nozzle SWOL Design & Field Implementation (BPS-C-1001)."
   c. 10032D14, Rev. 0, "Millstone Unit 2 RCS Shutdown Cooling Outlet Nozzle SWOL Design & Field Implementation (BSD-C-2001)."

d. 10031E61, Rev. 1, "Millstone Unit 2 RCS Safety Injection Nozzle SWOL Design & Field Implementation (BSI-C-4000)."

e. 10033D48, Rev. 0, "Millstone Unit 2 RCS Charging Inlet Nozzle SWOL Design & Field Implementation (BCH-C-1001)."

f. 10032D15, Rev. 0, "Millstone Unit 2 RCS Drain Nozzle SWOL Design & Field Implementation (BPD-C-2001)."

9. ASME Boiler and Pressure Vessel Code, Section II, 2001 Edition through 2003 Addenda, Materials, Part D – Properties.

10. ASME Boiler and Pressure Vessel Code, 2001 Edition, through 2003 Addenda, Section II, Materials, Part C – Specifications for Welding Rods, Electrodes, and Filler Metals.

11. E. F. Rybicki and R. B. Stonesifer, "Computation of Residual Stresses due to Multipass Welds in Piping Systems," Journal of Pressure Vessel Technology, Vol. 101, May 1979, pages 149-154.

12. Special Metals Corporation Publication, SMC-079, "INCONEL[(1)] Alloy 690," October 3, 2003.

13. ASME Code Case N-525, "Design Stress Intensities and Yield Strength Values for UNS N06690 with a Minimum Specified Yield Strength of 30 ksi, Class 1 Components Section III, Division 1," December 9, 1993.

14. ASM Metals Handbook, Volume 3, "Properties and Selection: Stainless Steels, Tool Materials and Special-Purpose Metals," Ninth Edition, Metals Park, OH, 1980.

15. Westinghouse Report, WCAP-13525-R1, Rev. 1, "RV Closure Head Penetration Alloy 600 PWSCC (Phase 2)," December 1992.

16. Westinghouse Letter, LTR-SST-06-21, Rev. 0, "Release of Ansys 10 for XP, HPUX 11.0, and HPUX 11.23 and ANSYS Error Reports," July 12, 2006.

17. EPRI Topical Report, EPRI NP-7103-D, Project T303-1, "Justification for Extended Weld-Overlay Design Life," January 1991.

18. Special Metals Corporation Publication No. SMC-027, "INCONEL Alloy 600," September 2004.

19. Westinghouse Letter, LTR-MRCDA-07-208, Rev. 0, "ANSYS Properties for Structural Weld Overlay Repair Residual Stress Calculations," November 12, 2007.

20. James, L. A., and W. J. Mills, "Fatigue Crack Propagation Behavior of Wrought Alloy 600 and Weld-Deposited EN82H in an Elevated Temperature Aqueous Environment," in ASME Publication PVP Vol. 303, 1995.

21. Van Der Sluys, W. A., B. A. Young, and D. Doyle, "Corrosion Fatigue Properties of Alloy 690 and some Nickel-Based Materials," in ASME Publication PVP Vol. 410-2, 2000.

22. Amzallag, C., G. Baudry, and J. L. Bernard, "Effects of PWR Environment on the Fatigue Crack Growth of Different Stainless Steels and Inconel Type Alloy," in Proc. Intl. Atomic Energy Agency Specialists Meeting on Subcritical Crack Growth, in NUREG/CP-0044, Vol. 1, 1983.

[1] INCONEL® is a registered trademark of Precision Castparts Corp.

23. Chopra O. K., W. K. Soppet, and W. J. Shack, "Effects of Alloy Chemistry, Cold Work, and Water Chemistry on Corrosion Fatigue and Stress Corrosion Cracking of Nickel Alloys and Welds," NUREG/CR-6721, May 2001.

24. Raju, I. S. and J. C. Newman, "Stress Intensity Factor Influence Coefficients for Internal and External Surface Cracks in Cylindrical Vessels," in Aspects of Fracture Mechanics in Pressure Vessels and Piping, ASME Publication PVP Vol. 58, 1982.

25. Mettu, S. R., I. S. Raju, and R. G. Forman, NASA Lyndon B. Johnson Space Center Report No. NASA-TM-111707, "Stress Intensity Factors for Part-Through Surface Cracks in Hollow Cylinders," in Structures and Mechanics Division, July 1992.

26. James, L. A., and D. P. Jones, "Fatigue Crack Growth Correlations for Austenitic Stainless Steel in Air," in Predictive Capabilities in Environmentally Assisted Cracking, ASME Publication PVP-99, December 1985.

27. Bamford, W. H., "Fatigue Crack Growth of Stainless Steel Piping in a Pressurized Water Reactor Environment," Trans ASME, Journal of Pressure Vessel Technology, February 1979.

28. Material Reliability Program: Technical Basis for Preemptive Weld Overlays for Alloy 82/182 Butt Welds in PWRs (MRP-169). EPRI, Palo Alto, CA: 2005. 1012843 (EPRI Proprietary Document).

29. WCAP-16597-P, "PCI/Westinghouse Assessment of First-Layer Chemistry in Structural Weld Overlay Deposits," February 6, 2008.

30. Combustion Engineering Design Specification, 18767-31-5, Rev. 16, "Engineering Specification for a Reactor Coolant Pipe & Fittings for Northeast Utilities Service Company Millstone Point Station, Unit No. 2," November 5, 1997.

31. Westinghouse Calculation Note, CN-MRCDA-07-82, Rev. 1, "Determination of Design Loads for Millstone Point Unit 2 Main Loop Piping Tributary Nozzles," January 8, 2008.

32. SWOL Residual Stress Analysis Reports

    a. Westinghouse Calculation Note, CN-MRCDA-07-98, Rev. 0, "Millstone Unit 2 RCS Spray Nozzle Residual Stress Analysis," February 20, 2008.

    b. Westinghouse Calculation Note, CN-MRCDA-07-100, Rev. 0, "Millstone Unit 2 RCS Surge Nozzle Residual Stress Analysis," February 20, 2008.

    c. Westinghouse Calculation Note, CN-MRCDA-07-102, Rev. 0, "Millstone Unit 2 RCS Shutdown Cooling Nozzle Residual Stress Analysis," February 19, 2008.

    d. Westinghouse Calculation Note, CN-MRCDA-07-99, Rev. 0, "Millstone Unit 2 RCS Safety Injection Nozzle Residual Stress Analysis," February 20, 2008.

    e. Westinghouse Calculation Note, CN-MRCDA-07-105, Rev. 1, "Millstone Unite 2 RCS Charging Inlet Nozzle Residual Stress Analysis," February 20, 2008.

    f. Westinghouse Calculation Note, CN-MRCDA-07-97, Rev. 0, "Millstone Unit 2 RCS Letdown/Drain Nozzle Residual Stress Analysis," February 20, 2008.

33. ANSI Code for Pressure Piping B31.7, Class 1, 1969.

34. Combustion Engineering Analytical Report, CENC-1192, Rev. 0, "Analytical Report for Northeast Utilities Service Company Millstone Point Station Unit No. 2 Piping," September 26, 1973.

35. Fatigue Crack Growth Analysis Reports:

a. Westinghouse Calculation Note, CN-MRCDA-08-7, Rev. 0, "Millstone Unit 2 Weld Overlay RCS Spray Nozzle Fatigue Crack Growth Analysis," February 22, 2008.

b. Westinghouse Calculation Note, CN-MRCDA-08-4, Rev. 0, "Millstone Unit 2 Weld Overlay RCS Surge Nozzle Fatigue Crack Growth Analysis," February 22, 2008.

c. Westinghouse Calculation Note, CN-MRCDA-08-6, Rev. 0, "Millstone Unit 2 Weld Overlay RCS Shutdown Cooling Nozzle Fatigue Crack Growth Analysis," February 28, 2008.

d. Westinghouse Calculation Note, CN-MRCDA-08-5, Rev. 0, "Millstone Unit 2 Weld Overlay RCS Safety Injection Nozzle Fatigue Crack Growth Analysis," February 22, 2008.

e. Westinghouse Calculation Note, CN-MRCDA-08-8, Rev. 0, "Millstone Unit 2 Weld Overlay RCS Charging Nozzle Fatigue Crack Growth Analysis," February 25, 2008.

f. Westinghouse Calculation Note, CN-MRCDA-08-9, Rev. 0, "Millstone Unit 2 Weld Overlay RCS Letdown/Drain Nozzle Fatigue Crack Growth Analysis," February 22, 2008.

36. Westinghouse Calculation Note, CN-MRCDA-07-107, Rev. 0, "Millstone Unit 2 Weld Overlay - RCS Response with Increased Nozzle Weight due to Overlays," January 14, 2008.